Establishing the *C. elegans* uterine seam cell (utse) as a novel model for studying cell behavior

Thesis by
Srimoyee Ghosh

In Partial Fulfillment of the Requirements for the degree
of
Doctor of Philosophy

CALIFORNIA INSTITUTE OF TECHNOLOGY
Pasadena, California
2015
Defended May 5, 2015

For মা

ACKNOWLEDGEMENTS

Excitement does not even cover how I feel right now. I am positively giddy. I cannot believe that I am at this point in my carrer and will soon transform from Ms. Ghosh to Dr. Ghosh. However, there is no way that I could even be typing the previous sentences without the help, love, and support of some key people.

First and foremost I want thank my parents, my father Prabhat Ghosh and my mother Indrani Ghosh. You have both continually had so much faith in me, and pushed me towards success every step of the way. Baba, I want to thank you for instilling a sense of discipline and structure in me that I may have hated when I was younger, but became my saving grace during graduate school. Ma, I want to thank you for always encouraging to "*neejer paye neje darao*" ('to stand on your own two feet' in Bengali), which gave me strength to take on whatever challenges I faced. I am the woman I am today because of your love and support and I am so proud to be your daughter.

Paul, I almost cannot put into words how much you have meant to me during this journey. People say that the perfect advisor does not exist, but I don't think those people have worked for you. As a mentor you somehow mix the right amount of guidance and direction with the right amount of independence, and it has made these past six years some of the best six years of my life. Thank you for your excitement and confidence in my work, from when I was just proposing I study the utse to fine-tuning experiments for publications. Your enthusiasm for *C. elegans* seeps into everyone around you, and you have honestly made me so excited to come into lab every day. And lastly, not only have you been an incredible advisor, but you have also been a great mentor and father figure to me. You once told me that during graduate school is a place where you achieve "life confidence" where you feel that you can successfully tackle any problem in front of you, no matter now complex or daunting. Working for someone as positive and encouraging as you has helped me find my "life confidence" and I am so excited for my future because of it.

I would also like to thank the members of the Sternberg Lab. This lab is an incredible place where egos are put aside and everyone is collaborative and genuinely wants everyone to succeed. I would like to thank the following individuals from the Sternberg lab: Mihoko Kato, for helping me bounce off ideas, and critically reading manuscripts, and always being excited and interested in what I am doing; James Lee, Pei Shih, Sylvia Vetrone, Han Wang, and Jon Liu for taking time out of their busy days to help me with experiments, no matter how long it took me to get a protocol; all of you

were so patient and helpful; Hillel Schwartz, for also critically reading manuscripts and catching things with the adeptness of a reviewer's eye but the kindness of someone who wants to you to publish; Barbara Perry, for not only providing me strains but also self confidence with your humor and positive words; David Angeles, for his excitement and interest; whenever I feel jaded I look to you and get excited again; Ping Hsueh, Chris Chronin, Ravi Nath, Alli Akagi, and Shahla Gharib for your friendship and always making lunch fun; Sarah Torres, for being so bright and cheerful and encouraging every day; you coming in and saying "you can do it!!!!!!!!" the month and a half I was writing my thesis meant so much to me! There are many others in lab I want to thank including Paul Minor, Erich Schwartz, Meenakshi Doma, Ryoji Shinya, Dan Leighton, Wen Chen, Katie Brugman, John Demodena, Gladys Medina, Carmie Robinson, and Kai Yuet. Lastly, I especially want to thank Andrea Choe for being a great mentor and friend and someone I could turn to anytime. Your wisdom and confidence in me has been fundamental to my success here, and I am so grateful to you! All of you made coming into lab a joy every day.

I also want to thank my summer students Stephanie Liu and Sang Nguyen. Thank you for your enthusiasm and eagerness to learn. Both of you were an absolute delight to work with and I'm so excited to see what you accomplish in the future.

I also owe thanks to the members of my thesis committee, Marianne Bronner, Bruce Hay, and David Chan. Thank you for taking time out of your busy schedules to meet with me, for providing me with great feedback, and for being so supportive and encouraging of my work. Marianne, I especially want to thank you for being my committee chair; you are such an inspiration and role model for women in science. I am so happy that you have been such an integral part of my career here, and thank you so much for all your support.

The *C. elegans* community has also played an essential role in my work here at Caltech. I want to thank Wendy Hanna-Rose, Dan Starr, and Matthew Buechner for helpful discussion when I first embarked upon characterizing the utse. I also want to thank Ian Hope, David Sherwood, David Baillie, Harald Hutter, and Nathalie Pujol for strains and reagents.

I would not even be in graduate school without the input of my undergraduate advisor John Wallingford. Thank you for being the first one to show me the wonder behind bench work and for giving me a project that led me to fall in love with developmental biology. Your honest input and enthusiasm helped me become the scientist and person I am today and I am ever so grateful.

Many members of the Caltech community outside of my lab have been key to my success here at Caltech. I specifically want to thank Angela Stathopoulos and members of the Stathopoulos Lab for being my initial home here at Caltech. Angela, my time working for you helped me realize how much I loved science, and your encouragement helped me truly gain confidence in my work. I also want to thank Snehalata Kadam for being an incredible mentor, and Young Bae, Amy McMahon, and Sarah Tulin for being my first family away from Texas when I moved out to California.

My friends have been a constant source of support while I have been here at Caltech. Going through graduate school with all of you by my side have made the last six years of my life incredible. I want to thank my classmate Alma Gharib for being my confidant and and giving me wise advice about life both in and outside the lab. I want to thank Alice Robinson for always wanting the best for me, whether it meant dragging me out to a party in the Cats because I was being antisocial my first year, or proofreading a chapter of my thesis; I am so happy to have you in my life. I also want to thank Sophie Katz for sharing my love for developmental biology and *C. elegans* and keeping our friendship solid even after your move from Caltech to UCLA, Crystal Dilworth for always reminding me of my worth, and Vikas Trivedi for your unfaltering faith in me and your laughter and humor.

Lastly I want to thank Aneesh Acharya. Your love, support and unyielding conviction that I am a strong, powerful, BOSS woman has helped me evolve into the person I am today. I am in awe of the person I have become in your presence. You are the reason I work so very hard and why I strive to do my absolute best every single day. I am so very thankful to have you in my life. I could not have done this without you.

PREFACE

"*All cell biologists are condemned to suffer an incurable secret sorrow: the size of the objects of their passion.... But those of us enamored of the cell must resign ourselves to the perverse, lonely fascination of a human being for things invisible to the naked human eye*."

- L.L. Larison Cudmore, Opening sentence from *The Center of Life: A Natural History of the Cell* (1977, 1978)

Growing up in the forests of southern New Hampshire, I always had a fascination for nature and the beauty within living things. You can only imagine my surprise and excitement when I first began working in developmental biology, and saw the splendor and intricacies of living cells. To me there is no greater beauty than seeing a glowing fluorescent image light up a pitch-black room, and taking in the wonder of directly being able to see something critical to the life and health of an organism.

Finding out exactly what makes an organism tick has been both trying and thrilling. The balance is so incredibly delicate and something as small as a change of a single base can create havoc and even death. My work has involved studying cell behavior, where cells move, twist, and bend until they reach their final shape and position within an organism. It has been an incredible journey documenting the many minute inputs necessary for a cell to do its job of creating a healthy, happy organism. Even if I have only found out the tip of the iceberg of what contributes to *C. elegans* utse biology, I am so grateful to have unearthed this information.

Someone once told me that it is a privilege to be in graduate school because you are basically creating knowledge. I am not pompous enough to say that I created knowledge on utse outgrowth (if anyone could be given credit for "creating this knowledge" it would the scores of nematodes whose uteruses I observed during my Ph.D.). However, I am so happy that my work has established this cell as a new model for studying outgrowth and shape change. There is much to be learned about the utse, and I am so excited to see what others discover next.

ABSTRACT

The molecular inputs necessary for cell behavior are vital to our understanding of development and disease. Proper cell behavior is necessary for processes ranging from creating one's face (neural crest migration) to spreading cancer from one tissue to another (invasive metastatic cancers). Identifying the genes and tissues involved in cell behavior not only increases our understanding of biology but also has the potential to create targeted therapies in diseases hallmarked by aberrant cell behavior.

A well-characterized model system is key to determining the molecular and spatial inputs necessary for cell behavior. In this work I present the *C. elegans* uterine seam cell (utse) as an ideal model for studying cell outgrowth and shape change. The utse is an H-shaped cell within the hermaphrodite uterus that functions in attaching the uterus to the body wall. Over L4 larval stage, the utse grows bidirectionally along the anterior-posterior axis, changing from an ellipsoidal shape to an elongated H-shape. Spatially, the utse requires the presence of the uterine toroid cells, sex muscles, and the anchor cell nucleus in order to properly grow outward. Several gene families are involved in utse development, including Trio, Nav, Rab GTPases, Arp2/3, as well as 54 other genes found from a candidate RNAi screen. The utse can be used as a model system for studying metastatic cancer. Meprin proteases are involved in promoting invasiveness of metastatic cancers and the meprin-likw genes *nas-21*, *nas-22,* and *toh-1* act similarly within the utse. Studying *nas-21* activity has also led to the discovery of novel upstream inhibitors and activators as well as targets of *nas-21*, some of which have been characterized to affect meprin activity. This illustrates that the utse can be used as an *in vivo* model for learning more about meprins, as well as various other proteins involved in metastasis.

TABLE OF CONTENTS

CHAPTER 1

Introduction Part I

1.1 Thesis Overview

During development, cells not only divide, but change their shape and move before reaching their final positions within an organism. This process is termed cell behavior, and is controlled by a variety of molecular and spatial inputs. Cell behavior is essential for the viability of an organism and disease models, including promoting formation of facial structures (neural crest cell migration, Le Douarin et al., 2007), forming the *Drosophila* gut (caudal visceral mesoderm cells, Kadam et al., 2012), and forming invasive structures in metastatic cancer (van Zijl et al., 2011). Characterizing genetic and tissue interactions not only creates a more thorough understanding of these processes but can lead to the creation of targeted therapies in diseases whose pathologies are characterized by changes in cell behavior.

C. elegans is a small free living nematode that has been well characterized for its roles in molecular biology. The cell lineage of *C. elegans* is stereotypic and well characterized (Brenner 1974; Byerly et al., 1976; Sulston et al., 1983) and therefore ideal for studying cell behavior. Specifically in this work, I have characterized one cell in the *C. elegans* uterus, the *C. elegans* uterine seam cell (utse).

In Chapter 2, I describe non-neuronal cell outgrowth in *C. elegans* (Ghosh and Sternberg, in prep 1), demonstrating that this organism is an ideal model for studying cell behavior. I discuss the spatial and molecular inputs necessary for eleven different systems including utse outgrowth, anchor cell invasion, sex muscle formation, male tail formation, excretory cell outgrowth, dorsal intercalation, ventral enclosure, early elongation, late elongation, muscle arm formation, and head mesodermal cell projection formation. I have also characterized genes that act in outgrowth of different tissues, identifying global regulators of cell outgrowth in *C. elegans*.

Chapter 3 involves characterizing the utse as a model for studying cell outgrowth (Ghosh and Sternberg, 2014). The utse is an H-shaped cell found in the hermaphrodite uterus (Newman et al., 1996). The utse functions in attaching the uterus to the seam cells of the body wall, and during the L4 larval stage, the utse changes from an ellipsoidal shape to an elongated shape by growing outward along the anterior-posterior axis (Newman et al., 1996, Ghosh and Sternberg, 2014). In this work, I have used laser ablation experiments to identify spatial inputs necessary for utse development. I show that the presence of two cells that line the lumen of the uterus (uterine toroid 1 and uterine toroid 2), the sex muscles, and the anchor cell of the nucleus are necessary for utse development. After determining that these tissues are necessary for mediating utse outgrowth, I

performed a candidate RNAi screen against genes that were expressed in these tissues and saw that several gene families were involved in utse development. Trio (*unc-73*), Nav (*unc-53*), RabGTPases (*rab-1, rab-5, rab-6.1, rab-10,* and *rab-11.1*), and their downstream factors promote outgrowth. Genes that are necessary for promoting anchor cell invasion (*fos-1, cdh-3, him-4, mig-10, zmp-1*, and *egl-43*) also must remain transcriptionally active for proper utse development. This work also presents a role for the novel gene RASEF ortholog *rsef-1,* which mediates signals from the uterine toroids to the utse.

Chapter 4 shows how the utse can be used as a model for studying genes that are involved in metastatic cancer (Ghosh et al., in prep). Meprin metalloproteases are a class of zinc metalloproteases upregulated in breast, pancreatic, and colorectal cancers (Matters and Bond, 1999; Bond et al., 2005; Dietrich et al., 1996; Minder et al., 2012) and are thought to promote invasive activity by degrading components of the extracellular matrix (Köhler et al., 2000; Kruse et al., 2004). The two human meprin metalloproteases, MEP1A and MEP1B, contain an astacin domain which is a HExxHxxG/NxxH/D zinc binding sequence (Rawlings and Barrett. 1995; Sterchi et al., 2008). *C. elegans* contains 40 astacin genes (Park et al., 2010), termed *nas* genes (nematode astacin), and three *nas* genes, *nas-21, nas-22,* and *nas-26*, are involved in utse development (Ghosh et al., in prep). RNAi knockdown of these genes results in utse outgrowth defects, and these three genes are either expressed in the utse or essential surrounding tissues (uterine toroids and sex muscles). Like meprins, *nas-21* and *nas-26* affect expression of components of the extracellular matrix. *nas-21* affects levels of laminin (*lam-1)* and *nas-26* affects levels of collagen IV (*emb-9*). *nas-21, nas-22,* and *nas-26* also affect levels of sydecan (*sdn-1),* a type I transmembrane heparan sulfate proteoglycan in the extracellular matrix (Kinnunen et al., 2014) that has not been previously associated to be a target of meprins. Overexpression of *nas-21* results in an expansion of the utse along the dorsal-ventral axis, and using this phenotype I was able to identify protease inhibitors and upstream activators that are acting on *nas-21*. Our network includes protease inhibitors that have been previously characterized to be acting upstream of meprins (cystatin, *cpi-1;* Hedrich et al., 2010; Jefferson et al., 2012; Hashmi et al., 2006), as well as protease inhibitors that have previously not been characterized to act with meprins (*F35B12.4, mec-1*). Therefore, in this work I present the utse as a model that can be used to study meprin activity *in vivo*, since I have recapitulated known interactions between meprins and its regulators as well as identified new players in the network.

Chapter 5 characterizes a candidate RNAi screen performed against genes that were thought to be affecting utse development (Ghosh and Sternberg, in prep 2). In order to identify the genetic inputs necessary for utse development, I created a list of 116 genes, 54 of which were shown to have significant utse defects upon RNAi knockdown. I have organized these genes into different subcategories, highlighting the diverse biological processes that are required for proper utse development. Categories included genes that had been previously characterized to affect neuronal guidance, cell adhesion, and nuclear migration, as well as genes that encoded structural components and transcription factors. This work indicates the breadth of information that remains to be investigated in utse development, and is meant to be a resource for those that plan on studying this cell in the future.

These findings present the utse as a powerful new model system for studying cell behavior. Not only is the utse an exciting new developmental system, but it also effectively serves as an *in vivo* model studying mechanisms involved in metastatic cancer. My work has identified the spatial cues necessary for utse development, and the molecular interactions necessary for mediating these spatial cues, and used the utse to create an interaction network used by genes that promote invasiveness of metastatic cancers. Much is left to be learned from the utse, and I hope that my work is the first of many studies that present this cell an incredible model for understanding cell biology.

References

Bond, J.S., Matters, G.L., Banerjee, S., Dusheck, R.E. 2005. Meprin metalloprotease expression and regulation in kidney, intestine, urinary tract infections and cancer. FEBS Lett.; **579**(15):3317-22.

Brenner S. 1974. The genetics of Caenorhabditis elegans. Genetics; **77**(1):71-94.

Byerly, L., Russell, R. L., & Cassada, R. C. 1976. The life cycle of the nematode Caenorhabditis elegans. I. Wild-type growth and reproduction. Dev Biol, **51**, 23-33.

Dietrich, J.M., Jiang, W., Bond, J.S. 1996. A novel meprin beta' mRNA in mouse embryonal and human colon carcinoma cells. J Biol Chem; **271**(4):2271-8.

Ghosh, S. and Sternberg, P.W. 2014. Spatial and molecular cues for cell outgrowth during C. elegans uterine development. Dev Biol; **396**(1):121-35.

Ghosh and Sternberg. Non-neuronal cell outgrowth in C. elegans. in prep. 1

Ghosh, Nguyen and Sternberg. An ECM protease/inhibitor network regulates cell outgrowth. in prep.

Ghosh and Sternberg. A candidate RNAi screen for cell outgrowth defects in the C. elegans utse. in prep. 2

Hashmi, S., Zhang, J., Oksov, Y., Ji, Q., Lustigman, S. 2006. The Caenorhabditis elegans CPI-2a cystatin-like inhibitor has an essential regulatory role during oogenesis and fertilization. J Biol Chem; **281**(38):28415-29.

Hedrich, J., Lottaz, D., Meyer, K., Yiallouros, I., Jahnen-Dechent, W., Stöcker, W., Becker-Pauly, C. 2010. Fetuin-A and cystatin C are endogenous inhibitors of human meprin metalloproteases. Biochemistry; **49**(39):8599-607.

Jefferson, T., Auf dem Keller, U., Bellac, C., Metz, V.V., Broder, C., Hedrich, J., Ohler, A., Maier, W., Magdolen, V., Sterchi, E., Bond, J.S., Jayakumar, A., Traupe, H., Chalaris, A., Rose-John, S., Pietrzik, C.U., Postina, R., Overall, C.M., Becker-Pauly, C. 2013. The substrate degradome of meprin metalloproteases reveals an unexpected proteolytic link between meprin β and ADAM10. Cell Mol Life Sci.; **70**(2):309-33.

Kadam, S., Ghosh, S., Stathopoulos, A. 2012. Synchronous and symmetric migration of Drosophila caudal visceral mesoderm cells requires dual input by two FGF ligands. Development.;**139**(4):699-708.

Kinnunen, T.K. 2014. Combinatorial roles of heparan sulfate proteoglycans and heparan sulfates in Caenorhabditis elegans neural development. PLoS One.; **9**(7):e102919.

Köhler, D., Kruse, M., Stöcker, W., Sterchi, E.E. 2000. Heterologously overexpressed, affinity-purified human meprin alpha is functionally active and cleaves components of the basement membrane in vitro. FEBS Lett.; **465**(1):2-7.

Kruse, M.N., Becker, C., Lottaz, D., Köhler, D., Yiallouros, I., Krell, H.W., Sterchi, E.E., Stöcker, W. 2004. Human meprin alpha and beta homo-oligomers: cleavage of basement membrane proteins and sensitivity to metalloprotease inhibitors. Biochem J.; **378**(Pt 2):383-9.

Le Douarin, N.M., Brito, J.M., Creuzet, S. 2007. Role of the neural crest in face and brain development. Brain Res Rev,; **55**(2):237-47.

Matters, G.L. and Bond, J.S. 1999. Expression and regulation of the meprin beta gene in human cancer cells. Mol Carcinog.; **25**(3):169-78.

Minder, P., Bayha, E., Becker-Pauly, C., Sterchi, E.E. 2012. Meprinα transactivates the epidermal growth factor receptor (EGFR) via ligand shedding, thereby enhancing colorectal cancer cell proliferation and migration. J Biol Chem.; **287**(42):35201-11.

Newman, A.P., White, J.G., Sternberg, P.W. 1996. Morphogenesis of the C. elegans hermaphrodite uterus. Development.; **122**(11):3617-26.

Park, J.O., Pan, J., Möhrlen, F., Schupp, M.O., Johnsen, R., Baillie, D.L., Zapf, R., Moerman, D.G., Hutter, H. 2010. Characterization of the astacin family of metalloproteases in C. elegans. BMC Dev Biol.; **10**:14.

Sulston, J.E., Schierenberg, E., White, J.G., Thomson, J.N. 1983. The embryonic cell lineage of the nematode Caenorhabditis elegans. Dev Biol.; **100**(1):64-119.

van Zijl, F., Krupitza, G., Mikulits, W. 2011. Initial steps of metastasis: cell invasion and endothelial transmigration. Mutat Res.; **728**(1-2):23-34.

CHAPTER 2

Introduction Part 2: An overview of non-neuronal outgrowth in *C. elegans*

2.1 Abstract

Cell outgrowth is a hallmark of developing cells, as well as certain diseases (i.e., metastatic cancers). Understanding the mechanisms that control cell outgrowth not only adds to our knowledge of tissue and organ development, but also can shed light on the pathologies of diseases. *C. elegans* is highly useful for analysis of gene and protein function and has several cell types that undergo outgrowth during development. Here we discuss the outgrowth mechanisms used by eleven different *C. elegans* cell types. We will focus specifically on the how the cell grows outward and what types of interactions the growing cell makes with its environment. We will also identify gene families that are involved in the outgrowth of each specific cell type. Our meta analysis identified genes that are involved in multiple cell outgrowth systems, defining potiential *C. elegans* master regulators of cell outgrowth.

2.2 Introduction

Cell outgrowth is the process in which cells expand outward to change their shape. This is a common behavior that occurs during morphogenesis, during which cells change their shape with the eventual goal of forming organs. Examples of normal outgrowth during morphogenesis include cell outgrowth in the mouse facial primodia (Yamaguchi et al., 1999), outgrowth of regenerating fins in zebrafish (Kujawski 2014), and dramatic cell shape changes in *Drosophila* cardioblast cells (Macabenta et al., 2013). Cell shape change is also characteristic of certain diseases such as endometriosis, which involves the outgrowth of endometrium cells outside the uterus (Baranov et al., 2015), and metastatic cancer, which is the spread of tumors from one tissue to another (Nguyen et al., 2009). Understanding the mechanisms that control cell outgrowth therefore not only sheds light on the genetic inputs that control development, but also provides information on the pathologies of certain diseases.

C. elegans is a small free-living nematode whose cell lineage is stereotypic and well characterized (Brenner 1974; Byerly et al., 1976; Sulston et al., 1983). This model organism is also transparent, which makes it a powerful tool to study cell morphology. Though much of *C. elegans* development is composed of cells simply dividing and taking on different fates, certain cell types undergo cell outgrowth during morphogenesis. In this review, we wish to describe the mechanisms these cell types use to undergo outgrowth. We are specifically focusing on non-neuronal cells because there

are numerous neuronal cells that undergo outgrowth, and addressing each neuronal cell type would result in content that would encompass its own review. Also, *C. elegans* neuronal outgrowth has already been well characterized (Hobert 2005; Forrester and Garriga 1997; Mehta et al., 2004; Wightman et al., 1996; Garriga et al., 1993; Stringham et al., 2002; Ackley 2013).

We will describe cell outgrowth behavior of the uterine seam cell (utse), the anchor cell (AC), excretory cell, sex muscles, male tail, four types of embryonic outgrowth (dorsal intercalation, ventral enclosure, early elongation and late elongation), muscle arms, and head mesodermal cells.

2.3 utse

The *C. elegans* uterine seam cell (utse) attaches the uterus to the lateral epithelial seam cells of the body wall (Newman et al., 1996).

The utse lineage begins with the Z1 and Z4 cells that generate the somatic gonad in the beginning of the L1 stage (Hubbard and Greenstein, 2000; Kimble and Hirsh, 1979). These cells divide anteriorly (a) and posteriorly (p) to give rise to Z1.ppa , Z4.aap, and Z4.aaa, all of which eventually become parts of the ventral uterus or VU cells. Either Z1.ppp or Z1.aaa will become the anchor cell (AC), with the other becoming a VU cell. Both Z1.ppp and Z4.aaa express low levels of the Notch family receptor LIN-12 and the Delta family ligand LAG-2; however, once Z1.ppp and Z4.aaa decide their fates, the VU cell expresses higher levels of LIN-12 and the AC expresses higher levels of LAG-2 (Riddle et al., 1997; Greenwald et al., 1983; Lambie and Kimble, 1991).

At late L3 stage, six of the VU granddaughter cells are induced via LAG-2-LIN-12 Notch-Delta signaling from the AC to become π cells (Newman et al., 1995). After these six π cells are induced, they divide to make 12 π-progeny cells (Newman et al., 1996). Four of these 12 π-progeny cells become uv1 cells via EGF signaling (Chang et al., 1999) from the vulval VulF cells. The eight π-progeny cells that do not become uv1 will form the utse nuclei as υ (upsilon) cells (Ghosh and Sternberg, 2014). During early L4, the AC has fuses with the υ cells (Newman et al., 1996; Ghosh and Sternberg, 2014). This fusion, enabled by the fusogen AFF-1 (Sapir et al., 2007), is essential for utse development because the expression of genes found within the anchor cell nucleus is necessary for utse outgrowth (Ghosh and Sternberg, 2014). Over the next eight hours after fusion, the utse cell body grows bi-directionally along the anterior-posterior axis, and the utse nuclei segregate into two groups, migrate along the anterior-posterior axis, and settle at the anterior/posterior edges of the utse

cell body (Figure 1; Newman et al., 1996; Ghosh and Sternberg, 2014). The utse cell body extends ahead of its nuclei during development, indicating that separate mechanisms control the movement of the cell body and the nuclei (Ghosh and Sternberg 2014).

During development, the utse needs to mediate interactions between several cells within the *C. elegans* uterus. Four uterine toroids line the lumen of the uterus. They are denoted uterine toroid 1 to uterine toroid 4, with numbers increasing for cells that are more distal to the vulva (Newman et al., 1996). The presence of uterine toroid 1 and uterine toroid 2 is essential for proper utse outgrowth because ablation of these cells leads to defects in utse outgrowth (Ghosh and Sternberg, 2014). The sex muscles, which lie proximal and distal to the utse or either side of the body wall, are also necessary for utse development, because both ablation and knockdown of genes expressed in the sex muscles lead to defects in utse development.

Several gene families are involved in utse development. These include the *unc-73/*TRIO and its interacting factors (*rho-1, let-502, unc-13,* and *unc-64*), Rab-like and RabGTPases (*rsef-1, rab-1, rab-11.1, rab-6.1, rab-10,* and *rab-5*), which are expressed within the uterine toroids, *unc-53*/NAV, which is found within the sex muscles, and the FGF receptor *egl-15,* as well as genes involved in anchor cell invasion (*aff-1, fos-1, cdh-3, egl-43, him-4, zmp-1,* and *mig-10*) that act on the utse after fusion with the anchor cell nucleus.

We have also performed a screen against candidate genes involved in cell behavior to identify genes that affect utse nuclear migration and cell outgrowth (Ghosh and Sternberg, in prep). From this screen, we identified 54 genes that affect utse development: the importins *ima-1, ima-2, ima-3, imb-2, imb-3,* the SUN/KASH proteins *nud-2, anc-1, unc-83,* and *unc-84*, the nuclear lamin *lmn-1,* the Arp2/3 complex components *arx-2* and *arx-3,* the WAVE/SCAR complex members *gex-1/wve-1, gex-2*, and *toca-1,* the globin *glb-12*, the integrins *ina-1* and *pat-3*, vinculin *deb-1,* paxilin *pxl-1,* beta-G spectrin *unc-70*, fibulin *fbl-1*, Wnt *cwn-1*, the Notch receptor *glp-1,* the LIM domain transcription factors *egl-13, lin-11* and *ttx-3,* the LIM PINCH domain containing genes *unc-97* and *lim-9*, orthologs of human GIPC PDZ domain containing 1 protein *C35D10.2/gipc-1* and *f44d12.4/gipc-2,* the homolog of isoform 2 of Suppressor of tumorigenicity 7 *F11A10.5*, the forkhead transcription factors *lin-31* and *daf-16,* the Deformed and Sex combs homeodomain protein *lin-39*, the ZFH class homeodomain protein *zag-1*, the inositol 1,4,5-trisphosphate receptor (IP(3)R) *itr-1*, the NCK-interacting kinase *mig-15,* the ortholog of the yeast SCC-2 protein *pqn-85*,

the ortholog of human FERM domain containing 6 protein *frm-2*, the *Pax-6* homeodomain protein *vab-3,* the homeobox protein *zc123.3/zfh-2*, the homolog of AF10 *zfp-1,* the component of the exocyst complex *sec-15,* the RhoGAP *rrc-1,* the synaptotagmin *dh11.5,* the serine/threonine kinase *sax-1,* the ortholog of human bridging integrator 2 *amph-1,* the RAB-11 homolog *f55c12.1,* the IgCAM *ncam-1,* the L1 CAM *sax-7,* the microtubule binding protein CRMP *unc-33,* and the GPCR *srsx-18,* and RanGAP *ran-2* and its guanine nucleotide exchange factor RCC-1 *ran-3.*

2.4 Anchor cell

The anchor cell (AC) undergoes cell shape change when it invades its underlying basement membrane to interact with vulval epithelial cells and establish vulval cell fates (Sherwood and Sternberg, 2003).

As mentioned earlier, either Z1.ppp or Z1.aaa will become the AC (with the other becoming a VU cell), and once fate has been established by lateral signaling (Sedoux and Greenwald, 1989), the VU cell expresses higher levels of LIN-12 and the AC expresses higher levels of LAG-2 (Greenwald et al., 1983; Lambie and Kimble, 1991; Sedoux and Greenwald, 1989). During the L3 larval stage, the AC extends a process ventrally to mediate a connection with the descendants of the 1° vulval precursor cell P6.p (Figure 2; Sherwood and Sternberg, 2003). Once the P6.p divides so that it reaches a two-cell stage (mid L3) (Figure 2B), the basement membrane underneath the AC is interrupted, and the basolateral portion of the anchor cell crosses the membrane (Figure 2C). At the P6.p four cell stage (mid to late L3), the basement membrane is interrupted, and the AC extends a fine cellular process that reaches ventrally between the P6.pap and P6.ppa cells (Figure 2D). This invasive structure remains in place as the P6.p granddaughter cells continue to divide and the vulva invaginates. By L3 lethargus/early L4, the anchor cell positions itself in the dorsal apex of the vulva and has completed the invasion process. The AC then induces surrounding ventral uterine cells to take on π cell fate through LAG-2-LIN-12 Notch-Delta, and at mid L4, the AC fuses with the υ (upsilon) cells to create the utse cell body (Newman et al., 1995; Ghosh and Sternberg, 2014; Sapir et al., 2007).

The presence of the 1° vulval cells are required for the AC to initiate invasion (Sherwood and Sternberg, 2003). The 1° vulval cells are specified via LIN-3 signaling from the AC in late L2 early L3 larval stage (Kimble, 1981, Hill and Sternberg, 1992). Without *lin-3,* all vulval precursor cells take on 3° fate and become external epithelial cells (Sulston and White, 1980; Kimble, 1981). *lin-3*

mutants, which have 3° vulval cells instead of 1° vulval cells, do not exhibit AC invasion (Sherwood and Sternberg, 2003). Also, when P8.p is ectopically induced by ablating all other vulval precursor cells in L2, the AC directs its projections to the distal P8.p cells, indicating that a long-range cue from the 1° vulval cells induces invasion.

Several gene families are involved in inducing AC invasion and removing the basement membrane underlying the AC. Our lab has identified a pathway involving the *c-fos* transcription factor ortholog *fos-1* and its downstream effectors zinc metalloprotease *zmp-1,* the protocadherin *cdh-3,* the zinc finger protein *egl-43,* the hemicentin extracellular matrix protein gene *him-4,* and lamillopodin/*mig-10* (Sherwood et al., 2005; Hwang et al. 2007; Wang et al., 2014; Rimann and Hajnal, 2007). Other genetic interactions/gene families that promote invasion include that between E3 ubiquitin ligase substrate-recognition subunit *zif-1*and *cdc-42* (Armenti et al., 2014; Matus et al., 2010), the netrins with the netrin ligand *unc-6* being expressed in the basement membrane and the netrin receptor *unc-40* in the AC plasma membrane (Ziel et al., 2009; Morrissey et al., 2013; Wang et al., 2014), the α/β integrin complex *ina-1/pat-3,* which targets the netrin receptor *unc-40* to the plasma membrane of the AC (Ihara et al., 2011; Hagedorn et al., 2009), the transcription factor *hlh-2,* which regulates levels of the cdh-3 and hemicentin *him-4* in a separate pathway from *fos-1* (Schindler and Sherwood, 2011), the protein kinase *vrk-1* (Klerkx et al., 2009), and the *Mid1* homolog *madd-2,* which prevents ectopic invasive structures from emanating from the AC (Morf et al., 2013).

2.5 Excretory cell

The excretory cell is the largest cell in *C. elegans* (Buechner, 2002). The excretory cell originates from the AB cell within the embryo, specifically AB plpappaap (Sulston, 1983). During the threefold embryonic stage, this cell grows outward dorsolaterally toward the lateral midline (Figure 3A-C; Buechner, 2002; McShea et al., 2013). The proximal and distal edges of the cell, known as canals, initially grow outward dorsally (Figure 3C), then branch out and extend anteriorly and posteriorly (Figure 3D). By the time the worm hatches, the posterior canal has extended outward, measuring half the length of the organism. Extension is completed within the L1 larval stage 12-14 hours after hatch, when the canal spans the entire worm body, from the anterior tip to the tip of the tail (Figure 3E; Buechner and Hedgecock, 1992). The canal connects to the hypodermis through gap junctions, and once canal extension is completed, the canal grows as the body of the worm

grows, growing from approximately 300 mm at L1 to its adult size of 1 mm (McShea et al., 2013). As the worm ages, the canal tip can detach from the hypodermis, causing the canal to shorten. Since this review focuses on cell outgrowth, we will not examine the luminal formation of the excretory cell.

The tail hypodermis acts in mediating excretory cell outgrowth (Sawa et al., 1996; Buechner 2002). Mutations in genes that control tail hypodermis integrity (*lin-17* and *bli-6)* result in exaggerated posterior canal growth (Park and Horvitz, 1996).

Several basement membrane proteins are necessary for proper excretory canal outgrowth. These include both α integrins *ina-1* and *pat-2* and their corresponding β integrin *pat-3* (Baum and Garriga, 1997; Gettner et al., 1995), the perlecan *unc-52* (Rogalski et al., 2001), and the laminins *epi-1* and *lam-1* (Zhu et al., 1999; Hutter et al., 2000). In *pat-3* mutants, canals grow approximately 30% slower than in wild type animals during the L1 and do not reach the ends of the animal. Canals continue to grow with the rest of the animal throughout later larval stages, but do not extend further along the hypodermis, indicating that separate mechanisms control canal outgrowth and passive canal growth as the worm grows. The seam cells may also affect excretory cell outgrowth, since knockdown of *cdh-3*, which is expressed in the seam, generates outgrowth defects (Pettitt et al., 1996).

Other genes that are involved in promoting excretory cell outgrowth are the Nck-interacting kinase *mig-15* (Poinat et al., 2002), NAV/*unc-53* (Stringham et al., 2002), which acts with the ADAM *unc-71* (Marcus-Gueret et al., 2012), TRIO/*unc-73* (Steven et al., 1998), lamellipodin *mig-10* (Manser et al., 1997), the *C. elegans* Enabled/VASP homolog *unc-34* (Forrester and Garriga, 1997), and three kinesins *unc-116, unc-104,* and *vab-8* (Patel et al., 1993; Otsuka et al., 1991; Wightman et al., 1996) The kinesin motor protein *vab-8* acts with *sax-3*/ROBO, *slt-1*/Slit, and *eva*-1 in the excretory cell (Marcus-Gueret et al., 2012). *vab-8* also acts on *unc-73b* in a parallel pathway to affect excretory cell outgrowth. Another gene that acts in multiple pathways in excretory cell outgrowth is *abi-1*. *abi-1* acts with both *mig-10* and *unc-53* to promote outgrowth of the excretory cell by promoting branched actin accumulation through activation of the Arp2/3 complex (McShea et al., 2013; Schmidt et al., 2009).

Netrins (the ligand *unc-6* and the receptor *unc-5*) act as dorsal guidance cues for the canals (Hedgecock et al., 1990; Merz et al., 2001; Wang and Wadsworth, 2002). Many of the genes in the

above paragraph, as well as *lin-17* and *bli-6,* also affect guidance of neurons, indicating that they could be diffusible cues from the basal surface that affect outgrowth of multiple tissues (Buechner, 2002).

2.6 Vulval muscles

During egg-laying, vulval muscles contract to open the vulva and allow eggs to be laid. Vulval muscles orginate from the M cell in L1 (Sulston and Horvitz, 1977). The M cell divides to create precursors for body wall muscles, coelomocytes, and two sex myoblasts. These sex myoblasts migrate anteriorly until they reach the position where the vulva will form. The sex myoblasts then divide in L3 larval stage to produce 16 muscle cells. The 16 cells are arranged in four sectors in the uterine/vulval area. The two sets of 4 cells that lie proximal to the vulva become vulval muscles (vm1 and vm2), and the two sets of 4 cells distal to the vulva become uterine muscles. Musculature takes its final position in L4 and twitches to allow egg laying.

In L3, the vulval myoblasts (two sets of 4 cells that will become vm1 and vm2) extend processes ventrally to attach the vulva to the hypodermis and longitudinally towards the seam cells (Figure 4; Sulston and Horvitz, 1977; Stringham et al., 2002). The NAV/*unc-53* is necessary for generating these longitudinal processes (Stringham et al., 2002). In *unc-53* mutants these processes fail to form, and muscles attach to myofilaments and take a rounded shape.

2.7 Male tail

The male *C. elegans* is distinguished from the hermaphrodite in a variety of ways, specifically in the development of its somatic gonad. The male somatic gonad can be found in the male tail, and consists of the fan, the rays, the spicules, the proctodeum, the gubernaculum, and the hook (Emmons, 2005). Cell shape change and outgrowth occur during fan and ray formation, and therefore we will be characterizing the development and molecular inputs for these two processes.

The male rays and fan originate from the lateral epidermal seam cells (Emmons and Sternberg, 1997). The three most posterior seam cells, V5, V5 and T, give rise to the ray precursor cells, or Rn.p cells (Sulston and White, 1980). These Rn.p cells eventually form nine pairs of sensory rays. These rays each consist of a hypodermal cell and two neurons, which allow the rays to function as peripheral sensory organs (Baird et al., 1991). During late L4, the tail tip becomes rounded and

retracts anteriorly by losing adhesion with the cuticle, leaving behind a clear fluid in the extracellular space (Figure 5B; Sulston and White, 1980; Nguyen et al., 1999). The hypodermal cells hyp8-11 fuse together and withdraw from the L4 cuticle, along with other anterior cells (Emmons, 2005). At the start of this process, the ray cells form papillae on the edge of the tail cell body (Figure 5C and Figure 5D) , and these papillae eventually become the distal edges of the rays, which attach to the fan cuticle through an adherens junction (Figure 5E; Baird et al., 1991; Chow et al., 1995). As the fan extends from the cell body, it pulls the papillae with it, allowing the rays to extend outward.

Several genetic inputs are required for the formation of the rays. *mab-21* is necessary for maintaining cell shape in ray 6. In wild-type males, ray 6 is thicker and more conical than other rays, whereas in *mab-21* mutants, ray 6 takes on the morphology of other rays. *sma-2* and *sma-3* are necessary for preventing rays 5 and 7 from taking on ray 6 morphology. In *sma-2* and *sma-3* mutants, ray 5 and ray 7 take on the thicker ray 6 shape. Also, *daf-4*, *mab-20, mab-21, mab-26, sma-2, sma-3,* and *sma-4* mutants can have rays that are fused together, caused by displacement of papillae prior to retraction (Emmons and Sternberg, 1997; Baird et al., 1991; Chow and Emmons, 1994; Savage et al., 1996; Chow et al., 1995). *mab-21* mutants also exhibit an ectopic tenth papillae between rays 5 and 7. Also the *ram* genes (ray morphology abnormal) *ram-1, ram-2,* and *ram-4* (Emmons, 2005; Baird and Emmons, 1990) affect collagen within the male tail, and mutants of these genes have rays with an expanded, lumpy shape. Other genes that affect ray shape include the thioredoxin-like protein *dpy-11*, and the prolyl hydroxylase *dpy-18*. (Hill et al., 2000; Ko and Chow, 2002; Winter and Page, 2000). The transmembrane protein *mab-7* and ray morphology abnormal gene *ram-5* also mediate communication between the ray cells and the hypodermis (Emmons, 2005; Yu et al., 2005).

Molecular regulatory inputs have also been characterized for male tail retraction. The C2H2 Zn-finger presumptive transcription factor *tlp-1* promotes hyp8-11 anterior retraction (Zhao et al., 2002). The *doublesex*-related DM gene *dmd-3* is also necessary to trigger retraction during L4 (Mason et al., 2008). Oftentimes if defects in retraction are present, ray formation is also affected. The RBCC (Ring finger-B box-Coiled coil) protein *lin-41* functions with *let-7* to regulate male tail retraction (Del Rio-Albrechtsen et al., 2006). Reduced function *lin-41* mutants begin retraction in L3, and either form disrupted fans or rays or no fans or rays at all. The hox gene *egl-5* mediates the retraction of cells other than hyp8-11, and in *egl-5* mutants, rays and the fan do not form (Chisholm,

1991). The notch homolog *let-765/nsh-1* also is necessary for retraction and ray formation; *let-765* reduced function mutants do not form rays or fans (Simms and Baillie, 2010). *rme-8*, which is necessary for receptor mediated endocytosis, also plays a role in both retraction and ray and fan morphogenesis; RNAi against this gene causes defects in the disruption of these behaviors (Nelson et al., 2011). Nelson et al. 2011 also identified 27 other genes that are involved in mail tail retraction: the ABC-transporter

abcx-1 and *wht-5,* the ADP-Ribosylation Factor *arl-1*, the zinc finger and SET domain-containing protein *blmp-1,* the serine/threonine kinases *bub-1,* the RhoGTPase *cdc-42,* DNA-replication licensing factor *cdt-1,* TGF-β Receptor *daf-4,* the GATA transcription factor *egl-18,* the innexins *inx-12* and *inx-13,* the chromosome condensation complex and condensin *mix-1* and *smc-4,* the nuclear hormone receptor *nhr-25,* the non-muscle myosin *nmy-2,* Abd-B Homeodomain transcription factor *nob-1,* the nucleoporins *npp-3* and *npp-6,* Abd-B Homeodomain transcription factor *php-3,* the polo-like serine/threonine kinase *plk-1,* the eukaryotic-type DNA primase *pri-2,* the Tau-like microtubule binding protein *ptl-1,* the RCC1 domain containing protein *ran-3,* the calcipressin and negative regulator of calcineurin *rcn-1,* the DNA-binding replication protein *rpa-1,* the SMAD *sma-3,* and the nuclear export factor *xpo-2*.

2.8 Embryonic epidermal cell outgrowth/shape change

The epidermal cells of *C. elegans* are generated during the ninth round of embryonic cell divisions, at which point the embryo is made up of around 365 cells (Chisholm and Hardin, 2005; Gendreau et al., 1994; Page et al., 1997). Epidermal cells originate from four cell types, ABarp, ABpla, ABpra, and C. These cells undergo several rounds of division, with the majority of epidermal cells localizing to the dorsal region of the embryo. Once terminal divisions are complete, three groups of major epidermal cells are generated. These groups are the dorsal epidermal cells, seam epidermal cells and ventral epidermal cells. The dorsal and ventral epidermal cells take on sheet-like shape and then undergo morphogenetic movements to encase the remaining cells of the embryo. Before the embryo can undergo elongation, two morphogenetic movements must occur: dorsal intercalation and ventral enclosure (Williams-Masson, 1998). Both dorsal intercalation and ventral enclosure require changes in cell shape and cell outgrowth, which is why we have characterized them in this review. After dorsal intercalation and ventral enclosure are complete, the embryo

undergoes an elongation, which also involves cell shape change. Different mechanisms are used in different phases of elongation, known as early and late elongation.

2.8.1 Dorsal intercalation

Dorsal intercalation is the process by which dorsal epidermal cells form a single row across the dorsal midline (Sulston et al., 1983; Williams-Masson, 1998; Priess and Hirsh, 1986). During this process, dorsal epidermal cells arrange themselves into six rows and change their shape from a more rounded shape to a wedged shape (Figure 6A; Williams-Masson, 1998). These cells then begin intercalating, with the anterior cells interdigitating first and then continuing down the anterior-posterior axis (Figure 6A-B). The interdigitating cells intercalate by forming basolateral protrusions (Figure 6B), which touch neighboring cells and help the cells move towards one another (Chisholm and Hardin, 2005; Williams-Mason, 1998; Hardin and Walston, 2004; Heid et al., 2001).

Molecular inputs controlling the cell shape change event in which rounded cells take on wedge shapes have been characterized. The T box transcription factors *tbx-8* and *tbx-9* are inputs for this process, for *tbx-8* and *tbx-9*(RNAi) treated animals do not form this wedge shape and intercalation arrests prematurely (Pocock et al., 2004). Another gene that affects cell shape of dorsal epidermal cells is Robo/*sax-3,* which functions cell autonomously within the dorsal epidermal cells (Ghenea et al., 2005).

Though many sets of genes have been found to be involved in dorsal intercalation, including those characterized above, as well as *apr-1, wve-1, gex-2, gex-3 arp-2, ced-10, mig-5, frk-1, rib-1* and *ten-1* (Hoier et al., 2000; Soto et al., 2002; Patel et al., 2008; Giuliani et al., 2009; Sawa et al., 2003; Walston et al., 2006; Putzke et al., 2005; Kitagawa et al., 2007; Mörck et al., 2010), none have been found to promote protrusion formation. Dorsal intercalation and protrusion formation may not be related, for in *die-1* mutants, protrusions form normally, but intercalation does not occur (Heid et al., 2001). Therefore, it may be useful to further analyze genes that have been implicated in dorsal intercalation for roles in dorsal protrusion formation.

2.8.2 Ventral enclosure

Ventral enclosure involves the ventral epidermal cells moving towards the ventral midline to encase underlying cells in an epithelial sheath (Chisholm and Hardin, 2005). Specifically, the epidermal

sheet migrates laterally and ventrally to encase the embryo (Figure 7A-B; Williams-Masson et al., 1997). This process commences when two anterior leading cells, known as ventral marginal cells (Figure 7A), extend large protrusions towards the ventral midline and then form epithelial junctions (Chisholm and Hardin, 2005; Williams-Masson et al., 1997). Once these cells reach the midline, the remaining cells, known as ventral pocket cells (Figure 7A), also move towards the midline via extending protrusions, eventually encasing the embryo. Presence of ventral marginal cells is necessary to mediate the rest of ventral enclosure, for if the marginal cells are ablated, ventral enclosure cannot occur (Williams-Masson et al., 1997). Marginal and pocket cell protrusions consist of actin filaments at the apical domain, which constrict as the ventral pocket closes.

The formation of these protrusions is modulated by several molecular cues. The WAVE complex and WASP and Ena/VASP activate the Arp2/3 complex, which enables actin polymerization at the leading edge of ventral marginal cells (Soto et al., 2002, Sawa et al., 2003; Withee et al., 2004). Knocking down components of each of these complexes, which include *unc-34*, *arx-1*, *arx-2, arx-3*, *arx-4, arx-5, arx-6, arx-7*, *gex-2, gex-3,* and *wsp-1,* causes defects in ventral enclosure. The 1,4,5-inositol trisphosphate receptor (IP_3) *itr-1* is also necessary for generating filopodia and organizing actin at the leading edge of marginal cells (Thomas-Virnig et al., 2004). Cadherin, α-catenin and β-catenin, encoded by *hmr-1, hmp-1* and *hmp-2,* respectively, and also known as the CCC complex, are necessary for enabling protrusions to make adhesive contacts with the ventral midline (Costa et al., 1998; Raich et al., 1999; Pásti and Labouesse, 2014). The receptor tyrosine kinase *vab-1* and its ligands *vab-2, efn-2,* and *efn-3* properly direct protrusions in both marginal and pocket cells (George et al. 1998; Wang et al., 1999; Chin-Sang et al., 1999; Ikegami et al., 2012). The semaphorin *mab-20* is necessary for preventing the formation of ectopic protrusions in the ventral pocket cells (Roy et al., 2000; Chin-Sang and Chisholm, 2000). The Plexin *plx-2* binds with *mab-20*, but acts redundantly with *mab-20* and *vab-1* to generate protrusions in the pocket cells (Ikegami et al., 2012; Nakao et al., 2007). *phy-1*, which encodes the catalytic domain of collagen prolyl 4-hydroxylase, acts with tenurin, *ten-1*, to prevent ectopic protrusion formation; in *ten-1 phy-1* double mutant animals, ventral protrusions were present after ventral enclosure had completed (Topf and Chiquet-Ehrismann, 2011). Dishevelled *dsh-2* is necessary for mediating the length of the protrusions formed by marginal cells, for *dsh-2* mutants have marginal cells with longer protrusions than normal (King et al., 2009). *dsh-2* mutant marginal cell protrusive activity also lags behind pocket cell protrusion formation, which prevents ventral enclosure from occurring.

Other genes that affect ventral enclosure but not protrustion formation have been characterized. These genes have been found to affect migration of epidermal cells and include the APC related gene *apr-1,* as well as *rib-1* and *rib-2*, which are involved in heparan sulfate biosynthesis (Hoier et al., 2000; Kitagawa et al. 2007)

The kalikrein *kal-1* acts with *efn-4* to mediate ventral epidermal cell migration (Hudson et al., 2006). *wip-1*, which activates WASP, also affects ventral epidermal cell migration, but since *wsp-1* affects protrusion formation, *wip-1* may also act in the protrustion formation pathway (Sawa and Takenawa, 2006). The Fer-related kinase-1 *frk-1* also affects enclosure (Putzke et al., 2005). Actin distribution is normal in mutants of the PAF1C complex member *ctr-9*; however, defects in closure are present (Kubota et al., 2014). The anilin *ani-1* is necessary for aligning cells as they come together during enclosure (Fotopoulos et al., 2012). The GTPase Arl2 homolog *evl-20* is necessary for mediating integrity of the hypodermis during ventral enclosure (Antoshechkin and Han, 2002).

2.8.3 Early embryonic elongation

Once ventral enclosure is complete, the hypodermis closes and then elongates through constriction of circumferentially aligned actin microfilaments and microtubules (Figure 8; Priess and Hirsh, 1986). This process changes the embryo from an ellipsoidal shape to an elongated shape (Chisholm and Hardin, 2005). Hypodermal epidermal cells elongate along the anterior posterior axis while constricting along the apical axis (Priess and Hirsh, 1986; Chisholm and Hardin, 2005). Prior to elongation, actin microfilaments and microtubules arrange themselves circumferentially on the apical surfaces of the dorsal and ventral hypodermal cells (Preiess and Hirsh, 1986; Costa et al. 1997). As these bundles contract, the internal cells are squeezed so that these cells can elongate along the anterior-posterior axis. The lateral epidermal cells strongly contract and act as a "motor" for elongation, while the dorsal and ventral epidermal cells act more passively and hold tension in the embryo (Wissman et al., 1999).

Several molecular inputs involved in early embryonic elongation have been characterized. The CCC complex, consisting of cadherin (*hmr-1)*, α-catenin (*hmp-1*) and β-catenin (*hmp-2)* promotes elongation; in fact, *hmp-1* and *hmp-2* are so named because of the "humpback" phenotype present in *hmp-1* mutants, which have defective elongation (Costa et al., 1998; Raich et al., 1999; Pásti and Labouesse, 2014). *hmr-1*, *hmp-1,* and *hmp-2* are necessary for mediating connections between the circumferentially arranged actin filaments in the dorsal hypodermis to adherens junctions (Costa et

al., 1998). The claudin-like protein *vab-9* is necessary for organization of circumferential actin bundles and requires *hmr-1* for its proper localization and *hmp-1* and *hmp-2* to maintain its distribution (Simske et al., 2003). Zonula occluden *zoo-1* acts with *hmr-1* and *vab-9* to mediate connections between actin and adherens juctions (Lockwood et al., 2008). Tropomodulin *unc-94* acts with *hmp-1* to weaken connections between actin filaments and adherens junctions (Cox-Paulson et al., 2012), as does the PDZ-domain containing, tight junction-associated protein *magi-1* (Lynch et al., 2012). The catenin homolog *jac-1* works with *hmp-1* to promote circumferential actin filament bundle formation (Pettitt et al., 2003). *ajm-1* localizes to a portion of the epidermis that is apical to the basal domain of the CCC complex (Köppen et al., 2001). *ajm-1* acts with *let-413* and *dlg-1* to maintain junctional integrity in epidermal cells.

The *let-502* mechanism controlling embryonic elongation is very well characterized. The rho binding kinase *let-502* is necessary for the elongation process and acts antagonistically with the myosin phosphatase *mel-11* in embryonic elongation (Piekny et al., 2000; Wissmann et al., 1999). Loss of function of *let-502* reduces elongation, whereas loss of function of *mel-11* causes excessive constriction of actin, causing hyper contraction; null mutations of either gene suppress the activity of the other gene. The serine/threonine-protein kinase *mrck-1* acts as an inhibitor of *mel-11*, which inhibits *mcl-4* (Gally et al., 2009). The PI3 kinase *age-1,* the insulin receptor *daf-2,* and Rho/Rac *mig-2* function in regulating *let-502/mel-11*. *unc-73* (Trio) acts parallel to *let-502* by acting upstream of *ced-10,* which acts on *pak-1* (described below) (Piekny et al., 2000; Martin et al*.,* 2014). The actin microfilament-associated RhoGAP *rga-2* acts as an inhibitor of the RhoGTPase *rho-1,* which in turns activates *let-502* (Diogon et al., 2007). The p21-activated kinase homolog *pak-1* phosphorylates the myosin light chain *mlc-4* (Gally et al., 2009)*,* which is a target of *let-502* (Shelton et al., 1999) and regulates two non-muscle myosin heavy chains *nmy-1* and *nmy-2* (Piekny et al., 2003). The CDC42/RAC-specific Guanine-nucleotide Exchange Factor (GEF) *pix-1* acts in parallel with *fem-2* as an upstream activator of *pak-1* (Martin et al, 2014). The formin *fhod-1* is necessary for formation of actin bundles and acts with *let-502* and *mel-11* to regulate *mlc-4* and *nmy-1* and *nmy-2* (Vanneste 2013).

Aside from the CCC and *let-502* pathway, many other genes also affect early elongation. The α-spectrin *spc-1* is necessary for actin organization during elongation (Norman and Moerman, 2002). The β spectrin *sma-1* mediates the interaction between actin and the apical membrane because in *sma-1* mutants, actin disassociates from the hypodermal membrane (Praitis et al., 2005). Therefore,

these two spectrins act together to organize and stabilize the actin cytoskeleton during elongation. Semaphorin *mab-20* is also necessary for alignment of the circumferential actin bundles (Roy et al., 2000). The PAF1C complex member *ctr-9* is necessary for microtubule alignment during elongation (mutations in *ctr9* affect microtubule organization more severely than actin filaments) (Kubota et al., 2014). The hedgehog related gene *wrt-5* also affects elongation in the two-fold stage, though its affects on elongation (specifically regarding how it affects actin distribution) have not been characterized (Hao et al., 2006). The ARL2 GTPase *evl-20* is necessary for mediating microtubule activity during elongation, specifically regulating levels of tubulin necessary for elongation (Antoshechkin and Han, 2002). Mutants of the transcription factor *hlh-1* also arrest during two-fold stage when elongation is occurring, though its specific effect on elongation has not been characterized (Chen et al., 1994). Other genes thought to be involved in early elongation are the nuclear hormone receptor transcription factor *nhr-2* (Sluder et al., 1997), the Fer-related kinase-1 *frk-1* (Putzke et al., 2005), the anilin *ani-1* (Fotopoulos et al., 2012), and the ESCRT-III protein *vps-32* (Michelet et al., 2009).

2.8.4 Late embryonic elongation

Elongation continues after the two-fold stage, but uses a different set of mechanisms. During this elongation stage, body wall muscles mediate connections with the epidermis (Gotenstein et al., 2010). Muscles induce hemidesmosome-containing attachment structures known as fibrous organelles to the epidermal and cuticle, and then forces generated via the muscles induce elongation (Francis and Waterston, 1991; Hresko et al., 1994).

The exact mechanism by which these muscles promote cell elongation is unknown (Chisholm and Hardin. 2005); however, many molecular inputs for later stage elongation have been characterized. These include the peroxidasin *pxn*-2 (Gotenstein et al., 2010), components of fibrous organelles such as the muscle positioning gene *mup-4* (Gatewood et al., 1997; Hahn and Labouesse, 2001), the fragile muscle attachment gene *mua-3* (Plenefisch et al., 2000; Hahn and Labouesse, 2001), myotactin *let-805* (Hresko et al., 1999; Hahn and Labouesse, 2001), and the HECT domain E3 ubiquitin ligase *eel-1,* which acts through *let-805* to coordinate fibrous organelle maturation (Zahreddine et al., 2010), the intermediate filaments *ifb-1* and *ifa-3* (Woo et al., 2004), SUMO (*smo-1*), which are involved in regulating *ifb-1* (Kaminsky et al., 2009), the plakin *vab-10,* which is necessary for connecting the epidermis to the cuticle (Bosher et al., 2003), tenurin *ten-1* and

collagen prolyl 4-hydroxylase *phy-1,* which act together to regulate distribution of *emb-9* (collagen IV) (Topf and Chiquet-Ehrismann, 2011), the serine-threonine kinase *unc-82,* which is necessary for M line localization (Hoppe et al., 2010), the ankyrin repeat protein *vab-19* (Ding et al., 2003), which recruits the signaling adaptor *eps-8* to fibrous organelles (Ding et al., 2008), the heparan sulfate transporter *pst-1* (Bhattacharya et al., 2009), the RNA binding protein *mec-8,* which is involved in alternative splicing for *unc-52* (also involved in elongation, see below) (Spike et al., 2002), the WD40 repeat protein *smu-1*, which also regulates alternative splicing for *unc-52* (Spike et al., 2001), *daf-18,* which also works with *mec-8* to regulate alternative splicing for *unc-52* (Suzuki and Han, 2006), the cyclin-dependent kinase *cki-1* (Fukuyama et al., 2003), the extracellular leucine-rich repeat only (eLRRon) proteins *let-4* and *sym-1,* which are necessary for epithelial junction integrity (Mancuso et al., 2012), the Mago nashi homolog *mag-1* (Li et al., 2000), the nuclear hormone receptor transcription factor *nhr-40,* which is involved in actin distribution in myofilaments (Brozová et al., 2006) and whose loss-of-function phenotypes result in embryonic arrest, the actopaxin *pat-6,* which is necessary for body wall muscle attachment (Lin et al., 2003), and *unc-45,* which controls muscle thick filament assembly (Venolia et al., 1999)

Components of the basement membrane are necessary for mediating adhesion between the body wall muscles and the epidermis during late elongation. These include the collagen *emb-9,* the F-spondin *spon-1,* and perlcan *unc-52* (Gupta et al., 1997; Woo et al., 2008; Hresko et al., 1994)

A class of phenotypes known as Pat (paralyzed, arrested elongation at twofold) has been characterized to affect later elongation (Williams and Waterson, 1994). Loss-of-function of certain genes causes this phenotype, and these genes include troponin-c *pat-10* (Terami et al., 1999), the α1 subunit of a putative voltage-activated Ca^{2+} channel protein *egl-19* (Lee et al., 1997), the flightless homolog *fli-1* (Lu et al., 2008), the α integrin *pat-2,* the β integrin *pat-3,* the pleckstrin homology domain-containing protein *unc-112,* the LIM domain-containing protein of the PINCH family *unc-97,* the serine/threonine kinase *pat-4,* actopaxin *pat-6* , perlecan *unc-52* (Williams and Waterson, 1994), and the nuclear zinc finger protein *pat-9* (Liu et al., 2012).

If mutants of a certain gene arrest in two-fold stage, they are thought to have defects in late elongation; however, the exact mechanism by which many of these genes affect elongation is not known. These genes include the nuclear hormone receptor transcription factor *nhr-25* (Gissendanner and Sluder, 1997), the protein O-fucosyltransferase gene *pad-2* (Menzel et al., 2004),

the clathrin adaptor *ap-1* (Shafaq-Zadah et al., 2012), and the uridine-5'-monophosphate synthase *umps-1* (Levitte et al., 2010).

2.9 Muscle arms

The plasma membrane of body wall muscles extends out protrusions to motor neurons called muscle arms in order to make neuromuscular junctions (Figure 9; White et al., 1986). These muscle extensions contain a thin stalk from the body wall muscle, and the ends of these protrusions bifurcate (Dixon and Roy, 2005). 79 of 95 body wall muscles create extensions, 16 of which extend from the neck to the nerve ring; the remaining 63 extend towards the nearest motor neuron on the nerve cord. When motor neurons take on aberrant paths, muscle arms extend in the paths of those aberrant neurons, indicating that these muscle arms respond to chemoattractant cues from motor neurons (Hedgecock et al., 1990). Muscle arms are also thought to direct their extensions towards areas containing dense core vesicles. In *unc-104* mutants, muscle arms extend towards areas with increased localizations of dense core vesicles (Hall and Hedgecock, 1991; Zhou et al., 2001). Muscle arms form stereotypically throughout development. L1 larvae have about 1-2 muscle arm extensions (Hall and Hedgecock, 1991), L2 have on average 3.4 muscle arms per body wall muscle, and adults have 3-5 muscle arms per body wall muscle (Dixon and Roy, 2005). Muscle arms use actin to generate protrusions, and knockdown of genes that affect actin (*act-1,act-2, act-3*) reduces muscle arm formation.

Alexander et al. 2009 performed a screen identifying genes necessary for muscle arm protrusion. They found ten genes which are listed as follows: *gex-2, madd-2, unc-33, unc-40, unc-51, unc-54, unc-60B, unc-73, unc-93,* and *unc-95*. Knockdown of these genes causes a muscle arm extension defect, also known as a Mad defect. The cofilin *unc-60B* specifically affects muscle arm extension by regulating actin severing activity (Dixon and Roy, 2005). Tropomyosin is known to antagonize cofilin activity (Bernstein and Bamburg, 1982; Blanchoin et al., 2000; DesMarais et al., 2002; Ono and Ono, 2002), and *C. elegans* tropomyosin *lev-11* acts to stabilize actin in muscle arms (Dixon and Roy, 2005). Other genes involved in muscle arm extension include adhesion factors such as the α integrin *pat-2*, the integrin linked kinase *pat-4*, actopaxin *pat-6*, the laminins *lam-1, lam-2,* and *epi-1*, and perlecan *unc-52* (Dixon et al., 2006). The dense body components *unc-97* and *unc-98* (Alexander et al. 2009), as well as components of the WAVE complex *gex-3*, *wve-1* and *wsp-1,* also regulate muscle arm extension. Myosin heavy chain B *unc-54* is also necessary for muscle arm

formation; loss-of-function results in fewer arms and changes in arm width (Dixon and Roy, 2005). The ADAMs ortholog *madd-4* and the netrin ligand *unc-6* also act with the netrin receptor *unc-40* and its coreceptor *eva-1* to form and guide muscle arm extensions (Seetharaman et al., 2011; Chan et al, 2014). *lin-12* and *madd-2* act through *unc-40* to affect muscle arm development (Alexander et al., 2010; Li et al, 2013).

The FGF pathway is also involved in forming muscle arm extensions; when *let-756*(FGF), *egl-15*(FGF receptor), *sem-5*(GRB2) are knocked down, ectopic muscle membrane extensions (EME) form (Dixon 2006). Loss-of-function of other FGF components such as *let-60, soc-2, ptp-2, egl-17, soc-1,* and *sos-1* also results in EME formation. The BWM-expressed receptor tyrosine phosphatase which inhibits *egl-15* activity (Kokel et al., 1998), also affects muscle arm extension by suppressing the EME phenotype from *egl-15* knockdown and by causing the MAD phenotype when knocked down on its own (Dixon et al., 2006).

2.10 Head mesodermal cells

The head mesodermal cells are branched cells that lie dorsal to the terminal bulb of the pharynx (Figure 10; Sulston et al., 1983; Altun and Hall, 2009). These cells, which originate from hmcR and hmcL (head mesodermal cell right and head mesodermal cell left), are the sister cells of Z1 and Z4 (Sulston et al., 1983). These cells migrate circumferentially to the dorsal midline, and once they reach this position, hmcR undergoes programmed cell death. hmcL then extends processes anteriorly and posteriorly along the dorsal and ventral margins of the body wall (Altun and Hall, 2009). These two branches split at the pharynx and grow adjacent to the terminal bulb of the pharynx. The ventral process grows along the anterior loop of the right excretory gland and adjacent to the ventral hypodermal ridge. This process also runs adjacent to the body wall muscle and makes gap junctions with the body wall muscle (Altun and Hall, 2009; White et al., 1976). The dorsal process grows adjacent to the dorsal hypodermal ridge and also makes gap junctions with arms from dorsal muscles.

The homolog of human myotonic dystrophy-associated homeodomain protein Six5 *unc-39* is involved in regulating the processes formed by head mesodermal cells (Yanowitz et al., 2004). When *unc-39* is knocked down, ectopic processes form around the nerve ring, and posterior directed processes become shorter.

Netrins (*unc-5, unc-6*, and *unc-40*) affect hmcL cell body positioning but not arm projections (Hedgecock et al., 1990).

2.11 Analysis of Gene Families

In this work, we have discussed 252 genes involved in 11 different systems (Table 1). We wished to determine which genes were acting as master regulators of non-neuronal cell outgrowth in *C. elegans*. Therefore, we identified genes that control cell outgrowth in multiple tissues (Table 1 and Table 2) and found that 54 (Table 2; Figure 11) genes were involved in affecting outgrowth in more than one tissue.

We created a matrix looking at pairwise interactions between different tissues (Table 2). From this matrix we saw that four genes were involved in four different tissues; these genes are Trio/*unc-73*, β-integrin/*pat-3*, the netrin ligand *unc-6*, and the WAVE complex component *gex-2*. Each of these three genes belongs to families that are also involved in cell outgrowth. *unc-73*/Trio is a Rho GNEF that acts with *rho-1* and *let-502* (Spencer et al., 2001; Steven et al., 1998) in both the utse (Ghosh and Sternberg, 2014) and in early elongation (Piekny et al., 2000; Wissmann et al., 1999) and with *unc-13* and *unc-64* (McMullan et al., 2006) in the utse only. The β-integrin/*pat-3* acts with the α integrin *ina-1,* which affects cell outgrowth in the utse, the anchor cell and the excretory cell (Ghosh and Sternberg, 2014; Ihara et al., 2011; Baum and Garriga, 1997; Gettner et al., 1995), and the α integrin *pat-2* in the excretory cell, late elongation, and muscle arms (Baum and Garriga, 1997; Gettner et al., 1995; Williams and Waterson, 1994; Dixon et al., 2006). Netrins are well-characterized guidance cues, and the netrin receptor *unc-40* is involved in regulating outgrowth in the anchor cell, ventral enclosure, and muscle arm extension (Ziel et al., 2009; Alexander et al. 2009; Seetharaman et al., 2011; Chan et al, 2014). *gex-2* is a member of the WAVE/SCAR complex necessary for actin initiation, and many components of the WAVE/SCAR complex are involved in multiple tissues characterized in this work (as described below). *gex-1/wve-1* is involved in the utse, dorsal intercalation, and muscle arms (Ghosh and Sternberg, 2014, Soto et al., 2002; Alexander et al. 2009). *gex-3* is involved in dorsal intercalation, ventral enclosure, and muscle arm extension (Soto et al., 2002; Patel et al., 2008; Dixon and Roy, 2005). Therefore, we believe that these four master cell outgrowth regulators function in multiple tissues and are differentially activated through interaction with other components of their gene families.

We also wanted to determine whether there were regulators of cell outgrowth that were specific to tissue type. In this work, we characterized two primary groups of tissues: the gonad (utse, anchor cell, and sex muscles) and the embryo (dorsal intercalation, ventral enclosure, early elongation, and late elongation). We categorized genes that were involved in multiple tissues based on whether they affected these two tissues, as well as the number of gonadal and embryonic tissues affected (Figure 11). By using a colored heat map to assign function in either gonadal or embryonic tissues, we were able to categorize genes that act as master regulators in these tissues. Yellow represents a more gonadal identity and blue represents a more embryonic identity.

Genes that exclusively affect gonadal tissues are the genes that regulate anchor cell invasion and utse outgrowth (*aff-1, fos-1, egl-43, zmp-1, him-4*). We also identified genes that affect two gonadal tissues and one non-gonadal/non-embryonic tissue, which were *cdh-3, ina-1, mig-10,* and *unc-53*. Aside from genes that have been found to control anchor cell invasion, we did not identify any specific gene or gene family that acted as a master regulator in gonadal outgrowth.

Conversely, we found 12 genes that act exclusively in embryonic cell outgrowth. Genes involved in multiple embryonic outgrowth processes are *frk-1, ten-1, apr-1, rib-1, ced-10, ani-1, ctr-9, evl-20, hmp-1, hmp-2, hmr-1,* and *phy-1*. Six of these genes are involved in both ventral enclosure and early elongation (*ani-1, ctr-9, evl-20, hmp-1, hmp-2, hmr-1)*. This is not surprising, because these two outgrowth processes occur temporally after one another in embryonic development (Chisholm and Hardin, 2005). The CCC complex consists of Cadherin, α-catenin and β-catenin and is encoded by *hmr-1, hmp-1,* and *hmp-2* (Costa et al., 1998; Raich et al., 1999; Pásti and Labouesse, 2014). From our list of genes that function exclusively in embryonic cell outgrowth, we observed that all members of the CCC complex were present. We therefore believe the CCC complex to be a master regulator of embryonic outgrowth.

2.12 Conclusions

In this chapter, we discussed both the process and mechanisms used by 11 tissues in *C. elegans* to control cell outgrowth. We have identified lineages from which these tissues emerge, as well as characterized in detail how these tissues and cells change their shape and grow outward during development. We have also characterized the genes that are necessary for mediating this outgrowth and shown that several gene families/gene types regulate outgrowth in multiple tissues, including WAVE/SCAR, integrins, and netrins.

We hope that this work can be used as a resource not only for better understanding cell outgrowth but for presenting a broad set of model organisms that can be used for studying cell outgrowth. In our previous work studying the mechanisms involved in utse development, we were able to glean more information about utse outgrowth by testing genes involved in outgrowth in other tissues. Cell outgrowth is a process that is present in a plethora of developing systems, and studying multiple cell outgrowth systems can shed light on the specific ways cells change their shape and how genes that regulate these behaviors function. Through this work, we hope to present a list of genes that can be characterized in other outgrowth systems, as well as other outgrowth systems that can be studied when trying to better understand the function of a specific gene.

References

Ackley, B.D. 2014. Wnt-signaling and planar cell polarity genes regulate axon guidance along the anteroposterior axis in C. elegans. Dev Neurobiol. **74**(8):781-96

Alexander, M., Chan, K.K., Byrne, A.B., Selman, G., Lee, T., Ono, J., Wong, E., Puckrin, R., Dixon, S.J., Roy, P.J. 2009. An UNC-40 pathway directs postsynaptic membrane extension in Caenorhabditis elegans. Development. **136**(6):911-22.

Alexander, M., Selman, G., Seetharaman, A., Chan, K.K., D'Souza, S.A., Byrne, A.B., Roy, P.J. 2010. MADD-2, a homolog of the Opitz syndrome protein MID1, regulates guidance to the midline through UNC-40 in Caenorhabditis elegans. Dev Cell;**18**(6):961-72.

Altun, Z.F. and Hall, D.H. 2009. Muscle system, head mesodermal cell. In WormAtlas. doi:10.3908/wormatlas.1.10

Antoshechkin, I. and Han, M. 2002 The C. elegans evl-20 gene is a homolog of the small GTPase ARL2 and regulates cytoskeleton dynamics during cytokinesis and morphogenesis. Dev Cell; **2**(5):579-91.

Armenti, S.T., Lohmer, L.L., Sherwood, D.R., Nance, J. 2014. Repurposing an endogenous degradation system for rapid and targeted depletion of C. elegans proteins. Development; **141**(23):4640-7.

Baird, S.E. and Emmons, S.W. 1990. Properties of a class of genes required for ray morphogenesis in Caenorhabditis elegans. Genetics;**126**(2):335-44.

Baird, S.E., Fitch, D.H., Kassem, I.A., Emmons, S.W. 1991. Pattern formation in the nematode epidermis: determination of the arrangement of peripheral sense organs in the C. elegans male tail. Development;**113**(2):515-26.

Baranov, V.S., Ivaschenko, T.E., Liehr, T., Yarmolinskaya, M.I.. 2015. Systems genetics view of endometriosis: a common complex disorder. Eur J Obstet Gynecol Reprod Biol; **185**C:59-65.

Baum, P.D. and Garriga, G. 1997. Neuronal migrations and axon fasciculation are disrupted in ina-1 integrin mutants. Neuron;**19**(1):51-62.

Bernstein, B. W. and Bamburg, J. R. 1982. Tropomyosin binding to F-actin protects the F-actin from disassembly by brain actin-depolymerizing factor (ADF). Cell Motil. **2**, 1-8.

Bhattacharya ,R., Townley, R.A., Berry, K.L., Bülow, H.E. 2009. The PAPS transporter PST-1 is required for heparan sulfation and is essential for viability and neural development in C. elegans. J Cell Sci;**122**(Pt 24):4492-504.

Blanchoin, L., Amann, K. J., Higgs, H. N., Marchand, J. B., Kaiser, D. A. and Pollard, T. D. 2000. Direct observation of dendritic actin filament networks nucleated by Arp2/3 complex and WASP/Scar proteins. Nature **404**, 1007-1011.

Bosher, J.M., Hahn, B.S., Legouis, R., Sookhareea, S., Weimer, R.M., Gansmuller, A., Chisholm, A.D., Rose, A.M., Bessereau, J.L., Labouesse, M. 2003. The Caenorhabditis elegans vab-10 spectraplakin isoforms protect the epidermis against internal and external forces. J Cell Biol;**161**(4):757-68.

Brenner S. 1974. The genetics of Caenorhabditis elegans. Genetics;**77**(1):71-94.

Brozová, E., Simecková, K., Kostrouch, Z., Rall, J.E., Kostrouchová, M. 2006. NHR-40, a Caenorhabditis elegans supplementary nuclear receptor, regulates embryonic and early larval development. Mech Dev.;**123**(9):689-701.

Buechner and Hedgecock. 1992. Worm Breeder's Gazette **12**(3): 97

Buechner M. 2002. Tubes and the single C. elegans excretory cell. Trends Cell Biol.;**12**(10):479-84.

Byerly, L., Russell, R. L., & Cassada, R. C. 1976. The life cycle of the nematode Caenorhabditis elegans. I. Wild-type growth and reproduction. Dev Biol, **51**, 23-33. doi:10.1016/0012-1606(76)90119-6

Chan, K.K., Seetharaman, A., Bagg, R., Selman, G., Zhang, Y., Kim, J., Roy, P.J.. 2014. EVA-1 functions as an UNC-40 Co-receptor to enhance attraction to the MADD-4 guidance cue in Caenorhabditis elegans. PLoS Genet.;**10**(8):e1004521.

Chang, C., Newman, A.P., Sternberg, P.W., 1999. Reciprocal EGF signaling back to the uterus from the induced C. elegans vulva coordinates morphogenesis of epithelia. Curr. Biol. **9**, 237-246

Chen, L., Krause, M., Sepanski, M., Fire, A. 1994. The Caenorhabditis elegans MYOD homologue HLH-1 is essential for proper muscle function and complete morphogenesis. Development. 1994 Jun;120(6):1631-41.

Chin-Sang, I.D., George, S.E., Ding, M., Moseley, S.L., Lynch, A.S., Chisholm, A.D.. 1999. The ephrin VAB-2/EFN-1 functions in neuronal signaling to regulate epidermal morphogenesis in C. elegans. Cell; **99**(7):781-90.

Chin-Sang, I.D. and Chisholm, A.D. 2000. Form of the worm: genetics of epidermal morphogenesis in C. elegans. Trends Genet;**16**(12):544-51.

Chisholm A. 1991. Control of cell fate in the tail region of C. elegans by the gene egl-5. Development.;**111**(4):921-32.

Chisholm, A.D. and Hardin, J. 2005. Epidermal morphogenesis , WormBook, ed. The C. elegans Research Community, WormBook, doi/10.1895/wormbook.1.35.1 , http://www.wormbook.org.

Chow, K.L., and Emmons, S.W. 1994. HOM-C/Hox genes and four interacting loci determine the morphogenetic properties of single cells in the nematode male tail. Development;**120**(9):2579-92.

Chow, K.L., Hall, D.H., Emmons, S.W. 1995. The mab-21 gene of Caenorhabditis elegans encodes a novel protein required for choice of alternate cell fates. Development.;**121**(11):3615-26.

Costa, M., Draper, B.W., Priess JR. 1997. The role of actin filaments in patterning the Caenorhabditis elegans cuticle. Dev Biol.;**184**(2):373-84.

Costa, M., Raich, W., Agbunag, C., Leung, B., Hardin, J., Priess, J.R. 1998. A putative catenin-cadherin system mediates morphogenesis of the Caenorhabditis elegans embryo. J Cell Biol;**141**(1):297-308.

Cox-Paulson, E.A., Walck-Shannon, E., Lynch, A.M., Yamashiro, S., Zaidel-Bar, R., Eno, C.C., Ono, S., Hardin, J. 2012. Tropomodulin protects α-catenin-dependent junctional-actin networks under stress during epithelial morphogenesis. Curr Biol.;**22**(16):1500-5.

Del Rio-Albrechtsen, T., Kiontke, K., Chiou, S.Y., Fitch, D.H. 2006. Novel gain-of-function alleles demonstrate a role for the heterochronic gene lin-41 in C. elegans male tail tip morphogenesis. Dev Biol; **297**(1):74-86.

DesMarais, V., Ichetovkin, I., Condeelis, J. and Hitchcock-DeGregori, S. E. 2002. Spatial regulation of actin dynamics: a tropomyosin-free, actin- rich compartment at the leading edge. J. Cell Sci. **115**, 4649-4660

Ding, M., Goncharov, A., Jin, Y., Chisholm, A.D. 2003. *C. elegans* ankyrin repeat protein VAB-19 is a component of epidermal attachment structures and is essential for epidermal morphogenesis. Development.;**130**(23):5791-801.

Ding, M., King, R.S., Berry, E.C., Wang, Y., Hardin, J., Chisholm, A.D. 2008. The cell signaling adaptor protein EPS-8 is essential for C. elegans epidermal elongation and interacts with the ankyrin repeat protein VAB-19. PLoS One.;**3**(10):e3346.

Diogon, M., Wissler, F., Quintin, S., Nagamatsu, Y., Sookhareea, S., Landmann, F., Hutter, H., Vitale, N., Labouesse, M. 2007. The RhoGAP RGA-2 and LET-502/ROCK achieve a balance of actomyosin-dependent forces in C. elegans epidermis to control morphogenesis. Development.;**134**(13):2469-79.

Dixon, S.J. and Roy, P.J. 2005. Muscle arm development in Caenorhabditis elegans. Development.; **132**(13):3079-92.

Dixon, S. J., Alexander, M., Fernandes, R., Ricker, N. and Roy, P. J. 2006. FGF negatively regulates muscle membrane extension in Caenorhabditis elegans. Development **133**, 1263-1275.

Emmons, S.W. and Sternberg P.W. 1997. Male Development and Mating Behavior. C. elegans II. 2nd edition. Cold Spring Harbor (NY): Cold Spring Harbor Laboratory Press; Chapter 12. Ed. Riddle DL, Blumenthal T, Meyer BJ, Priess JR,

Emmons, S.W. 2005. Male development, WormBook, ed. The C. elegans Research Community, WormBook, doi/10.1895/wormbook.1.33.1, http://www.wormbook.org.

Forrester, W.C. and Garriga, G. 1997. Genes necessary for C. elegans cell and growth cone migrations. Development.;**124**(9):1831-43.

Fotopoulos N1, Wernike D, Chen Y, Makil N, Marte A, Piekny A. 2012. Caenorhabditis elegans anillin (ani-1) regulates neuroblast cytokinesis and epidermal morphogenesis during embryonic development. Dev Biol.;**383**(1):61-74.

Francis, R. and Waterston, R.H. 1991. Muscle cell attachment in Caenorhabditis elegans. J Cell Biol;**114(**3):465-79.

Fukuyama, M., Gendreau, S.B., Derry, W.B., Rothman, J.H. 2003. Essential embryonic roles of the CKI-1 cyclin-dependent kinase inhibitor in cell-cycle exit and morphogenesis in C elegans. Dev Biol; **260**(1):273-86.

Gally, C., Wissler, F., Zahreddine, H., Quintin, S., Landmann, F., Labouesse, M. 2009. Myosin II regulation during C. elegans embryonic elongation: LET-502/ROCK, MRCK-1 and PAK-1, three kinases with different roles. Development.;**136**(18):3109-19.

Garriga, G., Desai, C., Horvitz, H.R. 1993. Cell interactions control the direction of outgrowth, branching and fasciculation of the HSN axons of Caenorhabditis elegans. Development.;**117**(3):1071-87.

Gatewood, B.K. and Bucher, E.A. 1997. The mup-4 locus in Caenorhabditis elegans is essential for hypodermal integrity, organismal morphogenesis and embryonic body wall muscle position. Genetics;**146**(1):165-83.

Gendreau, S.B., Moskowitz, I.P., Terns, R.M., Rothman, J.H. 1994. The potential to differentiate epidermis is unequally distributed in the AB lineage during early embryonic development in C. elegans. Dev Biol.;**166(**2):770-81.

George, S.E., Simokat, K., Hardin, J., Chisholm, A.D. 1998. The VAB-1 Eph receptor tyrosine kinase functions in neural and epithelial morphogenesis in C. elegans. Cell.;**92**(5):633-43.

Gettner, S.N., Kenyon, C., Reichardt, L.F. 1995. Characterization of beta pat-3 heterodimers, a family of essential integrin receptors in C. elegans. J Cell Biol.;**129**(4):1127-41.

Ghenea, S., Boudreau, J.R., Lague, N.P., Chin-Sang, I.D. 2005. The VAB-1 Eph receptor tyrosine kinase and SAX-3/Robo neuronal receptors function together during C. elegans embryonic

morphogenesis. Development.;**132**(16):3679-90.

Ghosh, S. and Sternberg, P.W. 2014. Spatial and molecular cues for cell outgrowth during *C. elegans* uterine development. Dev Biol.;**396**(1):121-35.

Ghosh, S. and Sternberg, P.W. "A candidate RNAi screen for cell outgrowth defects in the C. elegans utse". in prep

Gissendanner, C.R. and Sluder, A.E. 2000. nhr-25, the Caenorhabditis elegans ortholog of ftz-f1, is required for epidermal and somatic gonad development. Dev Biol.;**221**(1):259-72.

Giuliani, C., Troglio, F., Bai, Z., Patel, F.B., Zucconi, A., Malabarba, M.G., Disanza, A., Stradal, T.B., Cassata, G., Confalonieri, S., Hardin, J.D., Soto, M.C., Grant, B.D., Scita, G. 2009. Requirements for F-BAR proteins TOCA-1 and TOCA-2 in actin dynamics and membrane trafficking during Caenorhabditis elegans oocyte growth and embryonic epidermal morphogenesis. PLoS Genet.;**5**(10):e1000675.

Gotenstein, J.R., Swale, R.E., Fukuda, T., Wu, Z., Giurumescu, C.A., Goncharov, A., Jin, Y., Chisholm, A.D. 2010. The C. elegans peroxidasin PXN-2 is essential for embryonic morphogenesis and inhibits adult axon regeneration. Development;**137**(21):3603-13.

Greenwald, I.S., Sternberg, P.W., Horvitz, H.R. 1983. The lin-12 locus specifies cell fates in Caenorhabditis elegans. Cell; **34**(2):435-44.

Gupta, M.C., Graham, P.L., Kramer, J.M. 1997. Characterization of alpha1(IV) collagen mutations in Caenorhabditis elegans and the effects of alpha1 and alpha2(IV) mutations on type IV collagen distribution. J Cell Biol;**137**(5):1185-96.

Hagedorn, E.J., Yashiro, H., Ziel, J.W., Ihara, S., Wang, Z., Sherwood, D.R. 2009. Integrin acts upstream of netrin signaling to regulate formation of the anchor cell's invasive membrane in C. elegans. Dev Cell;**17**(2):187-98.

Hahn, B.S. and Labouesse, M. 2001. Tissue integrity: hemidesmosomes and resistance to stress. Curr Biol;**11**(21):R858-61.

Hall, D. H. and Hedgecock, E. M. 1991. Kinesin-related gene unc-104 is required for axonal transport of synaptic vesicles in C. elegans. Cell 65, 837- 847.

Hao, L., Aspöck, G., Bürglin, T.R. 2006. The hedgehog-related gene wrt-5 is essential for hypodermal development in Caenorhabditis elegans. Dev Biol; **290**(2):323-36.

Hardin, J. and Walston, T. 2004. Models of morphogenesis: the mechanisms and mechanics of cell rearrangement. Curr Opin Genet Dev. 2004 Aug;14(4):399-406.

Hedgecock, E.M., Culotti, J.G., Hall, D.H. 1990. The unc-5, unc-6, and unc-40 genes guide circumferential migrations of pioneer axons and mesodermal cells on the epidermis in C. elegans. Neuron; **4**(1):61-85.

Heid, P.J., Raich, W.B., Smith, R., Mohler, W.A., Simokat, K., Gendreau, S.B., Rothman,

J.H., Hardin, J. 2001. The zinc finger protein DIE-1 is required for late events during epithelial cell rearrangement in C. elegans. Dev Biol; **236**(1):165-80.

Hill, K.L., Harfe, B.D., Dobbins, C.A., L'Hernault, S.W. 2000. dpy-18 encodes an alpha-subunit of prolyl-4-hydroxylase in caenorhabditis elegans. Genetics;**155**(3):1139-48.

Hill, R.J., and Sternberg, P.W. 1992. The gene lin-3 encodes an inductive signal for vulval development in C. elegans. Nature 358, 470–476.

Hobert, O. 2005. Specification of the nervous system, WormBook, ed. The C. elegans Research Community, WormBook, doi/10.1895/wormbook.1.12.1, http://www.wormbook.org.

Hoier, E.F., Mohler, W.A., Kim, S.K., Hajnal, A. 2000. The Caenorhabditis elegans APC-related gene apr-1 is required for epithelial cell migration and Hox gene expression. Genes Dev; **14**(7):874-86.

Hoppe, P.E., Chau, J., Flanagan, K.A., Reedy, A.R., Schriefer, L.A. 2010. Caenorhabditis elegans unc-82 encodes a serine/threonine kinase important for myosin filament organization in muscle during growth. Genetics; **184**(1):79-90.

Hresko, M.C., Williams, B.D., Waterston, R.H. 1994. Assembly of body wall muscle and muscle cell attachment structures in Caenorhabditis elegans. J Cell Biol; **124**(4):491-506.

Hresko, M.C., Schriefer, L.A., Shrimankar, P., Waterston, R.H. 1999. Myotactin, a novel hypodermal protein involved in muscle-cell adhesion in Caenorhabditis elegans. J Cell Biol; **146**(3):659-72

Hubbard, E.J. and Greenstein, D. 2000. The Caenorhabditis elegans gonad: a test tube for cell and developmental biology. Dev Dyn; **218**(1):2-22.

Hudson, M.L., Kinnunen, T., Cinar, H.N., Chisholm, A.D. 2006. C. elegans Kallmann syndrome protein KAL-1 interacts with syndecan and glypican to regulate neuronal cell migrations. Dev Biol.; **294**(2):352-65. Epub 2006 May 3.

Hutter, H., Vogel, B.E., Plenefisch, J.D., Norris, C.R., Proenca, R.B., Spieth, J., Guo, C., Mastwal, S., Zhu, X., Scheel, J., Hedgecock, E.M. 2000. Conservation and novelty in the evolution of cell adhesion and extracellular matrix genes. Science.; **287**(5455):989-94.

Hwang, B.J., Meruelo, A.D., Sternberg, P.W., 2007. C. elegans EVI1 proto-oncogene, EGL-43, is necessary for Notch-mediated cell fate specification and regulates cell invasion. Development. **134**, 669-79.

Ihara, S., Hagedorn, E.J., Morrissey, M.A., Chi, Q., Motegi, F., Kramer, J.M., Sherwood, D.R. 2011. Basement membrane sliding and targeted adhesion remodels tissue boundaries during uterine-vulval attachment in Caenorhabditis elegans. Nat Cell Biol.;**13**(6):641-51. doi: 10.1038/ncb2233. Epub 2011 May 15.

Ikegami, R., Simokat. K., Zheng, H., Brown, L., Garriga, G., Hardin, J., Culotti, J. 2012. Semaphorin and Eph receptor signaling guide a series of cell movements for ventral enclosure in C.

elegans. Curr Biol.; **22**(1):1-11.

Kaminsky, R., Denison, C., Bening-Abu-Shach, U., Chisholm, A.D., Gygi, S.P., Broday, L. 2009**.** SUMO regulates the assembly and function of a cytoplasmic intermediate filament protein in C. elegans. Dev Cell.;**17**(5):724-35.

Kimble, J. and Hirsh, D. 1979. The postembryonic cell lineages of the hermaphrodite and male gonads in Caenorhabditis elegans. Dev Biol.; **70**(2):396-417.

Kimble, J. 1981. Alterations in cell lineage following laser ablation of cells in the somatic gonad of Caenorhabditis elegans. Dev. Biol. **87**, 286–300

King, R.S., Maiden. S.L., Hawkins. N.C., Kidd. A.R. 3rd, Kimble. J., Hardin. J., Walston. T.D. 2009. The N- or C-terminal domains of DSH-2 can activate the C. elegans Wnt/beta-catenin asymmetry pathway. Dev Biol.; **328**(2):234-44.

Kitagawa, H.1, Izumikawa. T., Mizuguchi. S., Dejima. K., Nomura. K.H., Egusa, N., Taniguchi, F., Tamura, J., Gengyo-Ando, K., Mitani, S., Nomura, K., Sugahara, K. 2007. Expression of rib-1, a Caenorhabditis elegans homolog of the human tumor suppressor EXT genes, is indispensable for heparan sulfate synthesis and embryonic morphogenesis. J Biol Chem.; **282**(11):8533-44. Epub 2007 Jan 19.

Klerkx, E.P., Alarcón, P., Waters, K., Reinke, V., Sternberg, P.W., Askjaer, P. 2009. Protein kinase VRK-1 regulates cell invasion and EGL-17/FGF signaling in Caenorhabditis elegans. Dev Biol.; **335**(1):12-21.

Ko, F.C. and Chow, K.L. 2002. A novel thioredoxin-like protein encoded by the C. elegans dpy-11 gene is required for body and sensory organ morphogenesis. Development; **129**(5):1185-94.

Kokel, M., Borland, C. Z., DeLong, L., Horvitz, H. R. and Stern, M. J. 1998. clr-1 encodes a receptor tyrosine phosphatase that negatively regulates an FGF receptor signaling pathway in Caenorhabditis elegans. Genes Dev. **12**, 1425- 1437.

Köppen, M., Simske, J.S., Sims, P.A., Firestein, B.L., Hall, D.H., Radice, A.D., Rongo, C., Hardin, J.D. 2001. Cooperative regulation of AJM-1 controls junctional integrity in Caenorhabditis elegans epithelia. Nat Cell Biol.; **3**(11):983-91.

Kubota, Y., Tsuyama, K., Takabayashi, Y., Haruta, N., Maruyama, R., Iida, N., Sugimoto, A. 2014. The PAF1 complex is involved in embryonic epidermal morphogenesis in Caenorhabditis elegans. Dev Biol.; **391**(1):43-53.

Kujawski, S., Lin, W., Kitte, F., Börmel, M., Fuchs, S., Arulmozhivarman, G., Vogt, S., Theil, D., Zhang, Y., Antos, C.L. 2014. Calcineurin regulates coordinated outgrowth of zebrafish regenerating fins. Dev Cell.; **28**(5):573-87.

Lambie , E.J. and Kimble, J. 1991. Two homologous regulatory genes, lin-12 and glp-1, have overlapping functions. Development.; **112**(1):231-40.

Lee, R.Y., Lobel, L., Hengartner, M., Horvitz, H.R., **Avery, L**. 1997. Mutations in the alpha1 subunit of an L-type voltage-activated Ca2+ channel cause myotonia in Caenorhabditis elegans.

EMBO J.; **16**(20):6066-76.

Levitte, S., Salesky, R., King, B., Coe Smith, S., Depper, M., Cole, M., Hermann, G.J. 2010. A Caenorhabditis elegans model of orotic aciduria reveals enlarged lysosome-related organelles in embryos lacking umps-1 function. FEBS J.; **277**(6):1420-39.

Li, P., Collins, K.M., Koelle, M.R., Shen, K. 2013. LIN-12/Notch signaling instructs postsynaptic muscle arm development by regulating UNC-40/DCC and MADD-2 in Caenorhabditis elegans. Elife.; **2**:e00378.

Li, W., Boswell, R., Wood, W.B. 2000. mag-1, a homolog of Drosophila mago nashi, regulates hermaphrodite germ-line sex determination in Caenorhabditis elegans. Dev Biol. 2000 Feb 15;218(2):172-82.

Lin, X., Qadota, H., Moerman, D.G., Williams, B.D. 2003. C. elegans PAT-6/actopaxin plays a critical role in the assembly of integrin adhesion complexes in vivo. Curr Biol.; **13**(11):922-32.

Liu, Q., Jones, T.I., Bachmann, R.A., Meghpara, M., Rogowski, L., Williams, B.D., Jones, P.L. 2012. C. elegans PAT-9 is a nuclear zinc finger protein critical for the assembly of muscle attachments. Cell Biosci.; **2**(1):18.

Lockwood, C., Zaidel-Bar, R., Hardin, J. 2008. The C. elegans zonula occludens ortholog cooperates with the cadherin complex to recruit actin during morphogenesis. Curr Biol.; **18**(17):1333-7.

Lu, J., Dentler, W.L., Lundquist, E.A. 2008. FLI-1 Flightless-1 and LET-60 Ras control germ line morphogenesis in C. elegans. BMC Dev Biol.; **8**:54. doi: 10.1186/1471-213X-8-54.

Lynch, A.M., Grana, T., Cox-Paulson, E., Couthier, A., Cameron, M., Chin-Sang, I., Pettitt, J., Hardin, J. 2012. A genome-wide functional screen shows MAGI-1 is an L1CAM-dependent stabilizer of apical junctions in C. elegans. Curr Biol; **22**(20):1891-9.

Macabenta, F.D., Jensen, A.G., Cheng, Y.S., Kramer, J.J., Kramer, S.G. 2013. Frazzled/DCC facilitates cardiac cell outgrowth and attachment during Drosophila dorsal vessel formation. Dev Biol.; **380**(2):233-42.

Mancuso, V.P., Parry, J.M., Storer, L., Poggioli, C., Nguyen, K.C., Hall, D.H., Sundaram, M.V. 2012. Extracellular leucine-rich repeat proteins are required to organize the apical extracellular matrix and maintain epithelial junction integrity in C. elegans. Development.; **139**(5):979-90.

Manser, J., Roonprapunt, C., Margolis, B. 1997. C. elegans cell migration gene mig-10 shares similarities with a family of SH2 domain proteins and acts cell nonautonomously in excretory canal development. Dev Biol.; **184**(1):150-64.

Marcus-Gueret, N., Schmidt, K.L., Stringham, E.G. 2012. Distinct cell guidance pathways controlled by the Rac and Rho GEF domains of UNC-73/TRIO in Caenorhabditis elegans. Genetics.; **190**(1):129-42.

Martin, E., Harel, S., Nkengfac, B., Hamiche, K., Neault, M., Jenna, S. 2014. pix-1 controls early elongation in parallel with mel-11 and let-502 in Caenorhabditis elegans. PLoS One.; **9**(4):e94684.

Mason, D.A., Rabinowitz, J.S., Portman, D.S. 2008. dmd-3, a doublesex-related gene regulated by tra-1, governs sex-specific morphogenesis in C. elegans. Development.; **135**(14):2373-82. doi: 10.1242/dev.017046. Epub 2008 Jun 11.

Matus, D.Q., Li, X.Y., Durbin, S., Agarwal, D., Chi, Q., Weiss, S.J., Sherwood, D.R. 2010. In vivo identification of regulators of cell invasion across basement membranes. Sci Signal.; **3**(120):ra35.

McMullan, R., Hiley, E., Morrison, P., Nurrish, S.J., 2006. Rho is a presynaptic activator of neurotransmitter release at pre-existing synapses in C. elegans. Genes Dev. **20**, 65-76.

McShea, M.A., Schmidt, K.L., Dubuke, M.L., Baldiga, C.E., Sullender, M.E., Reis, A.L., Zhang, S., O'Toole, S.M., Jeffers, M.C., Warden, R.M., Kenney, A.H., Gosselin, J., Kuhlwein, M., Hashmi, S.K., Stringham, E.G., Ryder, E.F. 2013. Abelson interactor-1 (ABI-1) interacts with MRL adaptor protein MIG-10 and is required in guided cell migrations and process outgrowth in C. elegans. Dev Biol.; 373(1):1-13.

Mehta, N., Loria, P.M., Hobert, O. 2004. A genetic screen for neurite outgrowth mutants in Caenorhabditis elegans reveals a new function for the F-box ubiquitin ligase component LIN-23. Genetics.; **166**(3):1253-67.

Menzel, O., Vellai, T., Takacs-Vellai, K., Reymond, A., Mueller, F., Antonarakis, S.E., Guipponi, M. 2004. The Caenorhabditis elegans ortholog of C21orf80, a potential new protein O-fucosyltransferase, is required for normal development. Genomics.; **84**(2):320-30.

Merz, D.C., Zheng, H., Killeen, M.T., Krizus, A., Culotti, J.G. 2001. Multiple signaling mechanisms of the UNC-6/netrin receptors UNC-5 and UNC-40/DCC in vivo. Genetics.; **158**(3):1071-80.

Michelet, X., Alberti, A., Benkemoun, L., Roudier, N., Lefebvre, C., Legouis, R. 2009. The ESCRT-III protein CeVPS-32 is enriched in domains distinct from CeVPS-27 and CeVPS-23 at the endosomal membrane of epithelial cells. Biol Cell.; **101**(10):599-615.

Mörck, C., Vivekanand, V., Jafari, G., Pilon, M. 2010. C. elegans ten-1 is synthetic lethal with mutations in cytoskeleton regulators, and enhances many axon guidance defective mutants. BMC Dev Biol.;**10**:55.

Morf, M.K., Rimann, I., Alexander, M., Roy, P., Hajnal, A. 2013. The Caenorhabditis elegans homolog of the Opitz syndrome gene, madd-2/Mid1, regulates anchor cell invasion during vulval development. Dev Biol. **1**;374(1):108-14.

Morrissey, M.A., Hagedorn, E.J., Sherwood, D.R. 2013. Cell invasion through basement membrane: The netrin receptor DCC guides the way. Worm.; **2**(3):e26169.

Nakao F1, Hudson ML, Suzuki M, Peckler Z, Kurokawa R, Liu Z, Gengyo-Ando K,

Nukazuka, A., Fujii, T., Suto, F., Shibata, Y., Shioi, G., Fujisawa, H., Mitani, S., Chisholm, A.D., Takagi, S. 2007. The PLEXIN PLX-2 and the ephrin EFN-4 have distinct roles in MAB-20/Semaphorin 2A signaling in Caenorhabditis elegans morphogenesis. Genetics.; **176**(3):1591-607.

Nelson, M.D., Zhou, E., Kiontke, K., Fradin, H., Maldonado, G., Martin, D., Shah, K., Fitch, D.H. 2011. A bow-tie genetic architecture for morphogenesis suggested by a genome-wide RNAi screen in Caenorhabditis elegans. PLoS Genet.;**7**(3):e1002010.

Newman, A.P., White, J.G., Sternberg, P.W. 1995. The Caenorhabditis elegans lin-12 gene mediates induction of ventral uterine specialization by the anchor cell. Development. **121**, 263-271.

Newman, A.P., White JG, Sternberg PW. 1996. Morphogenesis of the C. elegans hermaphrodite uterus. Development.; **122**(11):3617-26.

Nguyen, C.Q., Hall, D.H., Yang, Y., Fitch, D.H. 1999. Morphogenesis of the Caenorhabditis elegans male tail tip. Dev Biol.; **207**(1):86-106.

Nguyen, D.X., Bos, P.D., Massagué, J. 2009. Metastasis: from dissemination to organ-specific colonization. Nat Rev Cancer.; **9**(4):274-84.

Norman, K.R. and Moerman, D.G. 2002. Alpha spectrin is essential for morphogenesis and body wall muscle formation in Caenorhabditis elegans. J Cell Biol.; **157**(4):665-77. Epub 2002 May 6.

Ono, S. and Ono, K. 2002. Tropomyosin inhibits ADF/cofilin-dependent actin filament dynamics. J. Cell Biol. **156**, 1065-1076.

Otsuka, A.J., Jeyaprakash, A., García-Añoveros, J., Tang, L.Z., Fisk, G., Hartshorne, T., Franco, R., Born, T. 1991. The C. elegans unc-104 gene encodes a putative kinesin heavy chain-like protein. Neuron.; **6**(1):113-22.

Page, B.D., Zhang, W., Steward, K., Blumenthal, T., Priess, J.R. 1997. ELT-1, a GATA-like transcription factor, is required for epidermal cell fates in Caenorhabditis elegans embryos. Genes Dev.; **11**(13):1651-61.

Park, E.C. and Horvitz, H.R. 1986. Mutations with dominant effects on the behavior and morphology of the nematode Caenorhabditis elegans. Genetics.; **113**(4):821-52.

Pásti, G. and Labouesse, M. 2014. Epithelial junctions, cytoskeleton, and polarity. WormBook. **4**:1-35.

Patel, F.B., Bernadskaya, Y.Y., Chen, E., Jobanputra, A., Pooladi, Z., Freeman, K.L., Gally, C., Mohler, W.A., Soto, M.C. 2008. The WAVE/SCAR complex promotes polarized cell movements and actin enrichment in epithelia during C. elegans embryogenesis. Dev Biol.; **324**(2):297-309.

Patel, N., Thierry-Mieg, D., Mancillas, J.R. 1993. Cloning by insertional mutagenesis of a cDNA encoding Caenorhabditis elegans kinesin heavy chain. Proc Natl Acad Sci U S A.; **90**(19):9181-5.

Pettitt, J., Wood, W.B., Plasterk, R.H. 1996. cdh-3, a gene encoding a member of the cadherin superfamily, functions in epithelial cell morphogenesis in Caenorhabditis elegans. Development.; **122**(12):4149-57.

Pettitt, J., Cox, E.A., Broadbent, I.D., Flett, A., Hardin, J. 2003. The Caenorhabditis elegans p120 catenin homologue, JAC-1, modulates cadherin-catenin function during epidermal morphogenesis. J Cell Biol.; **162**(1):15-22.

Piekny, A.J., Wissmann, A., Mains, P.E. 2000. Embryonic morphogenesis in Caenorhabditis elegans integrates the activity of LET-502 Rho-binding kinase, MEL-11 myosin phosphatase, DAF-2 insulin receptor and FEM-2 PP2c phosphatase. Genetics.; **156**(4):1671-89.

Piekny, A.J., Johnson, J.L., Cham, G.D., Mains, P.E. 2003. The Caenorhabditis elegans nonmuscle myosin genes nmy-1 and nmy-2 function as redundant components of the let-502/Rho-binding kinase and mel-11/myosin phosphatase pathway during embryonic morphogenesis. Development.; **130**(23):5695-704.

Plenefisch, J.D., Zhu, X., Hedgecock, E.M. 2000. Fragile skeletal muscle attachments in dystrophic mutants of Caenorhabditis elegans: isolation and characterization of the mua genes. Development.; **127**(6):1197-207.

Pocock, R., Ahringer, J., Mitsch, M., Maxwell, S., Woollard, A. 2004. A regulatory network of T-box genes and the even-skipped homologue vab-7 controls patterning and morphogenesis in C. elegans. Development.; **131**(10):2373-85.

Poinat, P., De Arcangelis, A., Sookhareea, S., Zhu, X., Hedgecock, E.M., Labouesse, M., Georges-Labouesse, E. 2002. A conserved interaction between beta1 integrin/PAT-3 and Nck-interacting kinase/MIG-15 that mediates commissural axon navigation in C. elegans. Curr Biol.; **12**(8):622-31.

Praitis V1, Ciccone E, Austin J. 2005. SMA-1 spectrin has essential roles in epithelial cell sheet morphogenesis in C. elegans. Dev Biol.; **283**(1):157-70.

Priess, J.R. and Hirsh, D.I. 1986. Caenorhabditis elegans morphogenesis: the role of the cytoskeleton in elongation of the embryo. Dev Biol.; **117**(1):156-73.

Putzke, A.P., Hikita, S.T., Clegg, D.O., Rothman, J.H. 2005. Essential kinase-independent role of a Fer-like non-receptor tyrosine kinase in Caenorhabditis elegans morphogenesis. Development.; **132**(14):3185-95.

Raich, W.B., Agbunag, C., Hardin, J. 1999. Rapid epithelial-sheet sealing in the Caenorhabditis elegans embryo requires cadherin-dependent filopodial priming. Curr Biol.; **9**(20):1139-46.

Rimann, I. and Hajnal, A. 2007. Regulation of anchor cell invasion and uterine cell fates by the egl-43 Evi-1 proto-oncogene in Caenorhabditis elegans. Dev Biol.; **308**(1):187-95. Epub 2007 May 25.

Rogalski, T.M., Mullen, G.P., Bush, J.A., Gilchrist, E.J., Moerman, D.G. 2001. UNC-52/perlecan isoform diversity and function in Caenorhabditis elegans. Biochem Soc Trans.; **29**(Pt

2):171-6.

Roy, P.J., Zheng, H., Warren, C.E., Culotti, J.G. 2000. mab-20 encodes Semaphorin-2a and is required to prevent ectopic cell contacts during epidermal morphogenesis in Caenorhabditis elegans. Development.;**127**(4):755-67.

Sapir, A., Choi, J., Leikina, E., Avinoam, O., Valansi, C., Chernomordik, L.V., Newman, A.P., Podbilewicz, B., 2007. AFF-1, a FOS-1-regulated fusogen, mediates fusion of the anchor cell in C. elegans. Dev. Cell. 12, 683-698.

Savage, C., Das, P., Finelli, A.L., Townsend, S.R., Sun, C.Y., Baird, S.E., Padgett, R.W. 1996. Caenorhabditis elegans genes sma-2, sma-3, and sma-4 define a conserved family of transforming growth factor beta pathway components. Proc Natl Acad Sci U S A.; **93**(2):790-4.

Sawa, H., Lobel, L., Horvitz, H.R. 1996. The Caenorhabditis elegans gene lin-17, which is required for certain asymmetric cell divisions, encodes a putative seven-transmembrane protein similar to the Drosophila frizzled protein. Genes Dev.; **10**(17):2189-97.

Sawa, M., Suetsugu, S., Sugimoto, A., Miki, H., Yamamoto, M., Takenawa, T. 2003. Essential role of the C. elegans Arp2/3 complex in cell migration during ventral enclosure. J Cell Sci.; **116**(Pt 8):1505-18.

Sawa, M. and Takenawa, T. 2006. Caenorhabditis elegans WASP-interacting protein homologue WIP-1 is involved in morphogenesis through maintenance of WSP-1 protein levels. Biochem Biophys Res Commun.; **340**(2):709-17. Epub 2005 Dec 20.

Schindler, A.J. and Sherwood, D.R. 2011. The transcription factor HLH-2/E/Daughterless regulates anchor cell invasion across basement membrane in C. elegans. Dev Biol.; **357**(2):380-91.

Schmidt, K.L., Marcus-Gueret, N., Adeleye, A., Webber, J., Baillie, D., Stringham, E.G. 2009. The cell migration molecule UNC-53/NAV2 is linked to the ARP2/3 complex by ABI-1. Development.; **136**(4):563-74.

Seydoux, G. and Greenwald, I. 1989. Cell autonomy of lin-12 function in a cell fate decision in C. elegans. Cell.; **57**(7):1237-45.

Seetharaman, A., Selman, G., Puckrin, R., Barbier, L., Wong, E., D'Souza, S.A., Roy, P.J. 2011. MADD-4 is a secreted cue required for midline-oriented guidance in Caenorhabditis elegans. Dev Cell.; **21**(4):669-80.

Shafaq-Zadah, M., Brocard, L., Solari, F., Michaux, G. 2012. AP-1 is required for the maintenance of apico-basal polarity in the C. elegans intestine. Development.; **139**(11):2061-70

Shelton, C.A., Carter, J.C., Ellis, G.C., Bowerman, B. 1999. The nonmuscle myosin regulatory light chain gene mlc-4 is required for cytokinesis, anterior-posterior polarity, and body morphology during Caenorhabditis elegans embryogenesis. J Cell Biol.; **146**(2):439-51.

Sherwood, D.R. and Sternberg, P.W. 2003. Anchor cell invasion into the vulval epithelium in C. elegans. Dev Cell.; **5**(1):21-31.

Sherwood, D.R., Butler, J.A., Kramer, J.M., Sternberg, P.W. 2005. FOS-1 promotes basement-membrane removal during anchor-cell invasion in C. elegans. Cell.; **121**(6):951-62.

Simms, C.L. and Baillie, D.L. 2010. A strawberry notch homolog, let-765/nsh-1, positively regulates lin-3/egf expression to promote RAS-dependent vulval induction in C. elegans. Dev Biol.; **341**(2):472-85.

Simske, J.S., Köppen, M., Sims, P., Hodgkin, J., Yonkof, A., Hardin, J. 2003. The cell junction protein VAB-9 regulates adhesion and epidermal morphology in C. elegans. Nat Cell Biol.; **5**(7):619-25.

Sluder, A.E., Lindblom, T., Ruvkun, G. 1997. The Caenorhabditis elegans orphan nuclear hormone receptor gene nhr-2 functions in early embryonic development. Dev Biol.; **184**(2):303-19.

Soto, M.C., Qadota, H., Kasuya, K., Inoue, M., Tsuboi, D., Mello, C.C., Kaibuchi, K. 2002. The GEX-2 and GEX-3 proteins are required for tissue morphogenesis and cell migrations in C. elegans. Genes Dev.; **16**(5):620-32.

Spencer, A.G., Orita, S., Malone, C.J., Han, M., 2001. A RHO GTPase-mediated pathway is required during P cell migration in Caenorhabditis elegans. Proc. Natl. Acad. Sci USA. **98**, 13132-13137.

Spike, C.A., Shaw, J.E., Herman, R.K. 2001. Analysis of smu-1, a gene that regulates the alternative splicing of unc-52 pre-mRNA in Caenorhabditis elegans. Mol Cell Biol.; **21**(15):4985-95.

Spike, C.A., Davies, A.G., Shaw, J.E., Herman, R.K. 2002. MEC-8 regulates alternative splicing of unc-52 transcripts in C. elegans hypodermal cells. Development.; **129**(21):4999-5008.

Sternberg, P.W., 2005. Vulval development, WormBook, ed. The C. elegans Research Community, WormBook, doi/10.1895/wormbook.1.6.1, http://www.wormbook.org.

Steven, R., Kubiseski, T.J., Zheng, H., Kulkarni, S., Mancillas, J., Ruiz Morales, A., Hogue, C.W., Pawson, T., Culotti, J. 1998. UNC-73 activates the Rac GTPase and is required for cell and growth cone migrations in C. elegans. Cell.; **92**(6):785-95.

Stringham, E., Pujol, N., Vandekerckhove, J., Bogaert, T. 2002. unc-53 controls longitudinal migration in C. elegans. Development.; **129**(14):3367-79.

Sulston, J.E. and White, J.G. 1980. Regulation and cell autonomy during postembryonic development of Caenorhabditis elegans. Dev Biol.; **78**(2):577-97.

Sulston, J.E., Schierenberg, E., White, J.G., Thomson, J.N. 1983. The embryonic cell lineage of the nematode Caenorhabditis elegans. Dev Biol.; **100**(1):64-119.

Suzuki, Y. and Han, M. 2006. Genetic redundancy masks diverse functions of the tumor suppressor gene PTEN during C. elegans development. Genes Dev.; **20**(4):423-8.

Terami, H., Williams, B.D., Kitamura, S.i., Sakube, Y., Matsumoto, S., Doi, S., Obinata, T., Kagawa, H. Genomic organization, expression, and analysis of the troponin C gene pat-10 of Caenorhabditis elegans. J Cell Biol.; **146**(1):193-202.

Thomas-Virnig, C.L., Sims, P.A., Simske, J.S., Hardin, J. 2004. The inositol 1,4,5-trisphosphate receptor regulates epidermal cell migration in Caenorhabditis elegans. Curr Biol.; **14**(20):1882-7.

Topf, U. and Chiquet-Ehrismann, R. 2011. Genetic interaction between Caenorhabditis elegans teneurin ten-1 and prolyl 4-hydroxylase phy-1 and their function in collagen IV-mediated basement membrane integrity during late elongation of the embryo. Mol Biol Cell.; **22**(18):3331-43.

Vanneste, C.A., Pruyne, D., Mains, P.E. 2013. The role of the formin gene fhod-1 in C. elegans embryonic morphogenesis. Worm.; **2**(3):e25040.

Venolia, L., A.o., W., Kim, S., Kim, C., Pilgrim, D. 1999. unc-45 gene of Caenorhabditis elegans encodes a muscle-specific tetratricopeptide repeat-containing protein. Cell Motil Cytoskeleton.; **42**(3):163-77.

Walston T1, Guo C, Proenca R, Wu M, Herman M, Hardin J, Hedgecock E. mig-5/Dsh controls cell fate determination and cell migration in C. elegans. Dev Biol.; **298**(2):485-97. Epub 2006 Jul 7.

Wang, Q., Wadsworth, W.G. 2002. The C domain of netrin UNC-6 silences calcium/calmodulin-dependent protein kinase- and diacylglycerol-dependent axon branching in Caenorhabditis elegans. J Neurosci.; **22**(6):2274-82.

Wang, X., Roy, P.J., Holland, S.J., Zhang, L.W., Culotti, J.G., Pawson, T. 1999. Multiple ephrins control cell organization in C. elegans using kinase-dependent and -independent functions of the VAB-1 Eph receptor. Mol Cell.; **4**(6):903-13.

Wang, Z., Chi, Q., Sherwood, D.R. 2014. MIG-10 (lamellipodin) has netrin-independent functions and is a FOS-1A transcriptional target during anchor cell invasion in C. elegans. Development. **141**, 1342-1353

Wang, Z., Linden, L.M., Naegeli, K.M., Ziel, J.W., Chi, Q., Hagedorn, E.J., Savage, N.S., Sherwood, D.R. 2014. UNC-6 (netrin) stabilizes oscillatory clustering of the UNC-40 (DCC) receptor to orient polarity. J Cell Biol.; **206**(5):619-33.

White, J.G., Southgate, E., Thomson, J.N. and Brenner, S. 1976. The structure of the ventral nerve cord of Caenorhabditis elegans. Phil. Trans. Roy. Soc. Lond. **275**B: 327-348.

White, J. G., Southgate, E., Thomson, J. N. and Brenner, S. 1986. The structure of the nervous system of the nematode C. elegans. Philos. Trans. R. Soc. London Ser. B **314**, 1-340.

Wightman, B., Clark, S.G., Taskar, A.M., Forrester, W.C., Maricq, A.V., Bargmann, C.I., Garriga, G. 1996. The C. elegans gene vab-8 guides posteriorly directed axon outgrowth and cell migration. Development.; **122**(2):671-82.

Williams, B.D. and Waterston, R.H. 1994. Genes critical for muscle development and function in Caenorhabditis elegans identified through lethal mutations. J Cell Biol.; **124**(4):475-90.

Williams-Masson, E.M., Malik, A.N., Hardin, J. 1997. An actin-mediated two-step mechanism is required for ventral enclosure of the C. elegans hypodermis. Development.; **124**(15):2889-901.

Williams-Masson, E.M., Heid, P.J., Lavin, C.A., Hardin, J. 1998. The cellular mechanism of epithelial rearrangement during morphogenesis of the Caenorhabditis elegans dorsal hypodermis. Dev Biol.; **204**(1):263-76.

Winter, A.D. and Page, A.P. 2000. Prolyl 4-hydroxylase is an essential procollagen-modifying enzyme required for exoskeleton formation and the maintenance of body shape in the nematode Caenorhabditis elegans. Mol Cell Biol.; **20**(11):4084-93.

Wissmann, A., Ingles, J., Mains, P.E. 1999. The Caenorhabditis elegans mel-11 myosin phosphatase regulatory subunit affects tissue contraction in the somatic gonad and the embryonic epidermis and genetically interacts with the Rac signaling pathway. Dev Biol.; **209**(1):111-27.

Withee, J., Galligan, B., Hawkins, N., Garriga, G. 2004. Caenorhabditis elegans WASP and Ena/VASP proteins play compensatory roles in morphogenesis and neuronal cell migration. Genetics.; **167**(3):1165-76.

Woo, W.M., Goncharov, A., Jin, Y., Chisholm, A.D. 2004. Intermediate filaments are required for C. elegans epidermal elongation. Dev Biol.; **267**(1):216-29.

Woo, W.M., Berry, E.C., Hudson, M.L., Swale, R.E., Goncharov, A., Chisholm, A.D. 2008. The C. elegans F-spondin family protein SPON-1 maintains cell adhesion in neural and non-neural tissues. Development; **135**(16):2747-56.

Yamaguchi, T.P., Bradley, A., McMahon, A.P., Jones, S. 1999. A Wnt5a pathway underlies outgrowth of multiple structures in the vertebrate embryo. Development.; **126**(6):1211-23.

Yanowitz, J.L., Shakir, M.A., Hedgecock, E., Hutter, H., Fire, A.Z., Lundquist, E.A. 2004. UNC-39, the C. elegans homolog of the human myotonic dystrophy-associated homeodomain protein Six5, regulates cell motility and differentiation. Dev Biol.; **272**(2):389-402.

Yu, R.Y., Nguyen, C.Q., Hall, D.H., Chow, K.L. 2000. Expression of ram-5 in the structural cell is required for sensory ray morphogenesis in Caenorhabditis elegans male tail. EMBO J.; **19**(14):3542-55.

Zahreddine, H., Zhang, H., Diogon, M., Nagamatsu, Y., Labouesse, M. 2010. CRT-1/calreticulin and the E3 ligase EEL-1/HUWE1 control hemidesmosome maturation in C. elegans development. Curr Biol.; **20**(4):322-7.

Zhao, X., Yang, Y., Fitch, D.H., Herman, M.A. 2002. TLP-1 is an asymmetric cell fate determinant that responds to Wnt signals and controls male tail tip morphogenesis in C. elegans. Development.; **129**(6):1497-508.

Zhou, H. M., Brust-Mascher, I. and Scholey, J. M. 2001. Direct visualization of the movement of

the monomeric axonal transport motor UNC-104 along neuronal processes in living Caenorhabditis elegans. J. Neurosci. **21**, 3749-3755.

Zhu, X., Joh, K., Hedgecock, E.M., Hori, K. 1999. Identification of epi-1 locus as a laminin alpha chain gene in the nematode Caenorhabditis elegans and characterization of epi-1 mutant alleles. DNA Seq.; **10**(4-5):207-17.

Ziel, J.W., Hagedorn, E.J., Audhya, A., Sherwood, D.R. 2009. UNC-6 (netrin) orients the invasive membrane of the anchor cell in C. elegans. Nat Cell Biol; **11**(2):183-9. doi: 10.1038/ncb1825. Epub 2008 Dec 21.

Tables

Gene name	Description	utse	anchor cell	sex muscles	excretory cell	male tail	dorsal intercalation	ventral enclosure	early elongation	late elongation	muscle arms	head mesodermal cell
abcx-1	ABC-transporter					X						
abi-1	Abelson interactor-1				X							
act-1	actin isoform										X	
act-2	actin isoform										X	
act-3	actin isoform										X	
aff-1	fusogen	X	X									
age-1	PI3 kinase								X			
ajm-1	apical junction molecule								X			
amph-1	ortholog of human bridging integrator 2	X										
anc-1	homolog to SYNE1 and SYNE2 proteins, SUN/KASH complex member									X	X	
ani-1	anilin							X	X			
ap-1	clathrin adaptor									X		
apr-1	APC related gene						X	X				
arl-1	ADP-Ribosylation Factor					X						
arx-1	Arp 2/3 complex component							X				

Gene name	Description	utse	anchor cell	sex muscles	excretory cell	male tail	dorsal intercalation	ventral enclosure	early elongation	late elongation	muscle arms	head mesodermal cell
arx-2	Arp 2/3 complex component	X					X	X				
arx-3	Arp 2/3 complex component	X						X				
arx-4	Arp 2/3 complex component							X				
arx-5	Arp 2/3 complex component							X				
arx-6	Arp 2/3 complex component							X				
arx-7	Arp 2/3 complex component							X				
bli-6	collagen				X							
blmp-1	zinc finger and SET domain-containing protein					X						
bub-1	serine/threonine kinase					X						
C35D10.2/gipc-1	ortholog of human GIPC PDZ domain containing 1 protein	X										
cdc-42	RhoGTPase		X			X						
cdh-3	protocadherin	X	X		X							
cdt-1	DNA-replication licensing factor					X						
ced-10	RacGTPase						X		X			
cki-1	cyclin-dependent kinase									X		

Gene name	Description	utse	anchor cell	sex muscles	excretory cell	male tail	dorsal intercalation	ventral enclosure	early elongation	late elongation	muscle arms	head mesodermal cell
ctr-9	PAF1C complex member							X	X			
cwn-1	Wnt	X										
daf-16	forkhead transcription factor	X										
daf-18	lipid phosphatase									X		
daf-2	insulin receptor								X			
daf-4	TGF-β Receptor					X						
dh11.5	synaptotagmin	X										
die-1	zinc finger protein						X					
dlg-1	MAGUK protein								X			
dmd-3	doublesex-related DM gene					X						
dpy-11	thioredoxin-like protein					X						
dpy-18	prolyl hydroxylase					X						
dsh-2	Disheveled							X				
eel-1	E3 ligase									X		
efn-2	ortholog of human ephrin-B3							X				
efn-3	GPI-modified ephrin							X				
egl-13	LIM domain transcription factor	X										
egl-15	FGF receptor										X	
egl-17	FGF-like protein										X	
egl-18	GATA transcription					X						

Gene name	Description	utse	anchor cell	sex muscles	excretory cell	male tail	dorsal intercalation	ventral enclosure	early elongation	late elongation	muscle arms	head mesodermal cell
	factor											
egl-19	α1 subunit of a putative voltage-activated Ca2+ channel protein									X		
egl-43	EVI1 proto-oncogene	X	X									
egl-5	hox gene					X						
emb-9	collagen IV									X		
epi-1	α-laminin				X						X	
eps-8	cell signaling adaptor protein									X		
eva-1	Netrin co-receptor				X						X	
evl-20	ARL2 GTPase							X	X			
F11A10.5	homolog of isoform 2 of Suppressor of tumorigenicity 7	X										
f44d12.4/gipc-2	ortholog of human GIPC PDZ domain containing 1 protein	X										
f55c12.1	RAB-11 homolog	X										
fbl-1	fibulin	X										
fem-2	PP2c phosphatase								X			
fhod-1	formin								X			
fli-1	flightless homolog									X		
fos-1	c-fos transcription factor	X	X									
frk-1	Fer-related kinase-1						X	X	X			

Gene name	Description	utse	anchor cell	sex muscles	excretory cell	male tail	dorsal intercalation	ventral enclosure	early elongation	late elongation	muscle arms	head mesodermal cell
frm-2	ortholog of human FERM domain containing 6 protein	X										
gex-2	WAVE/SCAR complex component	X					X	X			X	
gex-3	WAVE/SCAR complex component						X	X			X	
glb-12	globin	X										
glp-1	Notch receptor	X										
him-4	hemicentin	X	X									
hlh-1	MYOD homologue								X			
hlh-2	Class I basic helix-loop-helix (bHLH) transcription factor, ortholog of the mammalian E and Drosophila Daughterless		X									
hmp-1	α-catenin							X	X			
hmp-2	β-catenin							X	X			
hmr-1	cadherin							X	X			
ifa-3	intermediate filament									X		
ifb-1	intermediate filament									X		

Gene name	Description	utse	anchor cell	sex muscles	excretory cell	male tail	dorsal intercalation	ventral enclosure	early elongation	late elongation	muscle arms	head mesodermal cell
ima-1	importin	X										
ima-2	importin	X										
ima-3	importin	X										
imb-2	importin	X										
imb-3	importin	X										
ina-1	α-integrin	X	X		X							
inx-12	innexin					X						
inx-13	innexin					X						
itr-1	1,4,5-inositol trisphosphate receptor (IP3)	X						X				
jac-1	p120 catenin homologue								X			
kal-1	kalikrein							X				
lam-1	laminin β				X						X	
lam-2	laminin γ										X	
let-4	extracellular leucine-rich repeat only (eLRRon) protein									X		
let-413	ERBIN								X			
let-502	Rho-binding Ser/Thr kinase	X							X			
let-60	Ras										X	
let-7	microRNA					X						
let-756	FGF					X					X	
let-805	myotactin									X		

Gene name	Description	utse	anchor cell	sex muscles	excretory cell	male tail	dorsal intercalation	ventral enclosure	early elongation	late elongation	muscle arms	head mesodermal cell
lev-11	tropomyosin										X	
lim-9	LIM PINCH domain	X										
lin-11	LIM domain transcription factor	X										
lin-12	Notch										X	
lin-17	Frizzled homolog				X							
lin-31	forkhead transcription factor	X										
lin-39	Deformed and Sex combs homeodomain protein	X										
lin-41	RBCC (Ring finger-B box-Coiled coil) protein					X						
lmn-1	nuclear lamin	X										
mab-20	semaphorin					X		X	X			
mab-21	MAB-21 ortholog					X						
mab-26	ephrin ligand					X						
mab-7	protein with hydrophobic type II transmembrane region at the N-terminus, an EGF-like motif, a ShKT motif and a long C-					X						

Gene name	Description	utse	anchor cell	sex muscles	excretory cell	male tail	dorsal intercalation	ventral enclosure	early elongation	late elongation	muscle arms	head mesodermal cell
	terminus											
madd-2	homolog of the Opitz syndrome gene		X								X	
madd-4	ADAMs ortholog										X	
mag-1	Mago nashi homolog									X		
magi-1	PDZ-domain containing, tight junction-associated protein								X			
mcl-4	myosin regulatory light chain								X			
mec-8	RNA binding protein									X		
mel-11	Rho-binding kinase								X			
mig-10	lamillopodin	X	X		X							
mig-15	NCK-interacting kinase	X			X							
mig-2	RhoGTPase								X			
mig-5	Dishevelled						X					
mix-1	SMC2 homolog					X						
mrck-1	serine/threonine kinase								X			
mua-3	ortholog of human collagen, type XIV, alpha 1									X		

Gene name	Description	utse	anchor cell	sex muscles	excretory cell	male tail	dorsal intercalation	ventral enclosure	early elongation	late elongation	muscle arms	head mesodermal cell
mup-4	muscle positioning gene									X		
ncam-1	IgCAM	X										
nhr-2	nuclear hormone receptor transcription factor								X			
nhr-25	nuclear hormone receptor					X			X			
nhr-40	nuclear hormone receptor transcription factor									X		
nmy-1	non-muscle myosin								X			
nmy-2	non-muscle myosin					X			X			
nob-1	Abd-B Homeodomain transcription factor					X						
npp-3	nucleoporin					X						
npp-6	nucleoporin					X						
nud-2	SUN/KASH complex member	X										
pad-2	protein O-fucosyltransferase									X		
pak-1	p21-activated kinase homolog								X			
pat-10	troponin C									X		
pat-2	α-integrin				X					X	X	
pat-3	β-integrin	X	X		X					X		

Gene name	Description	utse	anchor cell	sex muscles	excretory cell	male tail	dorsal intercalation	ventral enclosure	early elongation	late elongation	muscle arms	head mesodermal cell
pat-4	integrin linked kinase										X	
pat-6	actopaxin											
pat-9	nuclear zinc finger protein									X		
php-3	Abd-B Homeodomain transcription factor					X						
phy-1	collagen prolyl 4-hydroxylase							X		X		
pix-1	CDC42/RAC-specific Guanine-nucleotide Exchange Factor (GEF)								X			
plk-1	polo-like serine/threonine kinase					X						
pqn-85	ortholog of the yeast SCC-2 protein	X										
pri-2	eukaryotic-type DNA primase					X						
pst-1	PAPS transporter									X		
ptl-1	Tau-like microtubule binding protein					X						
ptp-2	SH2 domain-										X	

Gene name	Description	utse	anchor cell	sex muscles	excretory cell	male tail	dorsal intercalation	ventral enclosure	early elongation	late elongation	muscle arms	head mesodermal cell
	containing non-receptor protein tyrosine phosphatase											
pxl-1	paxilin	X										
pxn-2	peroxidasin									X		
rab-1	RabGTPase	X										
rab-10	RabGTPase	X										
rab-11.1	RabGTPase	X										
rab-5	RabGTPase	X										
rab-6.1	RabGTPase	X										
ram-1	abnormal RAy Morphology					X						
ram-2	abnormal RAy Morphology					X						
ram-4	abnormal RAy Morphology					X						
ram-5	abnormal RAy Morphology					X						
ran-2	RanGAP	X										
ran-3	RanGAP guanine nucleotide exchange factor RCC-1	X				X						
rcn-1	negative regulator of calcineurin					X						
rga-2	RhoGAP								X			

Gene name	Description	utse	anchor cell	sex muscles	excretory cell	male tail	dorsal intercalation	ventral enclosure	early elongation	late elongation	muscle arms	head mesodermal cell
rho-1	RhoGTPase	X							X			
rib-1	homolog of human tumor suppressor EXT gene						X	X				
rib-2	ortholog of human EXT2							X				
rme-8	DNA J domain-containing protein					X						
rpa-1	DNA-binding replication protein					X						
rrc-1	RhoGAP	X										
rsef-1	RASEF ortholog	X										
sax-1	serine/threonine kinase	X										
sax-3	Robo				X		X					
sax-7	L1 CAM	X										
sec-15	exocyst complex	X										
sem-5	GRB2										X	
slt-1	Slit				X							
sma-1	β-spectrin								X			
sma-2	SMAD					X						
sma-3	SMAD					X						
sma-4	SMAD					X						
smo-1	SUMO									X		
smu-1	WD40 repeat protein									X		
soc-1	multisubstrate										X	

Gene name	Description	utse	anchor cell	sex muscles	excretory cell	male tail	dorsal intercalation	ventral enclosure	early elongation	late elongation	muscle arms	head mesodermal cell
	adaptor (MSA) protein containing an amino-terminal pleckstrin homology domain (PHD)											
soc-2	leucine-rich repeat protein										X	
sos-1	ortholog of Son of sevenless										X	
spc-1	α-spectrin								X			
spon-1	F-spondin									X		
srsx-18	GPCR	X										
sym-1	extracellular leucine-rich repeat only (eLRRon) protein									X		
tbx-8	T box transcription factor						X					
tbx-9	T box transcription factor						X					
ten-1	tenurin						X	X		X		
tlp-1	C2H2 Zn-finger presumptive transcription factor					X						
toca-1	F-BAR protein	X										
ttx-3	LIM domain	X										

Gene name	Description	utse	anchor cell	sex muscles	excretory cell	male tail	dorsal intercalation	ventral enclosure	early elongation	late elongation	muscle arms	head mesodermal cell
	transcription factor											
umps-1	uridine-5'-monophosphate synthase									X		
unc-104	kinesin				X							
unc-112	pleckstrin homology domain-containing protein									X		
unc-116	kinesin				X							
unc-13	Rho target	X										
unc-33	microtubule binding protein CRMP	X									X	
unc-34	Enabled/VASP homolog				X			X				
unc-39	homolog of the human myotonic dystrophy-associated homeodomain protein Six5											X
unc-40	netrin receptor		X								X	X
unc-45	muscle-specific protein									X		
unc-5	Netrin receptor				X							X
unc-51	serine/threonine protein kinase										X	
unc-52	perlecan				X					X	X	

Gene name	Description	utse	anchor cell	sex muscles	excretory cell	male tail	dorsal intercalation	ventral enclosure	early elongation	late elongation	muscle arms	head mesodermal cell
unc-53	NAV	X		X	X							
unc-54	muscle myosin class II heavy chain										X	
unc-6	netrin ligand		X		X						X	X
unc-60B	cofilin										X	
unc-64	syntaxin	X										
unc-70	beta-G spectrin	X										
unc-71	ADAM protease				X							
unc-73	Trio	X			X				X		X	
unc-82	serine/threonine kinase									X		
unc-83	SUN/KASH complex member	X										
unc-84	SUN/KASH complex member	X										
unc-93	component of a multi-protein complex containing the SUP-9 two-pore potassium channel and the SUP-10 transmembrane protein										X	
unc-94	Tropomodulin								X			
unc-95	LIM domain-containing protein										X	
unc-97	LIM PINCH	X								X	X	

Gene name	Description	utse	anchor cell	sex muscles	excretory cell	male tail	dorsal intercalation	ventral enclosure	early elongation	late elongation	muscle arms	head mesodermal cell
	domain											
unc-98	dense body component										X	
vab-1	Ephrin receptor tyrosine kinase							X				
vab-10	plakin									X		
vab-19	ankyrin repeat protein									X		
vab-2	ephrin							X				
vab-3	Pax-6 homeodomain protein	X										
vab-8	kinesin				X							
vab-9	claudin								X			
vps-32	ESCRT-III protein								X			
wht-5	ABC-transporter					X						
wip-1	WASP-interacting protein homologue							X				
wrt-5	hedgehog related gene								X			
wsp-1	WAVE/SCAR complex component							X			X	
wve-1	WAVE/SCAR complex component	X					X				X	
xpo-2	nuclear export					X						

Gene name	Description	utse	anchor cell	sex muscles	excretory cell	male tail	dorsal intercalation	ventral enclosure	early elongation	late elongation	muscle arms	head mesodermal cell
	factor											
zag-1	ZFH class homeodomain protein	X										
zfh-2	homeobox protein	X										
zfp-1	homolog of AF10	X										
zif-1	E3 ubiquitin ligase substrate-recognition subunit		X									
zmp-1	zinc metalloprotease	X	X									
zoo-1	Zonula occluden								X			

Table 1: Table of all genes involved in cell outgrowth and their associated tissues.

Genes listed with their descriptions as well as the tissues in which they function.

	utse	anchor cell	sex muscles	excretory cell	male tail	dorsal intercalation	ventral enclosure	early elongation	late elongation	muscle arms	head mesodermal cell
utse		*aff-1, cdh-3, egl-43, fos-1, him-4, ina-1, mig-10, pat-3, zmp-1*	*unc-53*	*cdh-3, ina-1,mig-15, mig-10, pat-3, unc-53, unc-73*	*ran-3*	*arx-2, gex-2, wve-1*	*arx-2, arx-3, gex-2, itr-1*	*let-502, unc-73, rho-1*	*pat-3, unc-97*	*gex-2, unc-33, unc-97, wve-1*	*unc-40, unc-73*
anchor cell	*aff-1, cdh-3, fos-1, egl-43, him-4, ina-1, mig-10, pat-3, zmp-1*			*cdh-3, ina-1, mig-10, pat-3, unc-6*	*cdc-42*				*pat-3*	*madd-2, unc-6, unc-40*	*unc-6*
sex muscles	*unc-53*			*unc-53*							

excretory cell	*cdh-3, ina-1, mig-10, mig-15, pat-3, unc-53, unc-73*	*cdh-3, ina-1, mig-10, pat-3, unc-6*	*unc-53*	[redacted]		*sax-3*	*unc-34*	*unc-73*	*pat-2, pat-3, unc-52*	*epi-1, eva-1, lam-1, pat-2, unc-6, unc-52, unc-73*	*unc-5, unc-6*
male tail	*ran-3*	*cdc-42*			[redacted]		*mab-20*	*mab-20, nmy-2*	*nhr-25*	*let-756*	
dorsal intercalation	*arx-2, gex-2, wve-1*			*sax-3*		[redacted]	*apr-1, arx-2, frk-1, gex-2, gex-3, rib-1, ten-1*	*ced-10, frk-1*	*ten-1*	*gex-2, gex-3, wve-1*	
ventral enclosure	*arx-2, arx-3, gex-2, itr-1*			*unc-34*	*mab-20*	*apr-1, arx-2, frk-1, gex-2, gex-3 ,rib-1, ten-1*	[redacted]	*ani-1, evl-10, frk-1,hmp-1, hmp-2, hmr-1, mab-20, ctr-9*	*phy-1, ten-1*	*gex-2, gex-3, wsp-1*	
early elongation	*let-502, unc-73, rho-1*			*unc-73*	*mab-20, nmy-2*	*ced-10, frk-1*	*ani-1, evl-10, frk-1,hmp-1, hmp-2, hmr-1, mab-20, ctr-9*	[redacted]			*unc-73*

late elongation	*pat-3, unc-97*	*pat-3*	*pat-2, pat-3, unc-52*	*nhr-25*	*ten-1*	*ten-1, phy-1*			*pat-2, pat-6, unc-52, unc-97*
muscle arms head	*gex-2, wve-1, unc-33, unc-97*	*madd-2, unc-6, unc-40*	*epi-1, eva-1, lam-1, pat-2, unc-52, unc-6, unc-73*	*let-756*	*gex-2, gex-3, wve-1*	*gex-2, gex-3, wsp-1*	*unc-73*	*pat-2, pat-6, unc-52 unc-97*	*unc-6, unc-40*
mesodermal cell	*unc-73*	*unc-6, unc-40*	*unc-5, unc-6*						*unc-6, unc-40*

Table 2: Matrix of pairwise interactions of genes in different tissues

Rows and colums show which genes are shared between tissues in a pairwise fashion.

Figures

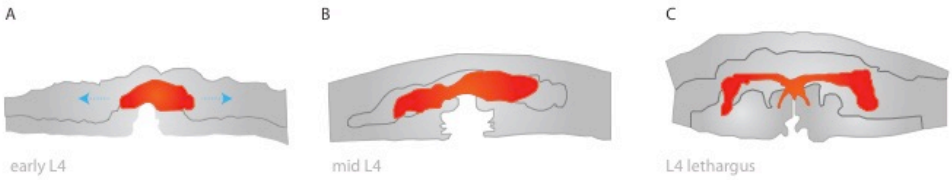

Figure 1: utse outgrowth over time

Schematic of utse outgrowth over time **(A)** Early L4 vulva and uterus. The utse has just for
this stage after the fusion of eight ρ cells and the anchor cell. The cell has an ellipsoidal
Outlines indicate positions of vulva and uterus. utse is indicated in red. Blue dashed arrows i
direction of outgrowth. **(B)** Mid L4 vulva and uterus. utse has begun elongating along the a
posterior axis. Outlines indicate positions of vulva and uterus. utse is indicated in red. **(**
lethargus vulva and uterus. utse has completed its outgrowth, and has taken on an elongated
with the edges of its arms extending along the dorsal/ventral axis. Outlines indicate positi
vulva and uterus. utse is indicated in red.

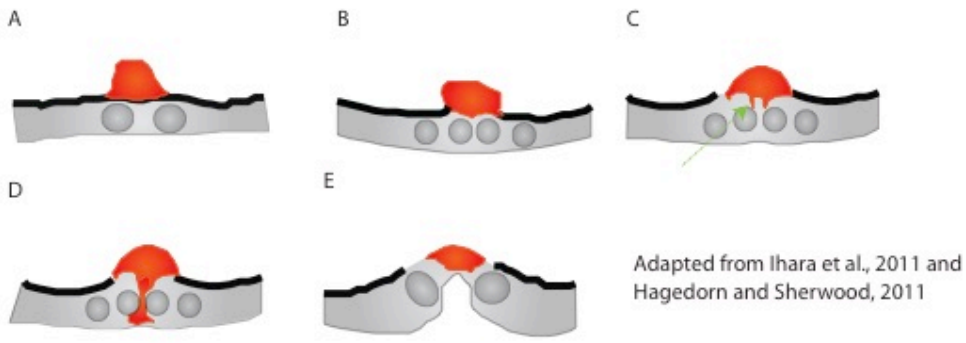

Figure 2: Anchor cell invasion

Schematic anchor cell invasion. Anchor cell shown in red, vulva shown in gray. Basement membrane shown in thick line. **(A)** Anchor cell at P6.p two cell stage during mid L3. Basement membrane (shown in thick line) is intact. Anchor cell is dorsal to the P6.p 1° VPC daughters (two circles below). **(B)** Anchor cell at P6.p four cell stage during mid to late L3. Anchor cell has generated a gap in the basement membrane (see separation between thick lines). Edges of the anchor cell are still in contact with the anchor cell. **(C)** Anchor cell at P6.p late four cell stage (late L3). The anchor cell has begun forming protrusions that will invade the vulva (see dashed green arrow). **(D)** Anchor cell at P6.p late four cell stage (late L3). The anchor cell has completely invaded the vulva, specifically invading between the 1° VPC granddaughters. **(E)** Anchor cell at early L4 stage. The 1◦ VPCs have divided and proximal cells are shown. Vulval invagination has occurred and anchor cell will soon fuse with the ρ cells to form the utse.

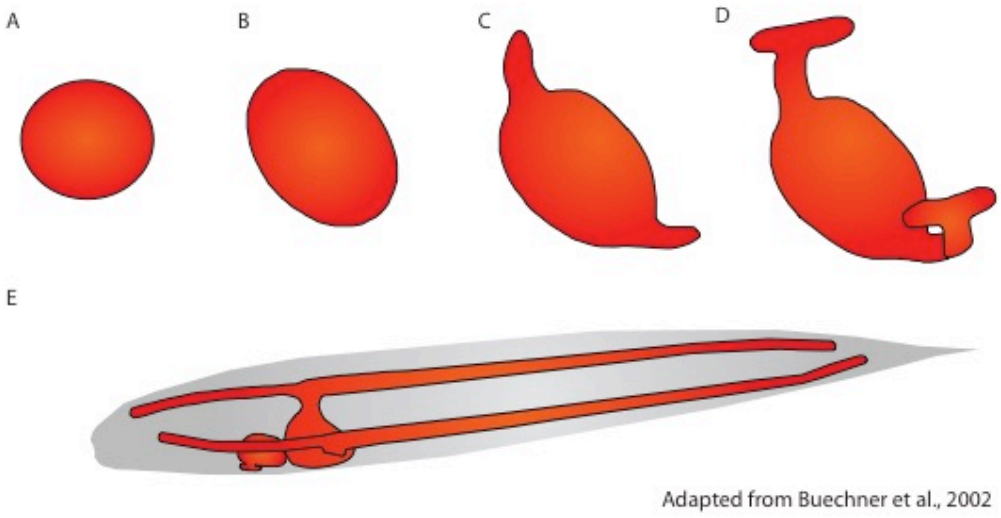

Figure 3: Excretory cell outgrowth

Schematic of excretory cell outgrowth. Excretory cell in red, outline of worm in black. **(A-D)** Excretory cell outgrowth during three-fold embryonic stage. **(A)** Excretory cell at birth, cell has a spherical shape. **(B)** Cell takes on an ellipsoidal shape as it is preparing to undergo outgrowth. **(C)** Apical and basal edges of the excretory cell begin migrating dorsally. **(D)** Edges of dorsal protrusions bifurcate and begin to grow outward laterally along the anterior posterior axis. **(E)** Completed excretory cell outgrowth (L1). Cell has extended laterally along the anterior posterior axis to span the entire length of the worm.

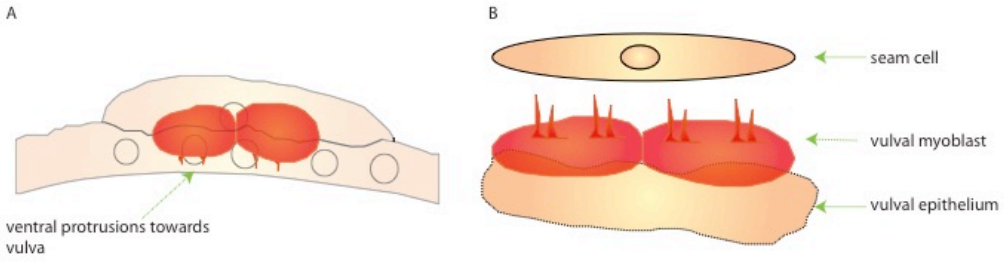

Figure 4: Sex muscle outgrowth

Schematic of sex myoblasts at L3 larval stage **(A)** Lateral view of L3 vulva. Sex myoblast daughter cells (shown in red) extend protrusions ventrally towards the vulva. **(B)** Top-down view of L3 vulva. Sex myoblasts are in between the vulval epithelium and the seam cells of the hypodermis. Sex myoblasts extend protrusions longitudinally towards the seam cells.

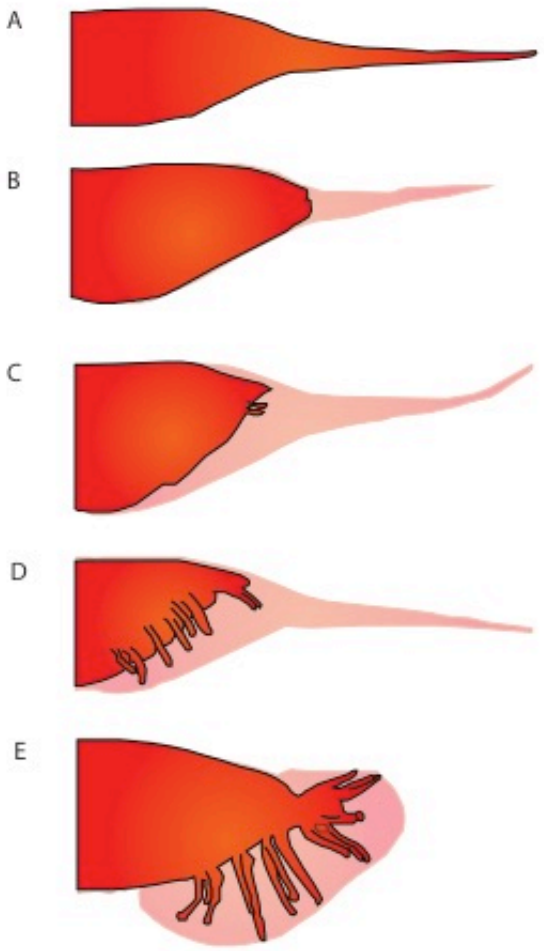

Figure 5: Male tail cell shape change and outgrowth

Schematic of male tail retraction and ray formation from L3 to adulthood. **(A)** Male tail at L3, retraction and ray formation have not occurred and entire cell is composed to tail epithelium. **(B)** Beginning of tale retraction in L4. Light red indicates fluid filled extracellular space previously inhabited by tail epithelium. **(C)** L4 stage. Continuation of retraction in male tail, start of ray formation. **(D)** L4 stage, male tail has finished retracting and rays have all formed. **(E)** Adult male tail. Rays have reached their final shape. Fluid filled extracellular space has taken peloderan shape.

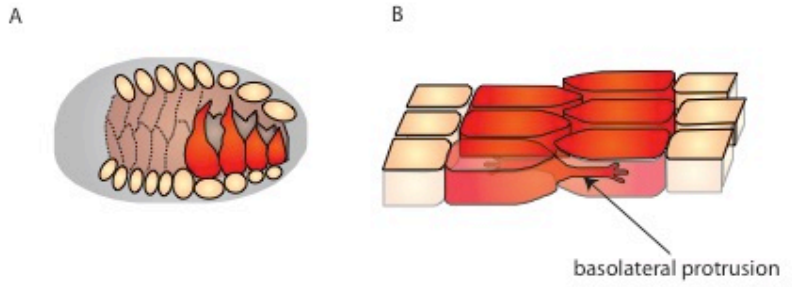

Adapted from Chisholm and Hardin, 2005

Figure 6: Dorsal intercalation

Schematic of dorsal intercalation. **(A)** Dorsal view of embryo undergoing intercalation. Intercalating epidermal cells shown in red. Dashed lines indicate cells that have already intercalated. Cells that are intercalation are changing from a rounded shape to a more wedge/protrusion like shape. **(**B) Expanded view of intercalating cells. Basolateral protrusions that also which touch neighboring cells, and help the intercalating cells move towards one another.

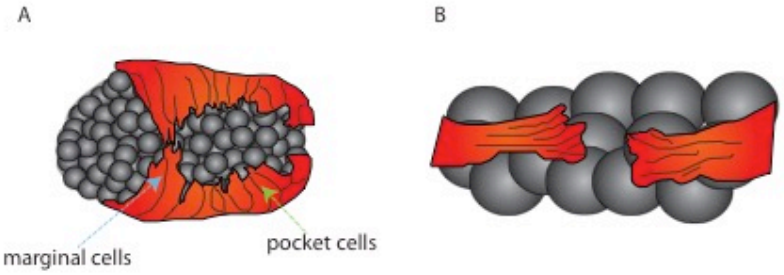

Adapted from Chisholm and Hardin, 2005

Figure 7: Ventral Enclosure

Schematic of ventral enclosure. Ventral epidermal cells shown in red, neuroblasts shown in gray spheres. **(A)** Outgrowth of epidermal cells during ventral enclosure. Ventral marginal cells are indicated with blue arrow and pocket cells are indicated with green arrow. **(B)** Expanded view of ventral epidermal cells moving along the neuroblast substratum.

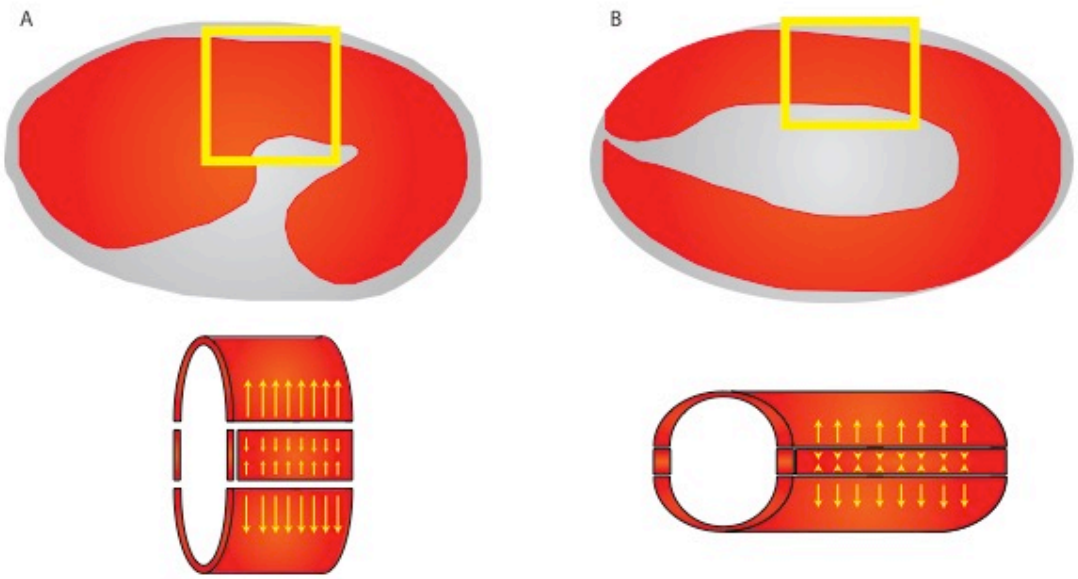

Adapted from Chisholm and Hardin, 2005

Figure 8: Embryonic Elongation

Schematic of embryonic elongation. Body of worm shown in red. **(A)** Beginning of embryonic elongation. Top image shows the shape of the worm body prior to elongation. Inset below is from yellow box. Yellow arrows in inset shows the forces that are mediated by circumferential actin bundles within the embryo. **(B)** Completion of embryonic elongation. Top image shows the shape of the worm after completed elongation. Inset below is from yellow box. Yellow arrows in inset shows the result of forces that are mediated by circumferential actin within the embryo.

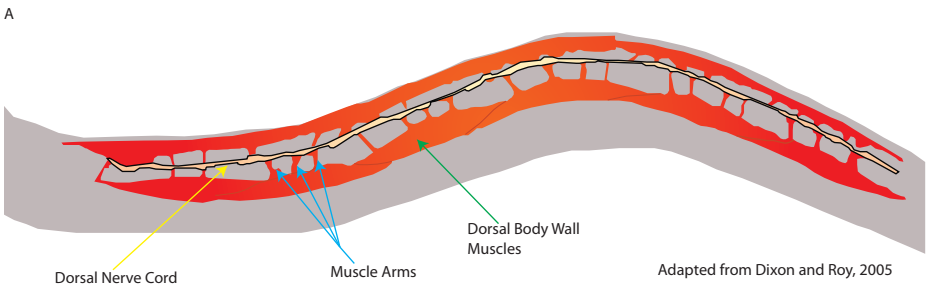

Figure 9: Muscle arm extension

Schematic of muscle arm extension **(A)** Example of muscle arms extension. Muscle arms have formed from the dorsal body wall muscles towards the dorsal nerve cord.

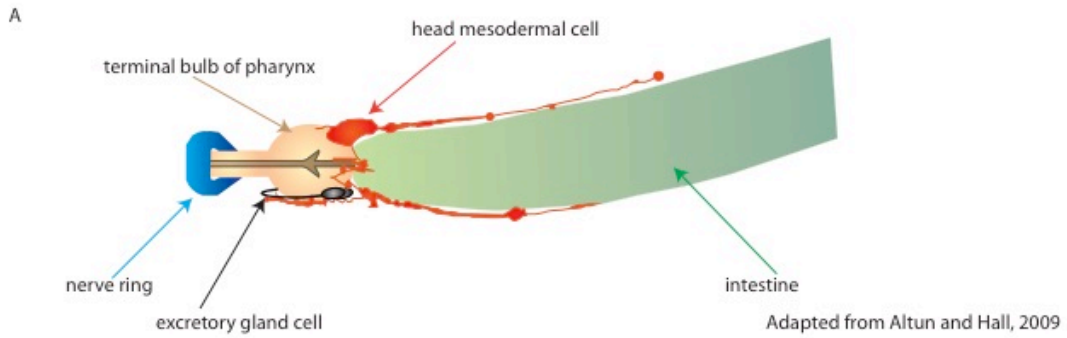

Figure 10: Head mesodermal cell

Schematic of head mesodermal cell. **(A)** Positioning of head mesodermal cell in adult worm. Head mesodermal cell lies dorsomedial to the terminal bulb of the pharynx. It extends out processes that split at the pharynx and extend anteriorly and posteriorly along the dorsal and ventral margins of the body wall. These processes also lie adjacent to the intestine as well as the excretory gland cell.

Gonad Embryo

Figure 11: Gene families figure

A) Schematic of types of tissues involved. Vertical axis shows number of tissues involved, horizontal axis indicates which tissue types genes are involved in. Yellow indicates genes that have greater involvement in gonad cell outgrowth and blue indicates genes that have greater involvement in embryonic cell outgrowth. By using a colored heat map to assign function in either gonadal or embryonic tissues, we were able to categorize genes that act as master regulators in these tissues. Yellow represent more gonadal identity and blue represents more of an embryonic identity.

CHAPTER 3

Spatial and molecular cues for cell outgrowth during *C. elegans* uterine development

3.1 Abstract

The *Caenorhabditis elegans* uterine seam cell (utse) is an H-shaped syncytium that connects the uterus to the body wall. Comprising nine nuclei that move outward in a bidirectional manner, this synctium undergoes remarkable shape change during development. Using cell ablation experiments, we show that three surrounding cell types affect utse development: uterine toroids, the anchor cell, and the sex myoblasts. The presence of the anchor cell (AC) nucleus within the utse is necessary for proper utse development, and AC invasion genes *fos-1, cdh-3, him-4, egl-43, zmp-1,* and *mig-10* promote utse cell outgrowth. Two types of uterine lumen epithelial cells, uterine toroid 1 (ut1) and uterine toroid 2 (ut2), mediate proper utse outgrowth, and we show roles in utse development for the following uterine toroid localized genes: RASEF ortholog *rsef-1* and Trio/*unc-73*. The SM localized gene *unc*-53/NAV regulates utse cell shape and ablation of sex myoblasts (SMs), which generate uterine and vulval muscles, and cause defects in utse morphology. Our results clarify the nature of the interactions that exist between utse and surrounding tissue, identify new roles for genes involved in cell outgrowth, and present the utse as a new model system for understanding cell shape change and, putatively, diseases associated with cell shape change.

3.2 Introduction

Understanding the mechanisms necessary for one cell's behavior can shed light on the genetic inputs necessary for a broad range of tissues. Many growing cells reorganize their cytoskeletons and respond to attractive and repulsive cues to reach their final developmental destinations, promoting tissue development, as seen with cells in the vertebrate neural crest, the *Drosophila* caudal visceral mesoderm, and neural growth cones (Hall, 2009; Le Douarin and Kalcheim 1999; Theveneau and Mayor, 2012; Bronner and Le Douarin, 2011; Kadam et al., 2012; Vitriol and Zheng, 2012; Ramón y Cajal, 1890; Gomez and Zheng, 2006). *C. elegans* is a useful model for understanding these types of cell behavior. For instance, the TLX/*tailless* ortholog *nhr-67* controls *C. elegans* male gonad linker cell migration (Kato and Sternberg, 2009), and is well characterized in the developing *Drosophila* nervous system (Pignoni 1990), and in mouse neural stem cell generation (Zhang et al., 2008). Netrin/UNC-6 and its receptor, UNC-40, were also discovered in *C. elegans* (Hedgecock et al., 1997; Hedgecock et al., 1990; Ishii et al., 1992) and are key attractive and repulsive cues necessary for growth cone outgrowth. Therefore, characterizing the cell biology

of *C. elegans* tissues has had broader implications in understanding mechanisms of other cell systems.

The *Caenorhabditis elegans* uterine seam cell (utse) is a syncytium that undergoes a striking outgrowth and nuclear migration during its development. Given the power of genetics in *C. elegans,* we thought that the utse offered an excellent system to study novel molecular mechanisms involved in cell outgrowth, cell shape change, and syncytial cell biology.

Studying cell outgrowth and shape change provides valuable insights for a variety of systems. Aside from its role in growth cone migration and metastatic cancers, cell outgrowth and cell shape change are also involved in wound healing, through the recruitment of keratinocytes that extend lamellipodia towards the wound site (Martin and Leibovich, 2005; Grinnell, 1992; Martin, 1997), as well as during TGF-β signaling driven transformation of fibroblast cells to myofibroblasts (which form cytoplasmic filamentious apparatuses cells in the presence of the wound) (Gabbiani 2003; Gabbiani et al., 1971). Study of utse outgrowth can provide important information to the regulation of these systems.

The utse is a syncytium formed by the fusion of nine cells. Several syncytial systems exist in biology, including embryonic and adult musculature, and vertebrate placenta (Biressi et al., 2007; Robertson et al., 1990; Robertson et al., 1993; Cross, 2000). The fusion events that contribute to the creation of these tissues have been well characterized; studying the cell behavior of the utse can contribute to understanding the morphogenetic movements that these syncytiums undertake. For instance, after fusion of post-mitotic precursor cells that make up the syncytial layer of the placenta, the syncytioblast, this syncytial layer expands and flattens to form a layer of tissue between the mother and fetus (Cross, 2000). Genetic inputs that control this behavior are not characterized and the utse can act as a model to study syncytial movement. Furthermore, abnormal placental formation can result in a slew of diseases, including preeclampsia, and therefore information contributing to the syncytium regulation can prove vital.

The utse is also a heterokaryon, since it results from the fusion of two cell types, uterine υ cells and the anchor cell. Investigating utse cell biology can contribute to our understanding of heterokaryons, which occur broadly in biology. Some examples include their presence in fungi, such as in *Schizophyllum commune,* where genes from two types of nuclei (SC3/SC4) come together to interact with one another transcriptionally (Schuurs et al., 1998); their involvement in cell

reprogramming (the fusion of embryonic stem cells with somatic cells induces pluripotency (Tada et al., 2001)); their promotion of tumor proliferation (through fusion of tumor cells with non-tumorigenic cells) (Berndt et al., 2013); and their association with multiple sclerosis (fusion of bone marrow cells and cerebelluar Purkinje cells in brain tissue of patients with multiple sclerosis) (Kemp et al., 2012).

Due to the unique characteristics of the utse being both a syncytium and a heterokaryon, and because its mechanisms for outgrowth are predominantly uncharacterized, we chose to study the molecular inputs involved in utse development. In this work, we sought to determine which surrounding uterine cells play a role in utse development. Using laser ablation we identified four cell types involved in utse development: the anchor cell (AC), uterine toroid 1 (ut1), uterine toroid 2 (ut2), and the sex myoblasts (SMs). We show that genes involved in AC invasion have an additional role promoting utse cell outgrowth. ut1 and ut2 are epithelial cells that are part of the uterine lumen, and through a candidate RNAi based screen on genes expressed in these cells, we identified two genes that play roles in for utse-ut interactions: RASEF/*rsef-1* and Trio/*unc-73*. The SMs form the uterine and vulval muscles that laterally flank the utse, and we show roles for the SM localized gene, *unc-53*/NAV, in utse outgrowth. These results identify both external and internal cues necessary for utse development and characterize genes contributing to the production of these cues.

3.3 Materials and Methods

Strains and genetics: *C. elegans* were handled as described previously (Brenner, 1974). All strains used (listed in supplementary material Table S1) are derivatives of *C. elegans* wild-type strain (N2 Bristol).

RNAi experiments: RNAi was performed by feeding nematodes dsRNA-producing bacteria using standard procedures (Timmons et al., 2001) modified as follows. Overnight starter cultures were grown with 1 ml LB supplemented with 25 μg/ml carbenicillin and 12.5 μg/ml tetracycline inoculated with a bacterial colony containing a plasmid producing dsRNA targeting a gene of interest. Starter cultures were diluted 1:80 the next day, using 100 ul of starter culture in 8ml LB containing 25 ug/ml carbenicillin. Cultures were grown between 6-8 hours to OD_{600} ~ 0.5. 6 cm Petri plates containing NGM agar that had been dried for at least three days at room temperature were prepared by using sterile glass beads to spread 50 μl of 25 mM carbenicillin, and 1 mM IPTG

in M9 on each plate. RNAi cultures were then transferred to 1.5 ml microcentrifuge tubes (1 tube/plate) and then spun at 5000 rpm for 5 minutes. The majority of the supernatant was removed, leaving about 50ul of liquid plus bacterial pellet. Pellets were then resuspended in this solution, and then spread using sterile glass beads on the NGM agar + carbenicillin + IPTG Petri plates described in the preceding step. Plates were grown at room temperature overnight, and, if not used immediately, were stored at 4˚C for no more than a week. On the day of the experiment, plates were pipetted with 50 µl of a 1:5 solution of 1M IPTG:M9. Plates were then dried for 10 minutes near a Bunsen burner. Eggs were bleached onto RNAi plates and allowed to hatch and develop. Phenotypes were scored at the L4 lethargus stage. For RNAis used see Table S2.

Scoring utse phenotypes: Animals were scored using a wide-field epifluorescence microscope at young adult or L4 lethargus stage. Wild-type utse cell body length is between 300-400 µm, and distance between wild-type nuclei is between 250-350 µm. Animals were classified as abnormal if both the utse cell body and nuclear distance were 50 µm greater or less than that of the wild type range (i.e., an animal was still classified as abnormal if its cell body was within the wild-type range but its nuclear distance was not.) All abnormal animals in this publication fit within this criteria and some exhibit other defects, such as missing arms, abnormal shape, or holes in portions of the cytoplasm.

Transgenics: To make the *exc-9::mcherry* construct, 20ng/µl of *exc-9::mcherry* plasmid (pBK162, *exc-9::mcherry* gateway plasmid, from M. Buechner, WBperson81) was injected into *unc-119(ed4)* with an *unc-119* rescue construct.

Ablations: Cell ablation experiments were performed as described (Bargmann and Avery, 1995). Dorsal uterine cells and uterine toroid cells were ablated at late L3 (see Figure 2B-B''' and Figure 3A). Anchor cells were ablated at early L4 (see Figure 2D-D''' and Figure 4A). Sex myoblasts were ablated at L1 (see Figure 9M,O,Q). All ablated worms were scored between late L4 and L4 lethargus.

3.4 Results

3.4.1 Wild-type *C. elegans* utse behavior

The hermaphrodite uterus is composed of several different cell types (Figure 1A). The uterus lies dorsal to the vulva, and is derived from the dorsal uterine (DU) and ventral uterine (VU) cell lineages (Figure S1A; Newman et al., 1996). The DU and VU lineages generate several different cell types, such as the dorsal uterine cell (du), which makes up the dorsal most portion of the uterus, uterine toroid (ut) cells, which line the uterine lumen, and the uterine-vulva (uv) cells, which connect the uterus to the vulva (Figure 1A, 1F, 3A and 4A).

The utse attaches the uterus laterally to the body wall via the seam cells (Figure 1A). The utse in *C. elegans* mid L4 hermaphrodite is shown in Figure 1B. utse nuclei are marked with *egl-13::gfp,* which marks the υ cells (see below for definition), and *cdh-3::PH::mcherry,* which uses the phospholipase-C plekstrin-homology (PH) domain fused to mCherry to direct expression in the utse cell body/plasma membrane (Figure 1D-E; Ihara et al., 2011). At mid L4 (Figure 1B-1E) the utse is undergoing both cell outgrowth and nuclear migration and it will reach its final shape at L4 lethargus (Figure 10-1R). The ventral view of the utse (Figure 1F) highlights its H-shaped form, with the middle of the H lying above the vulval opening, and the two sides mediating a connection between the seam cells of the body wall and ut2 (Figure 1F-1J).

At late L3 stage, six of the VU granddaughter cells are induced via LAG-2-LIN-12 Notch-Delta signaling from the AC to become π cells (Figure S1B-C; Newman et al., 1995). After these six π cells are induced they divide to make 12 π-progeny cells (Figure S1C-D; Newman et al., 1996). Four of these 12 π-progeny cells become the uv1 via EGF signaling (Figure S1E; Chang et al., 1999) from the vulval VulF cells; the remaining eight will later fuse with one another and then with the AC to form the syncytial cell body of the utse by the mid fourth larval (L4) stage via the fusogen AFF-1 (Figure S1F; Figure 1K-N; Sapir et al., 2007). We will henceforth refer to the eight π-progeny cells that do not become uv1 and form the utse nuclei as υ (upsilon) cells. During early L4, as visualized in Figure 2B-B’’’, the AC induces surrounding π cells but has not yet fused with these cells (since *cdh-3::PH::mcherry* expression is limited to the AC), and later in L4, as seen in Figure 2C’-C’’’, the AC has fused with the π-progeny cells, the υ cells (*cdh-3::PH::mcherry* has spread throughout the entire utse cell body).

Over the next eight hours the utse cell body grows bi-directionally along the anterior-posterior axis, and the utse nuclei segregate into two groups (Figure 2F’’-F’’’), migrate along the anterior posterior axis, and settle at the anterior/posterior edges of the utse cell body (Figure 2H-H’’’; Newman et al.,

1996). The utse cell body extends ahead of its nuclei during development (Figure 2E'''), indicating that separate mechanisms may be controlling these two behaviors; however, we observe defects in cell morphology associated with aberrant nuclear positioning (Figure 6). Therefore, both aberrations in nuclear migration and cell outgrowth were used to characterize defective utse development (see Materials and Methods for specific criteria for scoring phenotypes).

Two genes have been previously characterized for their roles in proper utse cell elongation and nuclear migration: the LIM domain transcription factor *lin-11* and the SOX domain transcription factor *egl-13* (Newman et al., 1999; Hanna-Rose and Han, 1999; Cinar et al. 2003). Both *lin-11* and *egl-13* are involved in AC fusion with the utse, as well as induction of π cell fate, and their role in utse cell outgrowth/nuclear migration has been attributed to these behaviors. We wished to better understand the role of the AC in utse development, as well as identify cues from surrounding uterine cells acting on the utse.

3.4.2 Surrounding uterine cells have an effect on utse development

We hypothesized that interactions between the utse and its surrounding tissues would be necessary for proper utse development. To this end, we ablated surrounding uterine cells and observed subsequent effects on utse development (Figure 3A). utse development was assessed by examining υ cell nuclei marked with nuclear-localized GFP driven by an *egl-13* promoter, and by examining utse cell bodies marked by *exc-9::gfp* translational fusion reporter. (Figure 3B-3I; Wendy Hanna-Rose personal communication, Tong and Buechner, 2008).

Without the presence of *egl-38*-dependent EGF signal necessary for uv1 cell fate, presumptive uv1 cells take on υ cells identities and fuse with the naturally occurring υ cells to form a wild-type utse with extra nuclei (Chamberlin et al., 1997). *cog-3/pnc-1* mutants lack the EGF signal necessary for uv1 fate and do not form uv1 cells, and these mutants show no defects in utse cell fate specification or morphology (Huang and Hanna-Rose, 2006). We therefore infer that uv1 cells do not affect utse development and chose not to ablate these cells.

We hypothesized that the du cell could potentially be pushing downward on the utse, causing it to stretch outward. However, du ablation had no effect on utse cell behavior (0%, n=26). Next, we tested the effect of the surrounding uterine toroid cells on utse development by ablating each set of

uterine toroid cells. Cell ablations were performed at early L4 stage. At this stage the four nuclei found within each toroid cell were easily visualized, lumen formation had not occurred (uterine toroid lumen formation occurs at mid L4), and utse development had not commenced (Figure 2B-B’’’, Figure 3A, Newman et. al, 1996). Figure 3A shows the progression of ut1 ablation. Animals were scored at L4 lethargus, approximately 6-8 hours after ablation. Mock ablations with exposure to anesthetic used (3mM levamisole) had no effect on utse development (0% defect, n=10; Table 1; Figure 3B-C). Ablations of uterine toroid 1 (ut1) or uterine toroid 2 (ut2) caused defects in utse development (Figure 3D-3G, Table 1). 88% percent of ut1-ablated worms (n=26) showed defects in nuclear migration (compare Figure 3D to 3B) and had utse cell bodies that were both shorter than wild type and missing portions (compare Figure 3E to 3C). ut2 is the second most proximal toroid cell to the utse, and is the last toroid cell with which the utse makes contact (Newman et al., 1996). 91% of ut2 ablated worms showed defects (n= 12, Table 1) including reduced distance between utse nuclei in ut2 ablated worms (compare Figure 3F to 3B), and shorter cell bodies containing missing portions and vacuoles (compare Figure 3G to 3C). Ablation of the next most distal ut cell, ut3, which has no direct contact with the utse, caused no defects in nuclear migration or cell outgrowth (Compare Figure 3H-I to Figure 3B-C). We conclude that ut1 and ut2 are involved in utse development.

3.4.3 Internal signals involved in utse development

Since the AC fuses with the utse during early L4 (Figure 2C-C’’’; Sapir et al., 2007) we asked if transcription within the AC-derived nucleus was necessary for utse development. We performed the cell ablations after mid L4, the stage at which the AC had already induced π cells and fused with the υ cell nuclei, and its nucleus could be easily identified due to its position in a unique plane of focus relative to other nuclei in the worm (Figure 2D-D’’’, Figure 4A; Félix and Sternberg, 1996). This timing of the ablation avoided any secondary effects that could have resulted from earlier ablations of the AC. AC nuclear ablation caused defects in utse development (86% abnormal, n=23). utse nuclei were clustered together in AC nuclear ablated worms (compare Figure 3B to 4B) and utse cell bodies were short and deformed (compare Figure 3C to 4C). As a control, we ablated υ cell nuclei to determine if defects were truly AC nuclei specific or a result of ablating any nucleus in the utse. Ablation of υ cell nuclei resulted in wild-type phenotypes (0% defects, n=6; Table 1). Since we specifically ablated the AC nucleus after fusion, we also eliminated the possibility that the AC

cytoplasm was contributing to utse outgrowth. The finding that the AC nucleus is necessary for utse development suggests that transcription factors expressed in the nucleus are required, as addressed below.

3.4.4 AC fusion is necessary for utse development

To verify if the AC was necessary for utse development, we observed utse development in the absence of AC-utse fusion. During early L4, the AC fuses with the utse via the fusogen *aff-1* (Sapir et al., 2007). *aff-1(RNAi)* treatment resulted in a clear failure of AC fusion as assayed by the *cdh-3::PH::mcherry; egl-13::gfp* marker initially expressed in the AC (Figure 5A-C; Table 2) and defective utse cell outgrowth, as assayed by *exc-9::gfp* (Figure 5D). Even though there is no AC fusion in these worms, the υ cell nuclei still migrated outward, albeit at a distance shorter than that of wild type (Figure 5C).

To rule out that these defects did stem from global issues in cell fusion, we examined the function of *eff-1,* which is involved in heterologous fusion events in *C. elegans* (Podbilewicz et al., 2006). Worms treated with *eff-1(RNAi)* showed a small but statistically significant defect in utse nuclear migration (11%, n= 43, P-value 0.0087; Table 2E) and no defects in utse cell outgrowth (0%, n=7; Table 2E).

3.4.5 AC invasion genes act during L4 to affect utse development

During late L3, the AC forms protrusions that span the basement membrane between the uterus and the vulva to invade the vulval epithelium (Sherwood and Sternberg, 2003). Because the AC changes its shape during protrusion formation, we hypothesized that genes involved in this process can also contribute to utse cell shape change. During AC invasion, the *c-fos* transcription factor ortholog *fos-1* promotes expression the zinc metalloprotease *zmp-1,* the protocadherin *cdh-3,* the zinc finger protein *egl-43,* of the hemicentin extracellular matrix protein gene *him-4,* and lamillopodin/*mig-10*; the activities of these genes induce the AC to form ventrally directed protrusions that breach the basement membrane (Figure 6A; Sherwood et al., 2005; Hwang et al. 2007; Wang et al., 2014). RNAi against the AC invasion genes resulted in defects in utse development (Table 2E; Figure 6B-D; 6F-H; 6J-L; 6N-P; 6R-T; 6V-X), supporting our hypothesis that genes involved in AC protrusion formation also affect utse development.

Each of these genes are expressed within the AC during invasion (Sherwood et al., 2005; Hwang et al. 2007; Wang et al., 2014). Since the AC nucleus is necessary for utse development, we asked if these genes were transcriptionally active throughout L4 and were present in the utse. We observed that transgene reporters for *fos-1, egl-43, zmp-1, cdh-3,* and *mig-10* were all expressed in the utse at L4 lethargus or young adult (Figure 6E, I, M, U), consistent with a role in utse development. *mig-10* is expressed in uterine toroids in L4 (Figure 6Y), and could be acting on the utse via signals from the uterine toroids, or internally like the other invasion genes. *him-4* encodes the extracellular matrix protein hemicentin, which assembles into polymers at areas of cell contact to help mediate the connection between the uterus and the hypodermis (Newman et al., 1995; Vogel et al., 2006). As it is necessary for mediating cell-cell interactions, and is expressed ventral to the utse (Figure 6Q), it is not surprising that lack of hemicentin in *him-4(RNAi)* also results in utse defects even though *him-4* is not expressed in the utse (Figure 6Q).

fos-1(RNAi) and *egl-43(RNAi)* treated worms showed severe defects not only in utse development but in somatic gonad development (data not shown). This effect was partially due to their involvement in π cell induction (Oommen and Newman, 2007; Rimann and Hajnal, 2007), which made nuclear migration difficult to score. The majority of *fos-1(RNAi)* and *egl-43(RNAi)* treated worms did not form π or υ cells (Table 2E), but those shown in Figure 6 and Table 2E were animals in which π and subsequently υ cell induction occurred. Both *fos-1* and *egl-43* are expressed in the utse at late L4 and young adult stages, indicating that they likely also act in the utse, and defective phenotypes from RNAi treatment against these genes is not wholly due to lack of π cell production.

Due to the presence of utse defects upon knockdown of AC invasion genes, as well as expression of the invasion genes within and surrounding the utse cell body, we believe to have discovered a new role for the AC in uterine development.

3.4.6 Molecular signals from ut1 and ut2 affect utse development

After determining that the uterine toroid cells (specifically ut1 and ut2) play a role in utse development we examined underlying genetic requirements. To this end, we generated a list of 37 genes expressed in the uterine toroids through a WormBase expression pattern search. We performed RNAi against these candidates and screened for defects in utse development (see Table 2A). Defects resulting from these genes would be significant since their expression (and potentially

site of action) in the uterine toroids would bolster our finding that the presence of the uterine toroids affect utse development.

Of the 37 genes, 7 exhibited extremely significant defects in utse development (Table 2A): helicase *dog-1,* the serine carboxypeptidase *F41C3.5*, the phosphatase *gsp-1,* the EGF vulval induction gene *lin-3,* the cell fusion annexin *nex-1,* the divergent Rab GTPase RASEF/*rsef-1* (formerly known as *tag-312),* and the GNEF (guanine nucleotide exchange factor) Trio-like protein *unc-73* (Youds et al., 2007; Saleh et al., 2006; Hristova et al., 2005; Rutledge et al., 2002; Hill and Sternberg, 1992; Hwang and Sternberg, 2004; Satoh et al., 2000; Daigle and Creutz, 1999; Shaye and Greenwald, 2011; Schmidt et al., 2009; Stringham et al., 2002; Wu et al., 2002). We focused on two of these genes: *rsef-1,* due to its uncharacterized nature, and *unc-73,* due to the high frequency and severity of utse defects from RNAi knockdown of this gene (Figure 9A-F).

rsef-1 is the *C. elegans* ortholog of RASEF (WormBase 2014), a potent tumor suppressor and lung cancer biomarker (Oshita et al., 2013). It is necessary for PLM axon growth and is a known *C. elegans* spermatheca and spermatheca-uterine junction (sujn) marker (Chen et al., 2011). Exposure to *rsef-1(RNAi)* caused defects both in utse nuclear migration (Figure 7E) as well as cell outgrowth (Figure 7F). *rsef-1(RNAi)* also caused problems in uterine lumen formation (Figure 7D), suggesting that the site of action is in the uterine toroids. To examine *rsef-1* expression we used a transcriptional fusion of *rsef-1* (Mounsey et al., 2002). Expression is absent during early and mid L4 stages, but is present both in the spermatheca and spermathecal-uterine junction at L4 lethargus (Figure 7G), and in the uterine toroids at young adult stage (Figure 7H; 7J). We observed phenotypic consequences of *rsef-1* silencing in the utse/uterine toroids prior to detecting expression of the *rsef-1::gfp* reporter, so we are likely missing some component of its expression.

3.4.7 Rab GTPases affect utse development

rsef-1 is largely uncharacterized and its upstream and downstream effectors are unknown. Using software that computationally predicts interactions between genes (geneorienteer.org; Zhong and Sternberg, 2006), we performed an RNAi screen against 14 of the top 15 predicted *rsef-1* interactors (Table 2B). (RNAi against *Y69H2.2* resulted in an absence of UTSE nuclei, data not shown.) RNAi treatment against three genes caused defects in utse development: the transcription factor *athp-1,* and two Rab GTPases, *rab-1* and *rab-11.1* (Figure 8D-G, 8U-X). *athp-1* has been shown to affect nuclear migration, potentially through the SUN/KASH pathway (S.G., unpublished observations).

RNAi against *rab-1* and *rab-11.1* resulted in severe defects (Figure 8D-G, 8U-X). *rab-1* is expressed in several cell types including the uterine toroids (Figure 8B). As *rsef-1* encodes a Rab family protein, we asked whether other Rab GTPases also affect utse development. Strikingly, of 21 tested, six Rab GTPases showed defects in utse development (Table 2C; Figure 8D-X). These Rab GTPases are involved in several parts of the cell trafficking pathway, including vesicle trafficking between the ER and the Golgi (*rab-1, rab-6, rab-10),* transport to the early endosome (*rab-5* and *rab-10),* and transport from the early endosome to the recycling endosome (*rab-11.1)* (Figure 8C, Nishimura and Sasaki, 2008; Chen et al., 1993; Martinez et al., 1994). Since Rab GTPases are expressed globally, site of action experiments will be necessary to determine whether these Rab proteins exert their effects on utse development by acting in the toroids, the utse, elsewhere, or in multiple tissues.

3.4.8 *unc-73* regulates the environment of utse

unc-73 encodes a Rho GNEF related to the mammalian Trio protein (Steven et al., 1998), which regulates cell outgrowth, cell migration, and cytoskeletal rearrangements (Seipel et al., 1999). We observed that 82% of *unc-73(RNAi)* (n= 50) treated worms showed defects such as a thick, truncated utse cell bodies (Figure 9B-C), and nuclei that failed to segregate into two groups and instead were linearly arranged (Figure 9A,C).

We next examined the expression pattern of *unc-73* in the uterus using the *unc-73* reporters. *unc-73* exists in eight isoforms which are as follows: *unc73a, unc-73b, unc-73c1, unc-73c2, unc-73f, unc-73d1,* and *unc-73d2)* (Steven et al., 2005). Of these different isoforms, combinations of four were reported to be expressed in the uterine epithelium at late L4 (*unc-73a,b::gfp* and *unc-73d::gfp)* (Ziel et al., 2009). *unc-73a,b::gfp* was expressed in the vulva at early L4 (specifically the vulE and vulF cells) and later in the uterine toroid4/spermatheca-uterine junction at mid and late L4 (data not shown). The *unc-73d::gfp* construct drove expression in ut2 in early L4 (Figure 9G), ut1 and ut2 and the utse at mid L4 (Figure 9H), and in both the uterine toroids and the utse by L4 lethargus (Figure 9I). Though *unc-73a,b::gfp* and *unc-73d::gfp* are predominantly expressed in the gonad, they are also expressed in other tissues, such as the pharynx and certain neurons. This, combined with the fact that the expression patterns of *unc-73c* and *unc-73f* have not been characterized, leads us to note that defects we are seeing from knockdown of *unc-73* may also be due to indirect effects of *unc-73* knockdown in other tissues.

We next identified genes downstream of *unc-73* that affect utse development. *unc-73* encodes a guanine nucleotide exchange factor required for activating Rho and Rac GTPases (Steven et al., 1998). The N-terminal RhoGEF-1 domain activates the Rac family of GTPases (Wu et al., 2002; Steven et al., 1998; Kubiseski et al., 2003) whereas the C-terminal RhoGEF-2 domain activates the RhoGTPase *rho-1* (Spencer et al., 2001). We noted that expression in ut1, ut2 and utse results from the *unc-73d::GFP* reporter. This isoform contains the RhoGEF2 domain (Ziel et al., 2009) responsible for activating RHO-1. We tested the *C. elegans* ortholog of RHO-1, *rho-1,* and observed significant defects in utse development (94% *rho-1(RNAi)* cause defects, n=17, Table 2D.) *let-502,* a Rho-binding serine-threonine kinase*,* is a downstream effector of *rho-1*, but does not have an effect on utse development (0% defects, n=10, see Table 3); however, another downstream effector of *rho-1, unc-13,* may play a role (50% *unc-13(RNAi)* caused defects*,* n= 24; Table 2D) (Spencer et al., 2001; McMullan et al., 2006). *unc-13* is a target of diacyl glycerol (DAG) signaling (Lackner et al., 1999), a pathway downstream of *rho-1* necessary for vesicle release. One of *unc-13*'s downstream effectors, *unc-64*/syntaxin, also affected utse development (50% *unc-64(RNAi)* caused defects, n= 30; Table 2D). Other members of the DAG pathway, such as *pkc-1*, a serine-threonine kinase, also yield utse defects (30% *pkc-1(RNAi)* caused defects, n= 30; Table 2D). (Note RNAi for *dgn-1/dystroglycan,* another downstream effector, was unavailable and therefore not tested.) The data suggests that UNC-73 acts on the utse by activating RHO-1, which then activates UNC-13 and potentially induces release of a chemoattractant through vesicle release via the DAG pathway.

3.4.9 The *unc-73* interactor, *unc-53,* affects utse development via the SMs

unc-73 acts together with *unc-53/*NAV and *unc-71* to promote guidance of SMs (uterine and vulval muscle progenitor cells) in the absence of the gonad (Branda and Stern, 2000; Chen et al., 1997) (Marcus-Gueret et al., 2012; Siddiqui, 1990; Wightman et al., 1997). *unc-53* is a cytoskeletal binding protein related to the mammalian NAV1 protein (neuronal navigators) (Maes et al., 2002). RNAi knockdown of *unc-53* resulted in high frequency of defects (73% of *unc-53(RNAi)* (n= 52)) that were phenotypically similar to defects caused by *unc-73(RNAi)* (Table 2D). Specifically*, unc-53(RNAi)* treated animals exhibit a thick, truncated utse cell body (Figure 9H-I) and nuclei are linearly arranged (Figure 9G, I). *unc-71(RNAi)* had slight utse defects (25%, n=8). Since *unc-73(RNAi)* and *unc-53(RNAi)* exhibit stronger and more penetrant phenotypes, we infer that these

two genes work together in utse development. *unc-73* and *unc-53* also work together without *unc-71* to direct posterior outgrowth of the excretory canal, axonal guidance and outgrowth of PLM neurons, and growth cone guidance along the ventral nerve cord (Marcus-Gueret et al., 2012; Siddiqui, 1990; Wightman et al., 1997.)

We determined the *unc-53* expression pattern using a reporter containing its full length promoter of *unc-53 (pABunc-53::gfp)* (Stringham et al., 2002). Expression was present in the sex myoblasts (SMs)(Figure 6K) as well as the vulval and uterine muscles they generate (Figure 9K, M, O). The SMs laterally flank the utse from L3 onwards (Figure 9J,L,N; Sulston and Horvitz, 1977). Since *unc-53* expression was limited to the SM lineage, we investigated the role of the SMs (and their descendants, the uterine and vulval muscles) in utse development via cell ablation. The SMs originate from the M cell, and migrate to the uterine region before generating the uterine and vulval muscles, also known as sex muscles (Sulston and Horvitz, 1977). We ablated the M cell in the L1 larval stage (Figure 9P), and then observed the utse at L4. In the absence of the SMs, the utse cell body exhibits abnormal morphology and expands beyond its normal position (Figure 9S, T, Table 1). Defective utse development occurs in the absence of other genes localized to the SMs, such as treatment the FGF receptor *egl-15(RNAi)* (78.9% defect, n = 19), substantiating our hypothesis that the SMs play a role in utse development. We conclude that the presence of the SMs or their descendants are necessary to mediate signals to the utse.

3.5 Discussion

Our results identify certain cellular and genetic requirements necessary for proper utse development (Figure 10). Using laser cell ablations, we identified four cell types in the environment of the utse that affect its development: AC, ut1, ut2, and the SMs. We show that genes involved in AC invasion have a secondary role in promoting utse outgrowth. An RNAi screen against two genes expressed in the uterine toroids, *rsef-1* and *unc-73,* was necessary for utse development. *rsef-1* is a divergent Rab GTPase and we found that several Rab GTPases affect utse development, indicating that membrane trafficking may play a crucial role. Our results also show that *rho-1, unc-13,* and *unc-64* potentially act downstream of *unc-73.* We also see that *unc-53* played a role in utse development through the SMs, and that the presence of SMs was necessary to maintain utse morphology.

3.5.1 Cell fusion and utse development

This study addressed the extent to which external cells affect the utse, and the role of cell fusion and subsequent internal signals on utse development. Transmission of genetic material between cells can change cell behavior; for instance, cell fusion between differentiated cells and embryonic stem cells can induce pluripotency in the formerly differentiated cell (Tada et al. 2001). Specifically, we found that the AC, which fuses with the utse during L4, affects utse development. The AC nucleus is necessary for utse development, and the AC invasion genes *fos-1, cdh-3, egl-43, him-4, zmp-1,* and *mig-10* promote utse cell outgrowth.

3.5.2 *rsef-1* and external cues in utse development

Surrounding tissues are known to have an impact on a cell's behavior and development; for instance, *C. elegans* dorsal muscle cells express *slt-1*/Slit1 ligand to repel axons that express its corresponding receptor *sax-3*/Robo, and the ventrally expressed *unc-6/*Netrin ligand attracts axons that express its receptor *unc-40/*DCC/Frazzled (Killeen and Sybingco, 2008). Though we have determined that *rsef-1* and *unc-73* are expressed in the environment of the utse, we do not know the cells in which they function to affect utse development. The RASEF ortholog, *rsef-1*, is detectable in the uterine toroids and it could act in the uterine toroids, the utse, or both.

3.5.3 Rab GTPses and vesicular trafficking in uterine development

This study addressed the extent to which external cells affect the utse, and the role of cell fusion and subsequent internal signals on utse development. Transmission of genetic material between cells can change cell behavior; for instance, cell fusion between differentiated cells and embryonic stem cells can induce pluripotency in the formerly differentiated cell (Tada et al. 2001). Specifically, we found that the AC, which fuses with the utse during L4, affects utse development. The AC nucleus is necessary for utse development, and the AC invasion genes *fos-1, cdh-3, egl-43, him-4, zmp-1,* and *mig-10* promote utse cell outgrowth.

rsef-1 is computationally predicted to interact with other Rab GTPases (*rab-11.1)* (Zhong and Sternberg, 2006). We showed that the predicted interactors *rab-1* and *rab-11.1,* and several other

Rab GTPases (*rab-5, rab-6.2,* and *rab-10)* are required for proper utse development (Figure 6, Table 2C). It is striking that we observe defects for multiple Rabs, which has not been the case in other *C. elegans* assays*,* suggesting that the utse development is sensitive to perturbations in membrane trafficking.

A potential role in the toroids could be that Rab GTPases are active in the uterine toroids and traffick cargo between the toroids to the utse. These Rab GTPases might deliver guidance cues to the utse that are necessary for development, or might deliver components of the extracellular matrix (ECM) to the growing utse. In some *C. elegans* tissues, Rab GTPase function has been found, but the cargo that these GTPases are transporting has not been identified. For instance, *rab-6.2* promotes vesicular transport necessary for grinder formation of *C. elegans*, yet its cargo is unknown (Straud et al., 2013). However, the Rab GTPases could also be transporting components of the extracellular matris to the utse. For instance, *rab-11.1* has been characterized to deliver cortical granules containing chondroitin proteoglycans to the developing embryonic extracellular matrix (Sato et al., 2008). Rab GTPases can also transport guidance cues for utse cell outgrowth. Wnts are well-known guidance cues for cell and neuronal migration in *C. elegans* (Zinovyeva et al., 2008; Minor et al., 2013). RAB-7 is required for trafficking proteins that mediate Wnt secretion (Wntless, Wls) between the endosome and trans-Golgi network and it affects Wnt protein EGL-20 function (Lorenowicz et al., 2013). RAB-10 is involved in trafficking of glutamate receptors (Glodowski et al., 2007) and glutamate receptors are necessary for transducing signals for both proper neural cell outgrowth (Beraldo et al., 2011) and migrating neural progenitor cells (Castrén et al., 2005).

3.5.4 Trio, NAV and internal and external cues affecting the utse

The Trio RhoGNEF *unc-73* affects utse development and is expressed in the cell's environment as well as within the utse. Since we see *unc-73* expression within the utse, *unc-73* could lead to the modification of components of the ECM to promote proper utse outgrowth. *unc-73* is expressed within the Q neuroblasts and promotes protrusion formation within these cells (Dyer et al. 2010) through rearrangements of the actin cytoskeleton. *unc-73* is also expressed in the uterine toroids, and could be involved in the secretion of guidance cues between the uterine toroids and the utse. Evidence for this type of function has a precedent in *unc-73's* role in growth cone formation, for *unc-73* increases the ability of *slt-1* (slit) and *unc-6* (netrin) to influence posterior guidance cues (Hu et al., 2011; Watari-Goshima et al., 2007).

unc-73 acts with *unc-53* and *unc-71* to guide SM migration in a gonad-independent mechanism (Branda and Stern, 2000; Chen et al., 1997). This led us to test *unc-53* and discover a new role of *unc-53* in utse development. Since *unc-53* is solely expressed in the SMs, we ablated the SMs to determine their role in utse development and saw that they are necessary for maintaining proper utse cell shape and size. Since the SMs generate the vulval and uterine muscles that flank the utse (Sulston and Horvitz, 1977) we propose that the SMs or their descendants secrete a cue that helps maintain utse cell shape. One precedent for SMs providing a cue to surrounding tissues is their role in providing sources of Wnt to the vulval precursor cell P7.p (Minor et al. 2013). *unc-53* is a homolog of the human neuronal navigator genes NAV1, NAV2, and NAV3 (Maes et al., 2002), and promotes guidance in muscle, excretory cells, and neurons, albeit in a cell autonomous manner (Stringham et al. 2002). Therefore, we propose a new non-autonomous role for *unc-53* promoting utse outgrowth via the SMs.

3.5.5 Broad implications of identification of utse genetic inputs

A variety of cell biological systems and disease models use mechanisms that function in utse development. Several of the genes identified, such as *unc-73* and *unc-53*, are key growth cone regulators, indicating that the utse could be used as a model to study genes involved in neurite outgrowth. RabGTPases are well characterized in several migratory systems, and the number of Rabs found in the utse makes it an ideal system for studying these GTPases.

Since the utse and the synctiotrophoblast layer of the placenta (Cross 2000) are both syncytia, the utse can act as a potential model to study morphogenetic movements in this system. Extravillious trophoblast (EVT) tissue invades the synctiotrophoblast and RhoA is necessary for migration of EVT (Nicola et al., 2008). Here we have shown that *rho-1,* a homolog of RhoA, is involved in utse outgrowth, illustrating the potential to use the utse as a model to study factors involved in placental development. Poor placental formation can deplete the fetus of nutrition, causing birth defects, and can cause preeclampsia, indicating a need for study of this tissue.

Metastatic cancers also use several of the mechanisms that function in utse development. The *unc-73* homologue Trio is involved with the migration and invasiveness of glioblastoma cells (Fortin et al., 2012) and in breast cancer cell metastasis (Li et al., 2011). Alterations of NAV3, an ortholog of *unc-53,* are characteristic of colorectal cancer cells (Carlsson et al., 2011), and certain Rab GTPases are upregulated in ovarian and breast cancer (Cheng et al., 2005). The utse grows outwards in a

manner similar to that of metastatic cancer cells (through rearranging its cytoskeleton and changing from an ellipsoid to a linear shape.) Therefore, the *C. elegans* utse may serve as a new model to understand the normal function of genes implicated in metastatic cell behavior.

3.6 Acknowledgements

We thank Matthew Buechner (University of Kansas), David Sherwood (Duke University), Ian Hope (University of Leeds), Nathalie Pujol (Centre d'Immunologie de Marseille-Luminy), and the Caenorhabditis Genetics Center (University of Minnesota) for worm strains; Sang Nguyen for verification of uterine toroid genes; Barbara Perry and Gladys Medina for technical assistance; Wendy Hanna-Rose, Marianne Bronner, Bruce Hay, David Chan, Amir Sapir, Mihoko Kato, Paul Minor, and Hillel Schwartz for helpful discussions and critically reading the manuscript. S.G. was supported by National Institutes of Health USPHS training grant GM07616. This work was supported by the Howard Hughes Medical Institute, with which P.W.S. is an investigator.

References

Bargmann, C.I. and Avery, L., 1995. Laser killing of cells in Caenorhabditis elegans. *Methods Cell Biol.* **48**, 225-250.

Beraldo, F.H., Arantes, C.P., Santos, T.G., Machado, C.F., Roffe, M., Hajj, G.N., Lee, K.S., Magalhães, A.C., Caetano, F.A., Mancini, G.L., Lopes, M.H., Américo, T.A., Magdesian, M.H., Ferguson, S.S., Linden, R., Prado, M.A., Martins, V.R., 2011. Metabotropic glutamate receptors transduce signals for neurite outgrowth after binding of the prion protein to laminin γ1 chain. *FASEB J*. **25**, 265-79.

Berndt, B., Zänker K.S., Dittmar T., 2013. Cell fusion is a potent inducer of aneuploidy and drug resistance in tumor cell/normal cell hybrids. *Crit. Rev. Oncog*. **18,** 97-113.

Biressi, S., Tagliafico, E., Lamorte, G., Monteverde, S., Tenedini, E., Roncaglia, E., Ferrari, S., Ferrari, S., Cusella-De Angelis, M.G., Tajbakhsh, S., Cossu, G., 2007. Intrinsic phenotypic diversity of embryonic and fetal myoblasts is revealed by genome-wide gene expression analysis on purified cells. *Dev. Biol*. **304,** 633-651.

Branda, C.S. and Stern, M.J., 2000. Mechanisms controlling sex myoblast migration in Caenorhabditis elegans hermaphrodites. *Dev Biol*. **226**, 137-151.

Brenner, S., 1974. The genetics of Caenorhabditis elegans. *Genetics*. **77,** 71-94.

Bronner, M.E., LeDouarin, N.M., 2011. Development and evolution of the neural crest: an overview. *Dev. Biol.* **366,** 2-9.

Carlsson, E., Ranki, A., Sipilä, L., Karenko, L., Abdel-Rahman, W.M., Ovaska, K., Siggberg, L., Aapola, U., Ässämäki, R., Häyry, V., Niiranen, K., Helle, M., Knuutila, S., Hautaniemi, S., Peltomäki, P., Krohn, K., 2012. Potential role of a navigator gene NAV3 in colorectal cancer. *Br. J. Cancer*. **106**, 517-524

Castrén, M., Tervonen, T., Kärkkäinen, V., Heinonen, S., Castrén, E., Larsson, K., Bakker, C.E., Oostra, B.A., Akerman, K. 2005. Altered differentiation of neural stem cells in fragile X syndrome. *Proc. Natl. Acad. Sci USA*. **102**, 17834-17839.

Chamberlin, H.M., Palmer, R.E., Newman, A.P., Sternberg, P.W., Baillie, D.L., Thomas, J.H., 1997. The PAX gene egl-38 mediates developmental patterning in Caenorhabditis elegans. *Development*. 124, 3919-28.

Chang, C., Newman, A.P., Sternberg, P.W., 1999. Reciprocal EGF signaling back to the uterus from the induced C. elegans vulva coordinates morphogenesis of epithelia. *Curr. Biol*. **9**, 237-246

Chen, E.B., Branda, C.S., Stern, M.J., 1997. Genetic enhancers of sem-5 define components of the gonad-independent guidance mechanism controlling sex myoblast migration in Caenorhabditis elegans hermaphrodites. *Dev. Biol*. **182**, 88-100

Chen, L., Wang, Z., Ghosh-Roy, A., Hubert, T., Yan, D., O'Rourke, S., Bowerman, B., Wu, Z., Jin, Y., Chisholm, A.D., 2011. Axon regeneration pathways identified by systematic genetic screening in C. elegans. *Neuron*. **71**, 1043-1057.

Chen, Y.T., Holcomb, C., Moore, H.P., 1993. Expression and localization of two low molecular weight GTP-binding proteins, Rab8 and Rab10, by epitope tag. *Proc. Natl. Acad. Sci. U. S. A*. **90**, 6508-6512.

Cheng, K.W., Lahad, J.P., Gray, J.W., Mills, G.B., 2005. Emerging role of RAB GTPases in cancer and human disease. *Cancer Res*. 65, 2516-2519.

Cinar, H.N., Richards, K.L., Oommen, K.S., Newman, A.P., 2003. The EGL-13 SOX domain transcription factor affects the uterine pi cell lineages in Caenorhabditis elegans. *Genetics*. **165**, 1623-1628.

Cross, J.C., 2000. Genetic insights into trophoblast differentiation and placental morphogenesis. *Semin. Cell Dev. Biol*. **11,** 105-113.

Daigle, S.N., Creutz, C.E., 1999. Transcription, biochemistry and localization of nematode annexins. *J. Cell Sci*. **112**, 1901-1913.

Dyer, J.O., Demarco, R.S., Lundquist, E.A., 2010. Distinct roles of Rac GTPases and the UNC-73/Trio and PIX-1 Rac GTP exchange factors in neuroblast protrusion and migration in C. elegans. *Small GTPases*. **1**, 44-61.

Félix, M.A. and Sternberg, P.W., 1996. Symmetry breakage in the development of one-armed gonads in nematodes. *Development.* **122**, 2129-2142.

Fortin, S.P., Ennis, M.J., Schumacher, C.A., Zylstra-Diegel, C.R., Williams, B.O., Ross, J.T.,

Winkles, J.A., Loftus, J.C., Symons, M.H., Tran, N.L., 2012. Cdc42 and the guanine nucleotide exchange factors Ect2 and trio mediate Fn14-induced migration and invasion of glioblastoma cells. *Mol. Cancer Res*. **10**, 958-968.

Gabbiani, G., Ryan, G.B., Majno, G., 1971. Presence of modified fibroblasts in granulation tissue and their possible role in wound contraction. *Experientia.* **27,** 549-550.

Gabbiani, G., 2003. The myofibroblast in wound healing and fibrocontractive diseases. *Journal of Pathology*. **200**, 500-503.

Glodowski, D.R., Chen, C.C., Schaefer, H., Grant, B.D., Rongo, C., 2007. RAB-10 regulates glutamate receptor recycling in a cholesterol-dependent endocytosis pathway. *Mol Biol Cell*. **18**, 4387-96.

Gomez, T.M., Zheng, J.Q., 2006. The molecular basis for calcium-dependent axon pathfinding. *Nat. Rev. Neurosci*. **7**, 115-125.

Grinnell F., 1992. Wound repair, keratinocyte activation and integrin modulation. *J Cell Sci.* **101**, 1-5.

Hall, B.K., 2009. *The Neural Crest and Neural Crest Cells in Vertebrate Development and Evolution*. New York , NY: Springer.

Hanna-Rose, W., Han, M., 1999. COG-2, a sox domain protein necessary for establishing a functional vulval-uterine connection in Caenorhabditis elegans. *Development*. **126**, 169-179.

Hedgecock, E.M., Culotti, J.G., Hall, D.H., and Stern, B.D., 1987. Genetics of cell and axon migrations in Caenorhabditis elegans. Development. 100, 365–382

Hedgecock, E.M., Culotti, J.G., Hall, D.H., 1990. The unc-5, unc-6, and unc-40 genes guide circumferential migrations of pioneer axons and mesodermal cells on the epidermis in C. elegans. *Neuron*. **4**, 61-85

Hill, R.J. and Sternberg, P.W., 1992. The gene lin-3 encodes an inductive signal for vulval development in C. elegans. *Nature*. **358**, 470-4776.

Hristova, M., Birse, D., Hong, Y., Ambros, V., 2005. The Caenorhabditis elegans heterochronic regulator LIN-14 is a novel transcription factor that controls the developmental timing of transcription from the insulin/insulin-like growth factor gene ins-33 by direct DNA binding. *Mol. Cell Biol*. **25**, 11059-11072.

Hu, S., Pawson, T., Steven, R.M., 2011. UNC-73/trio RhoGEF-2 activity modulates Caenorhabditis elegans motility through changes in neurotransmitter signaling upstream of the GSA-1/Galphas pathway. *Genetics*. **189**, 137-151.

Huang, L. and Hanna-Rose, W., 2006. EGF signaling overcomes a uterine cell death associated with temporal mis-coordination of organogenesis within the C. elegans egg-laying apparatus. *Dev. Biol*. 300, 599-611.

Hwang, B.J., Sternberg, P.W. 2004. A cell-specific enhancer that specifies lin-3 expression in the C. elegans anchor cell for vulval development. *Development*. **131**, 143-151.

Hwang, B.J., Meruelo, A.D., Sternberg, P.W., 2007. C. elegans EVI1 proto-oncogene, EGL-43, is necessary for Notch-mediated cell fate specification and regulates cell invasion. *Development*. **134**, 669-79.

Ihara, S., Hagedorn, E.J., Morrissey, M.A., Chi, Q., Motegi, F., Kramer, J.M., Sherwood, D.R., 2011. Basement membrane sliding and targeted adhesion remodels tissue boundaries during uterine-vulval attachment in Caenorhabditis elegans. *Nat. Cell Biol*. **13,** 669-679

Ishii, N., Wadsworth, W.G., Stern, B.D., Culotti, J.G., Hedgecock, E.M., 1992. UNC-6, a laminin-related protein, guides cell and pioneer axon migrations in C. elegans. Neuron. **9,** 873-881.

Kadam, S., Ghosh, S., Stathopoulos, A., 2012. Synchronous and symmetric migration of Drosophila caudal visceral mesoderm cells requires dual input by two FGF ligands. *Development*. **139,** 699-708.

Kato, M. and Sternberg, P.W., 2009. The C. elegans tailless/Tlx homolog nhr-67 regulates a stage-specific program of linker cell migration in male gonadogenesis. *Developmen*t. **136**, 3907-3915.

Kemp, K., Gray, E., Wilkins, A., Scolding, N., 2012. Purkinje cell fusion and binucleate heterokaryon formation in multiple sclerosis cerebellum. *Brain.* **135**, 2962-2972.

Killeen, M.T., Sybingco, S.S., 2008. Netrin, Slit and Wnt receptors allow axons to choose the axis of migration. *Dev. Biol*. **323**,143-151.

Kubiseski, T.J., Culotti, J., Pawson, T., 2003. Functional analysis of the Caenorhabditis elegans UNC-73B PH domain demonstrates a role in activation of the Rac GTPase in vitro and axon guidance in vivo. *Mol Cell. Biol*. **23**, 6823-6835.

Lackner, M.R., Nurrish, S.J., Kaplan, J.M., 1999. Facilitation of synaptic transmission by EGL-30 Gqalpha and EGL-8 PLCbeta: DAG binding to UNC-13 is required to stimulate acetylcholine release. *Neuron*. **24**, 335-346

Le Douarin, N.M, and Kalcheim, C., 1999. *The Neural Crest.* Cambridge, United Kingdom: Cambridge University Press

Li, Y., Guo, Z., Chen, H., Dong, Z., Pan, Z.K., Ding, H., Su, S.B., Huang, S., 2011. HOXC8-Dependent Cadherin 11 Expression Facilitates Breast Cancer Cell Migration through Trio and Rac. *Genes Cancer*. **2**, 880-888.

Lorenowicz, M.J., Macurkova, M., Harterink, M., Middelkoop, T.C., de Groot, R., Betist, M.C., Korswagen, H.C., 2013. Inhibition of late endosomal maturation restores Wnt secretion in Caenorhabditis elegans vps-29 retromer mutants. *Cell Signal*. 26, 19-31

Maes, T., Barceló, A., Buesa, C., 2002. Neuron navigator: a human gene family with homology to unc-53, a cell guidance gene from Caenorhabditis elegans. *Genomics*. **80**, 21-30.

Marcus-Gueret, N., Schmidt, K.L., Stringham, E.G., 2012. Distinct cell guidance pathways controlled by the Rac and Rho GEF domains of UNC-73/TRIO in Caenorhabditis elegans. *Genetics*. **190**, 129-142.

Martin, P., 1997. Wound healing--aiming for perfect skin regeneration. *Science*. **276**, 75-81.

Martin, P. and Leibovich, S.J., 2005. Inflammatory cells during wound repair: the good, the bad and the ugly. *Trends Cell Biol*. **15,** 599-607.

Martinez, O., Schmidt, A., Salaméro, J., Hoflack, B., Roa, M., Goud, B., 1994. The small GTP-binding protein rab6 functions in intra-Golgi transport. *J. Cell. Biol.* **127**,1575-88.

McMullan, R., Hiley, E., Morrison, P., Nurrish, S.J., 2006. Rho is a presynaptic activator of neurotransmitter release at pre-existing synapses in C. elegans. *Genes Dev*. **20**, 65-76.

Minor, P.J., He, T.F., Sohn, C.H., Asthagiri, A.R., Sternberg, P.W., 2013. FGF signaling regulates Wnt ligand expression to control vulval cell lineage polarity in C. elegans. *Development*. 140, 3882-3891.

Mounsey, A., Bauer, P., Hope, I.A., 2002. Evidence suggesting that a fifth of annotated Caenorhabditis elegans genes may be pseudogenes. *Genome Res.* **12,** 770-775.

Newman, A.P., White, J.G., Sternberg, P.W., 1995. The Caenorhabditis elegans lin-12 gene mediates induction of ventral uterine specialization by the anchor cell. *Development*. **121**, 263-271.

Newman, A.P., White, J.G., Sternberg, P.W., 1996. Morphogenesis of the C. elegans hermaphrodite uterus. *Development*.**122**, 3617-3626.

Newman, A.P., Acton, G.Z., Hartwieg, E., Horvitz, H.R., Sternberg, P.W., 1999. The lin-11 LIM domain transcription factor is necessary for morphogenesis of C. elegans uterine cells. *Development*. **126**, 5319-5326.

Nicola, C., Chirpac, A., Lala, P.K., Chakraborty, C., 2008. Roles of Rho guanosine 5'-triphosphatase A, Rho kinases, and extracellular signal regulated kinase (1/2) in prostaglandin E2-mediated migration of first-trimester human extravillous trophoblast. *Endocrinology*. **149,** 1243-1251.

Nishimura, N. and Sasaki, T., 2008. Regulation of epithelial cell adhesion and repulsion: role of endocytic recycling. *J. Med. Invest*. **55**, 9-16.

Oommen, K.S. and Newman, A.P., 2007. Co-regulation by Notch and Fos is required for cell fate specification of intermediate precursors during C. elegans uterine development. *Development*. 134, 3999-4009.

Oshita, H., Nishino, R., Takano, A., Fujitomo, T., Aragaki, M., Kato, T., Akiyama, H., Tsuchiya, E., Kohno, N., Nakamura, Y., Daigo, Y., 2013. RASEF is a novel diagnostic biomarker and a therapeutic target for lung cancer. *Mol Cancer Res*. **11**, 937-51.

Pignoni, F., Baldarelli, R.M., Steingrímsson, E., Diaz, R.J., Patapoutian, A., Merriam, J.R., Lengyel, J.A., 1990. The Drosophila gene tailless is expressed at the embryonic termini and is a member of the steroid receptor superfamily. *Cell*. **62**, 151-163.

Podbilewicz, B., Leikina, E., Sapir, A., Valansi, C., Suissa, M., Shemer, G., Chernomordik, L.V., 2006. The C. elegans developmental fusogen EFF-1 mediates homotypic fusion in heterologous cells and in vivo. *Dev. Cell*. **11**, 471-81.

Rimann, I. and Hajnal, A., 2007. Regulation of anchor cell invasion and uterine cell fates by the egl-43 Evi-1 proto-oncogene in Caenorhabditis elegans. *Dev. Biol*. 2007 **308**, 187-195.

Robertson, T. A., Grounds, M. D., Mitchell, C. A. and Papadimitriou, J. M., 1990. Fusion between myogenic cells in vivo: an ultrastructural study in regenerating murine skeletal muscle. *J. Struct. Biol***. 105,** 170-182**.**

Robertson, T. A., Maley, M. A., Grounds, M. D. and Papadimitriou, J. M., 1993. The role of macrophages in skeletal muscle regeneration with particular reference to chemotaxis. *Exp. Cell Res.* **207**, 321-331**.**

Rutledge, E., Denton, J., Strange, K., 2002. Cell cycle- and swelling-induced activation of a Caenorhabditis elegans ClC channel is mediated by CeGLC-7alpha/beta phosphatases. *J. Cell Biol*. **158**, 435-444.

Saleh, M.C., van Rij, R.P., Hekele, A., Gillis, A., Foley, E., O'Farrell, P.H., Andino, R., 2006.The endocytic pathway mediates cell entry of dsRNA to induce RNAi silencing. *Nat. Cell Biol.* **8**, 793-802.

Sapir, A., Choi, J., Leikina, E., Avinoam, O., Valansi, C., Chernomordik, L.V., Newman, A.P., Podbilewicz, B., 2007. AFF-1, a FOS-1-regulated fusogen, mediates fusion of the anchor cell in C. elegans. *Dev. Ce*ll. **12**, 683-698.

Sato, M., Grant, B.D., Harada, A., Sato, K., 2008. Rab11 is required for synchronous secretion of chondroitin proteoglycans after fertilization in Caenorhabditis elegans. *J. Cell Sci*. 12, 3177-3186.

Satoh, A., Miwa, H.E., Kojima, K., Hirabayashi, J., Matsumoto, I., 2000. Ligand-binding properties of annexin from Caenorhabditis elegans (annexin XVI, Nex-1). *J. Biochem*. **128**, 377-381.

Schmidt, K.L., Marcus-Gueret, N., Adeleye, A., Webber, J., Baillie, D., Stringham, E.G., 2009. The cell migration molecule UNC-53/NAV2 is linked to the ARP2/3 complex by ABI-1. *Development*. **136**, 563-574.

Schuurs, T.A., Dalstra, H.J., Scheer, J.M., Wessels, J.G., 1998. Positioning of nuclei in the secondary Mycelium of Schizophyllum commune in relation to differential gene expression. *Fungal Genet. Biol*. **23**, 150-161.

Seipel, K., Medley, Q.G., Kedersha, N.L., Zhang, X.A., O'Brien, S.P., Serra-Pages, C., Hemler, M.E., Streuli, M., 1999. Trio amino-terminal guanine nucleotide exchange factor domain expression promotes actin cytoskeleton reorganization, cell migration and anchorage-independent cell growth. *J Cell Sci.* 112, 1825-1834.

Shaye, D.D. and Greenwald, I., 2011. OrthoList: a compendium of C. elegans genes with human

orthologs. *PLoS One*. **6**, e20085.

Sherwood, D.R. and Sternberg, P.W., 2003. Anchor cell invasion into the vulval epithelium in C. elegans. *Dev. Cell*. **5**, 21-31.

Sherwood, D.R., Butler, J.A., Kramer, J.M., Sternberg, P.W., 2005. FOS-1 promotes basement-membrane removal during anchor-cell invasion in C. elegans. *Cell*. 121, 951-962.

Siddiqui SS., 1990. Mutations affecting axonal growth and guidance of motor neurons and mechanosensory neurons in the nematode Caenorhabditis elegans. *Neurosci. Re.s Suppl*. **13**, S171-190.

Spencer, A.G., Orita, S., Malone, C.J., Han, M., 2001. A RHO GTPase-mediated pathway is required during P cell migration in Caenorhabditis elegans. *Proc. Natl. Acad. Sci USA*. **98**, 13132-13137.

Steven, R., Kubiseski, T.J., Zheng, H., Kulkarni, S., Mancillas, J., Ruiz Morales, A., Hogue, C.W., Pawson, T., Culotti, J., 1998. UNC-73 activates the Rac GTPase and is required for cell and growth cone migrations in C. elegans. *Cell*. **92**, 785-795.

Steven, R., Zhang, L., Culotti, J., Pawson, T., 2005. The UNC-73/Trio RhoGEF-2 domain is required in separate isoforms for the regulation of pharynx pumping and normal neurotransmission in C. elegans. *Genes. Dev*. **19**, 2016-2029.

Straud, S., Lee, I., Song, B., Avery, L., You, Y.J., 2013. The jaw of the worm: GTPase-activating protein EAT-17 regulates grinder formation in Caenorhabditis elegans. *Genetics*. **195**, 115-125.

Stringham, E., Pujol, N., Vandekerckhove, J., Bogaert, T., 2002. unc-53 controls longitudinal migration in C. elegans. *Development*. **129**, 3367-3379.

Sulston, J.E., Horvitz H.R., 1977. Post-embryonic cell lineages of the nematode, Caenorhabditis elegans. *Dev. Biol.* **56**, 110-156

Tada, M., Takahama, Y., Abe, K., Nakatsuji, N., Tada, T., 2001. Nuclear reprogramming of somatic cells by in vitro hybridization with ES cells. *Curr. Biol*. **11**,1553-1558.

Theveneau, E. and Mayor, R., 2012. Neural crest delamination and migration: from epithelium-to-mesenchyme transition to collective cell migration. *Dev. Biol.* **366,** 34-54.

Timmons, L., Court, D.L., Fire, A., 2001. Ingestion of bacterially expressed dsRNAs can produce specific and potent genetic interference in Caenorhabditis elegans. *Gene*. **263**, 103-112.

Tong, X., Buechner, M. 2008. CRIP homologues maintain apical cytoskeleton to regulate tubule size in C. elegans. *Dev Biol.* **317,** 225-233

Vitriol, E.A., Zheng, J.Q., 2012. Growth cone travel in space and time: the cellular ensemble of cytoskeleton, adhesion, and membrane. *Neuron*. **73**, 1068-1081.

Vogel, B.E., Muriel, J.M., Dong, C., Xu, X., 2006. Hemicentins: what have we learned from worms? *Cell Res*. 16, 872-878.

Wang, Z., Chi, Q., Sherwood, D.R., 2014. MIG-10 (lamellipodin) has netrin-independent functions and is a FOS-1A transcriptional target during anchor cell invasion in C. elegans. *Development*. **141,** 1342-1353

Watari-Goshima, N., Ogura, K., Wolf, F.W., Goshima, Y., Garriga, G., 2007. C. elegans VAB-8 and UNC-73 regulate the SAX-3 receptor to direct cell and growth-cone migrations. *Nat. Neurosci*. **10**, 169-76.

Wightman, B., Baran, R., Garriga, G., 1997. Genes that guide growth cones along the C. elegans ventral nerve cord. *Development*. 124, 2571-2580.

Wormbase website, 2014., http://www.wormbase.org/species/c_elegans/gene/WBGene00016344?query=tag-312#0c-9d1b6-10, release WS241

Wu, Y.C., Cheng, T.W., Lee, M.C., Weng, N.Y., 2002. Distinct rac activation pathways control Caenorhabditis elegans cell migration and axon outgrowth. *Dev. Biol*. 250, 145-155.

Youds, J.L., Barber, L.J., Ward, J.D., Collis, S.J., O'Neil, N.J., Boulton, S.J., Rose, A.M., 2007. DOG-1 is the Caenorhabditis elegans BRIP1/FANCJ homologue and functions in interstrand cross-link repair. *Mol. Cell Biol*. **28**,1470-1479.

Zhang, C.L., Zou, Y., He, W., Gage, F.H., Evans, R.M., 2008. A role for adult TLX-positive neural stem cells in learning and behaviour. *Nature*. **7181**, 1004-1007

Zhong, W. and Sternberg, P.W., 2006**.** Genome-wide prediction of C. elegans genetic interactions. *Science*. **311**, 1481-1484.

Ziel, J.W., Matus, D.Q., Sherwood, D.R., 2009. An expression screen for RhoGEF genes involved in C. elegans gonadogenesis. *Gene Expr. Patterns*. **9**, 397-403.

Zinovyeva, A.Y., Yamamoto, Y., Sawa, H., Forrester, W.C., 2008. Complex network of Wnt signaling regulates neuronal migrations during Caenorhabditis elegans development. *Genetics*. 179, 1357-1371.

Tables

Table 1: Uterine cell ablations

Genotype	% Defect	n	P value
mock ablation	0	10	
du ablated	0	26	
UT1 ablated(nuclear)	84.6	13	<0.0001
UT1 ablated (cell membrane)	92.3	13	<0.0001
UT1 ablated (total)	88.5	26	<0.0001
UT2 ablated(nuclear)	85.7	7	<0.0001
UT2 ablated (cell membrane)	100	5	<0.0001
UT2 ablated (total)	91.67	12	<0.0001
UT2 ablated(nuclear)	0	7	
UT3 ablated (cell membrane)	0	4	
UT2 ablated (total)	0	11	
Anchor cell ablated (nuclear)	83.3	18	<0.0001
Anchor cell ablated (cell membrane)	100	5	<0.0001
Anchor cell ablated (total)	86.9	23	<0.0001
Sex Myoblasts	90	10	<0.0001
υ cell nuclei	0	6	

Table 1

Uterine toroid 1, uterine toroid 2, anchor cell, and sex myoblasts are necessary for utse development. All phenotypes were scored at L4 lethargus or young adult. P-values were were calculated in comparison with wild type cdh-3::mcherry;egl-13::worms using Fisher's exact test.

Table 2: RNAis tested on utse

Genotype	% Defect	N	P-value
empty vector RNAi	0.97	103	
A) genes expressed in the uterine toroids			
C25A1.5(RNAi)	0	20	1
cdh-4(RNAi)	0	11	1
ceh-24(RNAi)	8	25	0.1
ckb-2(RNAi)	0	20	1
cog-1(RNAi)	9	11	0.18
dcar-1(RNAi)	14	7	0.12
dog-1(RNAi)	50	20	<0.0001
egl-36(RNAi)	0	10	1
F22G12.5(RNAi)	0	10	1
F33H2.3(RNAi)	0	10	1
F41C3.2(RNAi)	30	10	0.002
F41C3.5(RNAi)	37	46	<0.0001
gly-2(RNAi)	0	4	1
gsp-1(RNAi)	38.5	39	<0.0001
hex-2(RNAi)	0	21	1
homt-1(RNAi)	0	10	1
inx-11(RNAi)	0	24	1
inx-8(RNAi)	0	14	1
lin-3(RNAi)	37.5	24	<0.0001
mls-1(RNAi)	0	20	1
nck-1(RNAi)	0	10	1
nex-1 (RNAi)	50	28	<0.0001
nhr-111(RNAi)	0	10	1
nhx-3(RNAi)	10.5	19	0.06
osm-9(RNAi)	15.4	13	0.03
pha-4(RNAi)	0	3	1
plc-3(RNAi)	0	10	1
rsef-1(RNAi)	66.7	18	<0.0001
sca-1(RNAi)	3.7	27	1
ser-2(RNAi)	21.4	14	0.01
tag-24(RNAi)	8.3	12	0.2
tdc-1(RNAi)	0	26	1
tyr-2(RNAi)	0	25	1
unc-73(RNAi)	82	50	<0.0001
unc-94(RNAi)	17.4	23	0.004

W01A11.1(RNAi)	12.5	8	0.14
Y45F10C.2(RNAi)	0	11	1
B) *rasf-1* predicted interactors* **			
athp-1(RNAi)	40	20	<0.0001
cdc-42(RNAi)	0	20	1
ced-10(RNAi)	0	13	1
F33A8.4(RNAi)	5.9	17	0.26
F55G1.13(RNAi)	9.5	21	0.07
let-502(RNAi)	0	10	1
let-60(RNAi)	9.1	11	0.18
rab-1(RNAi)	53	17	<0.0001
rab-11.1(RNAi)	90.6	32	<0.0001
rap-1(RNAi)	5	20	0.3
rap-2(RNAi)	0	10	1
ras-1(RNAi)	0	9	1
spt-5(RNAi)	20	20	0.002
tag-336(RNAi)	0	9	1
C) RabGTPases			
C56E6.2(RNAi) (rab-6 homolog*)*	0	20	1
F11A5.3 (RNAi) (rab-2 homolog*)*	0	14	1
rab-1 (RNAi)	52.9	17	<0.0001
rab-10(RNAi)	95.5	22	<0.0001
rab-11.1(RNAi)	90.6	32	<0.0001
rab-14(RNAi)	0	27	1
rab-19(RNAi)	0	9	1
rab-2(RNAi)	33.3	9	0.001
rab-21(RNAi)	0	15	1
rab-28(RNAi)	0	24	1
rab-30(RNAi)	0	2	1
rab-3(RNAi)	0	10	1
rab-33(RNAi)	0	10	1
rab-35(RNAi)	0	10	1
rab-37(RNAi)	0	13	1
rab-39(RNAi)	0	14	1
rab-5(RNAi)	70.8	24	<0.0001
rab-6.1(RNAi)	40	20	<0.0001
rab-6.2(RNAi)	68.2	22	<0.0001
rab-7(RNAi)	28.6	7	0.01
rab-8(RNAi)	18.2	11	0.02
D) *unc-73* and *unc-53* downstream genes			

cdc-42(RNAi)	0	20	1
ced-10(RNAi)	0	13	1
egl-15(RNAi)	79	19	<0.0001
mig-2(RNAi)	0	10	1
pkc-1(RNAi)	30	30	<0.0001
rho-1(RNAi)	94.1	17	<0.0001
sem-5(RNAi)	16	25	0.0051
unc-13(RNAi)	50	24	<0.0001
unc-53(RNAi)	73.1	52	<0.0001
unc-64(RNAi)	50	30	<0.0001
unc-71(RNAi)	25	8	0.01
E) genes involved in Anchor Cell fusion and invasion			
aff-1(RNAi)	67.9	28	<0.0001
aff-1(RNAi) cell fusion defective	100	11	<0.0001
cdh-3(RNAi)	38.5	26	<0.0001
eff-1(RNAi)	11.1	43	0.01
eff-1(RNAi) cell outgrowth	0	7	1
egl-43(RNAi)	100	29***	<0.0001
fos-1(RNAi)	100	15**	<0.0001
him-4(RNAi)	42.9	49	<0.0001
mig-10(RNAi)	86.7	15	<0.0001
zmp-1(RNAi)	62.5	24	<0.0001

* genes in this section have gene orienteer scores that designate computational interaction between *rsef-1*

**38 additional worms were scored but had no pi cell nuclei

***52 additional worms were scored but had no pi cell nuclei

Table 2

Phenotypes were scored at L4 lethargus. P-values were calculated in comparison to empty vector (RNAi) using Fisher's exact test.

Figures

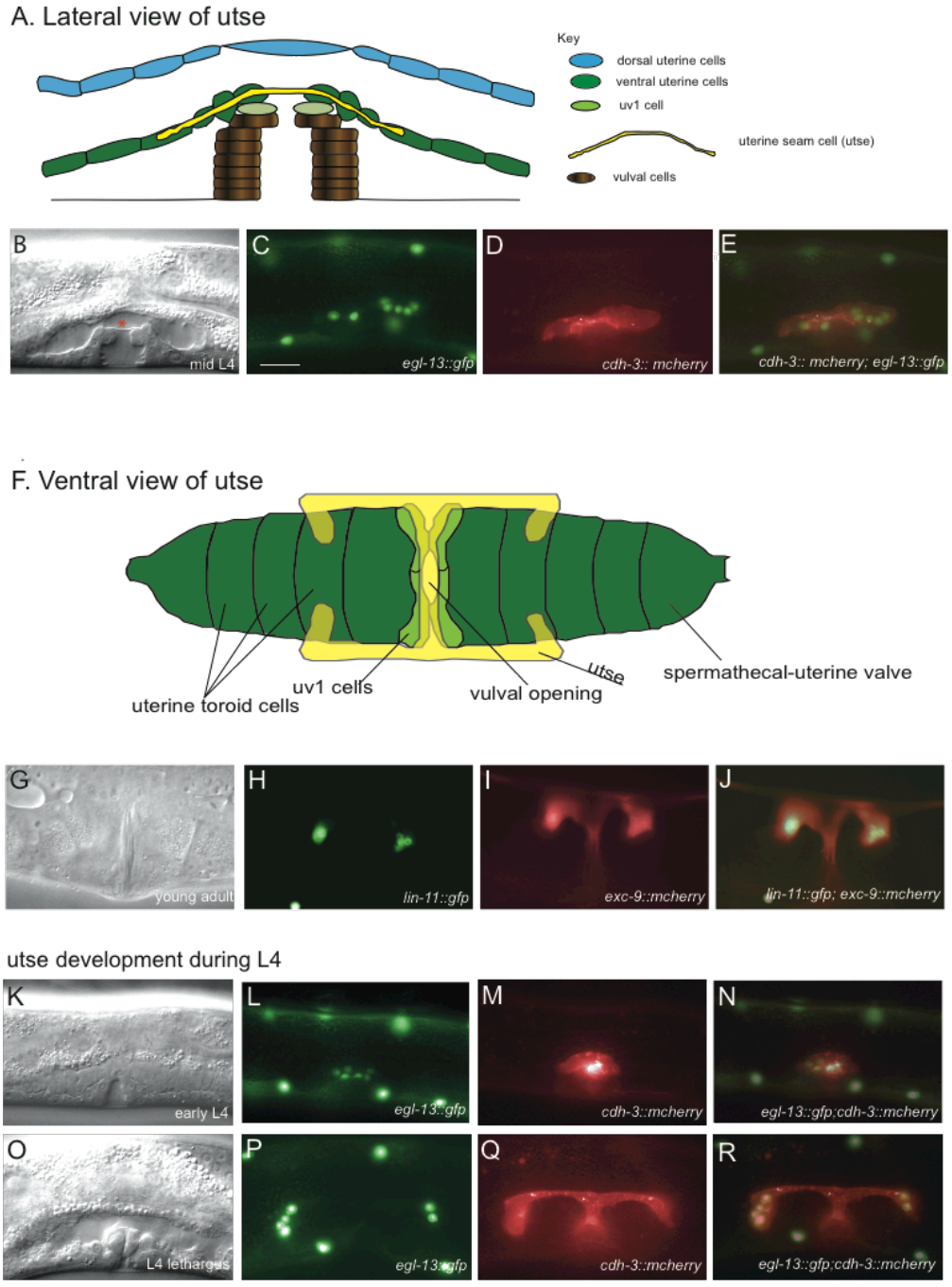

Figure 1 Wild-type utse development

Figure 1 Wild-type utse development

(A) Lateral schematic of a mid L4 uterus. **(B-E)** utse development at mid L4. **(B)** mid L4 somatic gonad; utse is shown underneath red asterisk. **(C)** υ cell nuclei (hereafter referred to as utse nuclei) shown with *egl-13::gfp*. **D)** utse cell body marked with *cdh-3::mcherry*. **(E)** merge of *C-D*. **(F)** Ventral schematic of L4 lethargus uterus. **(G-J)** Ventral view of young adult uterus. **(G)** young adult somatic gonad. **(H)** utse nuclei (υ cell nuclei) marked with *lin-11::gfp*. **(I)** cell body marked with *exc-9::mcherry*. **(J)** merge of *H-I*. **(K-R)** utse nuclei marked with *egl-13::gfp* and cell body marked with *exc-9::mcherry*. **(K-N)** utse development at early L4, here nuclei. **(L,N)** are clustered together and the cell body **(M,N)** has an ellipsoid shape. **(O-R)** utse development at L4 lethargus **(O)**; here the cell body **(Q,R)** has elongated in an anterior-posterior manner and nuclei **(P,R)** have migrated to distal tips of utse. Scale bar, 100μm.

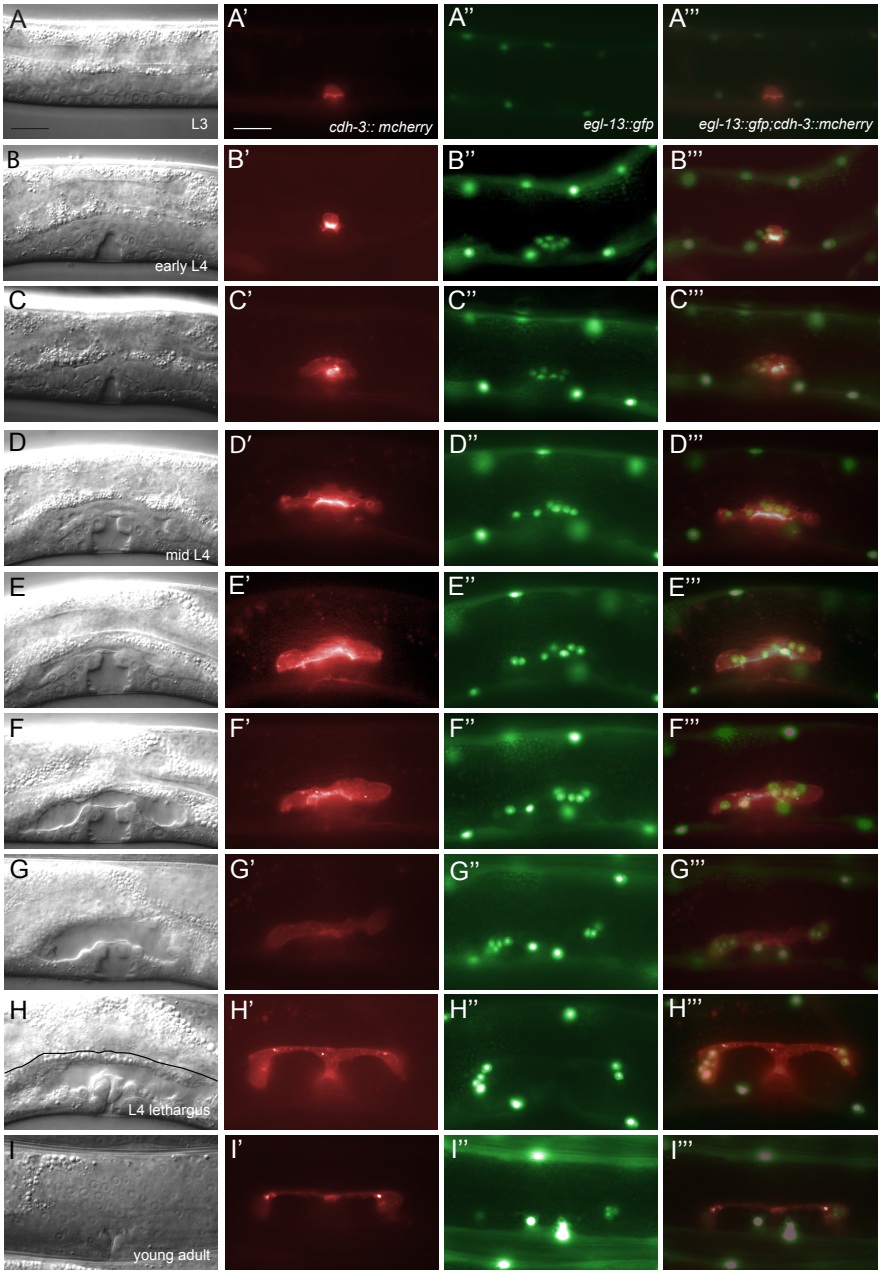

Figure 2 utse development from L3 to young adult

Sections **(A)** through **(I)** are in chronological order from earliest (L3) to latest (young adult). Each section includes a Nomarski image, expression of the *cdh-3::mCherry* marker in the cytoplasm of the AC and later the utse, expression of the *egl-13::gfp* marker in the nuclei of the υ cells and later the utse cell, and a merge of *mCherry* and *gfp* expression. Nuclei are marked with *egl-13::gfp* and

cell body is marked with *cdh-3::mcherry*. 10 worms were scored for each stage, and most representative image is shown. **(A-A''')** L3, AC invasion, pi cells have not been specified. **(B-B''')** Early L4, pi cells are specified by the anchor cell. **(C-C''')** fusion between υ cell nuclei an anchor cell. **(D-D''').** Mid L4, cell body outgrowth has commenced, nuclei are rearranging and have begun migrating slightly. **(E-G''')** Cell body outgrowth continues, with outgrowth occurring at a faster rate than nuclear migration. **(H-H''')** L4 lethargus, nuclear migration, and cell outgrowth have completed, and the utse has taken its final shape. **(I-I''')** Young adult, utse cell body will maintain this shape until egg-laying occurs. Scale bar, 100μm.

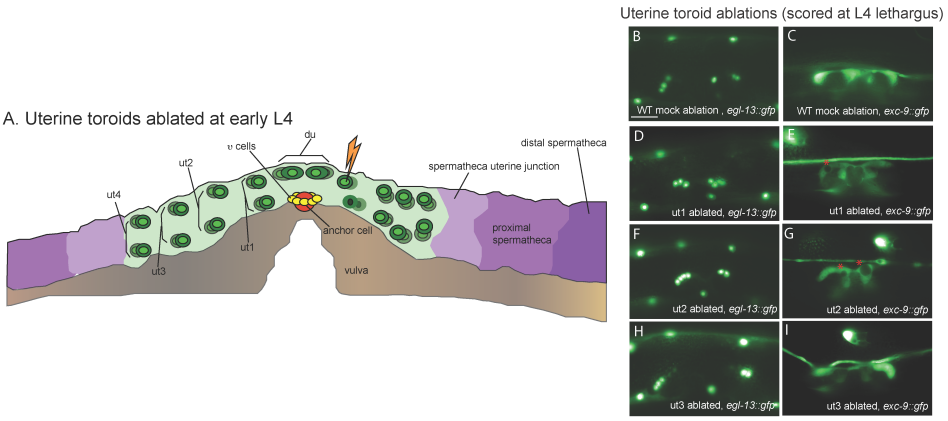

Figure 3 Uterine toroid ablations.

(A) Schematic of early L4 uterus. Lightning bolt indicates ablation of ut1 and borderless cells indicate cell death. **(B)** Completed nuclear migration in mock ablation worm (nuclei marked with *egl-13::gfp*). **(C)** Completed utse cell outgrowth in mock ablated worm (cell body marked with *exc-9::gfp*). **(D-E)** ut1 ablated worms. **(D)** Shorter nuclear migration. **(E)** Short and perforated cell body. **(F-G)** ut2 ablated worms. **(F)** Shorter nuclear migration. **(G)** Short and perforated cell body (see asterisks). **(H-I)** ut3 ablated worms **(H)** Nuclei distance in ut3 ablated worms is comparable to wild-type, **C**. **(I)** utse cell body in ut3 ablated worm looks similar to wild-type, **(E)** Scale bar, 100µm.

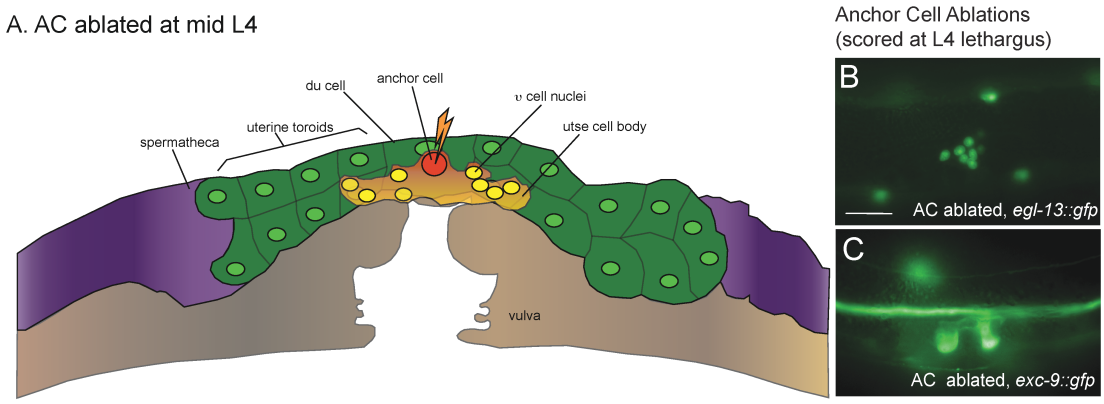

Figure 4 AC ablations

(A) Schematic of mid L4 uterus. Lightning bolt indicates point at which AC nucleus was ablated. **(B-C)** Images of worms with anchor cell ablated. **(B)** Nuclei are clustered together, migration has not occurred. **(C)** Cell body has not undergone cell outgrowth. Scale bar, 100µm.

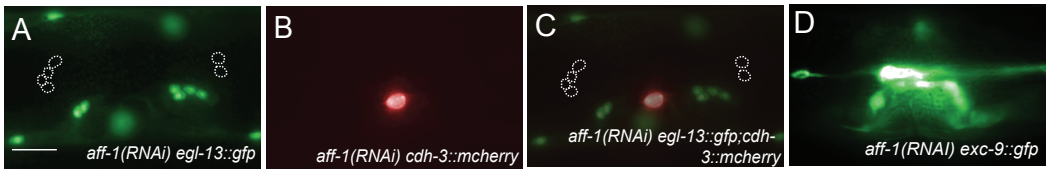

Figure 5 AC fusion and its role in utse development

(**A-C)** utse cell body is marked with *cdh-3::mcherry* and utse nuclei are marked with *egl-13::gfp.* **(A-D)** *aff-1(RNAi)* treated worms **(A,C)** shorter nuclear migration, cartoon in *F* and *C* indicate wild-type nuclear spacing. **(B,C)** AC has not fused with υ cells in *aff-1 (RNAi)* treated worms; however, nuclear migration has continued, though at a shorter distance comparable to wild-type. **(D)** Shorter utse cell body (marked with *exc-9::gfp*) upon treatment with *aff-1(RNAi).* Scale bar, 100μm.

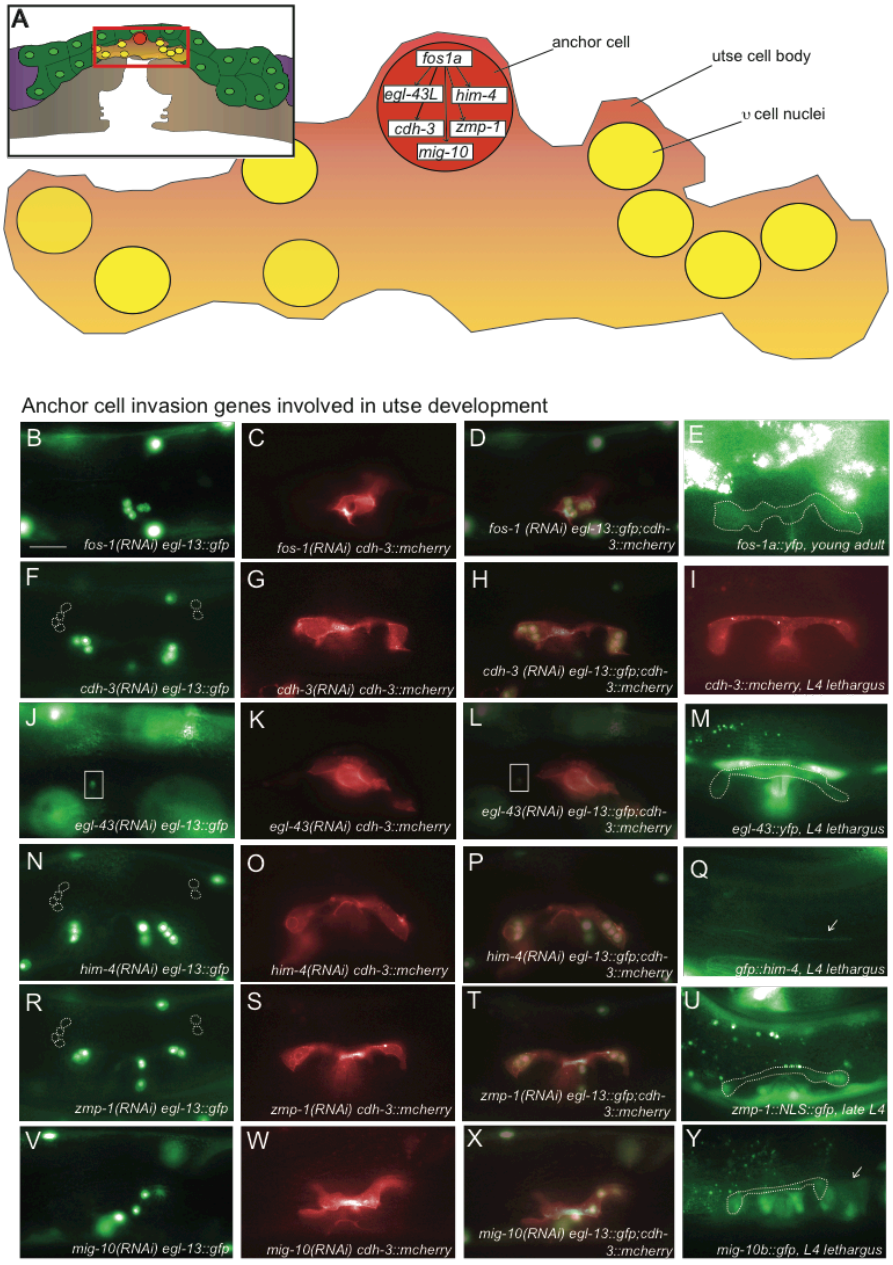

Figure 6 AC invasion genes effects on utse development

(**A)** Schematic of AC invasion genes. **(B-D, F-H, J-L, N-P, R-T, V-X)** utse cell body is marked with *cdh-3::mcherry* and nuclei are marked with *egl-13::gfp*. **(F,N,R)** Cartoons show wild-type utse nuclei positions. **(B-D)** *fos-1(RNAi)* treated worms. **(B,D)** When π cells were induced, nuclei clustered and ceased migrating. **(C,D)** Cell body is misshaped. **(E)** *fos-1a* expression pattern,

expressed in areas near the utse cell body at young adult (dashed lines show borders of expression). (**F-H)** *cdh-3(RNAi)* treated worms. **(F, H)** Shorter nuclear migration. **(G,H)** Cell body is misshapen and shorter. **(I)** *cdh-3* expression pattern, *cdh-3::mcherry* is expressed throughout the utse cell body. **(J-L)** *egl-43(RNAi)* treated worms. **(J, L)** υ cell is boxed, limited υ cell formation. **(K,L)** Cell body is misshapen. **(M)** *egl-43* expression pattern. Faint expression in area around utse at L4 lethargus (dashed lines show borders of expression). **(N-P)** *him-4(RNAi)* treated worms. **(N,P)** Shorter nuclear migration. **(O,P)** Shorter cell body. **(R)** *him-4* expression pattern, expression in the basement membrane underneath utse. **(R-T)** *zmp-1(RNAi)* treated worms. **(R,T)** Shorter nuclear migration. **(S,T)** Shorter cell body. **(U)** *zmp-1* expression pattern, expression at late L4, localizes to υ cell nuclei. **(V-X)** *mig-10(RNAi)* treated worms. **(V,X)** Misplaced and lower number of υ nuclei. **(W-X)** Shorter and misshapen cell body. **(Y)** *mig-10* expression pattern. *mig-10* localizes to utse (see dashed border) and uterine toroids (see arrow). Scale bar, 100μm.

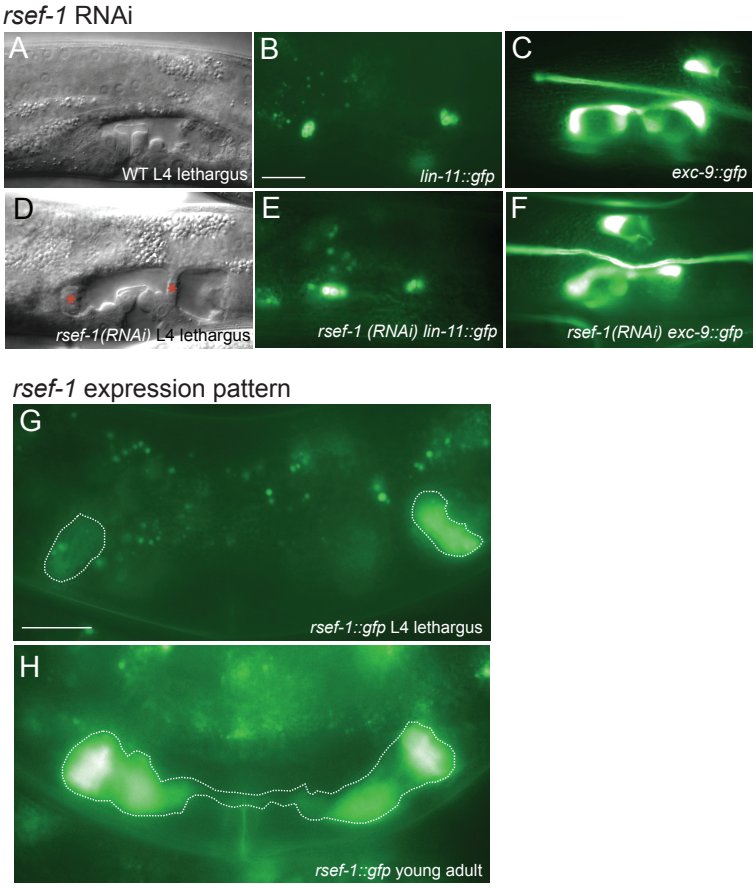

Figure 7 *rsef-1* in utse development

(A-F) utse cell body marked with *exc-9::gfp* and nuclei marked with *lin-11::gfp*. **(A-C)** Wild-type utse development. **(A)** Wild-type L4 lethargus. **(B)** Wild-type nuclear distance. **(C)** Wild-type cell shape. **(D-F)** *rsef-1(RNAi)* treated worms. **(D)** Problems in lumen formation in toroids (see asterisks). **(E)** Reduced nuclear migration. **(F)** Reduced cell outgrowth. **(G-J)** *rsef-1::gfp* expression. **(G)** *rsef-1* is expressed in the spermatheca at L4 lethargus. **(H)** *rsef-1* is expressed in the uterine toroids at young adult. Scale bar, 100μm.

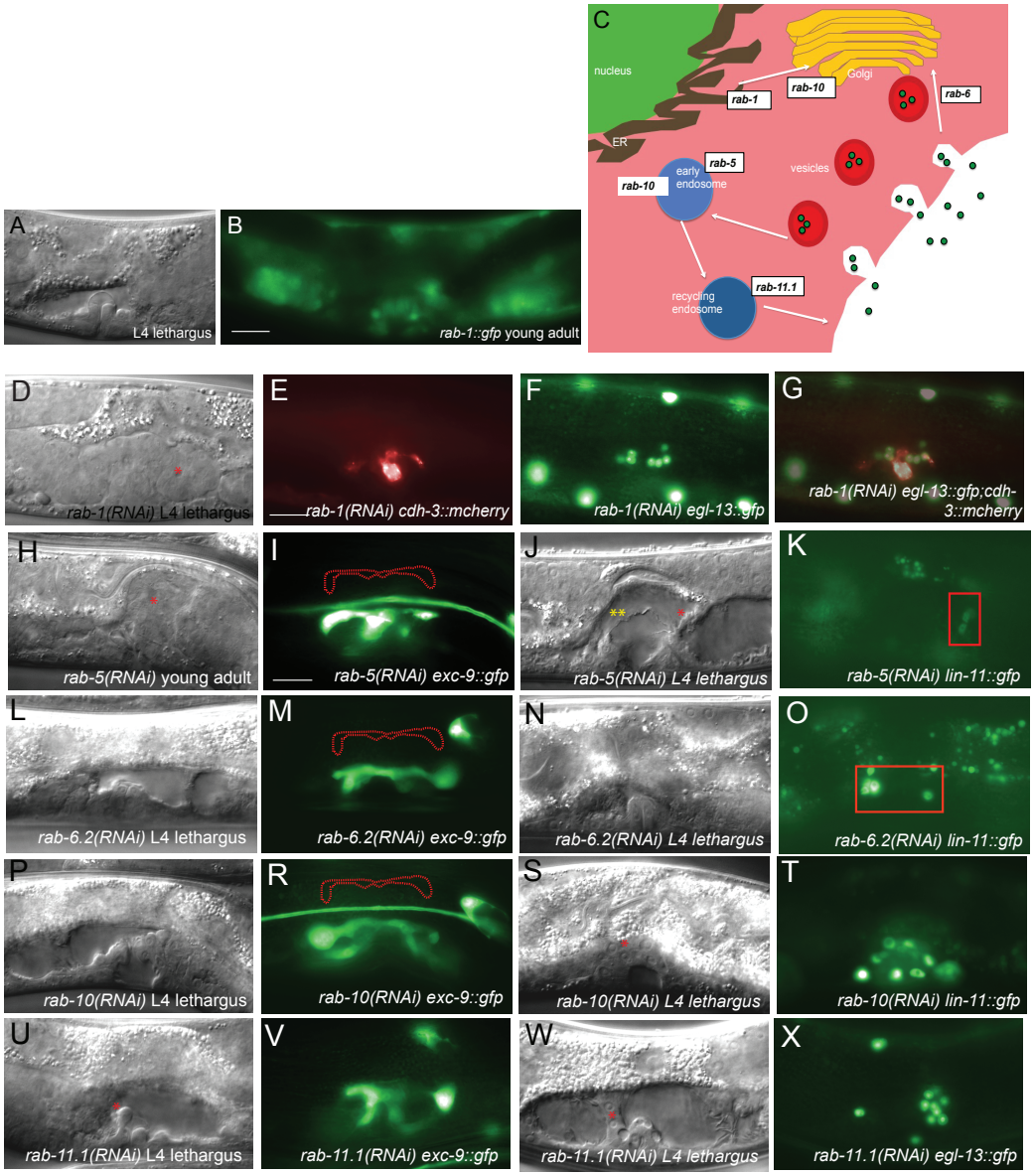

Figure 8 RabGTPases in utse development

(A,B) *rab-1* expression patterns at L4 lethargus in the uterine toroids. **(C)** Schematic of RabGTPases involved in utse development. **(D-G)** utse cell body is marked by *cdh-3::mcherry* and utse nuclei is marked by *egl-13::gfp*. *rab-1(RNAi)* treated worms (note *rab-1(RNAi)* treated worms grew three times slower than wild type, worms were staged based on vulval morphology and size). **(D)** stage for **E-G**. Uterine toroid lumen formation has not occurred (see red asterisk). **(E, G)** Cell body is misshapen and no outgrowth has occurred. **(F,G)** Nuclei have not migrated. **(H-X)** utse cell

body marked with *exc-9::gfp* and utse nuclei are marked with *lin-11::gfp.* **(I,M,R)** Dashed red cartoon indicates wild-type utse shape **(H-K)** *rab-5 (RNAi)* treated worms. **(H, J)** Stages for **I** and **K** were taken, respectively. Note, in **J**, lumen formation has not occurred (see red asterisk) and part of utse has detached (see yellow asterisks). (**I)** Cell body missing sections. **(K)** Nuclei are faint (see red box). **(L-O)** *rab-6.2 (RNAi)* treated worms. **(L, N)** Stages for **M** and **O**, respectively. **(M)** Cell body is misshapen. **(O)** Shorter nuclear migration, nuclei contained in red box. **(P-T)** *rab-10 (RNAi)* treated worms. **(P, S)** Stages for **R** and **T**, respectively. Note, in **S**, problems in lumen formation are present (see red asterisk). **(R)** Cell body is misshapen. **(T)** Nuclei are clustered. **(U-X)** *rab-11.1 (RNAi)* treated worms. **(U,W)** Stages for **V** and **X**, respectively. Bleb formed in cell membrane in **U** and defective lumen formation are present in **W** (see red asterisks). **(V)** Cell body is shorter and missing parts. **(X)** Shorter nuclear migration. Scale bar, 100μm.

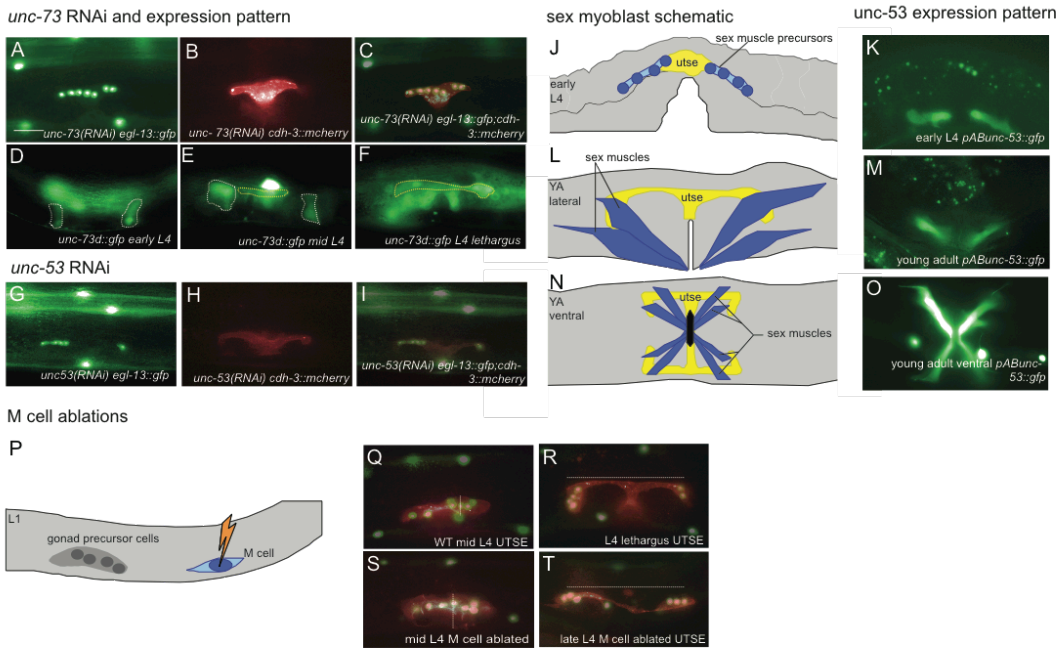

Figure 9 *unc-73, unc-53* and SMs in utse development

(**A-C; G-I)** utse cell body marked with *cdh-3::mcherry* and nuclei marked with *egl-13::gfp.* ***(*A-C)** *unc-73(RNAi)* treated worms. **(B, C)** Nuclei have not segregated into two groups or migrated. **(B, C)** Cell body is thick and misshapen. (**D-F)** *unc-73d::gfp* pattern. **(D)** Expression in early L4, white dashed lines indicate ut2 expression. **(E)** Expression in mid L4, white dashed lines show ut1 and ut2 expression and yellow dashed lines show utse expression. **(F)** Expression in L4 lethargus worms, yellow dashed lines show utse expression. **(G-I)** *unc-53(RNAi)* treated worms. **(G, I)** Nuclei are arranged linearly (similar to utse nuclei in *unc-73(RNAi)* treated worms), and have defective migration. **(H,I)** Cell body is thick and misshapen also similar to *unc-73(RNAi)* treated worms. **(J, L, N)** Schematics showing different stages of sex myoblast (SM) development. **(K, M, O)** *pABunc-53::gfp* expression pattern. **(J)** Sex myoblast position at early L4. **(K)** *unc-53* expression in sex myoblasts. **(L)** Lateral view of sex muscles in young adult. **(M)** *unc-53* expression in sex muscles (vulval muscles shown, uterine muscle expression in separate plane, not shown). (**N**) Ventral view of sex muscles in young adult. **(O)** *unc-53* expression in sex muscles. **(P)** Schematic of M cell (SM precursor) ablation at L1. **(Q-T)** utse cell body marked with *cdh-3::mcherry* and nuclei marked with *egl-13::gfp.* **(Q-R)** Wild-type utse development. **(Q)** Mid L4 utse, vertical dashed line shows widest

point of utse. **(R)** L4 lethargus utse, horizontal dashed line shows wild-type length. **(S)** Mid L4 utse in M cell ablated worm. utse is wider (see vertical dashed line at widest point). **(T)** Late L4 utse in M cell ablated worm, utse is longer (see horizontal dashed line for comparison to wild-type length). Scale bar, 100μm.

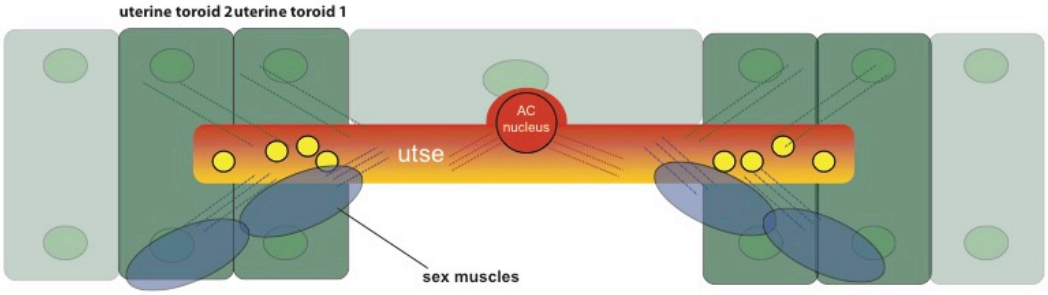

Figure 10 Mechanisms involved in utse development

(**A)** Schematic of different factors influencing utse development at mid L4. ut1 and ut2 are expressing *unc-73, rsef-1*, RabGTPases, and sex muscles are expressing *unc-53,* which together influence utse outgrowth exteriorly. AC invasion genes are directing outgrowth internally. Downstream factors are shown in box insets.

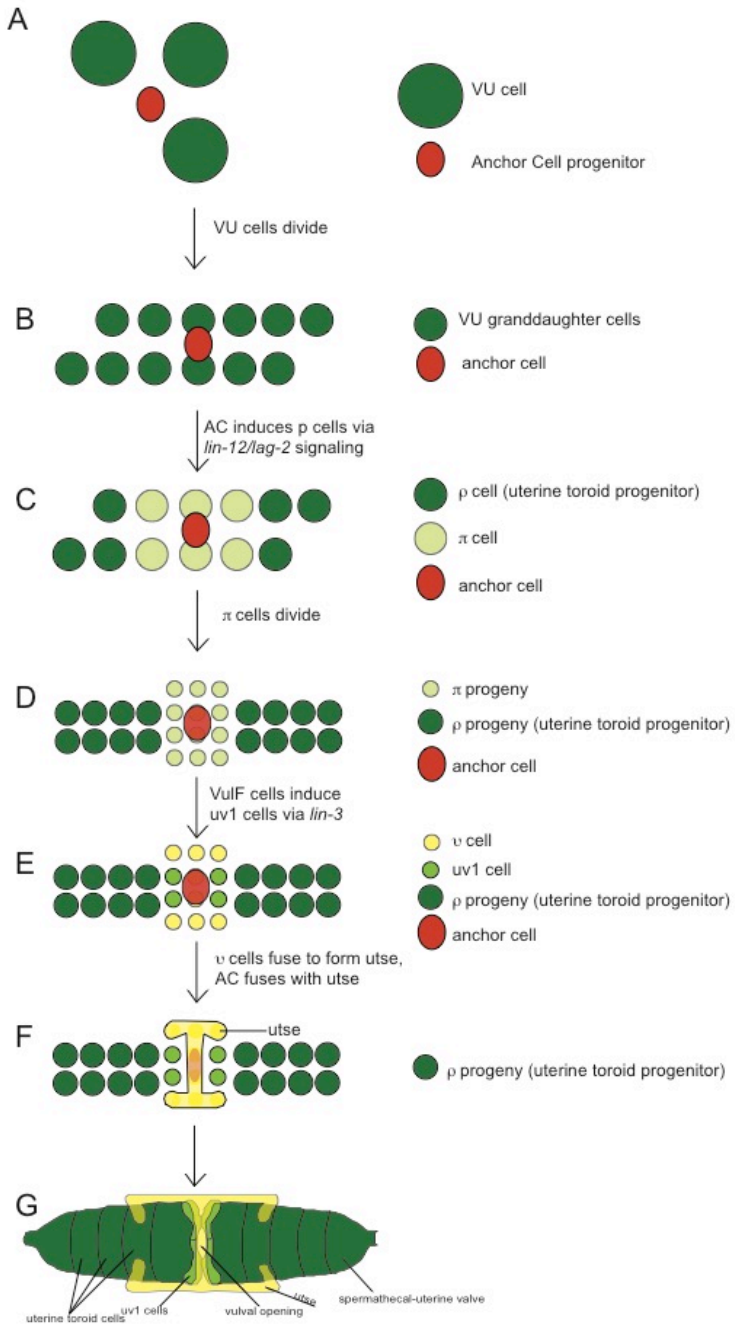

Figure S1: utse lineage

(A) L1 larval stage, ventral uterus is composed one anchor cell (AC) precursor (Z1.ppp or Z1.aaa) shown in red, and three remaining ventral uterine (VU) cells (from Z1.ppp, Z1.ppa , Z4.aap, and Z4.aaa). **(B)** L3, VU cells divided twice to produce 12 VU granddaughter cells, and AC has taken

its fate. **(C)** Late L3, AC induces surrounding VU granddaughter cells to π cell fate (shown in light green) via lin-12/lag-2 Notch-Delta signaling, remaining dark green cells show ρ cells which will eventually comprise the uterine toroid cells. **(D)** π cells divide to form 12 π daughter cells. **(E)** Vulval VulF cells induce 4 π daughter cells to take on uv1 (uterine-vulval 1) (lime green cells) fate, and the remaining 8 π cells take on υ cell fate (yellow cells). **(F)** Early L4, υ cells fuse together to form the utse syncytium, and the AC fuses with this syncytium. **(G)** L4 lethargus, hermaphrodite uterus with utse that had undergone full cell outgrowth.

CHAPTER 4

An ECM protease/inhibitor network regulates cell outgrowth

4.1 Abstract

Meprin metalloproteases have been characterized for their roles in metastatic cancer but have thus far been primarily studied *in vitro*. We have used the *C. elegans* uterine seam cell (utse) as a model to study meprin activity *in vivo*. Three meprin-like genes, *nas-21, nas-22,* and *toh-1*, exhibit high degrees of sequence similarity with the zinc metalloprotease active sites of human meprin gene MEP1A and MEP1B, and are necessary for proper utse outgrowth. Using *nas-21* gain-of-function phenotypes, we have identified four genes that act as protease inhibitors upstream of *nas-21*; two of these genes are known meprin protease inhibitors (*cpi-1* and *srp-2)* and two are novel protease inhibitors (*F35B12.4* and *mec-1*). *nas-21* and *toh-1* act on the *C. elegans* extracellular matrix in a similar manner to that of meprins, through controlling levels of collagen IV (*emb-9*) and laminin (*lam-1*). *nas-21, nas-22,* and *nas-26* control levels of a syndecan, an ECM protein target that has not yet been shown to interact with meprins. Our results present a new model for studying meprin activity, by identifying novel regulators and targets for meprin-like proteins.

4.2 Introduction

Metastasis is the major cause of death from cancer (WHO Cancer, 2014). Determining the underlying mechanisms that tumors use to invade other tissues can provide valuable information in stopping metastasis. Specifically, targeted drugs can be developed against molecular factors that are responsible for metastatic behaviors. For instance, autocrine motility factor (AMF) induces tumorigenicity, and causes cell detachment from the primary tumor site through promoting cell motility (Iiizumi et al., 2008; Liotta et al., 1986). This leads to an increase in metastasis in colorectal, lung, kidney, breast, and gastrointestinal carcinomas (Baumann et al., 1990; Filella et al., 1991; Patel et al., 1995; Dobashi et al., 2006; Tsutsumi et al., 2002; Yanagawa et al., 2004; Funasaka et al., 2007). Treatments have been developed against AMF, including carbohydrate phosphate inhibitors such as E4P, D- mannose-6-phosphate, and 5-phospho-D-arabinonate (5PAA), which block both AMF enzymatic activity and AMF-induced cell motility (Tanaka et al., 2002; Sun at al., 1999). Another treatment involves the use of antibodies against AMF (Talukder et al., 2000), which partially block HRG-induced invasiveness of human breast cancer MCF-7 cells. Therefore, identifying characteristics of metastatic cancers can yield effective treatments against this disease.

Metastasis occurs in several different stages, which include local invasion, intravasation (the entry of tumor cells into the bloodstream), circulation through the bloodstream, extravasation (the exit of tumor cells from capillary beds into the parenchyma of an organ), and colonization (Nguyen et al., 2009). Tumors initially begin by initiating genetic mutations that provide unlimited proliferative potential. These mutant cells tolerate cell division defects and an unstable genome, maintain progenitor-like phenotypes, and support other cell-autonomous functions that generate oncogenically transformed cells (Hanahan and Weinberg, 2000). However, in order to become metastatic, these tumors need to take on the additional ability to spread and proliferate in other tissues. This involves entering circulation, exiting circulation, and then infiltrating other organs. A subset of genes, known as metastasis initiation genes, promotes these invasive activities by inducing cell motility, epithelial to mesenchymal transition (EMT) and extracellular matrix (ECM) degradation (Chiang and Massagué, 2008).

Genes that encode proteases are a major type of metastasis initiation gene. In metastasis, proteases degrade components of the ECM so that tumor cells can breach barriers that exist between tissues. Several types of proteases are involved in degrading the ECM, including cathepsins, trypsins, threonine proteases, and matrix metalloproteases (Rakashanda et al., 2012). We are interested in studying the role of one family of zinc metalloproteases: the meprins. Meprins are a class of metalloproteases that are exclusively expressed in vertebrates and exist as two subunits: meprin α and meprin β (Sterchi et al., 2008). Meprins contribute to metastatic activity (Matters and Bond, 1999; Bond et al., 2005; Dietrich et al., 1996; Minder et al., 2012). Meprin β is upregulated in breast, pancreatic, and colon carcinoma cell lines (Matters and Bond, 1999; Bond et al., 2005; Dietrich et al., 1996) and meprin α is expressed in three fold higher levels in metastatic colorectal cancer cells versus nonmetastatic cells (Minder et al., 2012). *In vitro* studies have shown that meprins cleave components of the ECM including laminin-1, laminin-5 (Köhler et al., 2000), collagen IV, fibronectin, and nidogen (Kruse et al., 2004). All of this work has been done using *in vitro* cell culture, and though important insights regarding meprin function have been determined, studying meprins *in vivo* can provide many new insights. By studying meprins within an organism, we wish to shed light on the mechanisms meprins use to degrade components of the ECM, identify upstream and downstream regulators of meprins and determine how meprins, affect cell shape change.

Developing cells exhibit behaviors similar to that of metastatic cancers, and model organisms are valuable tools for studying genes involved in metastasis. Cell motility and shape change are a key aspects of organism development. The caudal visceral mesoderm (CVM) cells migrate anteriorly in the *Drosophila* embryo to eventually form muscles of the gut (Kadam et al., 2012). Vertebrate neural crest cells undergo epithelial to mesenchymal transition followed by migration to give rise to critical components of the craniofacial skeleton, such as the jaws and skull, as well as melanocytes and ganglia of the peripheral nervous system (Bronner and Le Dourian, 2012). And in *C. elegans,* the anchor cell degrades its underlying basement membrane to form protrusions, which allows the anchor cell to induce vulval fates (Sherwood et al., 2005). Each of these systems has not only elucidated aspects of cell behavior, but also clarified mechanisms involved in metastasis. For instance, the FGF receptor *heartless* is involved in regulating CVM migration (Kadam et al., 2012), and blockage of FGFR can reduce metastasis from prostate cancer cells into bones (Wan et al., 2014). Both migrating neural crest cells as well as colon carcinoma cells lose cadherin expression at their leading edge (Nakagawa and Takeichi 1998; Prall 2007). Netrin/UNC-6 and its receptor, UNC-40, guide protrusion formation during AC invasion (Hagedorn et al., 2013); similarly, netrins are known to promote liver, colorectal, and cervical cancer cell metastasis (Yan et al., 2014; Ko et al., 2013; Zhang et al., 2013).

We wish to study meprin activity using a *C. elegans* cell: the uterine seam cell (utse). The *C. elegans* uterine seam cell attaches the uterus to the body wall and undergoes cell outgrowth during development (Ghosh and Sternberg, 2014). During the L4 larval stage, the utse begins as an ellipsoidal cell, and then elongates outwards in a bidirectional manner along the anterior-posterior axis. Several genes involved in utse development have been implicated in cancer progression including Trio/*unc-73,* which is involved in the migration and invasiveness of gliblastoma cells (Fortin et al., 2012), NAV3/*unc-53,* which is found in colorectal cells (Carlsson et al., 2011), and several Rab GTPases (*rab-1*, *rab-5*, *rab-6.2*, *rab-10*, *rab-11.1*), which are upregulated in breast and ovarian cancers (Cheng et al., 2005). Since utse changes its shape and uses similar molecular inputs as metastatic cancer cells, we believe that it is an ideal model to study genes involved in cancer progression.

Here we focus on three *C. elegans* genes, *nas-21, nas-22,* and *nas-26*/*toh-1,* to study meprin activity. These three genes are members of a class of proteases known as nematode astacins (nas) (Möhrlen et al., 2003). The astacin family of proteases was isolated from the crayfish *Astacus*

astacus and encompass a family of than 120 reported sequences, detected in a wide range of organisms including bacteria, hexapodes, nematodes, molluscs, insects, and mammals (Gomis-Rüth 2003). Meprins belong to the astacin family (Sterchi et al., 2008) and therefore we believe that studying *nas-21*, *nas-22,* and *toh-1* will increase our understanding of meprin function and regulation. In this work we use the utse to identify upstream and downstream regulators of these three genes, and show that *nas-21*, *nas-22*, and *toh-1* are necessary for cell shape change, and characterize the effects of *nas-21*, *nas-22*, and *toh-1* on the extracellular matrix.

4.3 Materials and Methods

Strains and genetics: *C. elegans* were handled as described previously (Brenner, 1974). All strains used (listed in supplementary material Table S1) are derivatives of *C. elegans* wild-type strain (N2 Bristol).

RNAi experiments: RNAi was performed by feeding nematodes dsRNA-producing bacteria using standard procedures (Timmons et al., 2001) modified according to our previous work (Ghosh and Sternberg, 2014). For RNAis used see Table S2.

Scoring utse phenotypes: Animals were scored using a wide-field epifluorescence microscope at young adult or L4 lethargus stage. Abnormal utse outgrowth was classified using criteria from our previous work (Ghosh and Sternberg, 2014). Expanded utse were characterized as utse cell with portions of its cell membrane having widths of 40 μm or greater in areas that were not the anterior or posterior most edges of the cell.

Imaging: ECM protein expression patterns were acquired using a Zeiss LSM 710 Inverted confocal microscope with a ×100 Plan-APOCHROMAT objective and ZEN 2012 acquisition software Three-dimensional reconstructions were built from confocal z-stacks using Fiji (Schindelin et al., 2012). All acquired images were processed using Photoshop CS3 Extended (Adobe Systems). Fluorescent intensity of images in Figure 8 were quantified (through ROI manager and determining the mean average intensity) using Fiji (Schindelin et al., 2012).

Transgenics: To make the *nas-21(gk375710); exc-9::mcherry* strain, 60ng/μl of *exc-9::mcherry* plasmid (pBK162, *exc-9::mcherry* gateway plasmid, from M. Buechner, WBperson81) and 40ng/μl bluescript carrier DNA (pBSKS) was injected into *nas-21(gk375710)*. To create the *nas-21*

overexpression strain we created a construct that included 2989 bp upstream of the *nas-21* transcription start site, the entire coding region, as well as 794 bp of the *nas-21* 3'utr. Primers used were F: aaacaaacgttcacaacaatc and R: ctgtgcttgcaattgtgctt. This construct was highly toxic and 1ng/ µl was injected along with 60ng/ µl of pBK162 and 59ng/ µl of bluescript carrier DNA (pBSKS). To create the *F35B12.4p::GFP* construct, we fused a 643 bp region upstream of the *F35B12.4* transcription start site in front of a construct consisting of GFP and the *unc-54* 3'UTR. The PCR fusion was conducted according to techniques detailed in Hobert 2002. Primers used were (A) *F35B12.4* F: cgcttaatgcgaggtcatt, (B) F35B12.4 R + GFP: AGTCGACCTGCAGGCATGCAAGCTtcccgccccttttaaactatt, (C) GFP + F35B12.4: aatagtttaaaggggcgggaAGCTTGCATGCCTGCAGGTCGA, (D) *unc-54* utr R: AAGGGCCCGTACGGCCGACTAGTAGG. A nested: tgcgaggtcatttctgttaaa, D nested: GGAAACAGTTATGTTTGGTATATTGGG. We injected 60ng/ µl of pBK162, 20 ng/ µl of our *F35B12.4* construct, and 40 ng/ µl of bluescript carrier DNA (pBSKS).

Sequence analysis: Analysis of meprin and astacin protein sequences was performed using Clustal Omega (Sievers et al., 2011). Phylogenetic tree of astacins and meprins was created using Clustal X (Larkin et al., 2007) and FigTree v1.4.2 (FigTree).

4.4 Results

4.4.1 *nas-21*, *nas-22*, and *toh-1* affect utse development

The *C. elegans* utse is a cell whose function is to attach the uterus to the body wall (Figure 1A and 1E). During its development the utse begins as an ellipsoidal cell and then grows outward along the anterior posterior axis to become an elongated H- shaped cell (Ghosh and Sternberg 2014). The utse is a syncytium, and contains nine nuclei that also migrate along the anterior posterior axis (Newman et al., 1996). In our previous work (Ghosh and Sternberg, 2014) we found that the presence of certain cell types were necessary for proper utse outgrowth. These cell types included the uterine toroid cells (which comprise the lumen of the *C. elegans* uterus), and the sex myoblast cells (Figure 1E). While screening for genes expressed in these tissues, we found two genes, *nas-21* and *nas-22,* that were solely expressed in the utse or uterine toroid cells (Park et al., 2010, Figure 1B and 1C). *nas-21(RNAi)* and *nas-22(RNAi)* treated worms showed defective utse cell outgrowth and nuclear migration (Compare 1F-F''' to 1G-G''' and 1H-H'''). *nas-21(RNAi)* treatment caused defects that

were more severe than those caused by *nas-22(RNAi)*, indicating that this gene may play a greater role in utse development. *nas-21* and *nas-22* are members of the astacin family (Möhrlen et al., 2003). *C. elegans* contains 40 astacin genes, referred to as nematode astacins of *nas*- genes. We performed RNAi against 37 of the 40 astacin genes (the remaining three astacins did not have RNAi clones available) and screened for defects in utse development (Table 1). Using a P-value lower than 0.001 to assign significance in the face of multiple hypothesis, we saw that worms treated with RNAi against *nas-12, nas-19, nas-21, nas-22,* and *nas-26/toh-1* showed significant levels of defects. Of this group we chose to focus on genes that were expressed in the utse or cells involved in utse development (uterine toroids, sex muscle cells). This expanded our targeted astacin list to include *nas-26/toh-1* (hereby referred to as *toh-1*). *(nas-5* is also expressed in the utse (Park et al., 2010); however, RNAi treatment against *nas-5* did not result in a significant amount of defects.) *toh-1* is expressed in the sex muscles (Figure 1D) and RNAi against *toh-1* results in a shorter utse (Figure 1I''-I''') as well as a decreased nuclear migration (Figure 1I' and I''').

4.4.2 NAS-21, NAS-22, and TOH-1 exhibit similarity to meprins

Meprins are a subclass of the astacin protease family (Sterchi et at. 2008). Meprins are distinguished from other astacins by the presence of a transmembrane domain and are mainly found in vertebrates. Because meprins are upregulated in metastatic cancer (Matters and Bond, 1999; Bond et al., 2005; Dietrich et al., 1996, Minder et al., 2012), we were interested to see if *nas-21*, *nas-22,* and *toh-1* were related to human meprin genes. Human meprins exist in two forms: a gene that encodes the meprin α subunit, *Mep1A*, and a gene that encodes the meprin β subunit, *Mep1B* (Sterchi et at. 2008). These two subunits (hereby referred to as MEP1A for meprin α subunit and MEP1B for the meprin α subunit) can dimerize to form homo- (mep α, α) or heterodimers (mep α, β) (Bond and Benyon 1995).

We first wished to compare the sequences of MEP1A and MEP1B to NAS-21, NAS-22, and TOH-1. We used Clustal Omega (Sievers et al., 2011) to align their protein sequences (Figure 2B) and noted their percent identity to one another (Table 2). When comparing the sequence of MEP1A with all other nematode astacin sequences, NAS-21 shows 18.33% identity, NAS-22 shows 17.12%, and TOH-1 shows 19.22% similarity. NAS-14 exhibits the highest percent identity (26.04%) to MEP1A; however, RNAi treatment resulted in gross defects (worms did not develop past L2 stage), which prevented us from screening the utse (Table 1). When comparing MEP1B to all other nematode astacins, NAS-21 shares 21.59% identity, NAS-22 shares 22.45% identity, and

TOH-1 shares 20.36% identity (Table 2). NAS-4 shows the highest percent identity to MEP1B (33.21%); however, RNAi treatment of NAS-4 resulted in no utse defects (Table 1).

Comparison of the complete protein sequences of NAS-21, NAS-22, and TOH-1 show low percentage similarity with meprins, indicating that on the whole NAS-21, NAS-22, and TOH-1 may not be related to meprins. MEP1A, MEP1B, NAS-21, NAS-22, and TOH-1 do share similar domains (Figure 2A). We therefore analyzed these domains to determine if NAS-21, NAS-22, and TOH-1 shared domain similarity with the meprins.

MEP1A, MEP1B, NAS-21, NAS-22, and TOH-1 each contains a zinc metalloprotease domain (Figure 2A, domain shown in red) (astacins and meprins belong to the metzincin superfamily, which contains a zinc binding sequence at its active site) (Sterchi et at. 2008), an EGF domain (Figure 2A shown in blue), as well as a signal sequence and prodomain (Figure 2A in green and purple). These domains were annotated primarily using the SMART database (Schultz et al., 1998). Other domains were predicted by aligning sequences of NAS-21, NAS-22, and TOH-1 proteins from other nematode species using Clustal Omega (Sievers et al., 2011). We used sequences from *C. briggsae*, *C. remanei*, *C. brennerei,* and *C. japonica* sequences to identify conserved regions in NAS-21, NAS-22, and TOH-1 protein sequences, and were able to identify the signal peptide, prodomain of EGF domains of NAS-21, the prodomains of NAS-22 and TOH-1 (Figure S1).

MEP1A and MEP1B have three distinct domains from NAS-21, NAS-22, and TOH-1: the MAM domain, the TRAF domain, and a transmembrane domain. The MAM domain (shown in orange in Figure 2A), which spans amino acids 264-433 in MEP1A and 260-429 in MEP1B, is a domain that is characteristic to meprins and functions as an interaction and adhesion domain (Beckmann and Bork, 1993). The MAM domain is also necessary for correct folding and transport through the secretory pathway (Tsukuba and Bond, 1998). The MATH domain (shown in dark blue in Figure 2A, Table S3) is involved in self-association and receptor interaction (Sunnerhagen et al., 2002). MEP1A and MEP1B also contain transmembrane domains (shown in black in Figure 2A, Table S3). Although NAS-21, NAS-22, and TOH-1 do not have transmembrane domains, other nematode astacins (such as NAS-4, NAS-8, NAS-14, NAS-25, NAS-29, NAS-37, and NAS-39; see Table S3) have characterized transmembrane domains. The transmembrane domain anchors both MEP1A and MEP1B to the luminal side of the ER (endoplasmic reticulum) and to the plasma membrane in MEP1B (Sterchi et al, 2008). MEP1A also contains an I domain (shown in beige in Figure 2A) that

is necessary for proteolytic processing (Marchand et al, 1995). The I domain causes MEP1A to be secreted unless coexpressed with MEP1B to form a dimer. Therefore MEP1B exists as a transmembrane protein and MEP1A exists (when acting as a homodimer with itself) as a secreted protein.

NAS-21, NAS-22, and TOH-1 also share a distinct domain not found in MEP1A and MEP1B -- a CUB domain. This domain (shown in yellow in Figure 2A) is a developmentally regulated domain consisting of 110 residues found almost exclusively in extracellular and plasma membrane-associated proteins (Bork and Beckmann, 1993). Several other nematode astacins posses a CUB domain, specifically NAS-23 and NAS-27 through NAS-39 (Table S3). Since all nematode astacins do not posses these domains, we infer that these nematode astacins interact with factors involved in *C. elegans* development.

MEP1A and MEP1B, NAS-21, NAS-22, and TOH-1 all posses a signal peptide (shown in green, Figure 2A). Since NAS-21, NAS-22, and TOH-1 do not have transmembrane domains, we infer that NAS-21, NAS-22, and TOH-1 are all secreted extracellularly (according to SMART domain analysis, these proteins are also characterized as being secreted extracellularly) (Schultz et al., 1998). Using Clustal Omega (Sievers et al., 2011), we looked at the percent similarity between the signal peptides of NAS-21, NAS-22, TOH-1, MEP1A, and MEP1B (Table 2). The majority of nematode astacins also contain signal peptides, so we compared these signal sequences as well. When compared to the MEP1A signal peptide, NAS-21 shares 7.14% identity, NAS-22 shares 14.29% identity, and TOH-1 shares 14.29% identity. NAS-31 shares the highest percent identity with the signal sequence of MEP1A (37.5%); however, RNAi against NAS-31 did not any exhibit any utse defects (0%, Table 1). When compared to the signal peptide MEP1B, NAS-21 shares 6.67% identity, NAS-22 shares 20% identity, and TOH-1 shares 20% identity (Table 2). NAS-23 shared the highest percent identity with the signal peptide of MEP1B (41.67%), no RNAi against NAS-23 was present, and we were unable to determine if knockdown of this gene would affect utse development.

NAS-21, NAS-22, TOH-1, MEP1A, and MEP1B all posses prodomains. The prodomain of meprins must be cleaved off for activation (Sterchi et al., 2008). Meprins usually need trypsin-like proteinases to cleave off the prodomain from the N-terminus so that they can become active (Grünberg et al., 1993). Lack of the prodomain results in the biosynthesis of an immature and

transport-incompatible protein which is degraded intracellularly and cannot reach the plasma membrane. Therefore, the prodomain may potentially function as a chaperone that is essential for correct folding. The prodomain is near the N-terminus (Shown in purple in Figure 2A) and we compared the sequences of the meprin prodomains to the predicted prodomains of NAS-21, NAS-22, and TOH-1 (Table 2). When compared to the MEP1A prodomain, NAS-21 shares 7.69% identity and TOH-1 shares 22.73% identity (the NAS-22 prodomain sequence did not result in a Clustal output in the percent identity matrix). When compared to the MEP1B prodomain, NAS-21 shares 0% identity, and TOH-1 shares 25% identity (NAS-22 did not result in a Clustal output in the percent identity matrix).

Another domain that NAS-21, NAS-22, TOH-1, MEP1A, and MEP1B share is an EGF domain (shown in light blue in Figure 2A). The erole of EGF domains is not known in meprins; however, the EGF domain of MEP1A remains attached to the plasma membrane after MEP1A is secreted due to proteolytic cleavage at the I domain (Richter et al., 1999). EGF domains are characteristic of proteins that are membrane bound or secreted extracellularly (Davis 1990). Using Clustal Omega (Sievers et al., 2011), we looked at the percent similarity between the EGF domains of NAS-21, NAS-22, TOH-1, MEP1A and MEP1B (Table 2). Nematode astacins NAS-16 through NAS-39 contain EGF domains (Table S3), and we compared these sequences as well. When compared with the EGF domain of MEP1A (Table 2), NAS-21 shares no identity (0%), NAS-22 shares 18.18% identity, and TOH-1 shares 16.22% identity. The two EGF domains of NAS-39 (Table S3) share the highest percent identity among all the nematode astacins (33.33%), and although 23% of worms treated with NAS-39 (RNAi) exhibit defects (Table 1), we chose not to focus on this gene because its function as a BMP homolog has been characterized, specifically in molting (Park et al., 2010, Suzuki et al., 2004).

The zinc metalloprotease domain is a characteristic domain of MEP1A, MEP1B, NAS-21, NAS-22, and TOH-1 (shown in red in Figure 2A). This domain shares a conserved HExxHxxG/NxxH/D zinc binding sequence in its active site (Sterchi et al., 2008; Stöcker et al., 1995; see transparent red box in Figure 2B) as well as a conserved methionine-containing turn (Met-turn) backing the zinc site (see darker red box in Figure 2B). The HExxH (Rawlings and Barrett. 1995) is thought to have the highest degree of similarity between zinc metalloproteases (boxed in Figure 2B). Zinc activates these proteases, and is held in place with the amino acids present in the active site. Using Clustal Omega (Sievers et al., 2011), we looked at the percent similarity between the entire zinc

metalloprotease domain of NAS-21, NAS-22, TOH-1, MEP1A, and MEP1B, as well as the percent identity between their active sites (Table 2). Compared to entire zinc metalloprotease domain of nematode astacins to MEP1A (Table S3), NAS-21 shows 25.19% identity, NAS-22 shows 25.55% identity, and TOH-1 shows 27.21 percent identity (Table 2). NAS-13 and NAS-14 exhibited the highest percent identity (42.45%); however, RNAi against each of these astacins showed no utse defects (Table 1). When comparing the entire zinc metalloprotease domain of nematode astacins to MEP1B (Table S3), NAS-21 shows 28.03% identity, NAS-22 shows 28.36% identity, and TOH-1 shows 28.57% identity (Table 2). NAS-37 exhibits the highest percent identity with MEP1B (41.22%); however, NAS-37(RNAi) treatment showed a low percentage of utse defects (9.1%, Table 1) . We also compared the active site between MEP1A, MEP1B, NAS-21, NAS-22, and TOH-1 (outlined by green box Figure 2B). When compared to MEP1A, NAS-21 shares 47.37% identity, NAS-22 shares 57.89% identity, and TOH-1 shares 63.16% identity (Table 2). When compared with MEP1B, NAS-21 shares 47.37% identity, NAS-22 shares 63.16% identity and TOH-1 shares 68.42% identity. These percentages are significantly higher than any of the other domain comparisons, indicating that NAS-21, NAS-22, and TOH-1 are related to MEP1A and MEP1B through its zinc metalloprotease domain active site.

We also generated phylogenetic trees to determine relationships between MEP1A and MEP1B with NAS-21, NAS-22, and TOH-1 (Figure S2 and Figure S3). When comparing the entire sequence (Figure S2), we see that the astacins diverge into three major clades (which we have termed clade I, clade II, and clade III). Interestingly, the MEP1A and MEP1B fall into clade I, NAS-21 and NAS-22 fall into clade II, and NAS-26/TOH-1 falls into clade II, showing that there are high levels of sequence diversity between these proteins. We also created a tree using the zinc metalloprotease domains of MEP1A, MEP1B, NAS-21, NAS-22, and TOH-1 (Figure S3). Interestingly, MEP1A, MEP1B, and NAS-26/TOH-1 are all in the same clade (clade I), but NAS-21 and NAS-22 are in a different clade (clade II); however, if we move up one branching point, all become part of one monodelphic clade (see purple square). This verifies our findings that NAS-26/TOH-1 shows greater sequence similarity between MEP1A and MEP1B compared to NAS-21 and NAS-22.

Aside from comparisons with the active site of the zinc metalloprotease domain, NAS-21, NAS-22, and TOH-1 do not share significant sequence identity with MEP1A and MEP1B. Therefore it does not seem that NAS-21, NAS-22, or TOH-1 are taking on a specific role as one of the meprin subunits within *C. elegans* but rahter exhibit meprin-like qualities. Although other astacins show

greater sequence identity with MEP1A and MEP1B, we chose to focus on NAS-21, NAS-22, and TOH-1 because of their effect on utse development. Because the utse changes its cell shape in a manner similar to that of a metastasizing cell (Ghosh and Sternberg, 2014) we believe that better understanding how NAS-21, NAS-22, and TOH-1 function can provide insight into how meprins function in metastatic cancer.

4.4.3 Ectopic branch formation caused by *nas-21* loss-of-function

Because meprins are upregulated in metastatic cancer (Matters and Bond, 1999; Bond et al., 2005; Dietrich et al., 1996, Minder et al., 2012), we were interested to see how altering levels of NAS-21, NAS-22, and TOH-1 affected cell shape change. RNAi knockdown of these genes reduced utse outgrowth (Figure 1G'', 1H'', and 1I''). However, we observed additional cell body defects with knockdown of *nas-21*. In wild-type utse development the utse elongates, forming two arms (on the proximal side and one on the distal side), each with two branches on each side (Figure 3H; Ghosh and Sternberg, 2014); however, in some *nas-21(RNAi)* treated worms, we would see an additional small branch form on the proximal anterior utse branch (Figure 3A-3D). (*nas-22(RNAi)* and *toh-1(RNAi)* treated worms did not exhibit this phenotype). This defect occurred in a small percentage of *nas-21(RNAi)* treated worms (6.25%, Table 1). Interestingly, this branch also possessed nuclei (Figure 3B and 3D); however, the total number of nuclei (nine nuclei, Newman et al., 1996; Ghosh and Sternberg, 2014) remained constant, indicating that there was not a duplication event but rather a change in nuclear migration and cell outgrowth.

We observed similar ectopic branching phenotypes in the *nas-21* nonsense mutant *nas-21(gk375710)* (Figure 3G, Table 3). *nas-21(gk375710)* has a substitution that generates a premature stop codon at amino acid 38 (AGA to TGA) (Figure 3E, Thompson et al., 2013). This premature stop codon is within the prodomain of NAS-21; therefore, the mutant protein only contains the signal peptide and part of the prodomain (Figure 3E). The main defect that *nas-21(gk375710)* exhibits is the formation of ectopic branches, and there is no shortening of the utse (Figure 3G), which was the primary defect of *nas-21(RNAi)* treated worms.

One possibility as to why *nas-21(gk375710)* does not exhibit more severe defects is due to the presence of a potential secondary start site at amino acid 50 in NAS-21. Alternative start sites have circumvented mutations in other systems (Ozisik et al., 2003). This alternative start site would contain the entire astacin, EGF, and CUB domains (Figure 3E, Table S3). In meprins the

prodomain is cleaved off for activation (Grünberg et al., 1993); therefore, this mutant may be mimicking what is occurring endogenously to NAS-21. The presence of the stop codon at position 38 and not position 43 (which is the end of the NAS-21 prodomain) may also cause some misregulation in NAS-21 processing, which is why we are seeing some mutant phenotypes. Since the prodomain is thought to be involved in proper folding of meprins, it could also be affecting folding in NAS-21, which may cause this branching defect.

The *nas-22* deletion mutant, *nas-22(tm2888)*, in which a portion of the EGF and CUB domains are deleted (Figure S4A), showed no defects in utse development (Figure S4C; Table 3), which is why we chose to primarily focus on *nas-21* activity in the remainder of this work.

4.4.4 Overexpression of *nas-21* expands the utse cell membrane

After characterizing phenotypes that resulted from knockdown or loss-of-function of *nas-21* (Figure 1H'H''', Figure 3A-S, and Figure 3F-G), we wished to characterize nas-21 *gain-of-function* phenotypes. We generated a construct containing 2989 bp upstream of the *nas-21* transcription start site, the entire *nas-21* coding region and 794 bp downstream of the *nas-21* stop codon (Figure 4A), hereby referred to as the *nas-21* overexpression construct. This construct was extremely toxic, and we were only able to obtain survivorship at low concentrations (1ng/µl). When compared to wild type (Figure 4B-C), animals injected with 1ng/µl of the construct showed an expansion of the cell membrane along the dorsal-ventral axis (Figure 4G, Table 3), hereby referred to as blebbing (Charras 2008). We are certain that this was due to the construct itself, because when the construct was injected at an even lower concentration (0.1 ng/µl) we observed no defects (Figure 4E, Table 3). (We created an overexpression construct for *nas-22;* however, even low levels of injecting this construct resulted in lethal toxicity, which is why we were not able to screen *nas-22* overexpression phenotypes.)

Meprins are known to degrade components of the extracellular matrix (ECM) (Kruse et al., 2004; Köhler et al., 2000). We believe that worms overexpressing *nas-21* have expanded cell bodies, because an increase in levels of NAS-21 causes an increase in the degradation of the ECM (Figure 5B). Our hypothesis is that in wild type the utse expands outwards due to NAS-21, NAS-22, and TOH-1 cleaving/degrading components of the ECM (Figure 5A). This degradation cannot occur without the presence of these nematode astacins, which is why RNAi treatment of *nas-21, nas-22,* and *toh-1* inhibits utse outgrowth (Figure 1G'', Figure 1H'', and Figure 1I''). When one of these

three nematode astacins is overexpressed, the increased levels of this astacin (such as with *nas-21,* Figure 4G) cleaves larger numbers of ECM components, causing an expansion of the utse membrane (Figure 5B). This expansion occurs along the dorsal ventral axis (primarily ventrally) due to the presence of the basement membrane ventral to the utse (Ghosh and Sternbeg, 2014; Hagedorn and Sherwood, 2011).

4.4.5 Protease inhibitors act upstream of *nas-21*

We were interested in determining the mechanism NAS-21 uses to regulate utse outgrowth. We therefore wished to identify upstream and downstream regulators of NAS-21. We chose to screen known protease inhibitors to determine upstream regulators of NAS-21 and screen ECM components to identify downstream targets.

We generated a list of 51 protease inhibitors using WormBase and a publication containing a list of genes with putative protease inhibitor domains (WormBase; Ihara et al., 2011) (Table 1). We then used RNAi against these 51 genes and screened for utse defects, specifically defects that were comparable to the *nas-21* overexpression phenotype (Figure 5B). Knockdown of a NAS-21 protease inhibitor would cause higher levels of NAS-21, similar to the *nas-21* overexpression phenotype. Of the 51 genes test, we saw that RNAi against 15 genes exhibited high levels (greater than 25%) of membrane blebbing, similar to that of the overexpression mutants (Figure 6B, compare to Figure 4G). The genes are as follows: *C10G8.2, C10G8.3, cki-2, cpi-1, cpi-2, F35B12.4, K10D3.4, mec-1, mig-6, srp-2, T21D12.12, try-3, try-7, W0532.2, Y49G5A.1*.

We wished to determine if RNAi against these genes were causing the blebbling phenotype by specifically affecting levels of NAS-21. We created an assay where we treated wild-type, *nas-21* overexpression mutant, and *nas-21* loss-of-function mutant (*nas-21(gk375710)*) worms with protease inhibitor RNAi and identified interactions based on phenotypes observed. Increased levels of NAS-21 results in expanded membrane outgrowth and blebbing, and we hypothesized that using protease inhibitor RNAi in the *nas-21* overexpression strain would exaggerate its existing phenotype if it was specifically acting on NAS-21 (Figure 5C). Conversely, protease inhibitor RNAi in the *nas-21(gk375710)* would have no effect on its phenotype since there would be no NAS-21 for the protease inhibitor to act on (Figure 5D). *nas-21(gk375710)* may have an alternate start site that renders a functional protein; however, in this mutant the prodomain is separated from

the rest of the protein. Since the prodomain is implicated in proper folding, we believe that this protein may be misfolded, which could potentially hinder interactions with protease inhibitors.

We performed the aforementioned assay using RNAi against the 15 potential portease inhibitor genes and identified genes where RNAi treatment in the *nas-21* overexpression strain showed an exacerbated defect and RNAi treatment in the *nas-21(gk375710)* strain showed little to no defect (Table 4). Of the 15 genes, RNAi against five genes showed significant levels (under 0.0015 P-value) of exaggerated defects in the *nas-21* overexpression strain: *cpi-1*, *F35B12.4, mec-1, srp-2*, and *Y49G5A.1*. Of these five genes, RNAi against three of those genes did not have significant levels of defects (P-value above 0.09) in *nas-21(gk375710)*: *cpi-1*, *F35B12.4,* and *mec-1*. We therefore chose to characterize how these three genes in regulate *nas-21* activity.

4.4.6 Characterizing the role of specific protease inhibitors in utse development

Ideally we would verify interactions by observing changes in expression of *nas-21* caused by RNAi treatment of *cpi-1*, *F35B12.4,* and *mec-1.* However, we were unable to generate a *nas-21* translational fusion due to high levels of toxicity caused by injecting increased levels of NAS-21. Instead we have characterized the expression pattern of protease inhibitors (to predict if these inhibitors were in the vicinity of the utse/NAS-21 activity) and identified downstream effectors of these protease inhibitors by observing utse phenotypes.

cpi-1 is a homolog of cystatin, a cysteine protease inhibitor (Hashmi et al., 2006). *cpi-1* inhibits human cathepsin B, L, and S (Schierack et al., 2003) and is involved in defending nematodes against attack by plant parasites (Phiri et al., 2014). Interestingly, cystatin C is an inhibitor of MEP1A (Hedrich et al., 2010; Jefferson et al., 2012), and we are happy to have recapitulated finding with *nas-21* in the *C. elegans* utse. *cpi-1::gfp* can only be induced in the presence of cysteine proteinases, and cannot be detected without protease treatment (Phiri et al., 2014; Dr. David de Pomerai, personal communication). Any induced *cpi-1* expression was present globally through the worm. The other *C. elegans* cystatin homolog, *cpi-2*, was expressed in the gonad after protease treatment (Dr. David de Pomerai, personal communication); however, a low percentage and an insignificant level of utse defects were observed upon treatment with *cpi-2(RNAi)* (Table 1, 27%, P-value 0.4575).

F35B12.4 contains two Kunitz (KU) serine protease inhibitor domains (Ihara et al., 2011). *F35B12.4* contains one KU domain on its N-terminus (from amino acids 42 to 98) and one KU domain on its C-terminus (from amino acids 157 to 213) (Schultz et al., 1998). Kunitz domains are the active domains of certain serine protease inhibitors. We created an *F35B12.4p::GFP* expression construct using a 643 bp region to drive GFP (see Materials and methods). We saw expression in the pharyngeal neuron M4 (Figure 6D) but saw no expression in the uterine region. Therefore, we infer that F35B12.4 is being secreted or acting through another pathway to affect levels of NAS-21 activity.

Interestingly, *cpi-1* and *F35B12.4* are computationally predicted to interact with one another (geneorienteer.org; Zhong and Sternberg, 2006). Therefore they may be acting together on *nas-21*.

mec-1 is involved in regulating mechanosensory behavior in *C. elegans* (Chalfie and Sulston, 1981; Emtage et al., 2004) and contains eight KU serine protease inhibitor domains (Ihara et al., 2011; Schultz et al., 1998). Mutants defective in *mec-1* lack accumulation of ECM proteins, specifically accumulation of the collagen *mec-5.* This is interesting because meprins cleave collagen IV (Kruse at al., 2004; Köhler et al., 2000), and therefore *mec-1* affect accumulation of collagen through regulating levels of *nas-21.* *mec-5* RNAi does not induce utse defects, however, so we infer that *mec-1* is acting on a separate collagen in the utse outgrowth (Table 1). *mec-1* mutants have reduced sensitivity to touch response stimuli (Emtage et al., 2004). *mec-1* is expressed in touch receptor neurons, lateral neurons (the SDQ, PLN, and ALN neurons and two neurons of the dorsal sublateral cord), the PVT neuron and intestinal muscle. The touch neurons lie adjacent to the seam (Altun and Hall, 2011), which is adjacent to the utse, and therefore *mec-1* may be acting laterally on the utse and *nas-21*.

We wanted to determine if these three protease inhibitors were acting solely through *nas-21* or were affecting utse development via other downstream effectors. We therefore generated a list of genes predicted/known to interact with *cpi-1*, *F35B12.4,* and *mec-1* and tested the effects of RNAi against these genes. We tested predicted and known interactions using gene interaction database geneorienteer.org (Zhong and Sternberg, 2006).

For *cpi-1*, we tested RNAi that was available for the top five listed genes on geneorienteer.org (Table 1), two of which were known interactions (*dys-1* and *pat*-12) and all of which had a feature score higher than 16 (Figure S6). *dys-1(RNAi)* showed significant levels of utse defects (34.6%, P-

value <0.0001; Table 1). *dys-1* is the *C. elegans* homolog of the human dystrophin gene, mutations in which cause Duchenne muscular dystrophy (Bessou et al., 1998). *dys-1* mutants are hyperactive and hyper contracted and hypersensitive to aldicarb. *dys-1* is involved in cell positioning through tethering neurons to the actin cytoskeleton (Zhou and Chen, 2011). *dys-1* positively activates *cpi-1* (Towers et al., 2008). Unusually, the utse of *dys-1(RNAi)* treated worms was shorter than that of wild type (Figure S5) (since *dys-1* is predicted to activate cpi-1, we assumed that we would observe the overexpression phenotype), indicating that this gene may be involved in promoting utse outgrowth through a separate mechanism.

Three genes were significantly predicted to interact with *F35B12.4*, *cpi-1, cpi-2,* and *pat-2* (Table 1; Figure S6). We have already characterized *cpi-1*'s role as a potential protease inhibitor against *nas-21*. RNAi against *cpi-2* and *pat-2* did not cause significant defects in utse development.

Six genes were significantly predicted to interact with *mec-1* (Table 1): *unc-86, mec-4, mec-5, mec-9, dop-1,* and *mec-7*. RNAi against two of these genes caused defects in the utse – *unc-86* and *mec-9*. *unc-86* is a transcription factor expressed in the touch receptor neurons that acts positively acts upstream of *mec -1* (Baumeister et al., 1996). *mec-9* is an extracellular protein that has a similar structure to *mec-1*, containing six EGF repeats and five Kunitz domains that positively regulates levels of *mec-1* (Schultz et al., Emtage at al., 2004.) We believe that when we knockdown *mec-9* and *unc-86* we reduce expression of *mec-1,* which causes defects in utse development. RNAi against *unc-86* showed defects similar to that of the overexpression construct, which further validates this model (Figure S5; Figure S6).

We wished to further expand this network and also characterized the role of *C. elegans* homologues of known human cystatin and kunitz domain containing protease inhibitors in utse development.

Cystatin acts on two groups of proteases – cysteine proteases (Grzonka et al., 2001) and cathepsins, which are cysteine lysosomal proteases (Haves-Zburof et al., 2011). We identified 23 *C. elegans* cysteine proteases (both capthepsin and non-cathepsin-like) and cysteine protease targets (Table 5) and performed RNAi against these genes. Of these genes, 7 genes showed significant levels of utse defects (Table 5, P-value <0.001): the cathepsin-like cysteine proteases *cpr-1* and *cpr-6* (Laraminie and Johnstone, 1996), the cathepsin target *daf-4* (Jacobson et al., 1988), the cathepsin homolog *asp-3* (Tcherepanova et al, 2000), the cathepsin A homolog *Y40D12A.1* (Miedel et al., 2012; Xu et al., 2014) *mrp-4,* which acts upstream of cathepsin (Schaheen et al., 2006), and *clp-1,* which contains a

cysteine-protease active site (Joyce et al., 2012). All of these genes exhibited overexpression phenotypes (like that of *unc-86*), indicating that these genes are inhibiting some gene that acts similarly to *nas-21*.

Kunitz domain contains protease inhibitors with several types of proteases/proteins, including plasmin (Wan et al., 2013), thrombin (Wood et al., 2014), Factor Xa, and trypsin (Dennis and Lazarus 1994). We created a list of *C. elegans* genes that contain kunitz domains, are related to the known Kunitz domain inhibitor targets listed above, or are targets of the known Kunitz domain targets (Table 5). We tested RNAi against these 22 genes and 7 of these genes showed significant levels of utse defects (Table 5, P-value under 0.001). The genes are as follows: the kunitz domain containing *apl-1* (Salameh et al., 2009; Ewald and Li, 2012); the trypsins *try-3, try-5,* and *try-7* (Dennis and Lazarus, 1994; Shaye and Greenwald, 2011; Smith and Stanfied, 2011), the trypsin target *unc-45* (Gazda et al., 2013; papilin (*mig-6),* which contains a Kunitz domain (Kramerova et al., 2000) and the plasmin target ECM protein *nid-1* (Mayer et al., 1993; Kang et al., 2000).

Through categorizing utse phenotypes (blebbing due to negative/inhibitory interactions, and reduced outgrowth due to activating/positive interactions) and information found in literature, we have created a tentative network based on these interactions, shown in Figure S6.

4.4.7 Serine protease inhibitors regulate NAS-21

Meprin-like proteases and serine protease inhibitors localize within spider digestive fluid (Foradori et al., 2006). TAILS analysis has also shown that Mep1A and Mep1B interact with the serine protease inhibitor LEKTI (Jefferson et al., 2012). Therefore we wished to determine if serine protease affects NAS-21 activity.

While screening for protease inhibitors that were potentially affecting *nas-21,* we tested eight *C. elegans* serpins and saw that two showed overexpression phenotypes (*srp-1* and *srp-2*; Table 1). Though *srp-1* and *srp-2* did not meet our criteria for specifically affecting *nas-21* through our analysis used in Table 4, we were curious as to whether they could be affecting *nas-21* activity indirectly. We chose to focus specifically on *srp-2* due to its high level of severe overexpression phenotypes in the *nas-21* overxpression constructs.

We characterized the *srp-2* expression by using an *srp-2* transcriptional fusion construct (*srp-2::gfp*) (McKay et al., 2003). *srp-2* is expressed in the uterine toroid region, with expression concentrated at uterine toroid 1 (Figure 7D). The uterine toroids are cells that line the lumen of the uterus (Newman et al., 1996; Ghosh and Sternberg 2014) and we have shown that genes expressed in uterine toroid 1 contribute to utse outgrowth (Ghosh and Sternberg, 2014). *srp-2* is therefore localized to an ideal region for for regulating *nas-21* activity.

Since *srp-2* RNAi showed some defects in *nas-21(gk375710)*, we believe that *srp-2* may be acting on the utse through pathways other than *nas-21*. In order to determine what other pathways *srp-2* may be using to affect utse development we performed RNAi against genes that were characterized to act downstream of *srp-2* (Table 1) as well as genes that are targets of serpins (Table 5). We used geneorienteer.org (Zhong and Sternberg, 2006) to generate a list of the top five genes predicted to interact with *srp-2.* RNAi against one of these genes, *ubxn-3*, showed significant utse defects. *ubxn-3* and *srp-2* share a feature score of 7.22 on geneorienteer.org (Zhong and Sternberg, 2006). Specifically, both are expressed in *C. elegans* neurons, in *Arabidopsis,* and in mouse placenta. Both genes are also involved in regulating cell adhesion in rat, and are involved in similar biological processes in *Drosophila*, humans, and mouse. *ubxn-3* contains a ubiquitin regulatory X domain, and is involved in sperm production (Sasagawa et al., 2010)*)* and is expressed in the spermatheca (which lies proximal to the uterus and utse) and nerve cells (Yamauchi et al., 2007). Therefore, we believe that *srp-2* may also be acting on the utse through *ubxn-3* (Figure S6).

We also chose to look at proteins that have been characterized as serpin targets. Chymotrypsin-like peptidases have been characterized as targets of *srp-3*, another *C. elegans* serpin (Pak et al., 2006). We therefore looked at genes that show similar activity to chymotrypsin or are targets of chymotrypsin (Table 5). Interestingly, in addition to being a trypsin target, *unc-45* is also a chymotrypsin target (Lee et al., 2011; Price et al., 2002), and RNAi against *unc-45* shows significant defects (Table 5). *unc-45* is a muscle specific protein that controls muscle thick filament assembly (Venolia et al., 1999). *unc-45* is expressed in the sex muscles. We have shown that the sex muscles are one of the tissues that contributes to regulating proper utse outgrowth (Ghosh and Sternberg, 2014). Therefore we believe that *unc-45* also affects utse outgrowth, and is controlled by *srp-2,* as well as the two kunitz domain containing protease inhibitors *F35B12.4* and *mec-1* (Figure S6).

srp-2 also is an inhibitor of cathepsin-like proteases (Pak et al., 2004) We tested these proteases when investigating downstream effectors of cystatins and saw that *cpr-1, cpr-6*, *daf-4*, *asp-3*, *Y40D12A.1*, *mrp-4,* and *clp-1* all have effects on utse development (Table 5). We therefore believe that *srp-2* may be regulating these genes in utse development as well.

Through analyzing the *nas-21* overexpression phenotype we have identified four candidate protease inhibitors, and through scoring utse phenotypes we have added to this network by characterizing both upstream and downstream effectors of these protease inhibitors (Figure S6). This in itself shows the power of using *C. elegans* genetics to expand not only the NAS-21 regulatory network, but also the meprin regulatory network (Figure 11). In our study, not only have we recapitulated the presence of known meprin regulators (Cystatin/*cpi-1* and serine protease inhibibors/*srp-2),* but have identified new candidates in this network (*F35B12.4* and *mec-1*). We are excited to have generated these results and hope that this is just the beginning for using the *C. elegans* utse as a model to study meprins.

4.4.8 Effect of nematode astacins on *C. elegans* extracellular matrix proteins

Meprins cleave extracellular matrix proteins (ECM) *in vitro* (Kohler et al., 2000; Kruse et al., 2004). Specifically, meprin α (Mep1A) cleaves laminin 1 on the α1 chain and cleaves laminin 5 on the α3 chain (Kohler et al., 2000), and both meprin α and meprin β (Mep1A and Mep1B) degrade collagen IV (Kruse et al, 2004), and proteolytically cut fibronectin and nidogen at several sites.

These studies indicate that meprin either degrades or cleaves components of the extracellular matrix so that metastasizing cells can move into surrounding tissues. We wanted to determine if the presence of meprin-like proteins (specifically NAS-21, NAS-22, and TOH-1) affect distribution of extracellular matrix proteins in uterine tissues. We tested this by observing changes in expression levels of ECM proteins through treating translation fusion expression constructs of ECM proteins with *nas-21, nas-22,* and *toh-1* RNAi. We hypothesized that *nas-21, nas-22,* and *toh-1* knockdown will increase protein levels of ECM components.

C. elegans collagen genes were ideal targets since both meprin subunits completely degrade collagen IV (Kruse et al, 2004). In order to determine if collagen was necessary for utse development, we performed RNAi against known *C. elegans* collagen genes (Table 1) and scored for utse defects. We chose these three genes specifically because two of these genes (*emb-9* and *let-*

2) encode collagen IV in *C. elegans,* and *mec-5,* which is a collagen known to interact with protease inhibitor *mec-1* (Emtage et al., 2004).

RNAi against mec-5 resulted in no utse defects (Table 1). Instead we focused on *let-2* and *emb-9.* RNAi against *emb-9* generated utse defects (Table 1) and we used this protein to characterize the effect nematode astacins have on collagen distribution.

Changes in expression pattern were difficult to visualize using wide-field epifluorescence microscopy. We therefore used confocal imaging to finely observe changes in ECM expression due to *nas-21, nas-22,* and *toh-1* RNAi.

We used a *emb-9p::emb-9::dendra* line to observe changes in *emb-9* expression (Ihara et al., 2011). No changes in *emb-9* expression were observed in the presence of *nas-21* and *nas-22(RNAi)* (Figure 8B and 8C); however, *toh-1* RNAi did increase expression levels of *emb-9* in the vicinity of the uterus (Figure 8D). *emb-9* expression can be categorized into two types: puncta/globule-like accumulations of expression in the body wall, and a thin line of expression in the utse (Figure 8A). In *toh-1(RNAi)* treated worms, we saw a large increase in the number of *emb-9* globules in the body wall as well as an accumulation of gfp in the posterior uterine region (see red box Figure 8D). We therefore believe that *toh-1* specifically regulates levels of *emb-9* in the *C. elegans* uterus.

Since meprin α (Mep1A) cleaves laminin (Kohler et al., 2000), we also wanted to determine the effect of *nas-21*, *nas-22,* and *toh-1* knockdown on *C. elegans* laminins. *C. elegans* has four laminins: two encode the laminin α chain (*epi-1* and *lam-3*), one encodes the laminin β chain, *epi-1*, and one encodes the laminin γ chain, *lam-2* (Kramer 2005). We wanted to determine if these laminins involved in utse development, and to this end, we performed RNAi against these four genes and screened for utse defects (Table 1). Two of these genes, *lam-1* and *epi-1,* show significant utse defects.

Though RNAi against *epi-1* generates severe (Figure S7B-D) defects in utse, we saw that *epi-1* is not expressed in the vicinity of the uterus (Figure S7E). Therefore, we eliminated *epi-1* among the laminins potentially being regulated by *nas-21, nas-22,* and *toh-1*.

We used the *lam-1* translational fusion, *lam-1p::lam-1::gfp,* to observe *lam-1* expression (Ziel et al., 2009). *lam-1* is expressed in the dorsal utse edge as well at the lumen of the *C. elegans* uterus and

in the distal tip cell (DTC) (Figure 8E). RNAi against *nas-22* and *toh-1* had no effect on *lam-1* (Figure 8G and 8H). However, *nas-21(RNAi)* treated worms showed an increase in the intensity of *lam-1* expression in the uterus and in the distal tip cells (Figure 8F). We wished to quantify the change in intensity of *lam-1* expression so that we could determine the fold by which LAM-1 levels had increased. We chose two slices that were at comparable locations in the worm (based on vulval anatomy) from the *lam-1p::lam-1::gfp* and *nas-21(RNAi) lam-1p::lam-1::gfp* z-stacks (Figure 8M and Figure 8O). For each image, we quantified mean intensity in an area that contained the uterus (see whites boxes, Figure 8N and Figure 8P). Treatment of *nas-21(RNAi)* caused an 1.76 fold increase in fluorescent intensity. Therefore, we believe that presence of *nas-21* is necessary to control levels of *lam-1* expression (Figure 8A).

Since *nas-21* is affecting levels of LAM-1, we wanted to see if knockdown protease inhibitors acting on *nas-21* (*cpi-1, srp-2, mec-1, F35B12.*4) would affect levels of LAM-1. Ideally knockdown of protease inhibitors would increase *nas-21* activity, which would increase amount of laminin cleavage by NAS-21 and reduce levels of *lam-1* expression. *srp-2, F35B12.4,* and *mec-1* RNAi treatment of *lam-1p::lam-1::gfp* did not affect *lam-1* expression levels (Figure S8B-D). Since there are multiple genes that affect activity of *nas-21*, we believe that reducing the levels of these individual protease inhibitors by RNAi does not increase NAS-21 activity to the level where observable changes in *lam-1* expression are apparent.

Nidogen and fibronectin are also cleaved or degraded by meprins (Kruse et al., 2004). *nid-1* encodes the sole *C. elegans* nidogen homolog (Kang and Kramer 2000; Kim and Wadsworth 2000). RNAi against *nid-1* generated significant utse defects (Table 1). Antibody staining shows *nid-1* staining within the dorsal edge of the uterus (Kang and Kramer, 2000), indicating that it may be acting in this region. However, *nid-1::gfp* expression is limited to the PLM neurons, the intestinal cells, and the distal tip cells of the gonad (Kim and Wadsworth 2000). Therefore we were unable to evaluate changes in uterine expression of *nid-1* due to actacin knockdown.

C. elegans lacks fibronectin (Meighan et al., 2004); however, the *C. elegans* genome contains 23 genes that contain fibronectin domains (Table 1) We saw that RNAi treatment against two of these genes, *unc-73* and *unc-40,* resulted in significant utse defects (Table 1). Interestingly, both of these genes are involved in branch formation (Struckhoff and Lundquist 2003; Hao et al., 2010), a phenotype we observed as a result of *nas-21(RNAi)* treatment and in *nas-21(gk375710)* (Figure 3C,

3D, 3G). We hypothesize *nas-21* regulates both branch formation activity and fibronectin production by acting upstream of these genes.

We also wanted to use the utse to identify other meprin targets. One such target was the ECM protein *sdn-1*. *sdn-1* is the *C. elegans* homolog of vertebrate syndecan, a type I transmembrane heparan sulfate proteoglycan (Kinnunen 2014). *sdn-1* is expressed in the hypodermis, and is involved in HSN neuron migration. We used a *sdn-1p::sdn::gfp* reporter to visualize *sdn-1* localization, and saw expression in the hypodermis in the vicinity of the uterus (Figure 8I). *nas-21, nas-22,* and *toh-1(RNAi)* treatment of *sdn-1p::sdn::gfp* resulted in an expansion of the *sdn-1* expression pattern along the anterior posterior axis (Figure 8J-L), indicating that these three astacins may be cleaving/degrading *sdn-1*. Therefore, using our model we have identified an additional ECM protein that meprin-like *nas-21, nas-22,* and *toh-1* act on (Figure 11).

4.4.9 Specificity of astacin activity across multiple *C. elegans* tissues

We have shown that *nas-21, nas-22,* and *toh-1* cleave/degrade ECM components, but wished to determine if these astacins specifically affect the utse. Therefore, we designed an assay where we observed changes in ECM in a tissue distal to the utse.

Our distal tissue of choice was the *C. elegans* pharynx. The pharynx, or foregut, is used by *C. elegans* to intake food (Mango, 2007). The pharynx consists of two lobes connected by a tube, and is encased in a basement membrane. One of the components of this basement membrane is the type IV collagen *emb-9* (Gupta et al., 1997). Since we knew that *toh-1* affected *emb-9* localization in the utse, wished to see if nematode astacins could affect levels of *emb-9* within the pharynx.

We first wished to determine if the presence of *emb-9* was necessary for proper pharyngeal integrity. We performed *emb-9(RNAi)* on wild-type N2 worms and scored for pharyngeal defects. *emb-9(RNAi)* treated worms exhibited gaps within the tissue surrounding the pharynx (Figure 9B, Table 6), indicating that the integrity of the basement membrane had been compromised. Since *emb-9* plays a vital role in pharyngeal formation, we decided to characterize *emb-9* expression in the presence of nematode astacin knockdown.

As a positive control for our tissue specificity assay we chose three nematode astacins thought to affect pharyngeal function. Of the 40 *C. elegans* astacins, we chose three astacins that were either

solely expressed in the pharynx or expressed in the pharynx and tissues distal to the utse. These astacins, hereby referred to as the pharyngeal astacins, were *nas-1, nas-15,* and *nas-25* (Park et al., 2010). *nas-1, nas-15,* and *nas-25(RNAi)* treatment caused gaps in the tissue adjacent to the pharynx (Figure 9C-E), indicating that these astacins were affecting tissue integrity in the pharynx. In order to test for specificity, we also observed the effect of *nas-21, nas-22,* and *toh-1(RNAi)*, hereby referred to as the uterine astacins, on the pharynx. Surprisingly, *nas-21* and *nas-22(RNAi)* also caused gaps within the tissue adjacent to the pharynx. *toh-1(RNAi)* also showed similar defects, though at a significantly lower penetrance compared to the other uterine RNAis (10%, Table 6).

We next tested if pharyngeal astacins affect *emb-9* expression in the utse. *nas-1(RNAi)* and *nas-15(RNAi)* did not result in any gross utse defects; however, 16% of *nas-25(RNAi)* treated worms exhibited cell outgrowth defects (Table 1). Interestingly RNAi against all three pharyngeal astacins altered *emb-9* expression. *nas-1(RNAi)* treated worms exhibited increased *emb-9* expression in the utse (Figure 10B, see yellow arrow), and in globules ventral to the utse (Figure 10B, see white arrows). *nas-15*(RNAi) treated worms had reduced *emb-9* expression (Figure 10C). *nas-25(RNAi)* treated worms showed an increase in expression within collagen globules (Figure 10D, see white arrow). Since there was an increase in *emb-9* expression with knockdown of *nas-1* and *nas-25,* we believe that these two astacins act similarly to *toh-1* and cleave/degrade collagen IV within the utse. We also hypothesize that *nas-15* may be acting through an alterative pathway that positively regulates *emb-9*, which is why we see a reduction of *emb-9* expression upon *nas-15* knockdown.

We also observed effects of pharyngeal and uterine astacin RNAi knockdown on *emb-9* expression within the pharynx. RNAi against all six astacins affected *emb-9* pharyngeal expression. Specifically, number of collagen puncta in the vicinity of the pharynx decreased for all six astacins. Wild-type worms have 159 puncta, whereas *nas-1(RNAi)* treated worms had 121 puncta, *nas-15(RNAi)* treated worms had 87 puncta, *nas-25(RNAi)* treated worms had 94 puncta, *nas-21(RNAi)* treated worms had 138 puncta, *nas-22(RNAi)* treated worms had 66 puncta, and *toh(RNAi)* treated worms had 84 puncta. We may be seeing these results due to the presence of gaps in tissue -- number of puncta may be reduced because the amount of total tissue surrounding the pharynx has decreased. However, number of puncta did not correlate with level of defects seen in N2 worms treated with pharyngeal and uterins astacin RNAi. Therefore these astacins may be functioning in some pathway that positively regulates *emb-9* expression within the pharynx, which is why we see reduced numbers of puncta with astacin knockdown.

Our assay indicates that multiple astacins control integrity of the ECM in multiple tissues. We have added *nas-1, nas-15,* and *nas-25* to our network (Figure 11) because these astacins also affect collagen IV expression in the utse (Figure 10B-D). We also observe that *nas-1, nas-15*, *nas-25, nas-21,* and *nas-22* affect integrity of tissues surrounding the pharynx (Figure 9). This result is somewhat puzzling since these two groups of astacins are expressed distally from their target tissues. *nas-1, nas-15, nas-21, nas-22,* and *toh-1* all lack a transmembrane domain (Table S3), so it is possible that these astacins are secreted and have long-range effects. However, *nas-25* contains a transmembrane domain, although this domain may be cleaved in proteolytic processing. Since we have shown that astacins have long-range effects, we believe that a comprehensive study of how all 40 astacins is necessary to completely know the extent of how astacins affect the ECM.

4.5 Discussion

We have shown that three *C. elegans* nematode astacin genes, *nas-21*, *nas-22,* and *toh-1*, can be used to study meprin activity *in vivo*. Using the utse as a model, we demonstrate three meprin-like genes *nas-21, nas-22,* and *toh-1,* control cell shape change, regulate levels of ECM proteins (*emb-9, lam-1* and *sdn-1*), and use signaling pathways that are similar to meprins (*srp-2* and *cpi-1*). Additionally we identified two new upstream regulators of *nas-21* (*F35B12.4* and *cpi-1)* and 12 other members of the *nas-21* interaction network. We are eager to determine if these novel members of this interaction pathway are playing a role in meprin function and are plan on continuing to use the *C. elegans* utse as a model to study the *in vivo* function of meprins.

4.5.1 Characterizing the role of *nas-21* in the utse

Though we saw that three astacins were expressed in the utse and surrounding tissues (*nas-21, nas-22,* and *toh-1*), we primarily characterized *nas-21* for two reasons: the severity of utse defects caused by *nas-21* and availability of reagents. Using the cell outgrowth and overexpression phenotypes we were able to generate a network (Figure 11) of genes in which we believe *nas-21* is acting.

We observed an additional phenotype when characterizing *nas-21* – the formation of ectopic branches from the utse. Several gene families are involved in utse development (Ghosh and Sternberg, 2014), and we believe that knockdown of *nas-21* may be affecting function of other genes, which can induce branch formation. Specifically, two types of genes that we have

characterized in utse outgrowth, netrins and *unc-73* (Ghosh and Sternberg, 2014; Ghosh and Sternberg in prep; Table 1), have roles in branch formation in other tissues. *unc-73* mutants exhibit defects in axonal branching (Struckhoff and Lundquist 2003) and therefore knockdown of *nas-21* may be affecting *unc-73* activity. Misregulation of the Netrin ligand *unc-6* and its receptor *unc-40* also cause defects in branching (Hao et al., 2010). Netrins are expressed on the invasive edge of the anchor cell (Ziel et al., 2009) and RNAi knockdown of the two *C. elegans* netrin ligands (*unc-5* and *unc-6)* and the Netrin receptor (*unc-40)* results in defects in utse outgrowth (Table 1). Therefore we also hypothesize that *nas-21* may be affecting regulation of these proteins to induce branch formation.

4.5.2 Future directions

Since we have shown that *nas-21, nas-22,* and *toh-1* have meprin-like characteristics, including controlling levels of ECM proteins as well as using similar signaling pathways (*srp-2* and *cpi-1*), we wish to later test if human MEP1A or MEP1B within the *C. elegans* utse can rescue *nas-21* knockdown phenotypes. We plan on creating a construct by using a utse specific promoter region (*cdh-3*) to drive the human coding region of MEP1A and MEP1B in a vector that contains a *C. elegans* 3'utr (*unc-54*). This type of analysis will bolster the role of the utse as an ideal *in vivo* model for studying meprin activity.

4.5.3 Adding to the existing meprin interaction network

Prior to this work, the major findings of the meprin network were generated through *in vitro* studies (Kruse et al., 2004; Köhler et al., 2000; Ambort et al., 2010; Rösmann et al., 2002; Tang and Bond, 1998; Ohler et al., 2010; Herzog et al., 2014; Jefferson et al., 2012; Bien et al., 2012; Huguenin et al., 2008; Hedrich et al., 2010). The current network for meprin α and meprin β contains six upstream activators for meprin α and seven upstream activators for meprin β, and seven downstream targets for meprin α and 10 downstream targets for meprin β (Figure 11A). Of these interactions, 22 have been determined through *in vitro* work. Though this is valuable information, determining how these genes function *in vivo* can shed light on exactly how meprins affect a cell's environment and identify other potential regulators.

Certain *in vivo* studies of meprin activity have been conducted. Knockout mice for meprin α and meprin β have been generated (Banerjee et al., 2011; Normal et al., 2003). These knockouts have

been primarily used to determine phenotypes resulting from meprin loss-of-function. For example, knockout mice show decreased levels of collagen deposition in the skin, indicating an *in vivo* interaction between meprins and collagen I (Broder et al., 2013). Changes in renal gene expression have been determined using microarray analysis of kidney RNA from meprin β knockout mice, and MMP1 downregulated meprin β and meprin α knockout mice, but these results are from observing fold change (Normal et al., 2003; Broder et al., 2013). The meprin β knockout mouse has been used to determine certain interactions, such as Fra-2 acting as an inhibitor (Biasin et al., 2014) and Muc2 being a target (Schütte et al., 2014). Though this is promising, using a model such as *C. elegans*, with fast generation time and powerful genetics, allows us to not only identify genes that are affecting meprin activity but how these genes are affecting meprin activity.

4.5.4 Conclusions

In our work we have not only identified genetic new interactions between *nas-21, nas-22,* and *toh-1* in the *C. elegans* utse, but we have also shown that these three genes can be used to study meprin activity in a new *in vivo* system. We have identified similar interactions that exist between nematode astacins in the utse and meprins and their interaction network (Figure 10A). Both nematode astacins and meprins act on ECM proteins (collagen IV and nidogen) and are regulated by serine proteases (*srp-2* and KLKs) and cystatins (*cpi-1*). With the nematode astacin utse system we were able to identify multiple interactions systematically, and therefore we hope to continue using this powerful tool to further our understanding of meprins.

4.6 Acknowledgements

We thank Harald Hutter (Simon Fraser University), Matthew Buechner (University of Kansas), David Sherwood (Duke University), and the Caenorhabditis Genetics Center (University of Minnesota) for worm strains; Barbara Perry and Gladys Medina for technical assistance; and Marianne Bronner, Bruce Hay, and David Chan for helpful discussions. S.G. was supported by National Institutes of Health USPHS training grant GM07616; S.N. was supported by the Amgen Foundation through the Amgen Scholars Program. This work was supported by the Howard Hughes Medical Institute, with which P.W.S. is an investigator.

References

Altun, Z.F. and Hall, D.H. 2011. Nervous system, general description. In WormAtlas. doi:10.3908/wormatlas.1.18

Baumann, M., Kappl, A., Lang, T., Brand, K., Siegfried, W., Paterok, E. 1990. The diagnostic validity of the serum tumor marker phosphohexose isomerase (PHI) in patients with gastrointestinal, kidney, and breast cancer. Cancer Investigation; **8**:351–356.

Baumeister, R., Liu, Y., Ruvkun, G. 1996. Lineage-specific regulators couple cell lineage asymmetry to the transcription of the Caenorhabditis elegans POU gene unc-86 during neurogenesis. Genes Dev.; **10**(11):1395-410.

Becker, C., Kruse, M.N., Slotty, K.A., Köhler, D., Harris, J.R., Rösmann, S., Sterchi, E.E., Stöcker, W. 2003. Differences in the activation mechanism between the alpha and beta subunits of human meprin. Biol Chem.; **384**(5):825-31.

Beckmann, G. and Bork, P. 1993. An adhesive domain detected in functionally diverse receptors. Trends Biochem Sci.; **18**(2):40-1.

Bessou, C., Giugia, J.B., Franks, C.J., Holden-Dye, L., Ségalat, L. 1998. Mutations in the Caenorhabditis elegans dystrophin-like gene dys-1 lead to hyperactivity and suggest a link with cholinergic transmission. Neurogenetics.; **2**(1):61-72.

Bond, J.S. and Beynon, R.J. 1995. The astacin family of metalloendopeptidases. Protein Sci; **4**(7):1247–1261.

Bond, J.S., Matters, G.L., Banerjee, S., Dusheck, R.E. 2005. Meprin metalloprotease expression and regulation in kidney, intestine, urinary tract infections and cancer. FEBS Lett.; **579**(15):3317-22.

Bork, P. and Beckmann, G. 1993. The CUB domain. A widespread module in developmentally regulated proteins. J Mol Biol.; **231**(2):539-45.

Brenner, S. 1974. The genetics of Caenorhabditis elegans. Genetics.; **77**(1):71-94.

Bronner, M.E. and LeDouarin, N.M. 2012. Development and evolution of the neural crest: an overview. Dev Biol.; **366**(1):2-9.

Carlsson, E., Ranki, A., Sipilä, L., Karenko, L., Abdel-Rahman, W.M., Ovaska, K., Siggberg, L., Aapola, U., Ässämäki, R., Häyry, V., Niiranen, K., Helle, M., Knuutila, S., Hautaniemi, S., Peltomäki, P., Krohn, K., 2012. Potential role of a navigator gene NAV3 in colorectal cancer. Br. J. Cancer. **106**, 517-524

Chalfie, M. and Sulston, J. 1981. Developmental genetics of the mechanosensory neurons of Caenorhabditis elegans. Dev Biol.; **82**(2):358-70.

Charras, G.T. 2008. A short history of blebbing. J Microsc.; **231**(3):466-78.

Cheng, K.W., Lahad, J.P., Gray, J.W., Mills, G.B., 2005. Emerging role of RAB GTPases in cancer and human disease. Cancer Res. **65**, 2516-2519.

Chiang, A. C. and Massagué, J. 2008. Molecular basis of metastasis. N. Engl. J. Med. 359, 2814–2823.

Davis, C.G. 1990. The many faces of epidermal growth factor repeats. New Biol.; **2**(5):410-9.

Dennis, M.S. and Lazarus, R.A. 1994. Kunitz domain inhibitors of tissue factor-factor VIIa. II. Potent and specific inhibitors by competitive phage selection. J Biol Chem.; **269**(35):22137-44.

Dietrich, J.M., Jiang, W., Bond, J.S. 1996. A novel meprin beta' mRNA in mouse embryonal and human colon carcinoma cells. J Biol Chem.; **271**(4):2271-8.

Dobashi, Y., Watanabe, H., Matsubara, M., Yanagawa, T., Raz, A., Shimamiya, T., Ooi, A. 2006. Autocrine motility factor/glucose-6-phosphate isomerase is a possible predictor of metastasis in bone and soft tissue tumours. J. Pathol; **208**:44–53.

Emtage, L., Gu, G., Hartwieg, E., Chalfie, M. 2004. Extracellular proteins organize the mechanosensory channel complex in C. elegans touch receptor neurons. Neuron.; **44**(5):795-807.

Ewald, C.Y., and Li, C. 2012. Caenorhabditis elegans as a model organism to study APP function. Exp Brain Res.; **217**(3-4):397-411.

Filella, X., Molina, R., Jo, J., Mas, E., Ballesta, A.M. 1991. Serum phosphohexose isomerase activities in patients with colorectal cancer. Tumour Biology; **12**:360–367.

FigTree v1.4.2 http://tree.bio.ed.ac.uk/software/figtree/

Foradori, M.J., Tillinghast, E.K., Smith, J.S., Townley, M.A., Money, R.E. 2006. Astacin family metallopeptidases and serine peptidase inhibitors in spider digestive fluid. Comp Biochem Physiol B Biochem Mol Biol.; **143**(3):257-68.

Fortin, S.P., Ennis, M.J., Schumacher, C.A., Zylstra-Diegel, C.R., Williams, B.O., Ross, J.T., Winkles, J.A., Loftus, J.C., Symons, M.H., Tran, N.L., 2012. Cdc42 and the guanine nucleotide exchange factors Ect2 and trio mediate Fn14-induced migration and invasion of glioblastoma cells. Mol. Cancer Res. **10**, 958-968.

Funasaka, T., Hu, H., Yanagawa, T., Hogan, V., Raz, A. 2007. Down-regulation of phosphoglucose isomerase/ autocrine motility factor results in mesenchymal-to-epithelial transition of human lung fibrosarcoma cells. Cancer Res; **67**:4236–4243.

Gazda, L., Pokrzywa, W., Hellerschmied, D., Löwe, T., Forné, I., Mueller-Planitz, F., Hoppe, T. 2013. Clausen T. The myosin chaperone UNC-45 is organized in tandem modules to support myofilament formation in C. elegans. Cell.;**152**(1-2):183-95.

Ghosh, S. and Sternberg, P.W. 2014. Spatial and molecular cues for cell outgrowth during C. elegans uterine development. Dev Biol.; **396**(1):121-35.

Ghosh, S., and Sternberg, P.W. A candidate RNAi screen for cell outgrowth defects in the *C. elegans* utse. in prep.

GLOBOCAN. 2014. Section on Cancer Surveillance. http://globocan.iarc.fr/Pages/fact_sheets_cancer.aspx

Gomis-Rüth, F.X. 2003. Structural aspects of the metzincin clan of metalloendopeptidases. Mol Biotechnol.; **24**(2):157-202.

Grünberg, J., Dumermuth, E., Eldering, J.A., Sterchi, E.E. 1993. Expression of the alpha subunit of PABA peptide hydrolase (EC 3.4.24.18) in MDCK cells. Synthesis and secretion of an enzymatically inactive homodimer. FEBS Lett.; **335**(3):376-9.

Grzonka, Z., Jankowska, E., Kasprzykowski, F., Kasprzykowska, R., Lankiewicz, L., Wiczk, W., Wieczerzak, E., Ciarkowski, J., Drabik, P., Janowski, R., Kozak, M., Jaskólski, M., Grubb, A. 2001. Structural studies of cysteine proteases and their inhibitors. Acta Biochim Pol.; **48**(1):1-20.

Gupta, M.C., Graham, P.L., Kramer, J.M. 1997. Characterization of alpha1(IV) collagen mutations in Caenorhabditis elegans and the effects of alpha1 and alpha2(IV) mutations on type IV collagen distribution. J Cell Biol.; **137**(5):1185-96.

Hagedorn, E.J. and Sherwood, D.R. 2011. Cell invasion through basement membrane: the anchor cell breaches the barrier. Curr Opin Cell Biol.; **23**(5):589-96.

Hagedorn, E.J., Ziel, J.W., Morrissey, M.A., Linden, L.M., Wang, Z., Chi, Q., Johnson, S.A., Sherwood, D.R. 2013. The netrin receptor DCC focuses invadopodia-driven basement membrane transmigration in vivo. J. Cell Biol. **201**,903-913.

Hanahan, D. and Weinberg, R. A. 2000. The hallmarks of cancer. Cell **100**, 57–70

Hao, J.C., Adler, C.E., Mebane, L., Gertler, F.B., Bargmann, C.I., Tessier-Lavigne, M. 2010. The tripartite motif protein MADD-2 functions with the receptor UNC-40 (DCC) in Netrin-mediated axon attraction and branching. Dev Cell.; **18**(6):950-60.

Hashmi, S., Zhang, J., Oksov, Y., Ji, Q., Lustigman, S. 2006. The Caenorhabditis elegans CPI-2a cystatin-like inhibitor has an essential regulatory role during oogenesis and fertilization. J Biol Chem.; **281**(38):28415-29.

Haves-Zburof, D., Paperna, T., Gour-Lavie, A., Mandel, I., Glass-Marmor, L., Miller, A. 2011. Cathepsins and their endogenous inhibitors cystatins: expression and modulation in multiple sclerosis. J Cell Mol Med.; **15**(11):2421-9.

Hedrich, J., Lottaz, D., Meyer, K., Yiallouros, I., Jahnen-Dechent, W., Stöcker, W., Becker-Pauly, C. 2010. Fetuin-A and cystatin C are endogenous inhibitors of human meprin metalloproteases. Biochemistry.; **49**(39):8599-607.

Hobert, O. 2002. PCR fusion-based approach to create reporter gene constructs for expression analysis in transgenic C. elegans. Biotechniques.; **32**(4):728-30.

Ihara, S., Hagedorn, E.J., Morrissey, M.A., Chi, Q., Motegi, F., Kramer, J.M., Sherwood, D.R. 2011. Basement membrane sliding and targeted adhesion remodels tissue boundaries during uterine-vulval attachment in Caenorhabditis elegans. Nat Cell Biol.; **13**(6):641-51

Iiizumi, M., Liu, W., Pai, S.K., Furuta, E., Watabe, K. 2008. Drug development against metastasis-related genes and their pathways: a rationale for cancer therapy. Biochim Biophys Acta.; **1786**(2):87-104.

Jacobson, L.A., Jen-Jacobson, L., Hawdon, J.M., Owens, G.P., Bolanowski, M.A., Emmons, S.W., Shah, M.V., Pollock, R.A., Conklin, D.S. 1988. Identification of a putative structural gene for cathepsin D in Caenorhabditis elegans. Genetics.; **119**(2):355-63.

Jefferson, T., Auf dem Keller, U., Bellac, C., Metz, V.V., Broder, C., Hedrich, J., Ohler, A., Maier, W., Magdolen, V., Sterchi, E., Bond, J.S., Jayakumar, A., Traupe, H., Chalaris, A., Rose-John, S., Pietrzik, C.U., Postina, R., Overall, C.M., Becker-Pauly, C. 2012. The substrate degradome of meprin metalloproteases reveals an unexpected proteolytic link between meprin β and ADAM10. Cell Mol Life Sci.; **70**(2):309-33.

Joyce, P.I., Satija, R., Chen, M., Kuwabara, P.E. 2012. The atypical calpains: evolutionary analyses and roles in Caenorhabditis elegans cellular degeneration. PLoS Genet.; **8**(3):e1002602.

Kadam, S., Ghosh, S., Stathopoulos, A. 2012. Synchronous and symmetric migration of Drosophila caudal visceral mesoderm cells requires dual input by two FGF ligands. Development.; **139**(4):699-708.

Kang, S.H. and Kramer, J.M. 2000. Nidogen is nonessential and not required for normal type IV collagen localization in Caenorhabditis elegans. Mol Biol Cell.; **11**(11):3911-23.

Kim, S. and Wadsworth, W.G. 2000. Positioning of longitudinal nerves in C. elegans by nidogen. Science.; **288**(5463):150-4.

Kinnunen, T.K. 2014. Combinatorial roles of heparan sulfate proteoglycans and heparan sulfates in Caenorhabditis elegans neural development. PLoS One.; **9**(7):e102919

Ko, S.Y., Blatch, G.L., Dass, C.R. 2013. Netrin-1 as a potential target for metastatic cancer: focus on colorectal cancer. Cancer Metastasis Rev.

Köhler, D., Kruse, M., Stöcker, W., Sterchi, E.E. 2000. Heterologously overexpressed, affinity-purified human meprin alpha is functionally active and cleaves components of the basement membrane in vitro. FEBS Lett.; **465**(1):2-7.

Kramer, J.M. 2005. Basement membranes., WormBook, ed. The C. elegans Research Community, WormBook, doi/10.1895/wormbook.1.7.1, http://www.wormbook.org.

Kramerova, I.A., Kawaguchi, N., Fessler, L., Nelson, R.E., Chen, Y., Kramerov, A.A., Kusche-Gullberg, M., Kramer, J.M., Ackley, B.D., Sieron, A.L., Prockop, D.J., Fessler, J.H.

2000. Papilin in development; a pericellular protein with a homology to the ADAMTS metalloproteinases. Development.; **127**(24):5475-85.

Kruse, M.N., Becker, C., Lottaz, D., Köhler, D., Yiallouros, I., Krell, H.W., Sterchi, E.E., Stöcker, W. 2004. Human meprin alpha and beta homo-oligomers: cleavage of basement membrane proteins and sensitivity to metalloprotease inhibitors. Biochem J.; **378**(Pt 2):383-9.

Larminie, C.G. and Johnstone, I.L. 1996. Isolation and characterization of four developmentally regulated cathepsin B-like cysteine protease genes from the nematode Caenorhabditis elegans. DNA Cell Biol; **15**(1):75-82.

Larkin, M.A., Blackshields, G., Brown, N.P., Chenna, R., McGettigan, P.A., McWilliam, H., Valentin, F., Wallace, I.M., Wilm, A., Lopez, R., Thompson, J.D., Gibson, T.J., Higgins, D.G. 2007. Clustal W and Clustal X version 2.0. *Bioinformatics*, **23**, 2947-2948

Lee, C.F., Hauenstein, A.V., Fleming, J.K., Gasper, W.C., Engelke, V., Sankaran, B., Bernstein, S.I., Huxford, T. 2011. X-ray crystal structure of the UCS domain-containing UNC-45 myosin chaperone from Drosophila melanogaster. Structure.; **19**(3):397-408.

Liotta, L.A., Mandler, R., Murano, G., Katz, D.A., Gordon, R.K., Chiang, P.K., Schiffmann, E. 1986. Tumor cell autocrine motility factor. Proc. Natl. Acad. Sci. U.S.A; **83**:3302–3306.

Mango, S.E. 2007. The *C. elegans* pharynx: a model for organogenesis, *WormBook*, ed. The *C. elegans* Research Community, WormBook, doi/10.1895/wormbook.1.129.1, http://www.wormbook.org.

Marchand, P., Tang, J., Johnson, G.D., Bond, J.S. 1995. COOH-terminal proteolytic processing of secreted and membrane forms of the alpha subunit of the metalloprotease meprin A. Requirement of the I domain for processing in the endoplasmic reticulum. J Biol Chem.; **270**(10):5449-56.

Matters, G.L. and Bond, J.S. 1999. Expression and regulation of the meprin beta gene in human cancer cells. Mol Carcinog.; **25**(3):169-78.

Mayer, U., Mann, K., Timpl, R., Murphy, G. 1993. Sites of nidogen cleavage by proteases involved in tissue homeostasis and remodelling. Eur J Biochem.; **217**(3):877-84.

McKay, S.J., Johnsen, R., Khattra, J., Asano, J., Baillie, D.L., Chan, S., Dube, N., Fang, L., Goszczynski, B., Ha, E., Halfnight, E., Hollebakken, R., Huang, P., Hung, K., Jensen, V., Jones, S.J., Kai, H., Li, D., Mah, A., Marra, M., McGhee, J., Newbury, R., Pouzyrev, A., Riddle, D.L., Sonnhammer, E., Tian, H., Tu, D., Tyson, J.R., Vatcher, G., Warner, A., Wong, K., Zhao, Z., Moerman, D.G. 2003.Gene expression profiling of cells, tissues, and developmental stages of the nematode C. elegans. Cold Spring Harb Symp Quant Biol.; **68**:159-69.

Meighan, C.M., Cram, E.J., Schwarzbauer, J.E. 2004. Organogenesis: cutting to the chase. Curr Biol.; **14**(22):R948-50.

Miedel, M.T., Graf, N.J., Stephen, K.E., Long, O.S., Pak, S.C., Perlmutter, D.H., Silverman, G.A., Luke, C.J. 2012. A pro-cathepsin L mutant is a luminal substrate for endoplasmic-reticulum-associated degradation in C. elegans. PLoS One.; **7**(7):e40145.

Minder, P., Bayha, E., Becker-Pauly, C., Sterchi, E.E. 2012. Meprinα transactivates the epidermal growth factor receptor (EGFR) via ligand shedding, thereby enhancing colorectal cancer cell proliferation and migration. J Biol Chem.; **287**(42):35201-11.

Möhrlen, F., Hutter, H., Zwilling, R. 2003. The astacin protein family in Caenorhabditis elegans. Eur J Biochem.; **270**(24):4909-20.

Nakagawa, S. and Takeichi, M. 1998. Neural crest emigration from the neural tube depends on regulated cadherin expression. Development.; **125**(15):2963-71.

Newman, A.P., White, J.G., Sternberg, P.W. 1996. Morphogenesis of the C. elegans hermaphrodite uterus. Development.; **122**(11):3617-26.

Nguyen, D.X., Bos, P.D., Massagué, J. 2009. Metastasis: from dissemination to organ-specific colonization. Nat Rev Cancer.; **9**(4):274-84.

Ozisik, G., Mantovani, G., Achermann, J.C., Persani, L., Spada, A., Weiss, J., Beck-Peccoz, P., Jameson, J.L. 2003. An alternate translation initiation site circumvents an amino-terminal DAX1 nonsense mutation leading to a mild form of X-linked adrenal hypoplasia congenita. J Clin Endocrinol Metab.; **88**(1):417-23.

Pak, S.C., Kumar, V., Tsu, C., Luke, C.J., Askew, Y.S., Askew, D.J., Mills, D.R., Brömme, D., Silverman, G.A. 2004. SRP-2 is a cross-class inhibitor that participates in postembryonic development of the nematode Caenorhabditis elegans: initial characterization of the clade L serpins. J Biol Chem.; **279**(15):15448-59.

Pak, S.C., Tsu, C., Luke, C.J., Askew, Y.S., Silverman, G.A. 2006. The Caenorhabditis elegans muscle specific serpin, SRP-3, neutralizes chymotrypsin-like serine peptidases. Biochemistry.; **45**(14):4474-80.

Park, J.O., Pan, J., Möhrlen, F., Schupp, M.O., Johnsen, R., Baillie, D.L., Zapf, R., Moerman, D.G., Hutter, H. 2010. Characterization of the astacin family of metalloproteases in C. elegans. BMC Dev Biol.; **10**:14.

Patel, P.S., Raval, G.N., Rawal, R.M., Patel, G.H., Balar, D.B., Shah, P.M., Patel, D.D. 1995. Comparison between serum levels of carcinoembryonic antigen, sialic acid and phosphohexose isomerase in lung cancer. Neoplasma; **42**:271–274.

Phiri, A.M., De Pomerai, D., Buttle, D.J., Behnke, J.M. 2014. Developing a rapid throughput screen for detection of nematicidal activity of plant cysteine proteinases: the role of Caenorhabditis elegans cystatins. Parasitology.; **141**(2):164-80.

Prall, F. Tumour budding in colorectal carcinoma. Histopathology.; **50**(1):151-62.

Price, M.G., Landsverk, M.L., Barral, J.M., Epstein, H.F. 2002. Two mammalian UNC-45 isoforms are related to distinct cytoskeletal and muscle-specific functions. J Cell Sci; **115**(Pt 21):4013-23.

Rakashanda, S., Rana, F., Rafiq, S., Masood, A., Amin, S. 2012. Role of Proteases in Cancer: A Review. Biotechnology and Molecular Biology Review.: **7**(4): 90-101

Rawlings, N.D. and Barrett, A.J. 1995. Evolutionary families of metallopeptidases. Methods Enzymol.; **248**:183-228.

Richter, R., Schulz-Knappe, P., Schrader, M., Ständker, L., Jürgens, M., Tammen, H., Forssmann, W.G. 1999. Composition of the peptide fraction in human blood plasma: database of circulating human peptides. J Chromatogr B Biomed Sci Appl.; **726**(1-2):25-35.

Salameh, M.A., Robinson, J.L., Navaneetham, D., Sinha, D., Madden, B.J., Walsh, P.N., Radisky, E.S. 2010. The amyloid precursor protein/protease nexin 2 Kunitz inhibitor domain is a highly specific substrate of mesotrypsin. J Biol Chem.; **285**(3):1939-49.

Sasagawa, Y., Yamanaka, K., Saito-Sasagawa, Y., Ogura, T. 2010. Caenorhabditis elegans UBX cofactors for CDC-48/p97 control spermatogenesis. Genes Cells.; **15**(12):1201-15.

Schaheen, L., Patton, G., Fares, H. 2006. Suppression of the cup-5 mucolipidosis type IV-related lysosomal dysfunction by the inactivation of an ABC transporter in C. elegans. Development.; **133**(19):3939-48.

Schierack, P., Lucius, R., Sonnenburg, B., Schilling, K., Hartmann, S. 2003. Parasite-specific immunomodulatory functions of filarial cystatin. Infect Immun.; **71**(5):2422-9.

Schindelin, J., Arganda-Carreras, I., Frise, E., Kaynig, V., Longair, M., Pietzsch, T., Preibisch, S., Rueden, C., Saalfeld, S., Schmid, B., Tinevez, J.Y., White, D.J., Hartenstein, V., Eliceiri, K., Tomancak, P., Cardona, A. 2012. Fiji: an open-source platform for biological-image analysis. Nat Methods.; **9**(7):676-82.

Schultz, J., Milpetz, F., Bork, P., Ponting, C.P. 1998. SMART, a simple modular architecture research tool: identification of signaling domains. Proc Natl Acad Sci U S A.; **95**(11):5857-64.

Shaye, D.D. and Greenwald, I. 2011. OrthoList: a compendium of C. elegans genes with human orthologs. PLoS One.; **6**(5):e20085.

Sherwood, D.R., Butler, J.A., Kramer, J.M., Sternberg, P.W. 2005. FOS-1 promotes basement-membrane removal during anchor-cell invasion in C. elegans. Cell.; **121**(6):951-62.

Sievers F, Wilm A, Dineen DG, Gibson TJ, Karplus K, Li W, Lopez R, McWilliam H, Remmert M, Söding J, Thompson JD, Higgins D. 2011. Fast, scalable generation of high-quality protein multiple sequence alignments using Clustal Omega. Molecular Systems Biology **7**(539)

Smith, J.R. and Stanfield, G.M. 2011. TRY-5 is a sperm-activating protease in Caenorhabditis elegans seminal fluid. PLoS Genet.; **7**(11):e1002375.

Sterchi, E.E., Stöcker, W., Bond, J.S. 2008. Meprins, membrane-bound and secreted astacin metalloproteinases. Mol Aspects Med.; **29**(5):309-28.

Stöcker, W., Grams, F., Baumann, U., Reinemer, P., Gomis-Rüth, F.X., McKay, D.B., Bode, W. 1995. The metzincins--topological and sequential relations between the astacins, adamalysins, serralysins, and matrixins (collagenases) define a superfamily of zinc-peptidases.Protein Sci; **4**(5):823-40.

Struckhoff, E.C. and Lundquist, E.A. 2003. The actin-binding protein UNC-115 is an effector of Rac signaling during axon pathfinding in C. elegans. Development.; **130**(4):693-704.

Sun, Y.J., Chou, C.C., Chen, W.S., Wu, R.T., Meng, M., Hsiao, C.D. 1999. The crystal structure of a multifunctional protein: phosphoglucose isomerase/autocrine motility factor/neuroleukin. Proc. Natl. Acad. Sci. U.S.A; **96**:5412–5417.

Sunnerhagen, M., Pursglove, S., Fladvad, M. 2002. The new MATH: homology suggests shared binding surfaces in meprin tetramers and TRAF trimers. FEBS Lett.; **530**(1-3):1-3.

Suzuki, M., Sagoh, N., Iwasaki, H., Inoue, H., Takahashi, K. 2004. Metalloproteases with EGF, CUB, and thrombospondin-1 domains function in molting of Caenorhabditis elegans. Biol Chem.; **385**(6):565-8.

Talukder, A.H., Adam, L., Raz, A., Kumar, R. 2000. Heregulin regulation of autocrine motility factor expression in human tumor cells. Cancer Res; **60**:474–480.

Towers, P.R., Lescure, P., Baban, D., Malek, J.A., Duarte, J., Jones, E., Davies, K.E., Ségalat, L., Sattelle, D.B. 2006. Gene expression profiling studies on Caenorhabditis elegans dystrophin mutants dys-1(cx-35) and dys-1(cx18). Genomics.; **88**(5):642-9.

Tanaka, N., Haga, A., Uemura, H., Akiyama, H., Funasaka, T., Nagase, H., Raz, A., Nakamura, K.T. 2002. Inhibition mechanism of cytokine activity of human autocrine motility factor examined by crystal structure analyses and site-directed mutagenesis studies. J. Mol. Biol; **318**:985–997.

Tcherepanova, I., Bhattacharyya, L., Rubin, C.S., Freedman, J.H. 2000. Aspartic proteases from the nematode Caenorhabditis elegans. Structural organization and developmental and cell-specific expression of asp-1. J Biol Chem.; **275**(34):26359-69.

Thompson, O., Edgley, M., Strasbourger, P., Flibotte, S., Ewing, B., Adair, R., Au, V., Chaudhry, I., Fernando, L., Hutter, H., Kieffer, A., Lau, J., Lee, N., Miller, A., Raymant, G., Shen, B., Shendure, J., Taylor, J., Turner, E.H., Hillier, L.W., Moerman, D.G., Waterston, R.H. 2013. The million mutation project: a new approach to genetics in Caenorhabditis elegans. Genome Res.; **23**(10):1749-62.

Timmons, L., Court, D.L., Fire, A., 2001. Ingestion of bacterially expressed dsRNAs can produce specific and potent genetic interference in Caenorhabditis elegans. Gene. **263**, 103-112.

Tsukuba, T. and Bond, J.S. 1998. Role of the COOH-terminal domains of meprin A in folding, secretion, and activity of the metalloendopeptidase. J Biol Chem.; **273**(52):35260-7.

Tsutsumi S, Gupta SK, Hogan V, Collard JG, Raz A. 2002. Activation of small GTPase Rho is required for autocrine motility factor signaling. Cancer Res; **62**:4484–4490.

Venolia, L., A.o., W., Kim, S., Kim, C., Pilgrim, D. 1999. unc-45 gene of Caenorhabditis elegans encodes a muscle-specific tetratricopeptide repeat-containing protein. Cell Motil Cytoskeleton.; **42**(3):163-77.

Wan, H., Lee, K.S., Kim, B.Y., Zou, F.M., Yoon, H.J., Je, Y.H., Li, J., Jin, B.R. 2013. A spider-derived Kunitz-type serine protease inhibitor that acts as a plasmin inhibitor and an elastase inhibitor. PLoS One; **8**(1):e53343.

Wan, X., Corn, P.G., Yang, J., Palanisamy, N., Starbuck, M.W., Efstathiou, E., Tapia, E.M., Zurita, A.J., Aparicio, A., Ravoori, M.K., Vazquez, E.S., Robinson, D.R., Wu, Y.M., Cao, X., Iyer, M.K., McKeehan, W., Kundra, V., Wang, F., Troncoso, P., Chinnaiyan, A.M., Logothetis, C.J., Navone, N.M. 2014. Prostate cancer cell-stromal cell crosstalk via FGFR1 mediates antitumor activity of dovitinib in bone metastases. Sci Transl Med.; **6**(252):252ra122. doi: 10.1126/scitranslmed.3009332

WHO. 2014. "Cancer." World Health Organization. 7 November 2014. http://www.who.int/mediacentre/factsheets/fs297/en/

Wood, J.P., Ellery, P.E., Maroney, S.A., Mast, A.E. 2014. Biology of tissue factor pathway inhibitor. Blood.; **123**(19):2934-43.

WormBase web site, 2014. http://www.wormbase.org, release WS246, date 10-Oct-2014
Xu, M., Liu, Y., Zhao, L., Gan, Q., Wang, X., Yang, C. 2014. The lysosomal cathepsin protease CPL-1 plays a leading role in phagosomal degradation of apoptotic cells in Caenorhabditis elegans. Mol Biol Cell.; **25**(13):2071-83. doi: 10.1091/mbc.E14-01-0015. Epub 2014 May 14.

Yamauchi, S., Sasagawa, Y., Ogura, T., Yamanaka, K. 2007. Differential expression pattern of UBX family genes in Caenorhabditis elegans. Biochem Biophys Res Commun.; **358**(2):545-52.

Yan, W., Han, P., Zhou, Z., Tu, W., Liao, J., Li, P., Liu, M., Tian, D., Fu, Y. 2014. Netrin-1 Induces Epithelial-Mesenchymal Transition and Promotes Hepatocellular Carcinoma Invasiveness. Dig Dis Sci.; **59**(6):1213-21.

Yanagawa, T., Funasaka, T., Tsutsumi, S., Watanabe, H., Raz, A. 2004. Novel roles of the autocrine motility factor/phosphoglucose isomerase in tumor malignancy. Endocr. Relat. Cancer; **11**:749–759.

Zhang, J., Zheng, F., Yu, G., Yin, Y., Lu, Q. 2013. miR-196a targets netrin 4 and regulates cell proliferation and migration of cervical cancer cells. Biochem. Biophys. Res. Commun. **440**, 582-8.

Zhou, S. and Chen, L. 2011. Neural integrity is maintained by dystrophin in C. elegans. J Cell Biol.; **192**(2):349-63.

Zhong, W. and Sternberg, P.W. 2006. Genome-wide prediction of C. elegans genetic interactions. Science.; **311**(5766):1481-4.

Ziel, J.W., Hagedorn, E.J., Audhya, A., Sherwood, D.R. 2009. UNC-6 (netrin) orients the invasive membrane of the anchor cell in C. elegans. Nat Cell Biol.; **11**(2):183-9.

Tables

Table 1

Genotype	% Defect	N	P-value
Astacins			
empty vector RNAi	0.97	103	
nas-1(RNAi)	0	10	1
nas-2(RNAi)	No RNAi		
nas-3(RNAi)	No RNAi		
nas-4(RNAi)	0	13	1
nas-5(RNAi)	12.5	16	0.0472
nas-6(RNAi)	10	20	0.0684
nas-7(RNAi)	15.6	32	0.0029
nas-9(RNAi)	14.8	27	0.0066
nas-10(RNAi)	0	11	1
nas-11(RNAi)	10	10	0.1844
nas-12(RNAi)	9.1	22	0.0006
nas-13(RNAi)	0	8	1
nas-14(RNAi)		too young	
nas-15(RNAi)	0	10	1
nas-16(RNAi)	0	12	1
nas-17(RNAi)	0	12	1
nas-18(RNAi)	0	10	1
nas-19(RNAi)	28.6	14	0.0006
nas-20(RNAi)	0	23	1
nas-21(RNAi)	37.5	40	<0.0001
*nas-21(RNAi)**	6.25	16	0.2518
nas-22(RNAi)	42.6	47	<0.0001
nas-23(RNAi)	No RNAi		
nas-24(RNAi)	0	23	1
nas-25(RNAi)	25	16	0.0011
nas-26/toh-1(RNAi)	45.4	11	<0.0001
nas-27(RNAi)	9.5	21	0.074
nas-28(RNAi)	17.6	17	0.0088
nas-29(RNAi)	0	10	1
nas-30(RNAi)	No RNAi		
nas-31(RNAi)	0	23	1
nas-32(RNAi)	0	11	1
nas-33(RNAi)	30	10	0.002

nas-34/hch-1(RNAi)	0	11	1
nas-35/dpy-31(RNAi)	6.6	15	0.239
nas-36(RNAi)	0	22	1
nas-37(RNAi)	9.1	11	0.1844
nas-38(RNAi)	0	22	1
nas-39(RNAi)	23	13	0.0075
nas-40(RNAi)	No RNAi		

* indicates branching defect

Netrins

unc-5(RNAi)	35.00	40	<0.0001
unc-6(RNAi)	34.78	23	<0.0001
unc-40(RNAi)	34.29	35	<0.0001

Protease inhibitors

Genotype	% Defect	N	P-value
B0222.5(RNAi)	0	11	1
B0238.12(RNAi)	9.1	11	0.6853
bli-5(RNAi)	0	10	1
C02F12.5(RNAi)	10	10	0.6853
C10G8.2(RNAi)	42.9	28	0.0138
C10G8.3(RNAi)	25	28	0.5961
C10G8.4(RNAi)	0	10	1
C25E10.8(RNAi)	0	10	1
C25E10.10(RNAi)	0	9	1
C25E10.7(RNAi)	0	7	1
C34F6.1(RNAi)	7.7	13	0.4575
C53B7.2(RNAi)	18.2	11	1
cki-1(RNAi)	0	8	1
cki-2(RNAi)	70	30	<0.0001
cpi-1(RNAi)	58.1	31	<0.0001
cpi-2(RNAi)	27.3	11	0.4575
F30H5.3(RNAi)	0	10	1
F32D8.3(RNAi)	14.7	34	0.7963
F35B12.4(RNAi)	50	34	0.0013
K05F1.10(RNAi)	0	8	1
K07A1.6(RNAi)	0	7	1
K10D3.4(RNAi)	50	36	0.0008

K11D12.6(RNAi)	18.2	22	1
kal-1(RNAi)	0	10	1
mec-1(RNAi)	30.3	33	0.2251
mec-9(RNAi)	50	10	0.04
mig-6(RNAi)	72	25	<0.0001
mlt-11(RNAi)	0	10	1
R12A1.3(RNAi)	13	23	0.7635
srp-1(RNAi)	65	20	0.0004
srp-10(RNAi)	20	15	1
srp-2(RNAi)	58.8	17	0.0013
srp-3(RNAi)	0	12	1
srp-6(RNAi)	0	13	1
srp-7(RNAi)	16.7	6	1
srp-8(RNAi)	0	13	1
srp-9(RNAi)	10	20	1
T21D12.12(RNAi)	63.6	44	<0.0001
tag-290(RNAi)	8.3	12	0.6904
try-1(RNAi)	14.3	21	0.7616
try-10(RNAi)	20	10	1
try-3(RNAi)	60	10	0.0092
try-4(RNAi)	20	10	1
try-5(RNAi)	23.8	21	0.764
try-6(RNAi)	10	10	0.6853
try-7(RNAi)	44.4	9	0.0945
try-8(RNAi)	11.1	18	0.5213
W0532.2(RNAi)	40	10	0.2138
Y49G5A.1(RNAi)	36.7	30	0.0818
Downstream of *cpi-1*			
dys-1(RNAi)	26	34.6	<0.0001
cpr-5(RNAi)	No RNAi		
F57F5.1(RNAi)	9	0	1
cpr-6(RNAi)	13	0	1
pat-12(RNAi)	10	0	1
Downstream of *F35B12.4*			
pat-2(RNAi)	20.00	10	0.0203
Downstream of *mec-1*			
unc-86(RNAi)	70.00	10	<0.0001

mec-4(RNAi)	0.00	8	1
mec-5(RNAi)	0.00	19	1
mec-9(RNAi)	33.33	18	<0.0001
dop-1(RNAi)	23.07	13	0.0042
mec-7(RNAi)	0	11	1
Downstream of *srp-2*			
ZK1098.4(RNAi)	0.00	9	1
F15C11.2(RNAi)	5.56	18	0.2764
cpl-1(RNAi)	13.33	15	0.0422
nhr-48(RNAi)	no RNAi		
ubxn-3(RNAi)	27.58	18	0.0002
Collagen genes			
mec-5(RNAi)	0.00	19	1
emb-9(RNAi)	42.8	14	<0.0001
let-2(RNAi)	no RNAi		
Laminin genes			
epi-1(RNAi)	92.5	40	<0.0001
lam-1(RNAi)	17	29	0.0019
lam-3(RNAi)			
lam-2(RNAi)			
Nidogen			
nid-1(RNAi)	39.3	28	<0.0001
Fibronectin genes			
kal-1(RNAi)	0.00	10	1
unc-22(RNAi)	to be tested		
madd-2(RNAi)	to be tested		
let-805(RNAi)	to be tested		
ptp-3(RNAi)	to be tested		
rig-6(RNAi)	to be tested		
icgm-1(RNAi)	to be		

	tested		
	to be		
icgm-2(RNAi)	tested		
	to be		
hcf-1(RNAi)	tested		
	to be		
mam-7(RNAi)	tested		
	to be		
sax-3(RNAi)	tested		
unc-40(RNAi)	34.29	35	<0.0001
unc-73(RNAi)	66.67	48	<0.0001
	to be		
unc-89(RNAi)	tested		
	to be		
ttn-1(RNAi)	tested		
	to be		
syg-2(RNAi)	tested		
	to be		
syn-1(RNAi)	tested		
	to be		
syg-1(RNAi)	tested		
	to be		
vab-1(RNAi)	tested		
	to be		
lev-11(RNAi)	tested		
	to be		
lad-1(RNAi)	tested		
	to be		
ptp-1(RNAi)	tested		
	to be		
dig-1(RNAi)	tested		

Table 1: Table of RNAi treated animals scored for cell outgrowth defects

Phenotypes were scored at L4 lethargus. P-values were calculated in comparison to empty vector (RNAi) using Fisher's exact test.

Genotype	MEP1A	MEP1B	MEP1A Signal Peptide	MEP1B signal Peptide	MEP1A prodomain	MEP1B prodomain	MEP1A EGF domain	MEP1B EGF domain	MEP1A Zn Metalloprotease domain	MEP1B Zn Metalloprotease domain	MEP1A Zn Metalloprotease active site	MEP1B Zn Metalloprotease active site
nas-1	29.31	29.31	30.77	0					30.22	33.09		
nas-2	26.24	25.56	21.43	26.67					31.58	30.77		
nas-3	24.66	25.78	28.57	13.33					31.58	30		
nas-4	29.89	33.21							36.96	37.5		
nas-5	21.58	25.52	20	25					26.62	30.88		
nas-6	29.12	32.98	20	25					36.96	39.26		
nas-7	26.67	26.94							34.53	33.82		
nas-8	26.67	29.17	23.53	15.79					30.22	33.09		
nas-9	21.65	20.47	25	21.43					26.85	25.71		
nas-10	23.76	22.7							27.54	26.67		
nas-11	25.26	22.81	7.14	31.25					28.26	28.89		
nas-12	25.26	22.65	21.43	6.67					29.41	27.41		
nas-13	31.63	31.61	14.29	6.67					42.45	39.71		
nas-14	26.04	26.06	23.08	16.67					42.45	41.18		
nas-15	24.1	25.17	30.77	7.14					37.41	36.76		
nas-16	18.24	17.4					18.18	24.24	26.12	26.72		
nas-17	18.55	19.48	9.09	18.18			21.43	28.57	23.7	25.76		
nas-18	16.56	17.89					18.18	21.21	23.31	26.92		
nas-19	16.93	18.55	12.5	17.65			15.15	21.21	26.15	23.62		
nas-20	17.61	19.67	11.76	22.22			18.18	24.24	25.6	27.87		
nas-21	18.33	21.59	7.14	6.67	7.69	0	0	7.69	25.19	28.03	47.37	47.37
nas-22	17.12	22.45	14.29	20	n/a	n/a	18.18	18.18	25.55	28.36	57.89	63.16
nas-23	24.46	24.32	23.08	41.67			18.18	21.21	31.39	29.1		

nas-24	17.5	17.24	12.5	5.88			15.15	21.21	24.81	24.6		
nas-25	19.25	23.84	21.43	13.33			18.18	15.15	27.21	32.33		
toh-1	19.22	20.36	14.29	20	22.73	25	16.22	16.67	27.21	28.57	63.16	68.42
nas-27	22.97	24.93	15.38	6.67			18.18	12.12	27.74	29.85		
nas-28	22.04	24.73	16.67	7.14			12.9	16.13	32.61	34.07		
nas-29	22.46	23.66	19.05	35			27.27	21.21	32.85	32.09		
nas-30	22.61	23.4					25	25	38.81	39.69		
nas-31	18.87	19.83	37.5	25			21.62	27.78	31.11	32.58		
nas-32	18.7	22.75	16.67	15.38			21.62	22.22	28.57	33.85		
nas-33	21.85	22.84	23.08	14.29			18.18	15.15	38.81	39.69		
nas-34/hch-1	23.82	24.62	20	18.75			21.21	15.15	35.29	33.08		
nas-35/dpy-1	22.09	22.64	35.71	20			24.24	27.27	34.29	35.77		
nas-36	22.25	25.48	25	41.18			15.62	25	37.5	36.84		
nas-37	20.83	22.54	0	20			27.27	27.27	36.57	41.22		
nas-38	20.24	18.1	14.29	0			22.58	22.58	33.82	31.58		
nas-39	21.43	21.49	19.05	18.18			33.33, 33.33	25.71,28.57	35	37.96		
nas-40												

Table 2: Percent identity shared among meprin sequnces and domains

Percent identity determined using Clustal Omega.

Table 3: Gain-of-function and loss-of-function phenotypes

Genotype	% Defect	N	P-value
nas-21(gk375710)	5.88	17	1
nas-22(tm2888)	0	10	1
nas-21 overexpression (1ng/ul)	100	20	<0.0001
nas-21 overexpression (0.1ng/ul)	0	10	1

Table 3: Gain of Function and loss-of function phenotypes

Phenotypes were scored at L4 lethargus. P-values were calculated in comparison to empty (RNAi) using Fisher's exact test.

Table 4: *nas-21* specificity assay

	Wildtype			Overexpression			Mutant		
Protease inhibitor RNAi	**% defect**	**N**	**P-value**	**% severe defect**	**N**	**P-value ***	**% defect**	**N**	**P-value *****
C10G8.2	42.9	28	0.0138	24	17	0.036	70	10	0.0009
C10G8.3	25	28	0.5961	30	10	0.0296	58	19	0.0013
cki-2	70	30	<0.0001	33	6	0.0462	27	11	0.2694
cpi-1	58.1	31	<0.0001	46	3	0.0015	31	13	0.1377
F35B12.4	50	34	0.0013	60	20	<0.0001	21	19	0.342
K10D3.4	50	36	0.0008	41**	11	0.0018	32	19	0.0918
mec-1	30.3	33	0.2251	80	10	<0.0001	6	16	1
srp-1	65	20	0.0004	33***	16	0.0022	17	12	0.5534
srp-2	58.8	17	0.0013	68	19	<0.0001	42	19	0.0198
T21D12.12	63.6	44	<0.0001	36	11	0.0105	40	15	0.033
Y49G5A.1	36.7	30	0.0818	69	13	<0.0001	83	6	0.001

Table 4: *nas-21* specificity assay

Overexpression is from the *nas-21::nas-21; exc-9::mcherry* strain, mutant from the *nas-21(gk375710)* strain.

*compare to overexpression percentages

**91% showed oe phenotype

***88% showed oe phenotype

*****compared to mutant percentages

Table 5: Protein family targets/upstream regulators

Downstream of Cystatins

Genotype	type	Reference	% defect	N	P-value
cpl-1	cathepsin-like protease	(Britton and Murray, 2004)	13.33	15	0.0515
mec-4	cathepsin target	(Tavernarakis et al., 2001)	0.00	8	1
unc-52	cathepsin target	(Hawdon et al., 1989)	20.00	10	0.0203
ced-3	cysteine protease	(Xue D et al., 1996)	11.56	26	0.0257
cpr-1	cathepsin-like cysteine protease	(Larminie and Johnstone 1996)	37.5	16	<0.0001
cpr-2	cathepsin-like cysteine protease	(Larminie and Johnstone 1996)	No RNAi		
cpr-3	cathepsin-like cysteine protease	(Larminie and Johnstone 1996)	to be tested		
cpr-6	cathepsin-like cysteine protease	(Larminie and Johnstone 1996)	25	20	0.0004
cpr-5	cathepsin-like cysteine protease	(Larminie and Johnstone 1996)	No RNAi		
cpz-1	cathepsin like cysteine protease	(Hashmi et al., 2004)	to be tested		
clp-1	contains cysteine protease active site	(Cantacessi et al., 2010)	14.29	28	0.0074
clp-2	contains cysteine protease active site	(Cantacessi et al., 2010)	30	10	0.002
sep-1	cystine protease	(Siomos MF et al. 2001)	27.27	11	0.0026
usp-46	cystine protease	(Kowalski et al., 2011)	8.33	12	0.1986
clp-6	calpain, has cystine protease active site	(Syntichaki et al., 2002)	No RNAi		
clp-7	calpain, has cystine protease active site	(Syntichaki et al., 2002)	to be tested		
tra-3	calpain, has cystine protease active site	(Barnes TM ; Hodgkin JA 1996)	to be tested		
cad-1	cathepsin	(Jacobson et al., 1988)	to be tested		
asp-4	cathepsin homolog	(Phillips et al., 2006)	11.11	9	0.1699
asp-3	cathepsin homolog	(Tcherepanova et al, 2000)	50	8	0.0034
daf-4	cathepsin target	(Clokey and Jacobson 1984)	42.8	7	<0.0001
asp-1	cathepsin homolog	(Syntichaki et al, 2002)	to be tested		
mrp-4	upstream of cathepsin	(Schaheen et al., 2006)	33.33	6	0.0075

Y40D12A.1	cathepsin A homolog	(Murata et al., 2012)	60	10	<0.0001
Y40D12A.2	cathepsin A homolog	(Murata et al., 2012)	12.5	8	0.1396

Kunitz doman targets

Genotype	type	Reference	% defect	N	P-value
odr-2	related to uPA, plasmin target	(Chou et al., 2001)	8.00	25	0.0973
apl-1	contains Kunitz domain	(Ewald et al., 2012)	68.42	19	<0.0001
inx-6	related to thrombin	(Oshima et al., 2013)	9.52	21	0.074
C54D10.10	related to TFPI, contains Kunitz domain	(Wood et al., 2011); (Wormbase)	16.67	12	0.0284
C25E10.8	related to factor Xa	(Boag et al., 2002)	0.00	32	1
C25E10.7	related to factor Xa	(Boag et al., 2002)	0.00	18	1
C36C3.6b	contains BPTI (type of Kunitz domain)	(Teichmann and Chothia 2000)	No RNAi		
bli-5	contains BPTI (type of Kunitz domain)	(Stepek et al., 2010)	0.00	16	1
try-1	trypsin	(Dennis and Lazarus 1994)	14.29	21	0.0152
try-10	trypsin	(Dennis and Lazarus 1994)	20.00	10	0.0203
try-3	trypsin	(Dennis and Lazarus 1994)	60.00	10	<0.0001
try-4	trypsin	(Dennis and Lazarus 1994)	20.00	10	0.0203
try-5	trypsin	(Dennis and Lazarus 1994)	23.81	21	0.0005
try-6	trypsin	(Dennis and Lazarus 1994)	10.00	10	0.1699
try-7	trypsin	(Dennis and Lazarus 1994)	44.44	9	<0.0001
try-8	trypsin	(Dennis and Lazarus 1994)	to be tested		
unc-45	trypsin target	(Gazda et al., 2013)	36.36	11	0.0002
mig-6	papilin (contains Kunitz domain)	(Kramerova et al., 2000)	72.00	25	<0.0001
par-2	kalikrien target (Kunitz target)	(Skorkowska and Adamiec 2005)	0.00	10	1
nid-1	plasmin target	(Mayer et al., 1993)	39.29	28	<0.0001
unc-52	plasmin target	(Bix and Iozzo 2008)	20.00	10	0.0203
mec-8	interacts with unc-52	(Bix and Izzo 2008)	15.15	33	0.0033

Serpin targets

Genotype	type	Reference	% defect	N	P-value
gsnl-1	chymotrypsin target	(Liu and Ono 2013)	18.18	22	0.0033
unc-45	chymostrypsin target	(Price et al., 2002)(Lee et al., 2011)	36.36	11	0.0002
unc-18	chymotrypsin target	(Sassa et al., 1996)	0.00	20	1

Table 5: Protein family targets/upstream regulators

Phenotypes were scored at L4 lethargus. P-values were calculated in comparison to empty vector (RNAi) using Fisher's exact test

Table 6: Gross Pharyngeal defects

Genotype	% Defect	N	P-value
N2	0	10	1
emb-9(RNAi)	70	10	0.0031
nas-1(RNAi)	63.6	11	0.0039
nas-15(RNAi)	50	12	0.0152
nas-25(RNAi)	88.9	9	0.0001
nas-21(RNAi)	30	10	0.2105
nas-22(RNAi)	66.7	9	0.0031
toh-1(RNAi)	10	10	1

Table 6: Gross Pharyngeal defects

Phenotypes were scored at L4 lethargus. P-values were calculated in comparison to N2) using Fisher's exact test

Table S1 and S2 not included since they list strains and RNAis only.

Protein	signal peptide	Astacin domain	transmembrane	Shkt	EGF	CUB	TSP-1	MAM	MATH	
MEP1A	1 to 21	71 to 210	718 to 740		673 to 710			71 to 210	433 to 576	2
MEP1B	1 to 22	67 to 207	654 to 676		607 to 644			260 to 429	432 to 568	2
nas-1	1 to 17	76 to 217								
nas-2	1 to 17	77 to 228								
nas-3	1 to 16	66 to 225								
nas-4		100 to 242	7 to 24							
nas-5	1 to 21	67 to 220								
nas-6	1 to 19	77 to 217		299 to 335						
nas-7		85 to 226		347 to 382						
nas-8	1 to 29	117 to 258	13 to 30	337 to 373						
nas-9	1 to 14	309 to 456		509 to 546						
nas-10		321 to 469		523 to 560						
nas-11	1 to 17	337 to 485		538 to 576						
nas-12	1 to 25	79 to 216		286 to 326 and						

				347 to 364						
nas-13	1 to 31	115 to 256		367 to 405 and 413 to 450						
nas-14	1 to 25	121 to 265	5 to 27	379 to 415 and 468 to 503						
nas-15	1 to 15	119 to 260		353 to 389 and 415 to 434 and 535 to 571						
nas-16		76 to 228			267 to 306					
nas-17	1 to 21	64 to 206			251 to 284					
nas-18		83 to 220			256 to 295					
nas-19	1 to 20	46 to 186			225 to 264					
nas-20	1 to 20	36 to 164			203 to 244					
nas-21	1 to 24	52 to 182			263 to 279	299-377				27 to 43
nas-22	1 to 16	50 to 192			232 to	276 to				38 to 42

					270	365				
nas-23	1 to 16	120 to 262			309 to 346	356 to 469				
nas-24	1 to 20	46 to 186			224 to 263					
nas-25	1 to 20	46 to 188	3 to 25		232 to 275					
nas-26	1 to 20	67 to 216			251 to 307	308 to 413				26 to 66
nas-27	1 to 17	63 to 205			250 to 291	306 to 428				22 to 65
nas-28	1 to 14	126 to 269			324 to 354	374 to 483				23 to 61
nas-29	1 to 22	143 to 285	7 to 26		330 to 370	380 to 494				
nas-30		273 to 411			483 to 494	506 to 611				
nas-31	1 to 17	167 to 306		531 to 565	340 to 396	397 to 512				
nas-32	1 to 21	208 to 345		609 to 648	380 to 433	434 to 554				
nas-33	1 to 16	198 to 336			380 to 420	427 to 530	550 to 596			
nas-34	1 to 19	130 to 274			324 to 357	367 to 469	525 to 566			
nas-35/dpy-31	1 to 18	132 to 277			321 to 361	371 to 487	493 to 540			
nas-36	1 to 21	131 to 272			316 to 357	367 to 481	509 to 555			
nas-37	1 to 22	120 to 259	7 to 26		303 to 343	350 to 458	579 to 627			
nas-38	1 to 25	120 to 262			306 to	373 to	631 to			

					345	487	676			
nas-39	1 to 30	53 to 196	7 to 29		499 to 539, 648 to 688	249 to 381, 382 to 499, 542 to 648, 692 to 804, 805 to 923				

Table S3: Domain positions

Domain locations determined through SMART database.

Figures

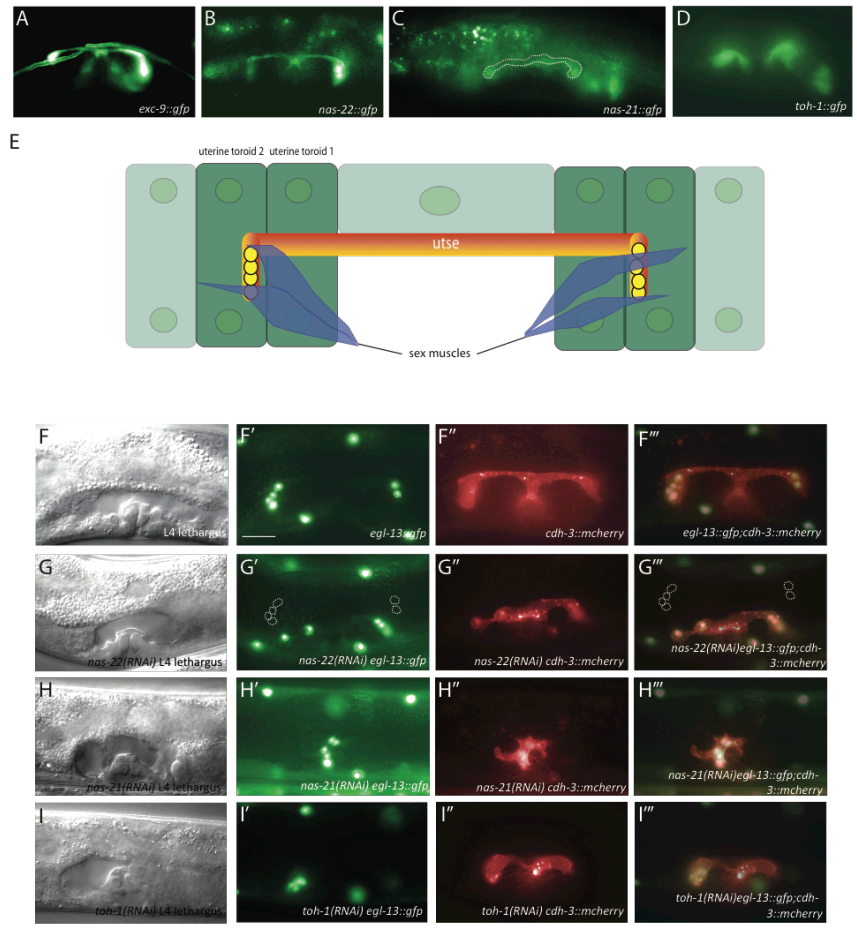

Figure 1: Astacins are involved in utse development

(A) Wild-type utse development, cell body marked with exc-9::gfp. Line behind uterine seam cell (utse) is the excretory cell. **(B)** *nas-22::gfp* expression. *nas-22* is expressed in the utse. **(C)** *nas-21::gfp* expression. *nas-21* is expressed in the utse and uterine toroids 1 and 2**. (D)** *toh-1::gfp* expression. *toh-1* is expressed in the sex muscles. **(E)** Schematic of *C. elegans* uterus. utse and cells contribute to its development (uterine toroid 1, uterine toroid 2 and the sex muscles). **(F-I)** nuclei marked with egl-13::gfp, cell body marked with cdh-3::mcherry. **(F, G, H, I)** L4 lethargus, stage at which each image set was taken. **(F-F’’’)** Wild-type utse development. **(F)** Stage at which B’-B’’’ were taken. **(F’, F’’’)** Normal nuclear migration. **(F’’, F’’’)** Normal cell outgrowth. **(F-F’’’)** *nas-21(RNAi)* treated worms. **(G)** Stage at which C’-C’’’ were taken. **(G’, G’’’)** Nuclei are slightly

closer together (see dashed white outlines of wild-type nuclei for comparison). **(G'', G''')** Cell body is malformed, slightly shorter. **(H-H''')** *nas-21(RNAi)* treated worms. **(H)** Stage at which D'-D''' were taken. **(H', H''')** Nuclei have not migrated outward. **(H'',H''')** Cell body is significantly shorter than wild type. **(I-I''')** *toh-1(RNAi)* treated worms. **(I)** Stage at which E'-E''' were taken. **(I', I''')** Nuclei have migrated to a distance shorter than that of wild type. **(I'', I''')** Cell body is shorter than that of wild type. Scale Bar 100 μm.

A

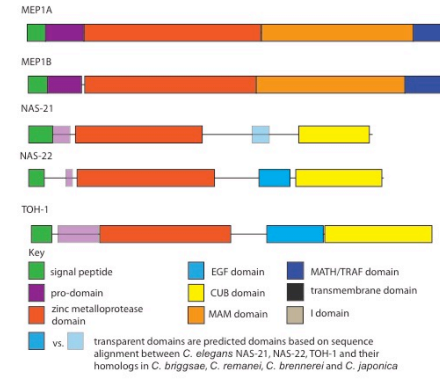

B

```
      Human MEP1A   -MAWIRSTCILFPTLLFAHIAAVPIKYLPEENVHDADFGEQKDISEINLAAGLDLFQG--
      Human MEP1B   MDLWNLSW-FLFLDAL------LVISGLATPENFDVDGGMDQDIFDINEGLGLDLFEG--
C. elegans NAS-21   -MN--------YFITFFFMHIAVLNFYF---------RFSNGNKIVMRVG--GSP------
C. elegans NAS-22   ------------MKSFFILLSIL-------------QECYGKDIVARIG--GRN------
 C. elegans TOH-1   -----------MTSSLVLILAPLALVA-----IGEAAFGNSSKIF-EIP--GLEVMASDK
                                :     :                ..*      *

      Human MEP1A   ---------DILLQ------KS--RNGLRDPNTRWTF-PIPY-ILADNLGLNAKGAILYA
      Human MEP1B   ---------DIRLD------RAQIRNSIIGEKYRWPH-TIPY-VLEDSLEMNAKGVILNA
C. elegans NAS-21   --------ETKRLERSK--RQA----LRMDNEPRWPRGTINYFFDEQRFDENSRATVLRA
C. elegans NAS-22   --------VAEKIGGARHRRQVLIRGSDEERRHKWFNNTVHYYFYEENFDFTVKESILRA
 C. elegans TOH-1   YPHFTTIETVSRTKVHRHRREVIA-----GQIYDWNSYEIPFQIWGG--DYNFQSLIRRG
                                .           *   : : .       . :  :  .

      Human MEP1A   FEMFRLKSCVDFKPYEGESS---YIIFQQFDGCWSEVGDQHVGQ-NISIGQGCAYKAIIE
      Human MEP1B   FERYRLKTCIDFKPWAGETN---YISVFKGSGCWSSVGNRRVGKQELSIGANCDRIATVQ
C. elegans NAS-21   MEKISNHTCIKFSPKDA-RIKLRIVSDK---GCQAAIGRVGGDQQYLSFPTSCYSVGSA-
C. elegans NAS-22   MELISNHTCIKFSTEPS-EKSIRMESDSTTIACYAEIGQVRE-NQLFSFNSDCYSAGVAV
 C. elegans TOH-1   IRMWEDSTCLRFKENQQSRDAIRYVLEKGDSCPTEYIGRNGG-HQDIIIGSECAEEYVVA
                    :.     :*: *.                        :*     .  : :   *

      Human MEP1A   HEIIHALGFYHEQSRTDRDDYVNIWWDQILSGYQHNFD-------TYDDSLITDLWTPYD
      Human MEP1B   HEFLHVLGFWHEQSRSDRDDYVRIWWDRILSGREHNFN-------TYSDDISDSLWVPYD
C. elegans NAS-21   SELIHVIGFLHSHQRADRDEYLKLNLQPWRLNDWFQTM-------QYKKYLDQWWIVPYD
C. elegans NAS-22   HELIHSLGFIHAHQRSDRDDYLEFKKNLDELNQTYQ-E-------QYKIWEYQEILVPYD
 C. elegans TOH-1   HETGHALGFWHTHQRPDRDDRHISINWKNVMEEATASFMPFRSMLQAFGIRQVSPREVPYD
                     *  * :** * :.* *** :: :  .       .          :        .***

      Human MEP1A   YESLMHYQPFSFNKNASVPTITAKIPEFNSIIGQRLDFSAIDLERLNRMY-NCTTTHTLL
      Human MEP1B   YTSVMHYSKTAFQN-GTEPTIVTRISDFEDVIGQRMDFSDSDLLKLNQLY-NCSSSLSFM
C. elegans NAS-21   YGSIMQYHDSDNE-----YGPK--NSKYFRTMGSQI-PSYFDYLMINEYY-QCSCEGEEQ
C. elegans NAS-22   VGSVMQYPNEEDE----EYYPVRKYRTMANTMGSAI-VAFYDYLMINKYY-ECSCAN--N
 C. elegans TOH-1   YGSLMHYHAVAHAVKVSDFTIVPKELKYVTTMGTEK-MAFLDAKVINDIYCPNACQGRNH
                      *:*:*                          :*     :  *   :*  *   :

      Human MEP1A   DHCT---FEKA---NIC-----------GMIQGTR------DDTDWAHQDSAQ-AGEVDH
      Human MEP1B   DSCS---FELE---NVC-----------GMIQSSG------DNADWQRVSQVPRGPESDH
C. elegans NAS-21   INCKNRGYPNPGNCSECNCPLE-------------------SSEEWKNITLNLDAGYMSL
C. elegans NAS-22   LSCKNHGYPNPSNCSQCNCPYGFGGADCSQRA--EPGATFQATETWQNVTISLDAGYRYL
 C. elegans TOH-1   LNCLAGGYPDPNNCNVCRCPEGLGGPDCGRLQPSPCGGEIHASDQWQTLSSPSGR-----
                      *    :      . *                          *

      Human MEP1A   TLLGQCTGAGYFMQFSTSSGSAEEAALLESR-ILYPKRKQQCLQFFYKMTGSPSDRLVVW
      Human MEP1B   SNMGQCQGSGFFMHFDSSSVNVGATAVLESR-TLYPKRGFQCLQFYLYNSGSESDQLNIY
C. elegans NAS-21   QNGTKLHQIDFVFRYLSISAPANKTIEVDIREITGVECNYGCYIGGIEVKTHEDRRMTSP
C. elegans NAS-22   ENNQKLPQVDFIYQFLWIMAPANKTTQIRVEKFVEGKCLPGCIRGGVEIKTNEDPRLTSP
 C. elegans TOH-1   ----------DVHCYWRISVPEGSRVRFRLS-DGEFPCSYGCQ-SYVEIKHKLDVRLTGF
                             .  :           .             *       .   . ::

      Human MEP1A   VRRDDSTGNVRKLVKVQTFQGDDDHNWKIAHVVLKEEQKFRYLFQGTKGDPQNSTGGIYL
      Human MEP1B   IREYSADNVDGNLTLVEEIKEIPTGSWQLYHVTLKVTKKFRVVFEGRKGSG-ASLGGLSI
C. elegans NAS-21   RLCCKND--------NEIYKSRNNPTIVMAFNS-EGLDKYNIFYRFTD------------
C. elegans NAS-22   RLCCEET--------S-------------------------------------------
 C. elegans TOH-1   RSCCYRP--------KEDTVSESNQIFVIYHPN-GRTARFSLRFRRQA------------

      Human MEP1A   DDITLTETPCPTGVWTVRNFSQVLENTSKGDKLQSPRFYNSEGYGFGVTLYPNSRESSGY
      Human MEP1B   DDINLSETRCPHHIWHIRNFTQFIGS--PNGTLYSPPFYSSKGYAFQIYLNLAHVTN---
C. elegans NAS-21   ------------------------------------------------------------
C. elegans NAS-22   ------------------------------------------------------------
 C. elegans TOH-1   ------------------------------------------------------------

      Human MEP1A   LRLAFHVCSGENDAILEWPVENRQVIITILDQEPDVRNRMSSSMVFTTSKSHTSPAINDT
      Human MEP1B   AGIYFHLISGANDDQLQWFCPWQQATMTLLDQNPDIRQRMSNQRSITTDPFM--TTDNGN
C. elegans NAS-21   ------------------------------------------------------------
C. elegans NAS-22   ------------------------------------------------------------
 C. elegans TOH-1   ------------------------------------------------------------

      Human MEP1A   VIWDRPSRVGTYHTD---CNCFRSIDLGWSGFISHQMLKRRSFLKNDDLIIFVDFEDITH
      Human MEP1B   YFWDRPSKVGTVALFSNGTQFRRGGGYGTSAFITHERLKSRDFIKGDDVYILLTVEDISH
C. elegans NAS-21   ------------------------------------------------------------
C. elegans NAS-22   ------------------------------------------------------------
 C. elegans TOH-1   ------------------------------------------------------------

      Human MEP1A   LSQTEVPTKGKRLSPQGLILQGQEQQVSEEGSGKAMLEEALPVSLSQGQPSRQKRSVENT
      Human MEP1B   LNSTQIQLTP------------------------------------------------------
C. elegans NAS-21   ------------------------------------------------------------
C. elegans NAS-22   ------------------------------------------------------------
 C. elegans TOH-1   ------------------------------------------------------------

      Human MEP1A   GPLEDHNWPQYFRDPCDPNPCQNDGICVNVKGMASCRCISGHAFFYTGERCQAVQVHGSV
      Human MEP1B   --------APSVQDLCSKTTCKNDGVCTVRDGKAECRCQSGEDWWYMGERCEKRGSTRDT
C. elegans NAS-21   ------------------------------------------------------------
C. elegans NAS-22   ------------------------------------------------------------
 C. elegans TOH-1   ------------------------------------------------------------

      Human MEP1A   IVIAVSSTVAVFALMLIITLVSVYCTRKKYRERMSSNRPNLTPQNQHAF
      Human MEP1B   LGMVIGGTAGVIFLTFSI--IAILSQRPRK-------------------
C. elegans NAS-21   ------------------------------------------------
C. elegans NAS-22   ------------------------------------------------
 C. elegans TOH-1   ------------------------------------------------
```

Figure 2: Astacins share sequence homology with Meprins

(A) Domain similarity between Human Meprin α, β, *C. elegans* NAS-21, NAS-22, and NAS-26/TOH-1. Domains are colored coded (see key). Transparent domains have been generated via sequence alignment with *C. briggsae, C. remanei, C. japonica,* and *C. breneri*. Proteins share signal peptide, prodomain, protease domain, and EGF domain. See Figure S1 for detailed alignment. **(B)** sequence alignment of MEP1A, MEP1B, NAS-21, NAS-22, and TOH-1. Red boxes indicate active site of zinc metalloprotease domain. Black outline shows high similarity between HEXXH site. Green outline shows part of active site used for aligment to determine percent identity. Dark red box indicates a conserved methionine-containing turn (Met-turn) backing the zinc site. An * (asterisk) indicates positions which have a single, fully conserved residue. A : (colon) indicates conservation between groups of strongly similar properties - scoring > 0.5 in the Gonnet PAM 250 matrix. A . (period) indicates conservation between groups of weakly similar properties - scoring =< 0.5 in the Gonnet PAM 250 matrix.

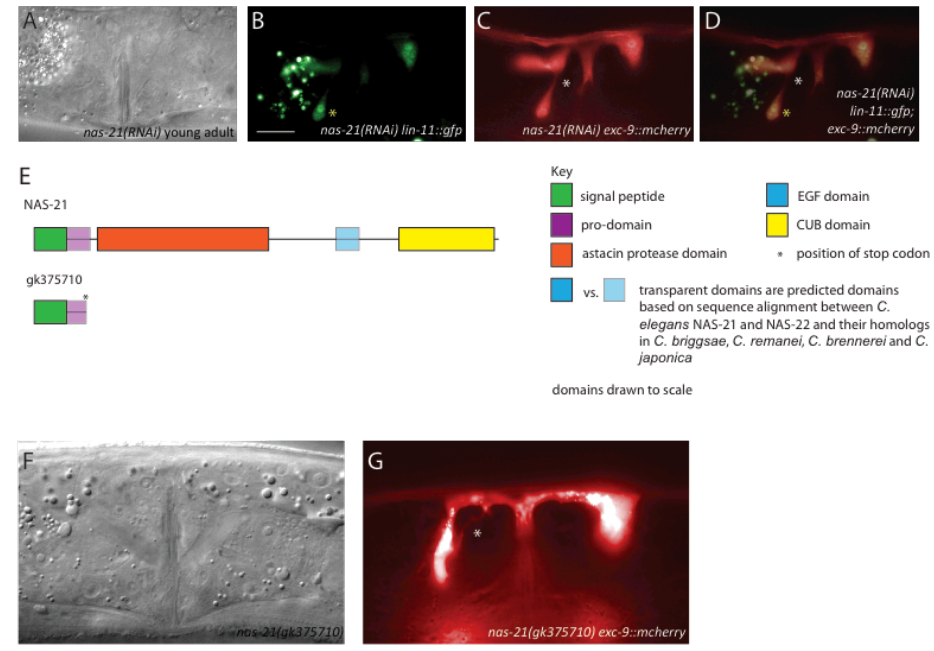
A
nas-21(RNAi) young adult
B
nas-21(RNAi) lin-11::gfp
C
nas-21(RNAi) exc-9::mcherry
D
nas-21(RNAi) lin-11::gfp; exc-9::mcherry
E
NAS-21
gk375710
Key
signal peptide
pro-domain
astacin protease domain
vs.
EGF domain
CUB domain
position of stop codon
transparent domains are predicted domains based on sequence alignment between C. elegans NAS-21 and NAS-22 and their homologs in C. briggsae, C. remanei, C. brennerei and C. japonica
domains drawn to scale
F
nas-21(gk375710)
G
nas-21(gk375710) exc-9::mcherry

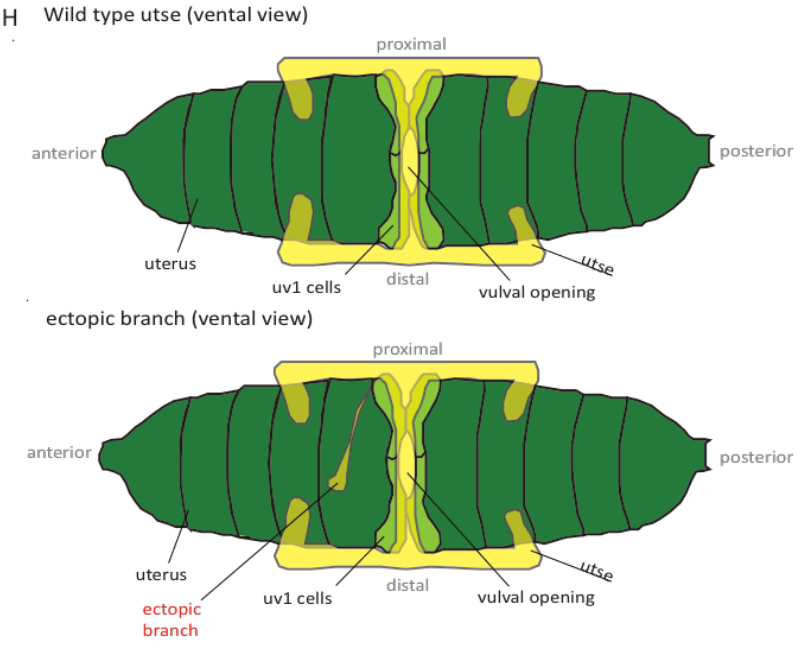
H
Wild type utse (ventral view)
proximal
anterior
posterior
uterus
uv1 cells
distal
vulval opening
utse
ectopic branch (ventral view)
proximal
anterior
posterior
uterus
ectopic branch
uv1 cells
distal
vulval opening
utse

Figure 3: Knockdown of *nas-21* results in cell body defects

(A-D) utse cell body marked with *exc-9::mcherry* and utse nuclei marked with *lin-11::gfp*. Worms treated with *nas-21(RNAi)*. **(A)** Stage at which B-D were taken. **(B.D)** utse nuclei are in aberrant positions in presence of *nas-21(RNAi)*. Yellow asterisk indicates position of abberant nuclei. **(C, D)** additional membrane branch formed in the presence of *nas-21(RNAi)*. White asterisk indicates location at which branch was initiated. (**E)** Schematic of *nas-21(gk375710)* mutation. Position of substitution mutation is indicated by black asterisk. **(F-G)** *nas-21(gk375710)* phenotype. Cell body marked with *exc-9::mcherry*. **(F)** Stage at which G was taken. **(G)** Formation of ectopic branch in the *nas-21(gk375710)* mutant. Ectopic branch indicated by white asterisk. **(H)** Schematic of wild type and mutant ventral uterus. Cell types labeled in black, utse shown in yellow. Locations labeled in gray and ectopic branch labeled in red. Scale Bar 100 µm.

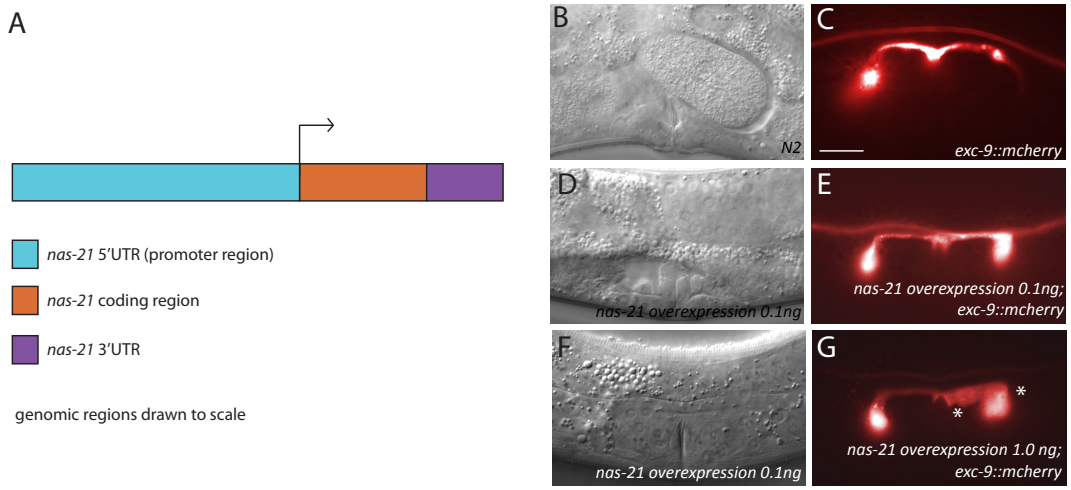

Figure 4: Overexpression of *nas-21* causes an expansion of the utse cell membrane

Cell body marked with *exc-9::mcherry*. **(A)** schematic of *nas-21* overexpression construct. **(B, D, F)** Stages at which B, D, and F were taken, respectively. **(B-C)** Wild type utse. **(C)** Proper utse outgrowth. **(E)** utse exhibits normal outgrowth and shape in the presence of low levels of additional endogenous *nas-21* (.1ng/µl) **(G)** utse cell body has expanded in the presence of high levels of additional endogenous (1ng/µl). White asterisks indicate areas of expansion. Scale Bar 100 µm.

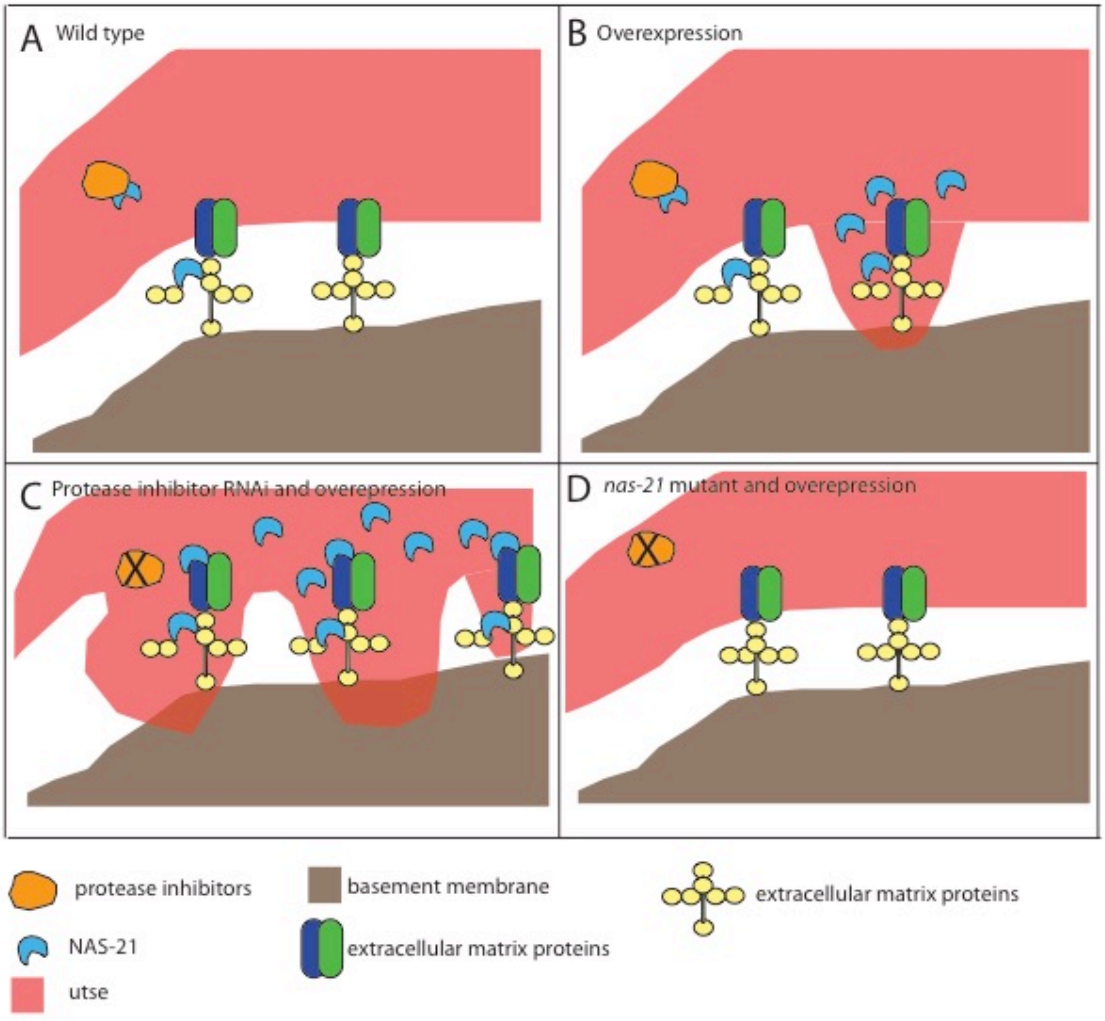

Figure 5: Schematic of how levels of NAS-21 affects utse outgrowth

(A) Wild type utse outgrowth. Normal levels of NAS-21 (shown in blue) cleave enough components of the extracellular matrix (ECM) (shown in yellow and green and dark blue) to allow for proper utse outgrowth (shown in red). **(B)** Over expression of NAS-21. Increased levels of NAS-21 causes increased cleavage of ECM components. This allows for expansion of the utse cell body along the dorsal-ventral axis and into the basement membrane. A similar phenotype occurs when protease inhibitors (which limit levels of NAS-21) are knocked down via RNAi. **(C)** Overexpression of NAS-21 in the presence of protease inhibitor knockdown. Increased levels of NAS-21 (due to the overexpression) along with protease inhibitor knockdown (which further increases levels of NAS-21) causes an exaggerated version of the phenotype from B. Further

expansion of the utse occurs on the dorsal-ventral axis into the basement membrane. **(D)** Protease inhibitor knockdown in NAS-21 mutants. Lack of presence of NAS-21 causes protease inhibitors to not have an effect. utse has wildtype or NAS-21 mutant phenotypes.

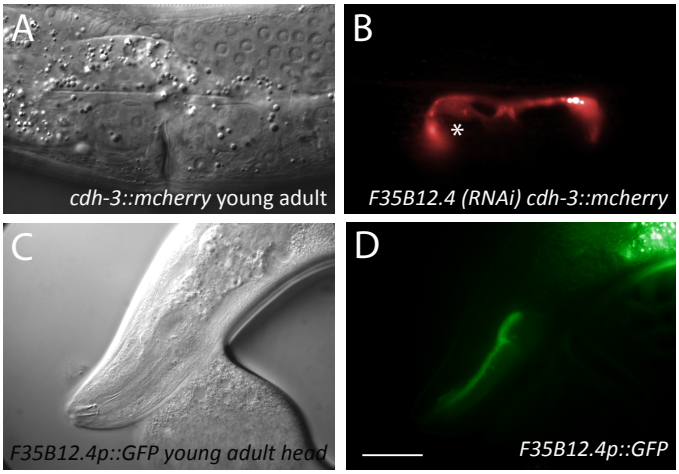

Figure 6: Protease inhibitors that affect NAS-21 activity

A) Stage at which B was taken. **(B)** Representative of RNAi phenotypes exhibited when protease inhibitors are knocked down. *F35B12.4(RNAi)* treated works exhibit blebbling on the dorsal ventral axis. Bleb indicated by white asterisk. **(C)** Stage at which D was taken. **(D)** *F35B12.4* is expressed in the pharyngeal neuron M4. Scale bar 100 µm.

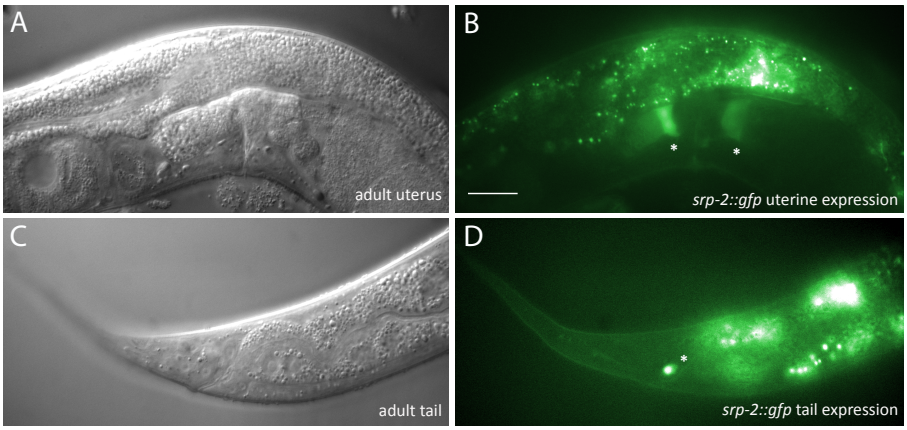

Figure 7: *srp-2* expression pattern

(A) Adult uterus, stage at which B was taken. **(B)** *srp-2* is expressed in the uterine toroids. Uterine toroids are marked by white asterisks. **(C)** Adult tail, stage at which D was taken. **(D)** *srp-2* is expressed in one of the tail neurons, potentially PDA. Scale bar 100 µm.

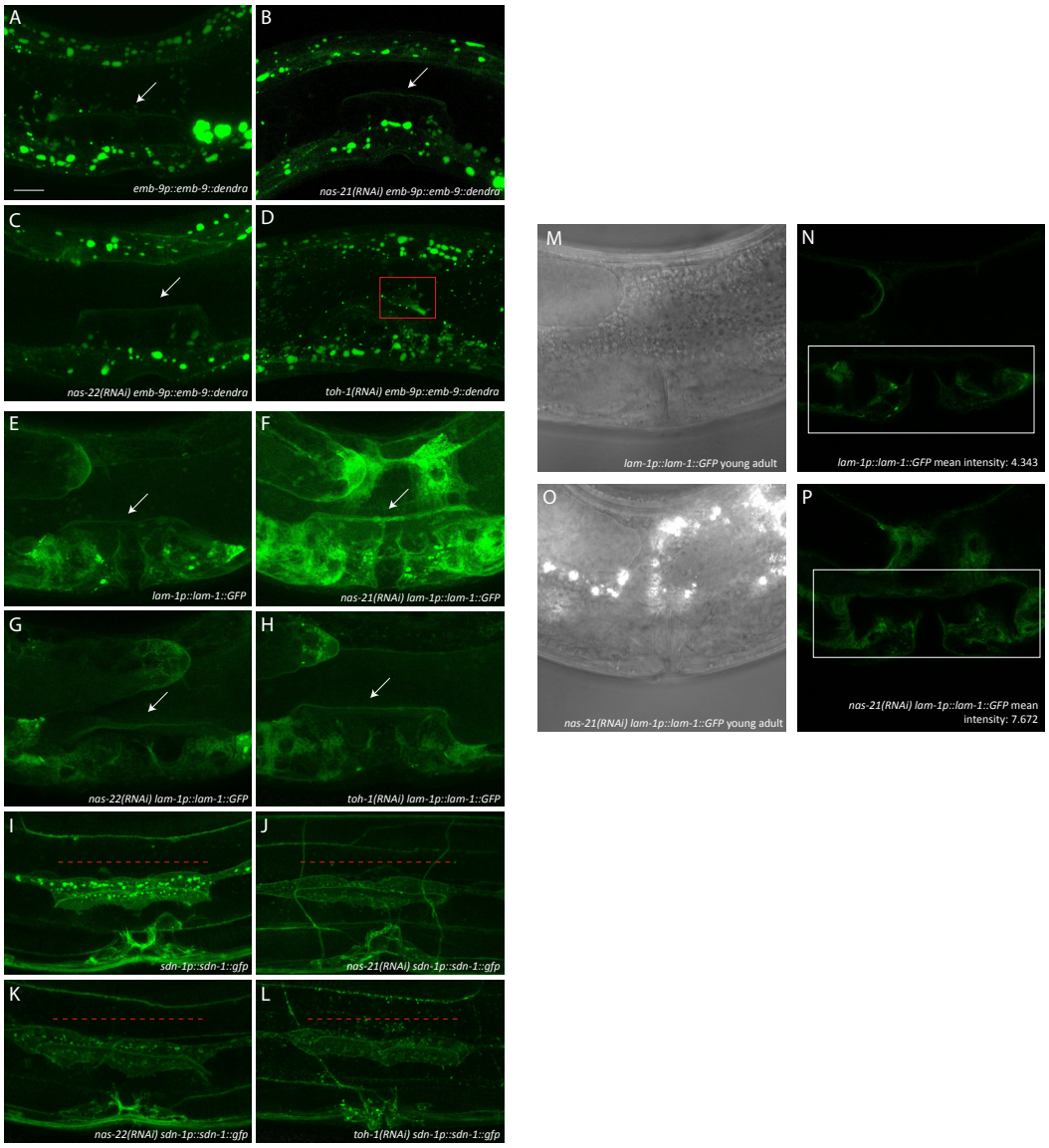

Figure 8: Changes in ECM levels due to *nas-21, nas-22,* and *toh-1* knockdown

(A-H) Images are z-projections of individual uterine sections. **(A-D)** Collagen IV accumulation marked using *emb-9p::emb-9::dendra* construct. **(A)** Wild-type *emb-9* gfp expression. Accumulation of *emb-9* expression in globule like structures in body wall muscle as well as along the dorsal edge of the utse (shown with white arrow). **(B)** *nas-21(RNAi)* treatment. Expression similar to that of wild type (presence of globules in body wall muscle) and dorsal edge of utse (white arrow). **(C)** *nas-22(RNAi)* treatment. Expression similar to that of wild type (presence of globules in body wall muscle) and dorsal edge of utse (white arrow). **(D)** *toh-1(RNAi)* treatment. *toh-1 RNAi* treated animals show an increased number of globules in the body wall muscle as well as an accumulation of expression in the posterior uterine area (see red box). **(E-H)** Laminin accumulation marked by *lam-1p::lam-1::gfp.* **(E)** Wild-type *lam-1* expression. *lam-1* is present in the dorsal edge of the utse (see white arrow) as well as the uterine lumen and distal tip cells (DTC). **(F)** *nas-21(RNAi)* treatment. *nas-21(RNAi)* treated worms show increased concentration of *lam-1* throughout the uterus and in the DTC. Worms in E and F were imaged using identical parameters. **(G)** *nas-22(RNAi)* treatment. Expression similar to that of wild type. **(H)** *toh-1(RNAi)* treatment. Expression similar to that of wild type. **(I-L)** Syndecan expression visualized by *sdn-1p::sdn-1::gfp*. **(I)** Wild-type *sdn-1* expression. *sdn-1* is present in the hypodermis lateral to the utse. Anterior-posterior length shown with red dashed arrow. **(J)** *nas-21(RNAi)* treatment. *sdn-1* expression has expanded along the anterior-posterior axis. See red dashed arrow for reference to wild type anterior-posterior length of expression. **(K)** *nas-22(RNAi)* treatment. *sdn-1* expression has expanded along the anterior-posterior axis. See red dashed arrow for reference to wild type anterior-posterior length of expression. **(L)** *toh-1(RNAi)* treatment. *sdn-1* expression has expanded along the anterior-posterior axis. See red dashed arrow for reference to wild type anterior-posterior length of expression. Also note increased amounts of *sdn-1* puncta after treatment with *toh-1(RNAi)*. **(M-P)** Images are individual slices taken from z-stacks of the uterine area. **(M)** Stack/stage at which J was taken. **(N)** *lam-1p::lam-1::gfp* wild type expression. Single slice taken from z-stack used to make projection in E. White box indicates area from which fluorescent intensity was quantified. **(O)** Stack/stage at which L was taken. K and L were taken at positions comparable to I and J based on vulval morphology. **(P)** *nas-21(RNAi) lam-1p::lam-1::gfp* expression pattern. Single slice taken from z-stack used to make projection in F. White box indicates area from which fluorescent intensity was quantified. Scale bar 100 μm.

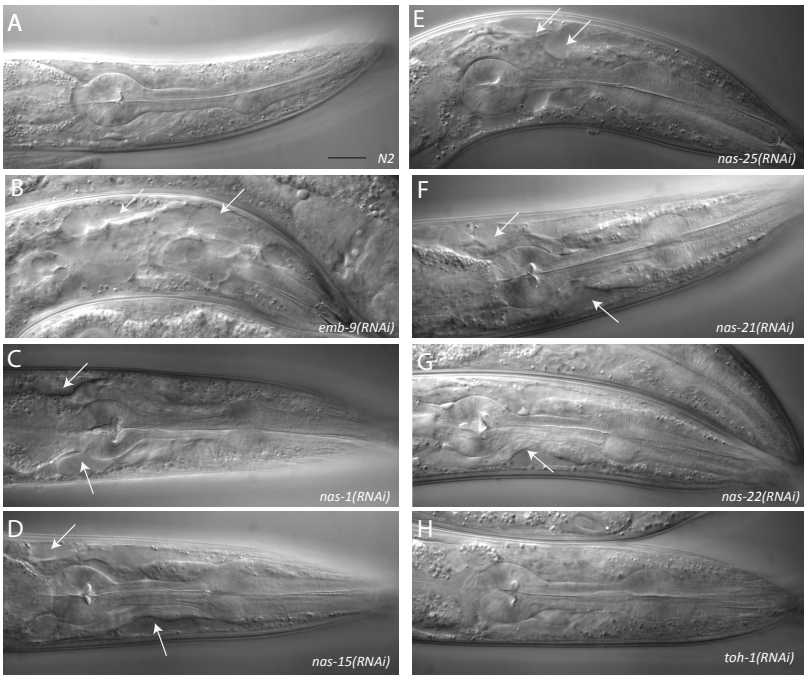

Figure 9: Pharyngeal defects caused by astacin RNAi

All RNAi was performed on N2 strain. White arrows indicate gaps present in the tissue adjacent to the pharynx. **(A)** Wild type N2 pharynx. **(B)** *emb-9(RNAi)* treated worms. **(C)** *nas-1(RNAi)* treated worms. **(D)** *nas-15(RNAi)* treated worms. **(E)** *nas-25(RNAi)* treated worms. **(F)** *nas-21(RNAi)* treated worms. **(G)** *nas-22(RNAi)* treated worms. **(H)** *toh-1(RNAi)* treated worms. Scale bar 100 μm.

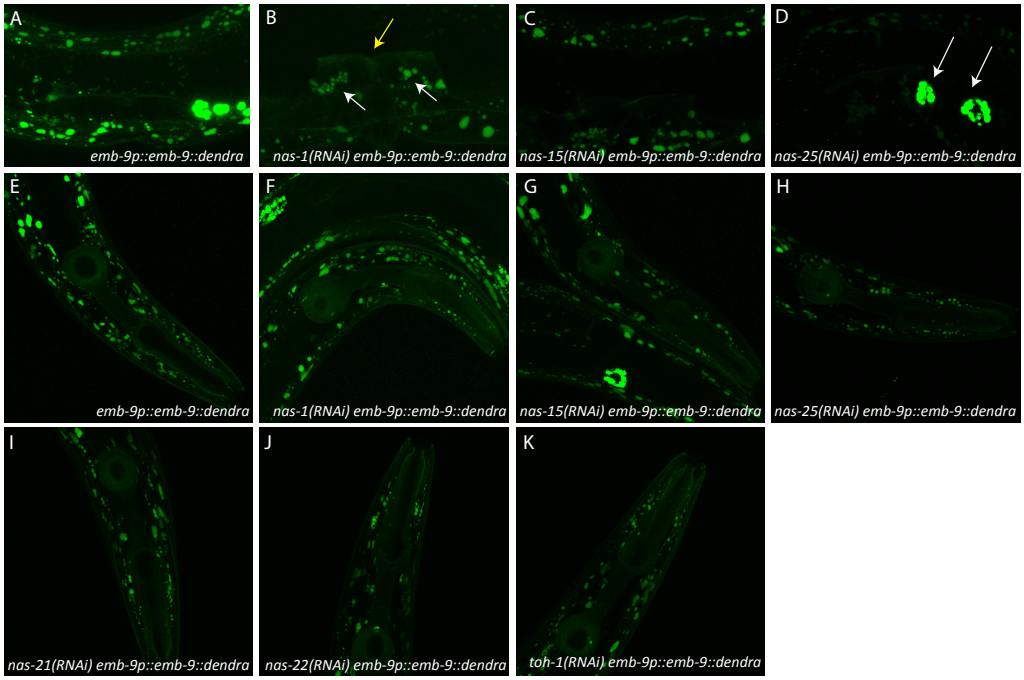

Figure 10: Changes in collagen IV expression with pharyngeal and uterine astacin knockdown

Collagen IV accumulation marked using *emb-9p::emb-9::dendra* construct. **(A-D)** Effect of pharyngeal astacin knockdown on the utse. **(A)** Wild-type uterine collagen distribution. **(B)** Collagen distribution in *nas-1(RNAi)* treated worms. Increased *emb-9* expression in the utse shown with yellow arrow. Increased *emb-9* expression ventral to the utse shown with white arrows. **(C)** Collagen distribution in *nas-15(RNAi)* treated worms. Lower levels of *emb-9* expression compared to wild-type. **(D)** Collagen distribution in *nas-25(RNAi)* treated worms. Increased *emb-9* expression in puncta shown with white arrows. **(E-K)** Effect of pharyngeal and uterine astacin knockdown on the pharynx. **(E)** Wild-type pharyngeal collagen distribution. **(F)** Pharyngeal collagen distribution in *nas-1(RNAi)* treated worms. **(G)** Pharyngeal collagen distribution in *nas-15(RNAi)* treated worms. **(H)** Pharyngeal collagen distribution in *nas-25(RNAi)* treated worms. **(I)** Pharyngeal collagen distribution in *nas-21(RNAi)* treated worms. **(J)** Pharyngeal collagen distribution in *nas-22(RNAi)* treated worms. **(K)** Pharyngeal collagen distribution in *toh-1(RNAi)* treated worms.

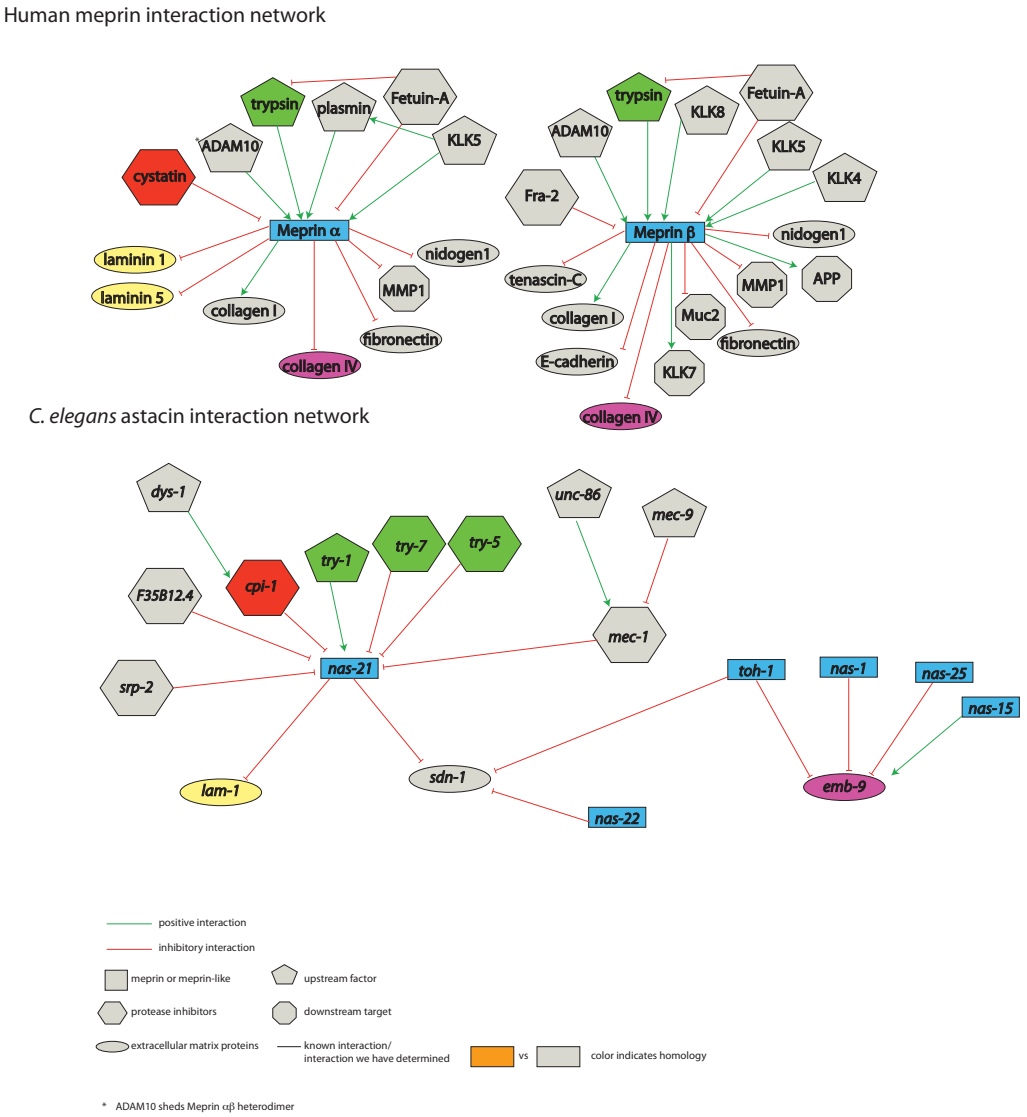

Figure 11: Meprin interaction network

A) Network of genes that regulate meprin α and meprin β. Genes are divided into subcategories (see legend). Genes are divided by shape (see legend). Colored boxes indicate genes that have been characterized to be involved in meprin regulation. Solid arrow indicates known interactions/interactions. Green arrows indicate positive interactions, red arrows indicate negative/inhibitory interactions.

Figure S1: Predicted domains using multiple species protein alignment

All alignments done using Clustal Omega (Sievers et al., 2011). **(A)** NAS-21 domain prediction. Sequences from *C. brenneri* NAS-21*, C. remanei* NAS-21, and *C. elegans* NAS-21 aligned with one another. Predicted signal peptide sequence highlighted in green, predicted prodomain sequence highlighted in purple, and predicted EGF domain shown in blue. **(B)** NAS-22 domain prediction. Sequences from *C. brenneri* NAS-22*, C. remanei* NAS-22, *C. briggsae* NAS-22, and *C. elegans* NAS-22 aligned with one another. Predicted prodomain shown in purple. **(C)** TOH-1 domain prediction. Sequences from *C. brenneri* TOH-1*, C. remanei* TOH-1, *C. briggsae* TOH-1, *C. japonica* TOH-1, and *C. elegans* TOH-1 aligned with one another. Prodomain shown in purple.

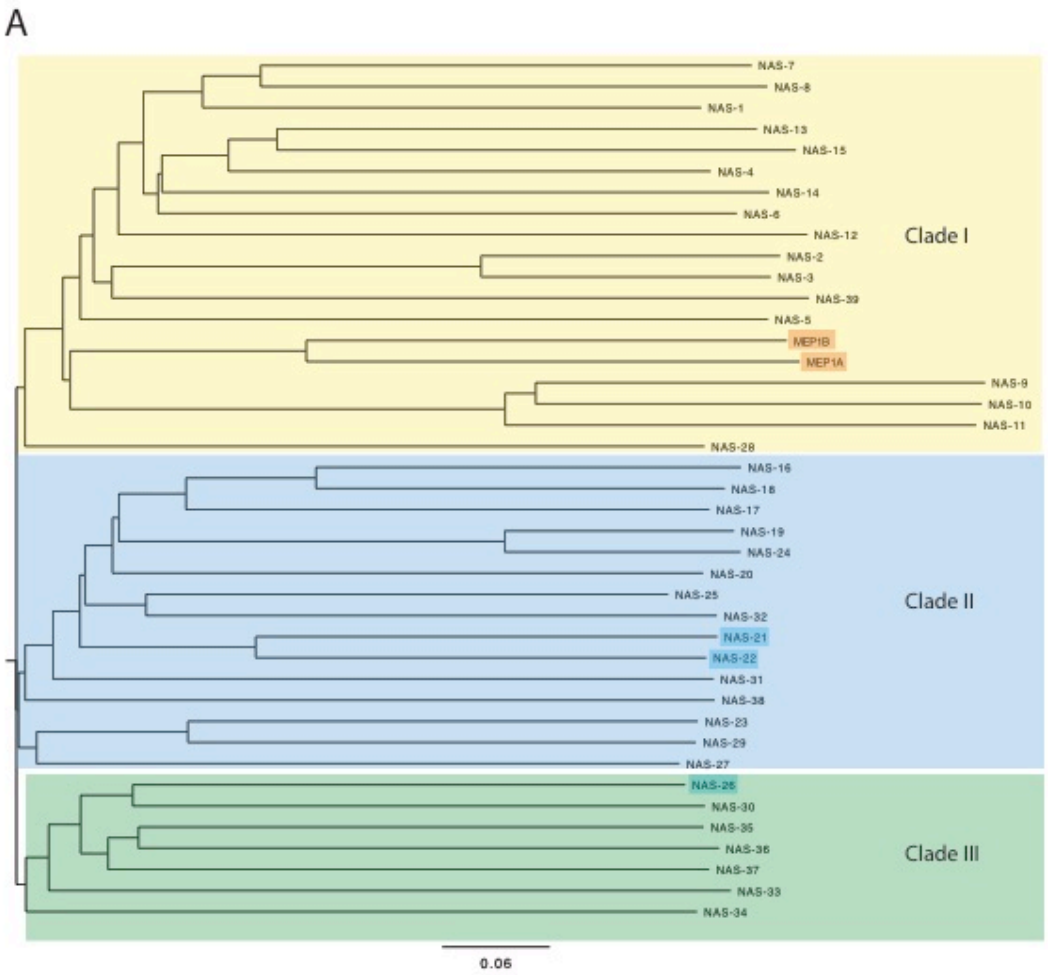

Figure S2: Phylogenetic tree of meprins and astacins

(A) Phylogenetic tree comparing entire meprin and astacin sequences. Red boxes show meprins, and blue boxes show astacins that we are characterizing in this work.

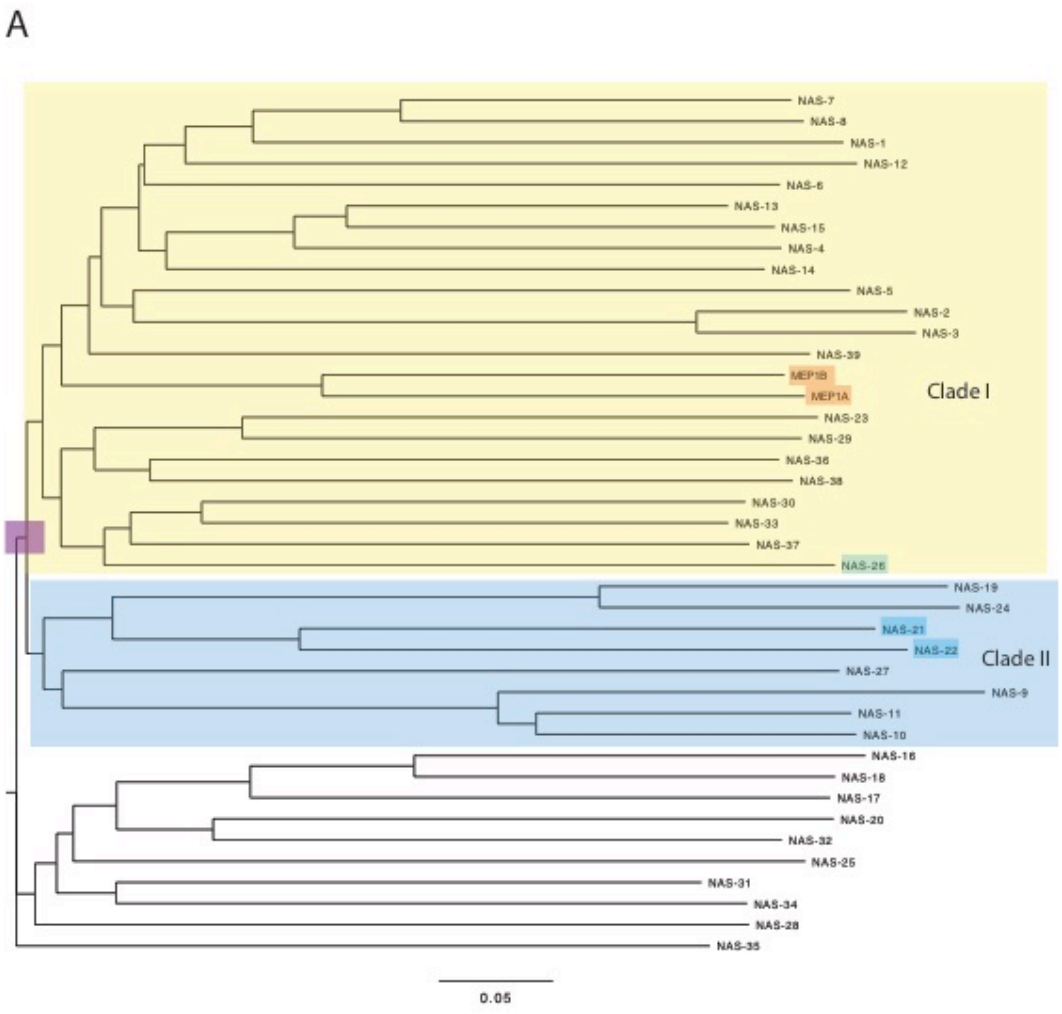

Figure S3: Phylogenetic tree astacin domain of meprins and astacins

(A) Phylogenetic tree comparing zinx metalloprotease (astacin) domain of meprin and astacin sequences. Red boxes show meprins, and blue boxes show astacins that we are characterizing in this work. Purple box shows potential monodelphic clade to which NAS-21, NAS-22, NAS-26/TOH-1, MEP1A, and MEP1B all belong.

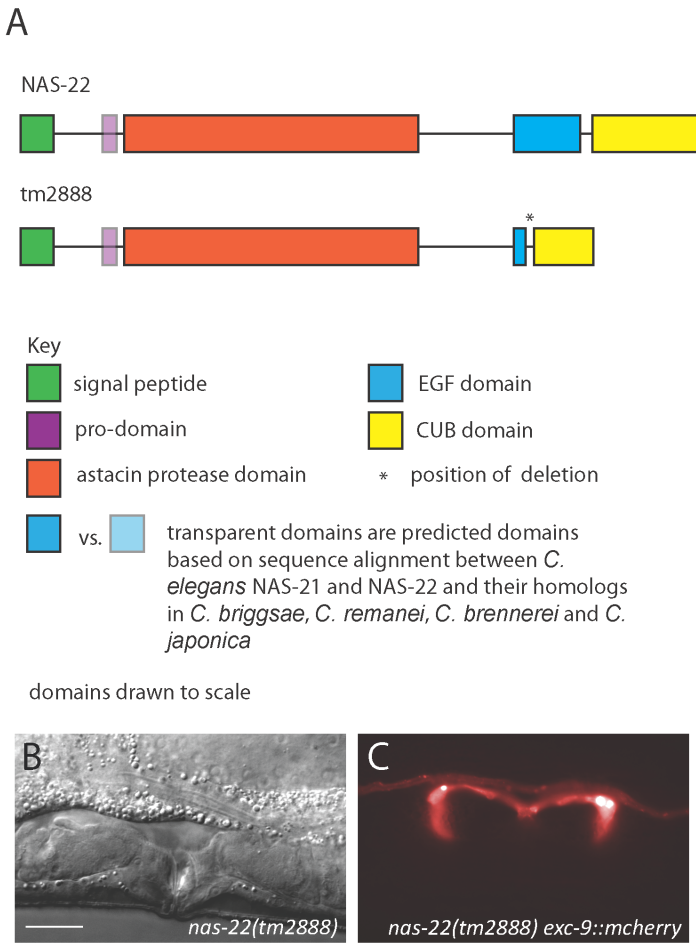

Figure S4: *nas-22(tm2888)* phenotypes

(**A)** Schematic of *nas-22(tm2888)* mutation. *tm2888* has a section of its EGF and CUB domains deleted (amino acids 244 to 334). **(B)** Stage at which C was taken. **(C)** Cell body marked by *exc-9::mcherry*. utse has wild type characteristics in *nas-22(tm2888)* mutation. Scale bar 100 µm.

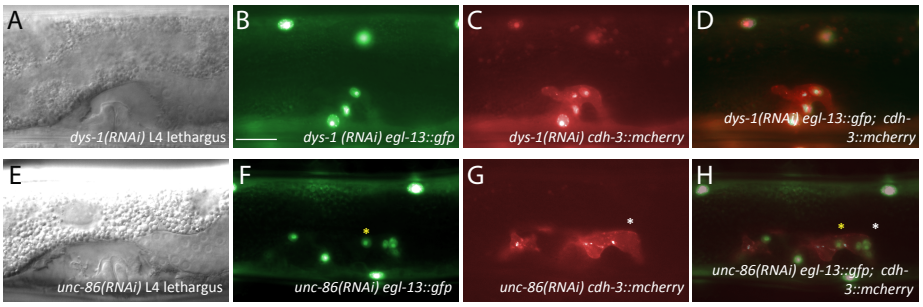

Figure S5: *unc-86(RNAi)* phenotypes

Cell body marked with *cdh-3::mcherry* and nuclei marked with *egl-13::gfp* **(A)** Stage at which B-D were taken. **(B)** Aberrant nuclear migration in *dys-1(RNAi)* treated worms. (compare to Figure 1F'). **(C)** Shorter cell body of in *dys-1(RNAi)* treated worms. (compare to 1F''). **(D)** Merge of B and C. **(E)** Stage at which F-H were taken. **(F)** Aberrant nuclear migration in *unc-86(RNAi)* treated worms. Yellow asterisk indicates nuclei that have not completely migrated to wild type positions (compare to Figure 1F'). **(G)** Cell body has extended along the dorsal-ventral axis similar to the *nas-21* overexpression construct (see Figure 4G). **(H)** Merge of F and G. Scale bar 100 µm.

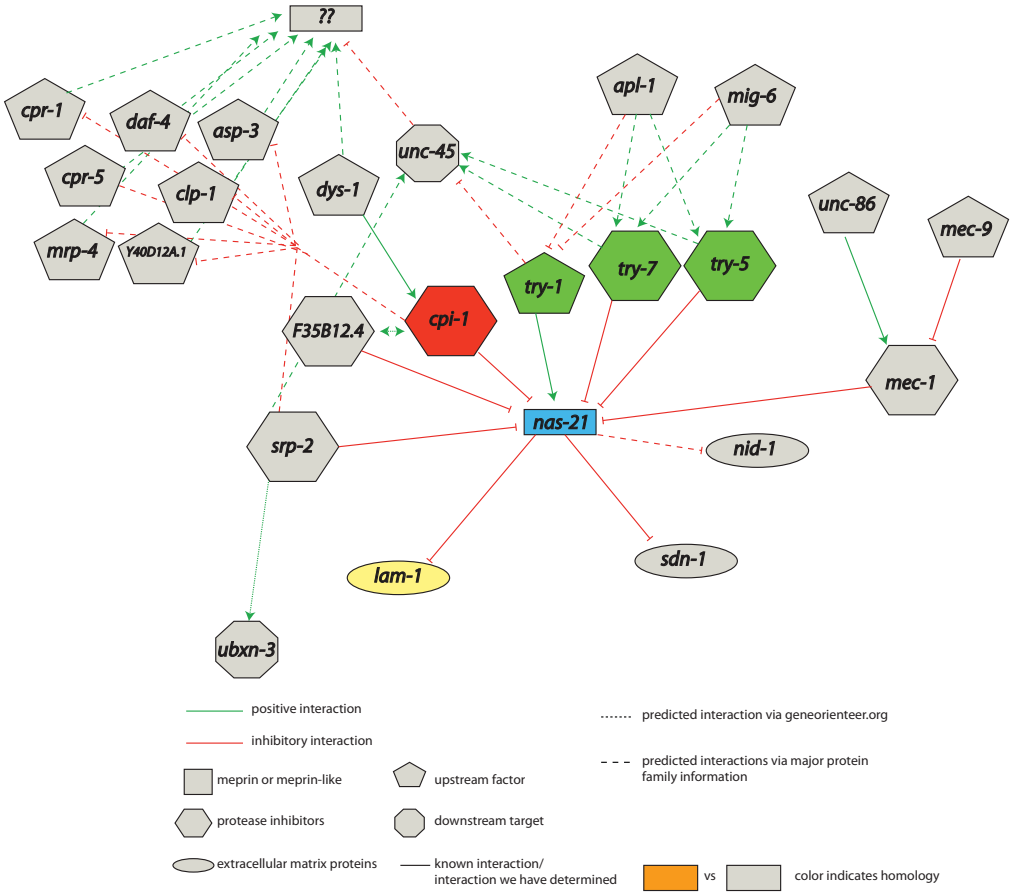

Figure S6: *nas-21* expanded interaction network

(A) Network of genes we believe are involved in regulating *nas-21*. Genes are divided by shape (see legend). Colored boxes indicate genes that have been characterized to be involved in meprin

regulation (see Figure 9). Solid arrow indicates known interactions/interactions. Dashed arrows indicate predicted interactions. Green arrows indicate positive interactions, red arrows indicate negative/inhibitory interactions.

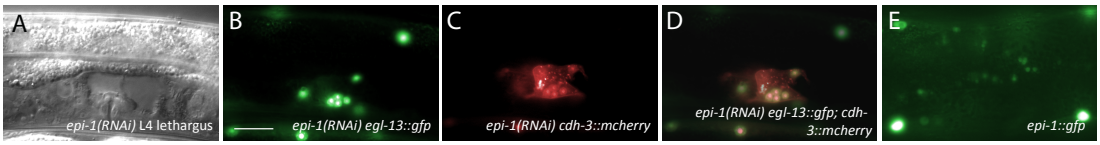

Figure S7: *epi-1* expression pattern and RNAi phenotypes

(A-D) *epi-1(RNAi)* treated worms. **(A)** Stage at which B-D was taken. **(B, D)** *epi-1(RNAi)* causes nuclear migration defects. Nuclei are marked with *egl-13::gfp*. Nuclei in *epi-1(RNAi)* treated worms fail to migrate at all. (Compare to Figure 1F' amd 1F'''). **(C, D)** *epi-1(RNAi)* causes cell outgrowth defects. Cell membrane marked with *cdh-3::mcherry*. utse takes a square shape versus an elongated H shape (compare to Figure 1F''and 1F'''). **(E)** *epi-1* expression pattern. *epi-1* is expressed in seam cells. Scale bar 100 μm.

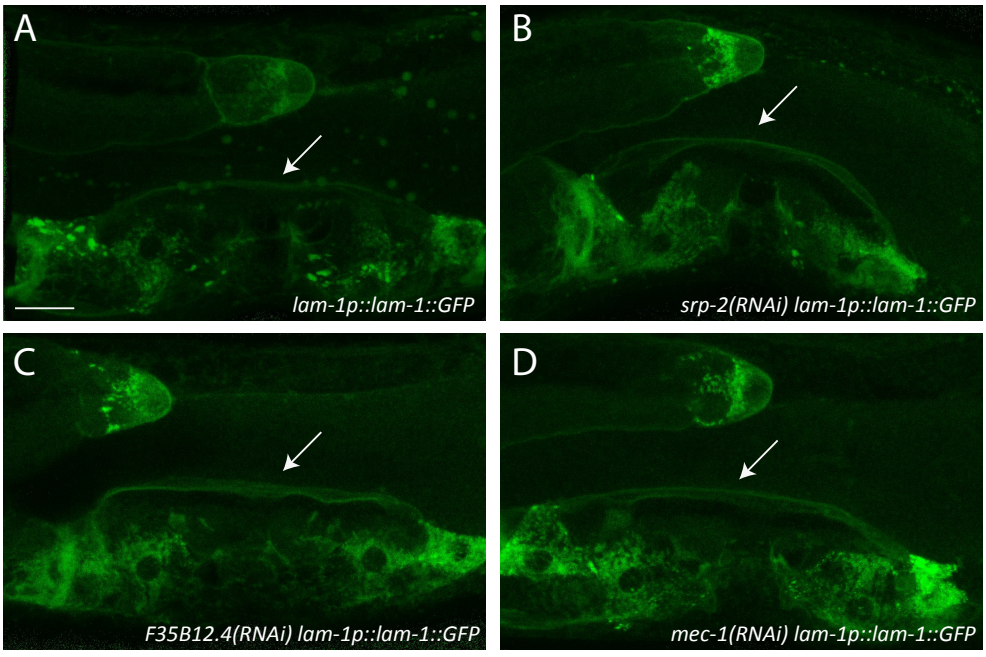

Figure S8: Effect of protease inhibitor knockdown on *lam-1* expression

(A) Wild-type *lam-1* expression. *lam-1* is present in the dorsal edge of the utse (see white arrow) as well as the uterine lumen and distal tip cells (DTC). **(B)** *srp-2(RNAi)* treatment. Expression similar to that of wild type. **(C)** *F35B12.4(RNAi)* treatment. Expression similar to that of wild type. **(D)** *mec-1(RNAi)* treatment. Expression similar to that of wild type.

CHAPTER 5

A Candidate RNAi screen for cell outgrowth defects in the *C. elegans* utse

5.1 Abstract

The *C. elegans* uterine seam cell (utse) undergoes cell outgrowth during development. In order to determine the molecular inputs necessary to mediate this outgrowth, we performed a candidate RNAi screen against 116 genes. These genes were selected using a three part criteria: genes with reported expression patterns within the utse or surrounding tissues, genes which characterized roles affecting cell outgrowth and nuclear migration in other tissues, and genes that encode structural cellular components as well as their predicted ability to interact with genes in the above three categories. We observed a high percentage of hits from our screen (46.6%, 54 genes of 116). We have categorized our hits into eight categories, including genes involved in neuronal regulation, nuclear migration, cell adhesion, cell structure, and cell transport. Our results expand the role of the utse from simply acting as a model for studying cell shape change. This work presents the utse as a powerful tool that can be used to understand a diverse array of genetic pathways and cell behaviors.

5.2 Introduction

The *C. elegans* uterine seam cell, or utse, is a syncytial cell within the hermaphrodite somatic gonad that functions in attaching the uterus to the body wall (Newman et al., 1996; Ghosh and Sternberg, 2014). During the L4 larval stage, the utse grows outward along the anterior-posterior axis, morphing from an ellipsoidal shape to that of a sideways H (lateral view in Figure 1A, Ghosh and Sternberg, 2014). The utse contains nine nuclei, and these nuclei migrate from the middle of the cell to the anterior and posterior edges of the cell during development. This migration occurs at a slower rate than the cell outgrowth indicating that these behaviors are not be linked.

Though the lineage of the utse is well characterized (Newman et al., 1996), the molecular inputs necessary to mediate cell outgrowth were not well known prior to our work. Specifically, two genes have been previously characterized for their roles in utse cell outgrowth and nuclear migration: the LIM domain transcription factor *lin-11* and the SOX domain transcription factor *egl-13* (Newman et al., 1999; Hanna-Rose and Han, 1999; Cinar et al. 2003). However, these genes were mainly characterized for the roles in utse precursor cell and anchor cell fusion.

We took a wide-scale approach to identifying additional genes that were necessary for utse cell outgrowth and nuclear migration. We designed a candidate RNAi screen against several classes of genes and scored for phenotypes exhibiting perturbed outgrowth and nuclear migration (Figure 3).

Specifically, we generated a list of the following types of genes: genes that were expressed in the utse and its surrounding tissues, genes characterized to affect cell behavior in other tissues and organisms, genes encoding structural components of cells, and genes that are predicted to act with genes of the previous three classes. We saw a high percentage of positive hits (Table 1; 46.6% of the 116 genes that we tested). These positive hits can be categorized into two major classes: genes that have been characterized to affect neurons and genes that play roles in nuclear dynamics. We also found genes that were involved in cell adhesion, encoded structural components of cells, and encoded transcription factors. We therefore not only present a list of genes that are involved in regulating utse development, but also present the utse as a powerful model for studying many aspects of cell biology.

5.3 Materials and Methods

Strains and genetics: *C. elegans* were handled as described previously (Brenner, 1974). All strains used (listed in supplementary material Table S1) are derivatives of *C. elegans* wild-type strain (N2 Bristol).

RNAi experiments: RNAi was performed by feeding nematodes dsRNA-producing bacteria using standard procedures (Timmons et al., 2001) modified according to our previous work (Ghosh and Sternberg, 2014). For RNAis used see Table S2.

Scoring utse phenotypes: Animals were scored using a wide-field epifluorescence microscope at young adult or L4 lethargus stage. Shortened or elongated utse outgrowth was classified using criteria from our previous work (Ghosh and Sternberg, 2014). Positive RNAi results were categorized in two categories, hits of high confidence (found by using Bonferroni correction), and hits of medium confidence (hits found with a false discovery rate of 0.05). Empty vector RNAi was used as a control.

5.4 Results and Discussion

The *C. elegans* uterine seam cell is a syncytial cell that grows outward bidirectionally along the anterior-posterior axis (Newman et al., 1996; Ghosh and Sternberg, 2014). Prior to our work, limited information was available about the genetic inputs necessary for mediating proper utse outgrowth. Therefore we chose to perform a large-scale candidate RNAi screen (Figure 2).

Specifically, we generated a list of genes using the following criteria: genes expressed in the utse and surrounding tissues, genes that affect cell and nuclear migration in other tissues and organisms, genes that encode components of the extracellular matrix, and genes characterized to act upstream and downstream of genes in the previous three categories. We fed worms bacteria containing plasmids with dsRNA of these genes (Figure 2), and scored for defective utse outgrowth phenotypes (Table 1). Our initial list consisted of 314 genes, and our findings from this list contributed to two publications. 84 of these genes were characterized in our publication where we examined spatial and molecular inputs that contribute to utse development (Ghosh and Sternberg, 2014). 114 of these genes were characterized in a publication where we used the utse as a model for studying protease activity (Ghosh et al., in prep). The remaining 116 genes from our list contained a high percentage of hits (Table 1; 54 genes out of 116). We wish to characterize these hits.

We have characterized our positive results into two categories: hits of high confidence (found by using Bonferroni correction), and hits of medium confidence (hits found with a false discovery rate of 0.05). 29 genes fit our high confidence category and 54 genes fit our medium confidence category. We will describe hits of both high confidence and medium confidence (54 genes) in this work.

Of the hits from our list, 18 genes were known to affect nuclear dynamics, 21 genes were either expressed in or affected behavior of neurons, 8 genes were involved in cell structure, 7 genes contained homeodomains, 7 genes affected cell adhesion, 5 genes were solely characterized as transcription factors, 4 genes were involved in intracellular transport, and 3 genes mediated cell signaling The remaining hits include a gene whose homolog regulates tumorigencity (*F11A10.5*), a gene involved in chromosome segregation (*pqn*-85), and a globin (*glb-12)*. We have characterized the positive hits from our list below.

5.4.1 Neuronal Genes

The largest category of genes from our list contained genes that were either expressed in neurons or controlled neuronal behavior (specifically neuronal outgrowth). The 23 genes in this category are *cwn-1*, *dh11.5, egl-13, gipc-1, gipc-2, ina-1, itr-1, lin-11, lin-39*, *mig-15, ncam-1, nud-2, pat-3, sax-1, sax-7, srsx-18, ttx-3, unc-33, unc-70, unc-97, vab-3, zag-1,* and *zfp-1*. The integrins *ina-1* and *pat-3* are characterized in the cell structure section and cell adhesion sections, and the remaining genes have been described below.

Several of the neuronal hits were genes that affect neuronal outgrowth, migration, guidance, and cell shape. These genes are *cwn-1*, *lin-11, lin-39, mig-15, ncam-1, sax-1, sax-7, ttx-3, unc-33, unc-70, zag-1,* and *zfp-1.* Since the utse undergoes anterior-posterior outgrowth during its development, we believe that these genes may be acting as guidance cues, or mediating structural components necessary for utse outgrowth. We have described the functions of these twelve neuronal outgrowth hits below.

cwn-1 encodes a Wnt-ligand necessary for establishing guidance for the ALM neuron (Hilliard and Bargmann et al., 2006). Specfically, in *cwn-1* and *egl-20* double mutants, ALM neurons migrate posteriorly rather than anteriorly. *cwn-1* is expressed in the body wall muscle and sex myoblasts (Minor et al., 2013), and we have shown that genes expressed in the sex myoblast (*unc-53*, Ghosh and Sternberg, 2014) are necessary for proper utse development. *cwn-1* is also necessary for establishing vulval polarity (Minor et al., 2013)

lin-11 is a LIM homeodomain transcription factor necessary for the formation of functional AIZ, RIC, AVG, AVH/AVJ neurons (Hobert et al., 1998). Specifically, *lin-11* null mutants exhibit neuronal outgrowth defects -- AIZ and RIC form posteriorly directed processes, and posteriorly displaced cells with these neurons take unusual paths, and AVG and AVH/AVJ processes terminate prematurely (Hobert et al., 1998; Hutter 2003). *lin-11* also specifies the fates of the AWA, ASG sensory neurons (Sarafi-Reinach et al., 2001). *lin-11* is also mediates the fusion between the utse and the AC, and specifies π cells (which are utse precursor cells that fuse with the AC to form the utse) (Newman et al., 1999). Therefore we may be seeing defects because of this role. However, due to its role in regulating genes involved in neuronal guidance we cannot elimate the possibility that *lin-11* may also act as a utse guidance cue.

Another LIM homeodomain protein that regulates neuronal outgrowth is TTX-3 (Hobert et al., 1997). *ttx-3* mutants exhibit defects in AIY axonal outgrowth. *ttx-3* is also necessary for temperature sensing (Hobert et al., 1997) and olfactory learning behaviors (Remy and Hobert, 2005).

lin-39 is a homeodomain protein homologous to the Deformed and Sex combs reduced family of homeodomain proteins (Clark et al., 1993). *lin-39* is necessary for QR neuroblast migration. The QR neuroblasts migrate along the anterior-posterior axis to form AVM, SDQR, and AQR neurons. In *lin-39* mutants, QR descents never reach their normal anterior positions. *lin-39* also specifies

vulval fates, and in the absence of *lin-39* function vulval precursor cells P(3-8).p fuse with hyp7 epidermis in the L1 larval stage (Sternberg, 2005; Clark et al., 1993). The utse lies dorsal to the vulva and therefore outgrowth phenotypes may be attributed to the vulval defects.

mig-15 is a NCK-interacting kinase necessary for proper axon outgrowth, specifically outgrowth in axon commisures (Poinat et al., 2002). Axon commissures are sites where axons cross the midline from one side of the nervous system to the other. *mig-15* interacts with beta integrin *pat-3* (which was another hit from our screen, Table 1) to guide GABAergic neurons crossing the ventral cord. Interestingly, *mig-15* is expressed in the vulval muscles, a tissue that we have identified to be involved in utse outgrowth (Ghosh and Sternberg, 2014).

ncam-1 is a cell adhesion molecule of the immunoglobulin superfamily (IgCAM) neurons (Schwarz et al., 2009). It mediates contact and communication between neurons. *ncam-1* is expressed in several neurons, including ASI, ASJ, AVB, AVE, PVC, AIB, AIN, DA, DB, M2, and NSM and affects directional outgrowth of DA2/DB3 motorneuron commissures.

sax-7 is another member of the immunoglobin superfamily involved in neural cell adhesion. *sax-7* encodes the sole *C. elegans* L1 CAM (an immunoglobin superfamily protein involved in neural cell adhesion (Chen et al., 2001)). *sax-7* is necessary for proper positioning of AWB, AWC, AFD, and RIA neurons (Sasakura et al., 2005). *sax-7* physically interacts with *unc-44* (ankyrin, an adaptor proteins that mediates the attachment of integral membrane proteins to spectrin-actin based cytoskeleton) (Zhou et al., 2008).

sax-1 encodes a serine/threonine kinase in the Ndr family and is necessary for maintaining cell shape in AWC, ASE, and ASJ (Zallen et al., 2000). *sax-1* mutants exhibit defects in neurite initiation and in neuronal cell shape, including an extended, irregularly shaped cell body and ectopic neurite-like processes.

unc-33 encodes the microtubule binding protein CRMP necessary for axon guidance and outgrowth (Li et al., 1992). In *unc-33* mutants, PVD and FLP neurons are prematurely terminated and PVD neurons have mislocalized dendrites (Maniar et al., 2011). *unc-33* affects outgrowth by increasing the steady-state level of axonal microtubules and orienting asymmetric, plus-end distal microtubule growth while preventing plus-end dendritic microtubules growth distally. Like *sax-7, unc-33* also interacts with ankyrin (*unc-44*) to organize microtubule positioning.

unc-70 encodes beta-G spectrin, a cytoskeletal protein that stabilizes the structure of cell membranes (Park et al., 1986; Hammarlund et al., 2000). *unc-70* mutants display defects in outgrowth of GABAergic axon commissures that extend from the ventral to the dorsal cord. The defects include in ectopic branching, axon mislocalization, and large terminal expansions resemble growth cones. *unc-70* is also necessary for sensation of mechanical stimuli in the AVM and ALM (Krieg et al., 2014) and maintenance of the muscle myofibril lattice (Hammarlund et al., 2000; Moorthy et al., 2000; Cox and Hardin, 2004).

zag-1 is a ZFH class homeodomain complex necessary for neuronal branch formation and guidance (Wacker et al., 2003; Clark and Chiu, 2003). *zag-1* is essential for proper development and behavior of several neurons, including the ALM, AVM, ADE, PDE, DA, DB, DD, and VD motor neurons, interneurons of the ventral cord, as well as the VA, AVB, AVD, AVE ,PVC, SABVR/L, AVEL/R, and PVQ interneurons (Wacker et al., 2003; Clark and Chiu, 2003). *zag-1* is also necessary for the differentiation of the HSN motor neuron, and induces *tph-1* expression for neuron maturation (Clark and Chiu, 2003).

zfp-1 is an ortholog of zinc finger protein 1, a plant homedomain protein and a homolog of AF10 (Acute Lympho- blastic Leukemia 1-Fused gene from chromosome 10) (Avgousti et al., 2013; Chaplin et al., 1995). *zfp-1* promotes HSM migration (Kennedy and Grishok, 2014). Specifically, *zfp-1* acts with RNAi DEficient 4 (*rde-1)* and other genes necessary for promoting RNAi in *C. elegans* to create an endogenous RNAi pathway within *C. elegans* (Grishok, 2012; Kennedy and Grishok, 2014). This endogenous RNAi system enables *zfp-1* to regulate levels of *pdk-1,* a component of the insulin-signaling pathway necessary for mediating reactions to stress and controlling *C. elegans* lifespan (Mansisidor et al., 2011). The *zfp-1/pdk-1* interaction also regulates levels of *daf-16* (a hit from our list that we have described in the nuclear genes section), which promotes HSN migration and nuclear localization within the hypodermis (Kennedy and Grishok, 2014). *zfp-1* is expressed in the germline and is necessary for the production of viable oocytes (Avgousti et al., 2013). *zfp-1* also interacts with the histone methyltransferase *dot-1* to negatively regulate the level of polymerase II of widely expressed genes (Cecere et al., 2013).

Nine of our hits were neuronal genes that regulated aspects of neurotransmitter release, cell fate, and behavior. Since the functions of these genes are not directly related to utse development, study

of these genes can shed light on connections between neurotransmitter release and utse development. The remaining nine hits are characterized below.

dh11.5 shares sequence homology with synaptotagmins. Synaptotagmins are proteins that localize to synaptic vesicles and mediate the release of neurotransmitters by sensing calcium levels (Fernández-Chacón et al., 2001).

egl-13 is a SOX domain transcription factor necessary for specifying the lineage of Q neuroblasts (Feng at el., 2013) and the fates of the BAG and URX O_2 and CO_2 sensing neurons (Gramstrup Petersen et al., 2013). *egl-13* is also necessary for anchor cell and utse precursor cell fusion (Hanna-Rose and Han 1999), which may be why we are observing utse defects as a result of its knockdown.

gipc-1 and *gipc-2* encode orthologs of human GIPC PDZ domain containing 1 protein (Hamamichi et al., 2008). *gipc-1* is involved in protecting against neurodegenration of DA neurons, and is a potential target screening against Parkinsons's diease. *gipc-2* exhibits a 0.49 fold change in *daf-2* mutants, which have defective insulin signaling (Ding et al., 2013)

itr-1 encodes the inositol 1,4,5-trisphosphate receptor (IP(3)R) and functions in mediating aversion responses to nose touch and the repellent benealdehyde in ASH (Walker et al., 2009). Gain-of-function *itr-1* rescues ovulation defects in the spermatheca in *fos-1(RNAi)* treated worms (Haitt et al., 2008). *fos-1* is a transcription factor involved in the formation of protrusions within the anchor cell (AC), a cell that eventually fuses with the utse (Sherwood et al., 2005). We have shown that *fos-1* activity is necessary for mediating mediating proper utse outgrowth (Ghosh and Sternberg, 2014). Therefore *itr-1* may be acting with *fos-1* in utse outgrowth as well. *itr-1* is also involved in *C. elegans* aging (Iwasa et al., 2010).

srsx-18 is expressed in the linker cell and is an ortholog of human olfactory receptor 56B1 (Schwarz et al., 2012). Olfactory receptors detect odorants to allow for odor perception. (Malnic et al., 2004).

nud-2 encodes an ortholog of human NDE1 and NDEL1 (Locke et al., 2006). *nud-2* attaches the SUN/KASH complex to dynein during nuclear migration (Fridolfsson et al., 2010, see following section for more information on the SUN/KASH complex), and is necessary for preventing susceptibility of GABAergic neurons to pentylenetetrazole (which causes convulsions) and to

maintain proper distribution of synaptic vesicles in the GABAergic neurons (Locke et al., 2006). Therefore, study of *nud-2* can shed light on mechanisms causing epilepsy.

unc-97 is a LIM domain containing protein (Hobert et al., 1999). Behavioral assays of *unc-97* mutants indicate that it is necessary for mechanosensory touch perception. *unc-97* is also involved in regulating adhesion in other tissues, and its adhesive functions will be discussed further in the cell adhesion section.

vab-3 is a homeodomain protein related to the *Pax6 Drosophila* eye development genes (Chisholm and Horvitz, 1995). *vab-3* is necessary for the patterning of cells in the head, including neurons, seam cells, and alae of the cuticle. *vab-3* is also necessary for the development of the male copulatory spicules and post cloacal sensilla (Johnson and Chamberlin, 2008).

5.4.2 Genes that affect nuclear dynamics

This category includes the following genes: *arx-2, arx-3, anc-1, gex-1/wve-1, gex-2, ima-1, ima-2, ima-3, imb-2, imb-3, lmn-1, nud-2, ran-2, ran-3 toca-1, unc-83,* and *unc-84* (Table 1).

Several of the above genes are involved in nuclear positioning. For instance, five of our hits (*unc-83, unc-84, anc-1, lmn-1,* and *bicd*-1) are either members of or associate with the SUN, KASH and Syne families. The SUN, KASH, and Syne protein families anchor the nucleus to the cytoskeleton and promote nuclear migration (Tapley and Starr, 2009). *unc-84/*SUN and *anc-1/*SYNE anchor nuclei in the *C. elegans* syncytial hypodermis (Starr and Han, 2003; Malone et al., 1999, Hedgecock and Thompson, 1982). *unc-83/*KASH coordinates nuclear migration necessary for hyp7 nuclear positioning (Malone et al., 1999; Starr et al., 2001). If the nucleus is to maintain its position within the cell (by tethering nuclei to actin), UNC-84 localizes to the inner nuclear membrane and attaches to the outer nuclear membrane protein ANC-1 (Hedgecock and Thompson, 1982; Starr and Han, 2003; Starr and Han, 2002). If the nucleus will undergo migration, UNC-84 attaches to the outer nuclear membrane protein UNC-83 (Starr et al., 2001). UNC-83 promotes migration by tethering the nucleus to dynenin motor proteins on microtubules via *nud-2* (a hit from our screen, Table 1) (Fridolfsson et al., 2010). LMN-1 is the sole *C. elegans* lamin and binds with nucleoplasmic domain of UNC-84 to further tether this protein to the inner nuclear membrane (Bone et al., 2014).

We also saw hits from two other complexes involved in nuclear migration: the Arp2/3 complex (*arx-2, arx-3*) and the WAVE/SCAR complex (*gex-1/wve-1, gex-2)* (Xiong et al., 2011). Arp2/3 and WAVE/SCAR complex affect embryonic nuclear migration (pronuclear migration is perturbed when embryos are treated with *arx-2* and *gex-3* RNAi and in *wve-1* and *gex-3* mutants). The WAVE/SCAR complex acts as a switch to activate the Arp2/3 complex, which induces actin polymerization, leading to the formation of branched actin (Takenawa and Miki, 2001). This mechanism has been characterized in migrating cells, since branched actin accumulates on the leading edge of migrating *C. elegans* embryonic epithelial cells (Patel et al 2008). Although the exact mechanism used by the WAVE/SCAR and Arp 2/3 complex in nuclear migration has not been elucidated, initiation of branched actin within the nucleus may be one way these complexes enable this nuclear migration.

toca-1 is an F-BAR protein that binds the WAVE/SCAR complex to membranes (Giuliani et al., 2009). *toca-1* mutants exhibit defective embryonic P-cell migration in the *C. elegans* embryo(Chang et al*.,* 2012). It therefore may be acting with the WAVE/SCAR complex to mediate nuclear migration.

It is not surprising that RNAi knockdown of genes involved in nuclear migration affect utse development. The utse is a syncytium composed of nine nuclei (Newman et al., 1996), and during L4 larval stage these nuclei migrate from the central portion of the cell to the anterior and posterior edges of the cell (Ghosh and Sternberg, 2014). Both the SUN/KASH and WAVE/SCAR (with Arp2/3) complexes could potentially regulate utse nuclear migration since RNAi knockdown of genes in these complexes results in utse nuclear migration defects. We also sometimes observe defects in nuclear migration only (*unc-83(RNAi)* S.G. unpublished observation), though not always (*arx-2(RNAi)* induces cell outgrowth defects as well, unpublished observation) and therefore the utse can be used as a model to determine specificity of nuclear migration defects.

RNAi against several *C. elegans* importins (*ima-1, ima-2, ima-3, imb-2, imb-3)* also cause utse defects (Table 1). Importins mediate nuclear transport. Importin α and β bind to proteins containing a nuclear localization sequence (NLS) and shuttle these proteins from the cytoplasm to the nucleus (Görlich and Kutay, 1999). The *ima* genes encode the importin α subunit and the *imb* genes encode the importin β subunit (Geles and Adam, 2001). Importins play a variety of roles in *C. elegans* development. IMA-1 localizes to the P0 germline (Geles and Adam, worm meeting abstract 1999).

IMA-3 is required for the progression of meiotic prophase I during oocyte development (Geles and Adam, 2001). IMA-2 is required for chromosomal dynamics in the germ line and early embryonic mitosis and nuclear envelope assembly (Geles et al., 2002). IMA-2 and IMB-1 also aid in embryonic mitotic spindle formation by interacting with the RanGAP *ran-2* and its guanine nucleotide exchange factor for RCC-1 (*ran-3)* (*ran-2* and *ran-3* were hits from our screen, Table 1) (Askjaer et al., 2002). IMB-2 shares sequence homology with human TNPO1 (Transportin-1) and is necessary for localization and activation of the forkhead transcription factor *daf-16* (another hit from our screen, Table 1) in L1 nuclei (Putker et al., 2013). IMB-3 shares sequence homology with yeast importin/karyopherin-beta3, which functions with RanGTPases to regulate nuclear import of ribosomal proteins (Yaseen and Blobel, 1997).

Since the *C. elegans* utse is a syncytium it is not surprising that the activity of these importins are necessary to mediate proper utse development. We hypothesize that importins transport factors necessary for mediating nuclear migration and positioning. Since we have observed that knockdown of *daf-16* also affects utse development, the utse can also be used as a model to study the role of importins in transporting transcription factors into the nucleus.

5.4.3 Genes that encode structural components of cells

The utse changes its shape over time. Rearrangements of the ECM, or structural proteins that make up the outer portion of a cell, are necessary. We therefore were not surprised to see that eight genes encoding structural proteins, or proteins that associate with structural proteins, were present in our hits. The genes are *deb-1, fbl-1, frm-2, ina-1, pat-3, pxl-1, toca-1,* and *unc-70*. *toca-1* and *unc-70* have been described in the nuclear and neuronal genes sections of this work. The remaining genes are characterized below.

deb-1 encodes vinculin, which is a cytoskeletal protein that links integrins to the actin cytoskeleton (Barstead and Waterston, 1989). *deb-1* is expressed in the myoepithelial sheath of the hermaphrodite gonad and dense bodies of muscles (Ono et al., 2007; Mackinnon et al., 2002). *deb-1* acts with the β-integrin *pat-3* (found in our screen, Table 1) and the a serine/threonine kinase orthologous to human integrin-linked kinase *pat-4* to recruit actin to the dense bodies of muscles (Mackinnon et al., 2002). *deb-1* also acts with two other hits from our screen, paxillin *pxl-1* and the LIM domain-containing protein of the PINCH family *unc-97*, and its role interacting with those genes has been described in the neuronal and cell adhesion sections. Since *deb-1* acts with three

other genes that from our screen, we believe that these interactions may have led us to discover an additional pathway involved in utse development.

fbl-1 encodes fibulin, a basement membrane glycoprotein necessary for distal tip cell migration (DTC) (Barth et al., 1998; Hesselson et al., 2004). *fbl-1* acts antagonistically with the ADAMS metalloprotease *gon-1* to control gonadal shape. *gon-1* promotes elongation through its expression in the gonad, and the fibulin keeps gonad migration on track since it is present in the ECM and the edge of the DTC (Hesselson et al., 2004). This is particularly interesting because we have identified metalloprotease involvement in utse development (three astacin metalloproteases, *nas-21, nas-22,* and *toh-1,* Ghosh et al., in prep) and fibulin may be interacting with astacin metalloproteases within the utse.

frm-2 encodes an ortholog of human FERM domain containing 6 protein and contains an ERM domain (Wormbase, INTERPRO:IPR000798). The ERM domain, or Ezrin/radixin/moesin-like domain, crosslinks the actin cytoskeleton with the plasma membrane (Tsukita et al., 1997). *frm-2* is expressed in the epithelial seam cells and utse (McKay et al., 2003).

Two *C. elegans* integrins were positive hits from our screen: the α integrin *ina-1* and its corresponding β integrin *pat-3* (Baum and Garriga, 1997). Integrins are surface receptors of the basement membrane (Harburger and Calderwood, 2009). The *ina-1/pat-3* complex is necessary for creating a breach in the basement membrane through which the anchor cell (AC) invases into vulval epithelium (Ihara et al., 2011). This is the same basement membrane that lies ventral to the utse, and we believe that pat-3/ina-1 may act on the utse by either degrading the underlying basement membrane or providing guidance cues for outgrowth (see below for ina-1/pat-3's role in generating guidance cues).

ina-1/pat-3 activity is also required for migrations of the CAN, ALM, and HSN neurons, axon fasciculation, distal tip cell migration, embryonic cell corpse removal, and localization of cell cycle proteins in the hypodermis (Baum and Garriga, 1997; Meighan and Schwarzbauer, 2007; Hsieh et al., 2012; Kihira et al., 2012).

pat-3 also associates with another alpha integrin -- *pat-2. pat-2/pat-3* is involved in muscle cell organization and muscle attachment (Lee et al., 2001; Rogalski et al., 2000; Etheridge et al., 2012).

pxl-1 encodes paxilin, a signal transduction adaptor protein that links integrin to focal adhesions (Warner et al., 2011; Turner et al., 1990). *pxl-1* localizes to the pharyngeal muscle and is necessary for pharyngeal muscle contractions (Warner et al., 2011). *pxl-1* also localizes to the dense bodies, adhesion plaques, and M-lines in body wall muscle and binds with *deb-1* (which was characterized earlier in this section) *in vitro*.

5.4.4 Homeodomain genes

Eight genes from our list contain homeodomains. The genes are *lin-11, ttx-3, lin-39, vab-3, zag-1, zfh-2,* and *zfp-1* (Table 1). For the descriptions of l*in-11, ttx-3, lin-39, vab-3, zag-1,* and *zfp-1* see neuronal genes section. *zfh-2* has been described in the transcription factor section.

Interestingly, two of the genes encoding homeodomain proteins posses LIM homeodomains (*lin-11* and *ttx-3*). Proteins that contain LIM domains are known to associate with LIM homeodomain proteins. We found an additional two hits that contained LIM domains, *unc-97* and *lim-9*. Both are members of the LIM PINCH family (Hobert et al., 1999; Qadota et al., 2007) and are described in the cell adhesion and cell signaling sections of this work.

5.4.5 Cell adhesion genes

Seven of the hits from our list were genes involved in cell adhesion. The genes are *ina-1, pat-3, ncam-1, pxl-1, unc-33, unc-70,* and *unc-97*. The integrins *ina-1* and *pat-3* have been described in the structural components section. *ncam-1, unc-33,* and *unc-70* are involved in adhesion activities necessary for neuronal outgrowth and have been discussed in the neuronal genes section. *pxl-1* was discussed in the cell structure section. *unc-97* is characterized below.

Aside from regulating mechanosensory responses, *unc-97* is necessary for the assembly of adhesion complexes in *C. elegans* body wall muscle (Hobert et al., 1999; Norman et al., 2007). *unc-97* regulates levels of the ECM proteins perlecan (*unc-52*) , vinculin (*deb-1),* and β-integrin (*pat-3)* (Hobert et al., 1999; Norman et al., 2007). In *unc-97* mutants, integrin and vinculin fail to organize properly at the basement membrane, preventing proper myosin organization within musculature. Interestingly *unc-52*, *pat-3,* and *deb-1* are necessary for proper utse development (Table 1, Ghosh et al., in prep). *unc-97* is also expressed in the vulval muscles (specifically sites in which vulval muscle attaches to the hypodermis) (Hobert et al., 1999). Genes expressed in vulval muscles are

necessary for utse development (Ghosh and Sternberg, 2014), and therefore *unc-97* may be acting through the vulval muscles to regulate levels of ECM proteins and promote adhesion between the utse and the uterine epithelium during outgrowth.

During its development, the utse grows outwards along the basement membrane of the ventral uterine epithelium (Newman et al., 1996 ; Ghosh and Sternberg, 2014). This adhesion behavior is mediated by a variety of genes, some of which we have characterized in our previous work (Ghosh and Sternberg, 2014); however, we believe that the seven genes described above play additional roles in utse outgrowth. Study of these genes will lead to a clearer and more complete understanding of the molecular inputs necessary to mediate adhesion behavior of the growing utse.

5.4.6 Transcription factors

Our screen has five hits that were primarily characterized as transcription factors. These transcription factors are as follows: *daf-16,* e*gl-13, lin-11, lin-31,* and *zfh-2*. We have already described three of these transcription factors in previous sections (*daf-16* in the nuclear and neuronal genes section and *egl-13* and *lin-11* in the neuronal genes section). The remaining two transcription factors are discussed below.

lin-31 is a forkhead transcription factor involved in vulva development (Miller et al., 1993). *lin-31* is secifies the Pn.p vulval precursor cells and acts downstream of the ras homolog *let-60*. *mpk-1* phosphorylates *lin-31,* which disrupts a complex with *lin-1* and promotes primary fate of P6.p (Tan et al., 1998). Since *lin-31* is necessary for specifying primary vulval fates, RNAi against *lin-31* may be affecting vulva development, and disrupting the vulva induces secondary effects on utse development.

zfh-2 is a homeobox protein expressed in the vulval muscles (Reece-Hoyes et al., 2007). *zfh-2* regulates lifespan (Walter et al., 2011). Genes expressed in vulval muscles can affect utse development (Ghosh and Sternberg, 2014) and therefore *zfh-2* may be controlling utse development by acting through this tissue.

5.4.7 Intracellular transport genes

Four of the genes from our list affect intracellular transport. The genes are *sec-15, rrc-1, amph-1,* and *f55c12.1.*

sec-15 encodes a component of the exocyst complex, a protein complex that directs vesicles from the Golgi complex to the plasma membrane and tethers said vesicles to the plasma membrane prior to fusion (Wu et al., 2005; Winter et al., 2012; Zhang et al., 2004). *sec-15* is necessary for the distribution of *rab-11* positive vesicles in the *C. elegans* intestine (Zhang et al., 2004; Chen et al, 2014). *rab-11.1* is necessary for utse development (Ghosh and Sternberg, 2014) and therefore *sec-15* may be acting with *rab-11.1* to contribute to utse development.

rrc-1 is a RhoGAP, which activates the RhoGTPases *rac-1* and *cdc-42* (Delawary et al., 2007). *rrc-1* is expressed in the coelomocytes, excretory cell, GLR cells, and utse. RhoGTPases regulate intracelleular signals necessary for organization of the actin cytoskeleton (Hall, 1998), and therefore *rrc-1* may be acting in the utse by regulating actin cytoskeleton organization.

amph-1 is the the ortholog of human bridging integrator 2 and localizes to the recycling endosome (Pant et al., 2009). *amph-1* colocalizes with *rme-1* (receptor mediated endocytosis/Eps15 homology-domain containing 1) in the recycling endosome and *amph-1* null mutants are defective in recycling cargo between the plasma membrane and early endosome.

f55c12.1, also known as *rfip-1*, encodes the RAB-11 effector NUF (Winter et al., 2012). Loss of *f55c12.1* causes defects in recycling endosome and late endosome positiong. As mentioned earlier, we have shown that *rab-11.1* is involved in utse development (Ghosh and Sternberg, 2014), and therefore *f55c12.1* may act through rab-11.1 to affect utse development.

Mediating cell transport is an important aspect of utse behavior. In our previous work we have shown that six RabGTPases and one divergent Rab (*rsef-1)* are necessary for utse development (Ghosh and Sternberg, 2014). Though we have not yet identified the cargo being transported between the utse and its environment, further study of the hits in this section could shed light on how intracellular transport occurs within the utse.

5.4.8 Genes involved in signaling pathways

Three genes were involved in cell-cell signaling or were part of characterized signaling pathways. The genes are as follows: *cwn-1, glp-1,* and *lim-9. cwn-1* has been describedin the neuronal genes section of this work, and we discuss the remaining two genes below.

glp-1 encodes a Notch receptor necessary for germ cell proliferation, specifying the distal tip cell and vulval cells, and promoting cell-cell interactions between pharyngeal precursor cells, while maintaining polarity within the embryo (Roehl et al., 1996; Austin and Kimble, 1987; Priess et al., 1987; Crittenden et al., 1997; Berry et al., 1997). *glp-1* exhibits specificity by interacting with different Delta ligands in different tissues, such as *lag-2* in the germ cells and *apx-1* in the embryo (Henderson et al., 1994; Gao and Kimble; 1995).

lim-9 is a LIM domain protein that is part of the non-canonical Wnt pathway (planar cell polarity pathway) necessary for asymmetric division of the male specific blast cell (B cell) (Qadota et al., 2007; Wu and Herman, 2006). *lim-9* is expressed in the pharyngeal and body wall muscles, neurons, vulva, spermatheca, anal sphincter and depressor muscles, gonadal sheath, and the excretory canal (Qadota et al., 2007).

Results from our screen show that several classical development pathways are involved in utse development, including Notch/Delta and Wnt, and therefore the utse can be used as a model system to better understand how these pathways regulate *C. elegans* development.

5.4.9 Additional genes

F11A10.5 is a homolog of isoform 2 of Suppressor of tumorigenicity 7 (Wormbase). *F11A10.5* is expressed in the pharynx, intestine, and body wall muscle (McKay et al., 2003; Hunt-Newbury et al., 2007).

glb-12 is a globin (Hoogewijs et al., 2004; Hoogewijs et al., 2007). *glb-12* is expressed in the utse (Dehenau personal communication), and is an active inhibitor of germline apoptosis through modulating levels of reactive oxygen (Dehenau et al., 2013, International Worm Meeting abstract). *glb-12* is also necessary for vulva development (*glb-12(RNAi)* causes a protruding vulva phenotype) (Dehenau et al., 2011, International Worm Meeting abstract).

pqn-85 (also known as *scc-2*) is the ortholog of the yeast SCC-2 protein, which is involved in sister chromatid cohesion (van Haaften et al., 2006; Ciosk et al., 2000). *pqn-85* localizes to binding sites of condensin on the X chromosome (Kranz et al., 2013) and processes DNA double-strand breaks during meiotic recombination in the germ cells (Lightfoot et al., 2011). *pqn-85* also acts with guidance factor *mau-2* to regulate chromosome segregation in *C. elegans* embryos (Seitan et al., 2006).

5.4.10 Conclusions

In this work we have described the functions of 54 genes whose knockdown cause utse defects. We hope that the results from this screen will highlight the endless possibilities of using the *C. elegans* utse as a model for studying a variety of behaviors and pathways.

5.5 Acknowledgements

We thank Matthew Buechner (University of Kansas) and David Sherwood (Duke University) for worm strains; Barbara Perry and Gladys Medina for technical assistance; Mihoko Kato for critically reading the manuscript and Wendy Hanna-Rose, Marianne Bronner, Bruce Hay, and David Chan for helpful discussions. S.G. was supported by National Institutes of Health USPHS training grant GM07616. This work was supported by the Howard Hughes Medical Institute, with which P.W.S. is an investigator.

References

Ahringer, J., ed. 2006. Reverse genetics, WormBook, ed. The C. elegans Research Community, WormBook, doi/10.1895/wormbook.1.47.1, http://www.wormbook.org.

Askjaer, P., Galy, V., Hannak, E., Mattaj, I.W. 2002. Ran GTPase cycle and importins alpha and beta are essential for spindle formation and nuclear envelope assembly in living Caenorhabditis elegans embryos. Mol Biol Cell.; **13**(12):4355-70.

Austin J1 and Kimble J. 1987. glp-1 is required in the germ line for regulation of the decision between mitosis and meiosis in C. elegans. Cell.; **51**(4):589-99.

Avgousti, D.C., Cecere, G., Grishok, A. 2012. The conserved PHD1-PHD2 domain of ZFP-1/AF10 is a discrete functional module essential for viability in Caenorhabditis elegans. Mol Cell Biol.; **33**(5):999-1015.

Barstead RJ1 and Waterston RH. The basal component of the nematode dense-body is vinculin. J Biol Chem.; **264**(17):10177-85.

Barth, J.L., Argraves, K.M., Roark, E.F., Little, C.D., Argraves, W.S. 1998. Identification of chicken and C. elegans fibulin-1 homologs and characterization of the C. elegans fibulin-1 gene. Matrix Biol.; **17**(8-9):635-46.

Baum, P.D. and Garriga, G. 1997. Neuronal migrations and axon fasciculation are disrupted in ina-1 integrin mutants. Neuron.; **19**(1):51-62.

Berry, L.W., Westlund, B., Schedl, T. 1997. Germ-line tumor formation caused by activation of glp-1, a Caenorhabditis elegans member of the Notch family of receptors. Development.; **124**(4):925-36.

Bone, C.R., Tapley, E.C., Gorjánácz, M., Starr, D.A. 2014. The Caenorhabditis elegans SUN protein UNC-84 interacts with lamin to transfer forces from the cytoplasm to the nucleoskeleton during nuclear migration. Mol Biol Cell.; **25**(18):2853-65.

Brenner, S. 1974. The genetics of Caenorhabditis elegans. Genetics.; **77**(1):71-94.

Byerly, L., Russell, R. L., Cassada, R. C. 1976. The life cycle of the nematode Caenorhabditis elegans. I. Wild-type growth and reproduction. Dev Biol, **51**, 23-33.

Cecere, G., Hoersch, S., Jensen, M.B., Dixit, S., Grishok, A. 2013. The ZFP-1(AF10)/DOT-1 complex opposes H2B ubiquitination to reduce Pol II transcription. Mol Cell.; **50**(6):894-907.

Chang, Y.T., Dranow, D., Kuhn, J., Meyerzon, M., Ngo, M., Ratner, D., Warltier, K., Starr, D.A. 2013. toca-1 is in a novel pathway that functions in parallel with a SUN-KASH nuclear envelope bridge to move nuclei in Caenorhabditis elegans. Genetics.; **193**(1):187-200.

Chaplin, T., Ayton, P., Bernard, O.A., Saha, V., Della Valle, V., Hillion, J., Gregorini, A., Lillington, D., Berger, R., Young, B.D. 1995. A novel class of zinc finger/leucine zipper genes identified from the molecular cloning of the t(10;11) translocation in acute leukemia. Blood; **85**(6):1435-41.

Chen, L., Ong, B., Bennett, V. 2001. LAD-1, the Caenorhabditis elegans L1CAM homologue, participates in embryonic and gonadal morphogenesis and is a substrate for fibroblast growth factor receptor pathway-dependent phosphotyrosine-based signaling. J Cell Biol.; **154**(4):841-55.

Chen, S., Li, L., Li, J., Liu, B., Zhu, X., Zheng, L., Zhang, R., Xu, T. 2014. SEC-10 and RAB-10 coordinate basolateral recycling of clathrin-independent cargo through endosomal tubules in Caenorhabditis elegans. Proc Natl Acad Sci U S A.; **111**(43):15432-7.

Chisholm, A.D. and Horvitz, H.R. 1995. Patterning of the Caenorhabditis elegans head region by the Pax-6 family member vab-3. Nature.; **377**(6544):52-5.

Cinar, H.N., Richards, K.L., Oommen, K.S., Newman, A.P. 2003. The EGL-13 SOX domain transcription factor affects the uterine pi cell lineages in Caenorhabditis elegans. Genetics. **165**, 1623-1628.

Ciosk, R., Shirayama, M., Shevchenko, A., Tanaka, T., Toth, A., Shevchenko, A., Nasmyth, K. 2000. Cohesin's binding to chromosomes depends on a separate complex consisting of Scc2 and Scc4 proteins. Mol Cell.; **5**(2):243-54.

Clark, S.G., Chisholm, A.D., Horvitz, H.R. 1993. Control of cell fates in the central body region of C. elegans by the homeobox gene lin-39. Cell.; **74**(1):43-55.

Clark, S.G. and Chiu, C. 2003. C. elegans ZAG-1, a Zn-finger-homeodomain protein, regulates axonal development and neuronal differentiation. Development.; **130**(16):3781-94.

Cox, E.A. and Hardin, J. 2004. Sticky worms: adhesion complexes in C. elegans. J Cell Sci.; **117**(Pt 10):1885-97.

Crittenden, S.L., Rudel, D., Binder, J., Evans, T.C., Kimble, J. 1997. Genes required for GLP-1 asymmetry in the early Caenorhabditis elegans embryo. Dev Biol.; **181**(1):36-46.

Delawary, M., Nakazawa, T., Tezuka, T., Sawa, M., Iino, Y., Takenawa, T., Yamamoto, T. 2007. Molecular characterization of a novel RhoGAP, RRC-1 of the nematode Caenorhabditis elegans. Biochem Biophys Res Commun.1; **357**(2):377-82.

Ding, Y.H., Du, Y.G., Luo, S., Li, Y.X., Li, T.M., Yoshina, S., Wang, X., Klage, K., Mitani, S., Ye, K., Dong, M.Q. 2013. Characterization of PUD-1 and PUD-2, two proteins up-regulated in a long-lived daf-2 mutant. PLoS One.; **8**(6):e67158

Etheridge, T., Oczypok, E.A., Lehmann, S., Fields, B.D., Shephard, F., Jacobson, L.A., Szewczyk, N.J. 2012. Calpains mediate integrin attachment complex maintenance of adult muscle in Caenorhabditis elegans. PLoS Genet.; **8**(1):e1002471.

Feng, G., Yi, P., Yang, Y., Chai, Y., Tian, D., Zhu, Z., Liu, J., Zhou, F., Cheng, Z., Wang, X., Li, W., Ou, G. 2013. Developmental stage-dependent transcriptional regulatory pathways control neuroblast lineage progression. Development.; **140**(18):3838-47.

Fernández-Chacón R1, Königstorfer A, Gerber SH, García J, Matos MF, Stevens CF, Brose N, Rizo J, Rosenmund C, Südhof TC. 2001. Synaptotagmin I functions as a calcium regulator of release probability. Nature.; **410**(6824):41-9.

Fire, A., Xu, S., Montgomery, M.K., Kostas, S.A., Driver, S.E., and Mello, C.C. 1998. Potent and specific genetic interference by double-stranded RNA in Caenorhabditis elegans. Nature **391**, 806–811

Fridolfsson, H.N., Ly, N., Meyerzon, M., Starr, D.A. 2010. UNC-83 coordinates kinesin-1 and dynein activities at the nuclear envelope during nuclear migration. Dev Biol.; **338**(2):237-50.

Gao, D. and Kimble, J. 1995. APX-1 can substitute for its homolog LAG-2 to direct cell interactions throughout Caenorhabditis elegans development. Proc Natl Acad Sci U S A.; **92**(21):9839-42.

Geles, K.G. and Adam, S.A. 2001. Germline and developmental roles of the nuclear transport

factor importin alpha3 in C. elegans. Development.; **128**(10):1817-30.

Geles, K.G., Johnson, J.J., Jong, S., Adam, S.A. 2002. A role for Caenorhabditis elegans importin IMA-2 in germ line and embryonic mitosis. Mol Biol Cell. ; **13**(9):3138-47.

Ghosh, S. and Sternberg, P.W. 2014. Spatial and molecular cues for cell outgrowth during C. elegans uterine development. Dev Biol.; **396**(1):121-35.

Ghosh, S., Nguyen, S. and Sternberg, P.W. An ECM protease/inhibitor network regulates cell outgrowth, in prep.

Giuliani, C., Troglio, F., Bai, Z., Patel, F.B., Zucconi, A., Malabarba, M.G., Disanza, A., Stradal, T.B., Cassata, G., Confalonieri, S., Hardin, J.D., Soto, M.C., Grant, B.D., Scita, G. 2009. Requirements for F-BAR proteins TOCA-1 and TOCA-2 in actin dynamics and membrane trafficking during Caenorhabditis elegans oocyte growth and embryonic epidermal morphogenesis. PLoS Genet.; **5**(10):e1000675.

Görlich, D. and Kutay, U. 1999. Transport between the cell nucleus and the cytoplasm. Annu Rev Cell Dev Biol.; **15**:607-60.

Gramstrup Petersen, J., Rojo Romanos, T., Juozaityte, V., Redo Riveiro, A., Hums, I., Traunmüller, L., Zimmer, M., Pocock, R. 2013. EGL-13/SoxD specifies distinct O2 and CO2 sensory neuron fates in Caenorhabditis elegans. PLoS Genet.; **9**(5):e1003511.

Grishok, A. 2012. Endogenous RNAi and adaptation to environment in C. elegans. Worm.; **1**(2):129-33.

Hall, A. 1998. Rho GTPases and the actin cytoskeleton. Science.; **279**(5350):509-14.

Hamamichi, S., Rivas, R.N., Knight, A.L., Cao, S., Caldwell, K.A., Caldwell, G.A. 2008. Hypothesis-based RNAi screening identifies neuroprotective genes in a Parkinson's disease model. Proc Natl Acad Sci U S A.; **105**(2):728-33.

Hamilton, B., Dong, Y., Shindo, M., Liu, W., Odell, I., Ruvkun, G., Lee, S.S. 2005. A systematic RNAi screen for longevity genes in C. elegans. Genes Dev.; **19**(13):1544-55.

Hammarlund, M., Davis, W.S., Jorgensen, E.M. 2000. Mutations in beta-spectrin disrupt axon outgrowth and sarcomere structure. J Cell Biol.; **149**(4):931-42.

Hanna-Rose, W. and Han, M. 1999. COG-2, a sox domain protein necessary for establishing a functional vulval-uterine connection in Caenorhabditis elegans. Development. **126**, 169-179.

Harburger, D.S. and Calderwood, DA. 2009. Integrin signalling at a glance. J Cell Sci. 2009 Jan 15; **122**(Pt 2):159-63.

Hedgecock, E.M. and Thomson, J.N. 1982. A gene required for nuclear and mitochondrial attachment in the nematode Caenorhabditis elegans. Cell.; **30**(1):321-30.

Henau, S. D., Tilleman, L., Hoogewijs, D., Moens, L., Dewilde, S., Vanfleteren, J. R., &

Braeckman, B. P. 2011. Caenorhabditis elegans' GLB-12 regulates germline apoptosis levels and vulval development presented in International Worm Meeting

Henau, S. D., Tilleman, L., Pauwels, M., Pesce, A., Nardini, M., Bolognesi, M., Wael, K. D., Moens, L., Dewilde, S., & Braeckman, B. P. 2013. A Redox Signaling Globin Regulates Germ Cell Apoptosis in Caenorhabditis elegans presented in International Worm Meeting.

Henderson, S.T., Gao, D., Lambie, E.J., Kimble, J. 1994. lag-2 may encode a signaling ligand for the GLP-1 and LIN-12 receptors of C. elegans. Development.; **120**(10):2913-24.

Hesselson, D., Newman, C., Kim, K.W., Kimble, J. 2004. GON-1 and fibulin have antagonistic roles in control of organ shape. Curr Biol.; 14(22):2005-10.

Hiatt, S.M., Duren, H.M., Shyu, Y.J., Ellis, R.E., Hisamoto, N., Matsumoto, K., Kariya, K., Kerppola, T.K., Hu, C.D. 2009. Caenorhabditis elegans FOS-1 and JUN-1 regulate plc-1 expression in the spermatheca to control ovulation. Mol Biol Cell.; **20**(17):3888-95.

Hilliard, M.A. and Bargmann, C.I. 2006. Wnt signals and frizzled activity orient anterior-posterior axon outgrowth in C. elegans. Dev Cell.; **10**(3):379-90.

Hobert, O., Mori, I., Yamashita, Y., Honda, H., Ohshima, Y., Liu, Y., Ruvkun, G. 1997. Regulation of interneuron function in the C. elegans thermoregulatory pathway by the ttx-3 LIM homeobox gene. Neuron.; **19**(2):345-57.

Hobert, O., D'Alberti, T., Liu, Y., Ruvkun, G. 1998. Control of neural development and function in a thermoregulatory network by the LIM homeobox gene lin-11. J Neurosci.; **18**(6):2084-96.

Hobert, O., Moerman, D.G., Clark, K.A., Beckerle, M.C., Ruvkun, G. 1999. A conserved LIM protein that affects muscular adherens junction integrity and mechanosensory function in Caenorhabditis elegans. J Cell Biol.; **144**(1):45-57.

Hoogewijs, D., Geuens, E., Dewilde S, Moens L, Vierstraete A, Vinogradov S, Vanfleteren J. 2004. Genome-wide analysis of the globin gene family of C. elegans. IUBMB Life.; **56**(11-12):697-702.

Hoogewijs, D., Geuens, E., Dewilde, S., Vierstraete, A., Moens, L., Vinogradov, S., Vanfleteren, J.R. 2007. Wide diversity in structure and expression profiles among members of the Caenorhabditis elegans globin protein family. BMC Genomics.; **8**:356.

Hsieh, H.H., Hsu, T.Y., Jiang, H.S., Wu, Y.C. 2012. Integrin α PAT-2/CDC-42 signaling is required for muscle-mediated clearance of apoptotic cells in Caenorhabditis elegans. PLoS Genet. **2012**;8(5):e1002663.

Hunt-Newbury, R., Viveiros, R., Johnsen, R., Mah, A., Anastas, D., Fang, L., Halfnight, E., Lee, D., Lin, J., Lorch, A., McKay, S., Okada, H.M., Pan, J., Schulz, A.K., Tu, D., Wong, K., Zhao, Z., Alexeyenko, A., Burglin, T., Sonnhammer, E., Schnabel, R., Jones, S.J., Marra, M.A., Baillie, D.L., Moerman, D.G. 2007. High-throughput in vivo analysis of gene expression in Caenorhabditis elegans. PLoS Biol.; **5**(9):e237.

Hutter, H. 2003. Extracellular cues and pioneers act together to guide axons in the ventral cord of C. elegans. Development.; **130**(22):5307-18.

Ihara, S., Hagedorn, E.J., Morrissey, M.A., Chi, Q., Motegi, F., Kramer, J.M., Sherwood, D.R. 2011. Basement membrane sliding and targeted adhesion remodels tissue boundaries during uterine-vulval attachment in Caenorhabditis elegans. Nat Cell Biol.; **13**(6):641-51.

Iwasa, H., Yu, S., Xue, J., Driscoll, M. 2010. Novel EGF pathway regulators modulate C. elegans healthspan and lifespan via EGF receptor, PLC-gamma, and IP3R activation. Aging Cell.; **9**(4):490-505. doi: 10.1111/j.1474-9726.2010.00575.x. Epub 2010 May 22.

Johnson, R.W. and Chamberlin, H.M. 2008. Positive and negative regulatory inputs restrict pax-6/vab-3 transcription to sensory organ precursors in Caenorhabditis elegans. Mech Dev; **125**(5-6):486-97.

Kennedy, L.M. and Grishok, A. 2014. Neuronal migration is regulated by endogenous RNAi and chromatin-binding factor ZFP-1/AF10 in Caenorhabditis elegans. Genetics.; **197**(1):207-20.

Kihira, S., Yu, E.J., Cunningham, J., Cram, E.J., Lee, M. 2012. A novel mutation in β integrin reveals an integrin-mediated interaction between the extracellular matrix and cki-1/p27KIP1. PLoS One.; **7**(8):e42425.

Kranz, A.L., Jiao, C.Y., Winterkorn, L.H., Albritton, S.E., Kramer, M., Ercan, S. 2013. Genome-wide analysis of condensin binding in Caenorhabditis elegans. Genome Biol.; **14**(10):R112.

Krieg, M., Dunn, A.R., Goodman, M.B. 2014. Mechanical control of the sense of touch by β-spectrin. Nat Cell Biol.; **16**(3):224-33.

Lee, M., Cram, E.J., Shen, B., Schwarzbauer, J.E. 2001. Roles for beta(pat-3) integrins in development and function of Caenorhabditis elegans muscles and gonads. J Biol Chem.; **276**(39):36404-10.

Li, W., Herman, R.K., Shaw, J.E. 1992. Analysis of the Caenorhabditis elegans axonal guidance and outgrowth gene unc-33. Genetics.; **132**(3):675-89.

Lightfoot, J., Testori, S., Barroso, C., Martinez-Perez, E. 2011. Loading of meiotic cohesin by SCC-2 is required for early processing of DSBs and for the DNA damage checkpoint. Curr Biol.; **21**(17):1421-30. doi: 10.1016/j.cub.2011.07.007.

Locke, C.J., Williams, S.N., Schwarz, E.M., Caldwell, G.A., Caldwell, K.A. 2006. Genetic interactions among cortical malformation genes that influence susceptibility to convulsions in C. elegans. Brain Res.;1120(1):23-34. Epub 2006 Sep 22.

Mackinnon, A.C., Qadota, H., Norman, K.R., Moerman, D.G., Williams, B.D. 2002. C. elegans PAT-4/ILK functions as an adaptor protein within integrin adhesion complexes. Curr Biol.; **12**(10):787-97.

Malnic, B., Godfrey, P.A., Buck, L.B. 2004. The human olfactory receptor gene family. Proc Natl

Acad Sci U S A.; **101**(8):2584-9.

Malone, C.J., Fixsen, W.D., Horvitz, H.R., Han, M. 1999. UNC-84 localizes to the nuclear envelope and is required for nuclear migration and anchoring during C. elegans development. Development; **126**(14):3171-81.

Maniar, T.A., Kaplan, M., Wang, G.J., Shen, K., Wei, L., Shaw, J.E., Koushika, S.P., Bargmann, C.I. 2011. UNC-33 (CRMP) and ankyrin organize microtubules and localize kinesin to polarize axon-dendrite sorting. Nat Neurosci.; **15**(1):48-56. doi: 10.1038/nn.2970.

Mansisidor, A.R., Cecere, G., Hoersch, S., Jensen, M.B., Kawli, T., Kennedy, L.M., Chavez, V., Tan, M.W., Lieb, J.D., Grishok, A. 2011. A conserved PHD finger protein and endogenous RNAi modulate insulin signaling in Caenorhabditis elegans. PLoS Genet.; **7**(9):e1002299.

McKay, S.J., Johnsen, R., Khattra, J., Asano, J., Baillie, D.L., Chan, S., Dube, N., Fang, L., Goszczynski, B., Ha, E., Halfnight, E., Hollebakken, R., Huang, P., Hung, K., Jensen, V., Jones, S.J., Kai, H., Li, D., Mah, A., Marra, M., McGhee, J., Newbury, R., Pouzyrev, A., Riddle, D.L., Sonnhammer, E., Tian, H., Tu, D., Tyson, J.R., Vatcher, G., Warner, A., Wong, K., Zhao, Z., Moerman, D.G. 2003. Gene expression profiling of cells, tissues, and developmental stages of the nematode C. elegans. Cold Spring Harb Symp Quant Biol.; **68**:159-69.

Meighan CM1 and Schwarzbauer JE. 2007. Control of C. elegans hermaphrodite gonad size and shape by vab-3/Pax6-mediated regulation of integrin receptors. Genes Dev.; **21**(13):1615-20.

Miller, L.M., Gallegos, M.E., Morisseau, B.A., Kim, S.K. 1993. lin-31, a Caenorhabditis elegans HNF-3/fork head transcription factor homolog, specifies three alternative cell fates in vulval development. Genes Dev.; **7**(6):933-47.

Minor, P.J., He, T.F., Sohn, C.H., Asthagiri, A.R., Sternberg, P.W. 2013. FGF signaling regulates Wnt ligand expression to control vulval cell lineage polarity in C. elegans. Development.; **140**(18):3882-91.

Moorthy, S., Chen, L., Bennett, V. 2000. Caenorhabditis elegans beta-G spectrin is dispensable for establishment of epithelial polarity, but essential for muscular and neuronal function. J Cell Biol.; **149**(4):915-30.

Newman, A.P., White, J.G., Sternberg, P.W. 1996. Morphogenesis of the C. elegans hermaphrodite uterus. Development.; **122**(11):3617-26.

Newman, A.P., Acton, G.Z., Hartwieg, E., Horvitz, H.R., Sternberg, P.W. 1999. The lin-11 LIM domain transcription factor is necessary for morphogenesis of C. elegans uterine cells. Development. 126, 5319-5326.

Norman, K.R., Cordes, S., Qadota, H., Rahmani, P., Moerman, D.G. 2007. UNC-97/PINCH is involved in the assembly of integrin cell adhesion complexes in Caenorhabditis elegans body wall muscle. Dev Biol.; **309**(1):45-55.

Ono, K., Yu, R., Ono, S. 2007. Structural components of the nonstriated contractile apparatuses in the Caenorhabditis elegans gonadal myoepithelial sheath and their essential roles for ovulation. Dev

Dyn.; **236**(4):1093-105.

Pant, S., Sharma, M., Patel, K., Caplan, S., Carr, C.M., Grant, B.D. 2009. AMPH-1/Amphiphysin/Bin1 functions with RME-1/Ehd1 in endocytic recycling.;**11**(12):1399-410.

Park EC and Horvitz HR. 1986. Mutations with dominant effects on the behavior and morphology of the nematode Caenorhabditis elegans. Genetics.; **113**(4):821-52.

Patel, F.B., Bernadskaya, Y.Y., Chen, E., Jobanputra, A., Pooladi, Z., Freeman, K.L., Gally, C., Mohler, W.A., Soto, M.C. 2008. The WAVE/SCAR complex promotes polarized cell movements and actin enrichment in epithelia during C. elegans embryogenesis. Dev Biol.; **324**(2):297-309.

Poinat, P., De Arcangelis, A., Sookhareea, S., Zhu, X., Hedgecock, E.M., Labouesse, M., Georges-Labouesse, E. 2002. A conserved interaction between beta1 integrin/PAT-3 and Nck-interacting kinase/MIG-15 that mediates commissural axon navigation in C. elegans. Curr Biol.; **12**(8):622-31.

Priess JR1, Schnabel H, Schnabel R. 1987. The glp-1 locus and cellular interactions in early C. elegans embryos. Cell.; **51**(4):601-11.

Putker, M., Madl, T., Vos, H.R., de Ruiter, H., Visscher, M., van den Berg, M.C., Kaplan, M., Korswagen, H.C., Boelens, R., Vermeulen, M., Burgering, B.M., Dansen, T.B. 2013. Redox-dependent control of FOXO/DAF-16 by transportin-1. Mol Cell.; **49**(4):730-42.

Qadota, H., Mercer, K.B., Miller, R.K., Kaibuchi, K., Benian, G.M. 2007. Two LIM domain proteins and UNC-96 link UNC-97/pinch to myosin thick filaments in Caenorhabditis elegans muscle. Mol Biol Cell.; **18**(11):4317-26.

Reece-Hoyes JS1, Shingles J, Dupuy D, Grove CA, Walhout AJ, Vidal M, Hope IA. 2007. Insight into transcription factor gene duplication from Caenorhabditis elegans Promoterome-driven expression patterns. BMC Genomics.; **8**:27.

Remy, J.J. and Hobert, O. 2005. An interneuronal chemoreceptor required for olfactory imprinting in C. elegans. Science.; **309**(5735):787-90.

Roehl, H., Bosenberg, M., Blelloch, R., Kimble, J. 1996. Roles of the RAM and ANK domains in signaling by the C. elegans GLP-1 receptor. EMBO J.; **15**(24):7002-12.

Rogalski, T.M., Mullen, G.P., Gilbert, M.M., Williams, B.D., Moerman, D.G. 2000. The UNC-112 gene in Caenorhabditis elegans encodes a novel component of cell-matrix adhesion structures required for integrin localization in the muscle cell membrane.
J Cell Biol.; **150**(1):253-64.

Sarafi-Reinach, T.R., Melkman, T., Hobert, O., Sengupta, P. 2001. The lin-11 LIM homeobox gene specifies olfactory and chemosensory neuron fates in C. elegans. Development.; **128**(17):3269-81.

Sasakura, H., Inada, H., Kuhara, A., Fusaoka, E., Takemoto, D., Takeuchi, K., Mori, I. 2005.

Maintenance of neuronal positions in organized ganglia by SAX-7, a Caenorhabditis elegans homologue of L1. EMBO J.; **24**(7):1477-88.

Schwarz, E.M., Kato, M., Sternberg, P.W. 2012. Functional transcriptomics of a migrating cell in Caenorhabditis elegans. Proc Natl Acad Sci U S A; **109**(40):16246-51.

Schwarz, V., Pan, J., Voltmer-Irsch, S., Hutter, H. 2009. IgCAMs redundantly control axon navigation in Caenorhabditis elegans. Neural Dev; **4**:13.

Seitan, V.C., Banks, P., Laval, S., Majid, N.A., Dorsett, D., Rana, A., Smith, J., Bateman, A., Krpic, S., Hostert, A., Rollins, R.A., Erdjument-Bromage, H., Tempst, P., Benard, C.Y., Hekimi, S., Newbury, S.F., Strachan, T. 2006. Metazoan Scc4 homologs link sister chromatid cohesion to cell and axon migration guidance. PLoS Biol.; **4**(8):e242.

Sherwood, D.R., Butler, J.A., Kramer, J.M., Sternberg, P.W. 2005. FOS-1 promotes basement-membrane removal during anchor-cell invasion in C. elegans. Cell.; **121**(6):951-62.

Starr, D.A. and Han, M. 2003. ANChors away: an actin based mechanism of nuclear positioning. J Cell Sci.; **116**(Pt 2):211-6.

Starr, D.A., Hermann, G.J., Malone, C.J., Fixsen, W., Priess, J.R., Horvitz, H.R., Han, M. 2001. unc-83 encodes a novel component of the nuclear envelope and is essential for proper nuclear migration. Development.; **128**(24):5039-50.

Starr, D.A. and Han, M. 2002. Role of ANC-1 in tethering nuclei to the actin cytoskeleton. Science.; **298**(5592):406-9.

Sternberg, P.W., 2005. Vulval development, WormBook, ed. The C. elegans Research Community, WormBook, doi/10.1895/wormbook.1.6.1, http://www.wormbook.org.

Sulston, J.E., Schierenberg, E., White, J.G., Thomson, J.N. 1983. The embryonic cell lineage of the nematode Caenorhabditis elegans. Dev Biol.; **100**(1):64-119.

Takenawa, T. and Miki, H. 2001. WASP and WAVE family proteins: key molecules for rapid rearrangement of cortical actin filaments and cell movement. J Cell Sci.; **114**(Pt 10):1801-9.

Tan, P.B., Lackner, M.R., Kim, S.K. 1998. MAP kinase signaling specificity mediated by the LIN-1 Ets/LIN-31 WH transcription factor complex during C. elegans vulval induction. Cell.; **93**(4):569-80.

Tapley, E.C. and Starr, D.A. 2013. Connecting the nucleus to the cytoskeleton by SUN-KASH bridges across the nuclear envelope. Curr Opin Cell Biol.; **25**(1):57-62.

Timmons, L., and Fire, A. 1998. Specific interference by ingested dsRNA. Nature 395, 854.

Tsukita, S., Yonemura, S., Tsukita, S. 1997. ERM proteins: head-to-tail regulation of actin-plasma membrane interaction. Trends Biochem Sci.; **22**(2):53-8.

Turner, C.E., Glenney, J.R. Jr, Burridge, K. 1990. Paxillin: a new vinculin-binding protein

present in focal adhesions. J Cell Biol.; **111**(3):1059-68.

van Haaften, G., Romeijn, R., Pothof, J., Koole, W., Mullenders, L.H., Pastink, A., Plasterk, R.H., Tijsterman, M. 2006. Identification of conserved pathways of DNA-damage response and radiation protection by genome-wide RNAi. Curr Biol.; **16**(13):1344-50.

Wacker, I., Schwarz, V., Hedgecock, E.M., Hutter, H. 2003. zag-1, a Zn-finger homeodomain transcription factor controlling neuronal differentiation and axon outgrowth in C. elegans. Development.; **130**(16):3795-805.

Walker, D.S., Vázquez-Manrique, R.P., Gower, N.J., Gregory, E., Schafer, W.R., Baylis, H.A. 2009. Inositol 1,4,5-trisphosphate signalling regulates the avoidance response to nose touch in Caenorhabditis elegans. PLoS Genet.; **5**(9):e1000636.

Walter, L., Baruah, A., Chang, H.W., Pace, H.M., Lee, S.S. 2011. The homeobox protein CEH-23 mediates prolonged longevity in response to impaired mitochondrial electron transport chain in C. elegans. PLoS Biol.; **9**(6):e1001084. doi: 10.1371/journal.pbio.1001084.

Warner, A., Qadota, H., Benian, G.M., Vogl, A.W., Moerman, D.G. 2011. The Caenorhabditis elegans paxillin orthologue, PXL-1, is required for pharyngeal muscle contraction and for viability; **22**(14):2551-63.

Winter, J.F., Höpfner, S., Korn, K., Farnung, B.O., Bradshaw, C.R., Marsico, G., Volkmer, M., Habermann, B., Zerial, M. 2012. Caenorhabditis elegans screen reveals role of PAR-5 in RAB-11-recycling endosome positioning and apicobasal cell polarity. Nat Cell Biol.; **14**(7):666-76.

WormBase web site, http://www.wormbase.org, release WS246, date 10-Oct-2014

Wu, S., Mehta, S.Q., Pichaud, F., Bellen, H.J., Quiocho, FA. 2005. Sec15 interacts with Rab11 via a novel domain and affects Rab11 localization in vivo. Nat Struct Mol Biol.; **12**(10):879-85.

Wu, M. and Herman, M.A. 2006. A novel noncanonical Wnt pathway is involved in the regulation of the asymmetric B cell division in C. elegans. Dev Biol.; **293**(2):316-29. Epub 2006 Apr 24.

Xiong, H., Mohler, W.A., Soto, M.C. 2011. The branched actin nucleator Arp2/3 promotes nuclear migrations and cell polarity in the C. elegans zygote. Dev Biol. 2011; **357**(2):356-69.

Yaseen, N.R. and Blobel, G. 1997. Cloning and characterization of human karyopherin beta3. Proc Natl Acad Sci U S A.; **94**(9):4451-6.

Zallen, J.A., Peckol, E.L., Tobin, D.M., Bargmann, C.I. Neuronal cell shape and neurite initiation are regulated by the Ndr kinase SAX-1, a member of the Orb6/COT-1/warts serine/threonine kinase family. Mol Biol Cell.; **11**(9):3177-90.

Chen, S., Li, L., Li, J., Liu, B., Zhu, X., Zheng, L., Zhang, R., Xu, T. 2014. SEC-10 and RAB-10 coordinate basolateral recycling of clathrin-independent cargo through endosomal tubules in Caenorhabditis elegans. Proc Natl Acad Sci U S A.; **111**(43):15432-7.

Zhou, S., Opperman, K., Wang, X., Chen, L. 2008. unc-44 Ankyrin and stn-2 gamma-syntrophin regulate sax-7 L1CAM function in maintaining neuronal positioning in Caenorhabditis elegans. Genetics.; **180**(3):1429-43.

Tables

Genotype	% Defect	N	P-value	class	confidence level
empty vector	0.97	103			
abi-1	10.6	19	0.0629		
amph-1	20	25	0.001	cell transport	medium
anc-1	39.4	66	<0.0001	nuclear	high
app-1	10	20	0.0684		
arx-2	82.8	29	<0.0001	nuclear	high
arx-3	50	26	<0.0001	nuclear	high
bar-1	6.7	15	0.239		
bicd-1	0	10	1		
c35a5.8	10.5	19	0.0629		
C35D10.2/gipc-1	26.1	23	<0.0001	neuronal	high
ced-5	0	9	1		
ckb-2	0	20	1		
cls-1	10	10	0.1699		
cwn-1	14.3	21	0.0152	neuronal, cell signaling	medium
d2092.1	0	9	1		
daf-16	37.5	8	0.001	transcription factor	medium
daf-18	0	8	1		
deb-1	40	10	0.0002	cell structure	high
dh11.5	21.7	23	0.0007	neuronal	medium
dpy-31	6.7	15	0.239		
egal-1	0	5	1		
egl-13	23.5	102	<0.0001	transcription factor; neuronal	high
egl-17	0	11	1		
egl-26	0	10	1		
egl-5	5.9	17	0.2643		
F11A10.5	23.4	47	<0.0001	regulates tumorigencity	high
f44d12.4/gipc-2	20	10	0.0203	neuronal	medium

f55c12.1	30	10	0.002	cell cycle , cell transport	medium
fbl-1	14.3	21	0.0152	cell structure	medium
fmi-1	12.5	8	0.1396		
frm-2	20	10	0.0203	cell structure	medium
gei-13	7.7	13	0.2124		
gei-4	0	10	1		
gex-1/wve-1	59.4	32	<0.0001	nuclear	high
gex-2	50	20	<0.0001	nuclear	high
glb-12	72.2	18	<0.0001	globin	high
glp-1	14.3	21	0.0152	cell signaling	medium
gpb-1	10	10	0.1699		
gpb-2	15.4	13	0.0328		
him-1	0	10	1		
hlh-2	0	15	1		
hmp-2	10	20	0.0684		
hsp-12.3	0	17	1		
ima-1	25	16	0.0011	nuclear	medium
ima-2	57.9	19	<0.0001	nuclear	high
ima-3	57.7	26	<0.0001	nuclear	high
imb-2	29.4	17	0.0002	nuclear	high
imb-3	42.9	14	<0.0001	nuclear	high
ina-1	77.4	53	<0.0001	neruonal, cell structure	high
itr-1	33.3	30	<0.0001	neuronal	high
klc-2	0	12	1		
let-23	0	17	1		
let-756	9.1	11	0.1844		
let-99	0	10	1		
lim-9	37.5	24	<0.0001	cell signaling	high
lin-11	18.8	32	0.0007	transcription factor, neuronal, homeodomain	medium
lin-26	0	14	1		
lin-31	50	10	<0.0001	transcription factor	high
lin-39	100	10	<0.0001	neuronal, homeodomain	high
lis-1	18.2	11	0.0242		
lmn-1	26.3	19	0.0003	nuclear	high
mig-15	87.5	8	<0.0001	neuronal	high

mnp-1	0	10	1		
msp-19	10.3	29	0.0331		
msp-3	5.9	17	0.2643		
mua-6	20	5	0.0909		
ncam-1	21.1	19	0.002	neuronal, cell adhesion	medium
nob-1	0	15	1		
nud-2	22.2	9	0.0166	neuronal	medium
ooc-3	0	10	1		
pat-3	66.7	6	<0.0001	neuronal, cell structure	high
pat-4	0	11	1		
plc-3	0	10	1		
pqn-85	34.6	26	<0.0001	chromosome segregation	high
ptc-1	0	20	1		
pxl-1	37.5	8	0.001	cell adhesion, cell structure	medium
r06f6.6	9.1	22	0.0797		
rab-11.2	12.5	8	0.1396		
ran-1	6.3	16	0.2518		
ran-2	15	20	0.0135	nuclear	medium
ran-3	17.6	17	0.0088	nuclear	medium
rbf-1	11.1	9	0.1549		
rrc-1	28.6	14	0.0006	cell transport	medium
sax-1	20.8	24	0.0009	neuronal	medium
sax-2	0	10	1		
sax-7	22.2	9	0.0166	neuronal	medium
sec-15	29.4	17	0.0002	cell transport	high
slt-1	11.1	9	0.1549		
sma-6	0	9	1		
smf-1	0	5	1		
snt-4	16.7	6	0.1075		
sos-1	0	9	1		
srsx-18	11.5	52	0.006	neuronal	medium
syd-9	7.7	13	0.2124		
sym-4	0	10	1		
t16g12.6	11.1	9	0.1549		
ten-1	0	20	1		
toca-1	13.9	36	0.0045	cell structure, nuclear	medium

tsr-1	0	20	1		
ttx-3	21.4	14	0.0052	neuronal, homeodomain	medium
uig-1	11.1	9	0.1549		
unc-112	5.9	17	0.2643		
unc-33	30	10	0.002	neuronal, cell adhesion	medium
unc-44	25	4	0.0737		
unc-70	15.8	19	0.0118	neuronal, cell structure, cell adhesion	medium
unc-76	10	10	0.1699		
unc-83	52.4	21	<0.0001	nuclear	high
unc-84	33.3	30	<0.0001	nuclear	high
unc-97	64.3	14	<0.0001	neuronal, cell adhesion	high
vab-3	29.6	27	<0.0001	homeodomain protein	high
Y40H4A.2	4.8	21	0.3112		
y69h2.2	0	0	1		
zag-1	30	10	0.002	neuronal, homeodomain	medium
zc123.3/zfh-2	44.4	45	<0.0001	neuronal, transcription factor, homeodomain	high
zfp-1	35.3	34	<0.0001	homeodomain protein	high
zyg-8	0	10	1		
zyg-9	10	10	0.1699		

Table 1: RNAi screen list of genes

Phenotypes were scored at L4 lethargus. P-values were calculated in comparison to empty vector (RNAi) using Fisher's exact test.

Figures

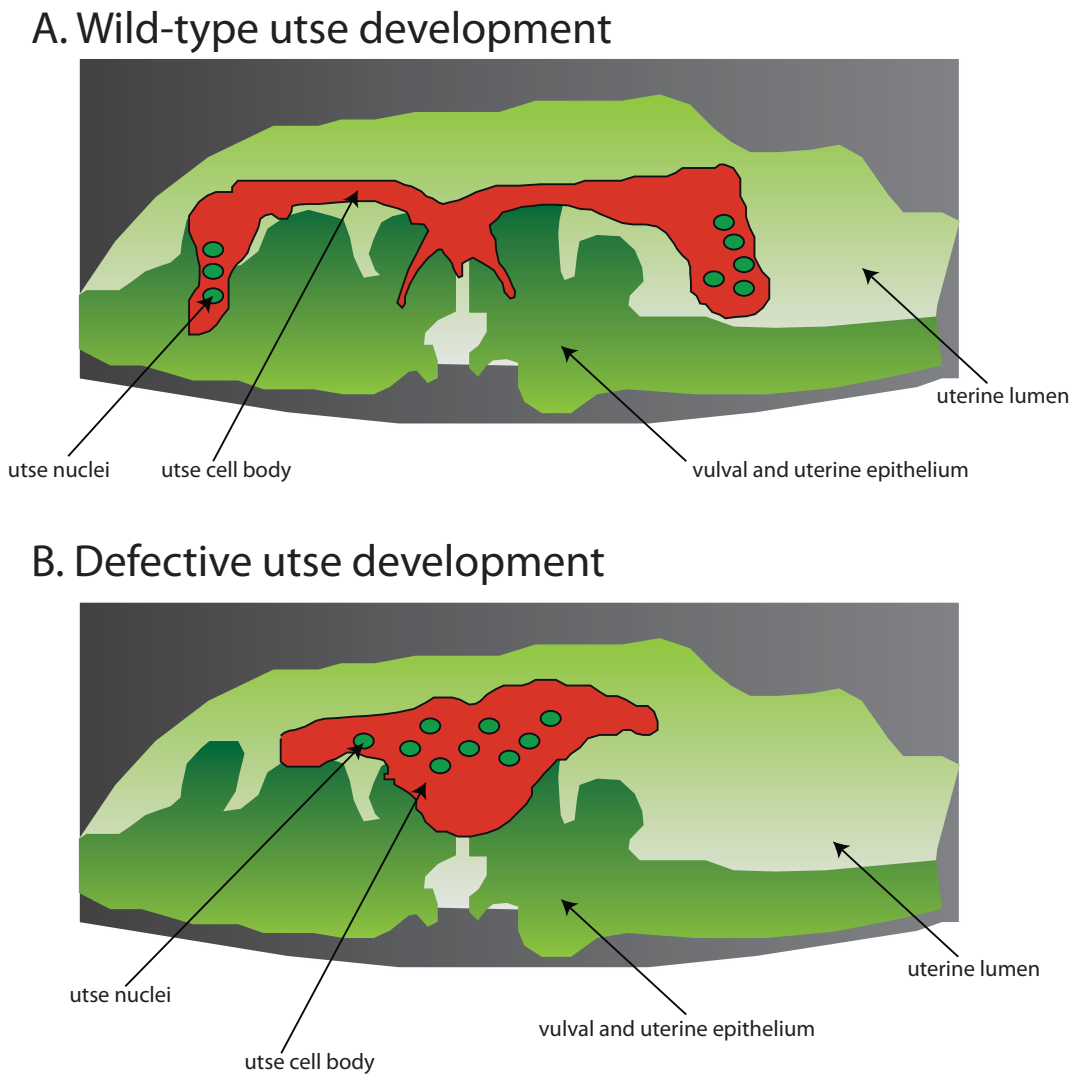

Figure 1: utse outgrowth phenotypes

utse cell body is shown in red and utse nuclei is shown in solid green. **(A)** Wild-type utse development at L4 lethargus. utse has properly elongated along the anterior-posterior axis and nuclei have migrated to the anterior and posterior edges of the utse. **(B)** Defective utse development at L4 lethargus. utse exhibits shorter outgrowth and nuclei have not migrated.

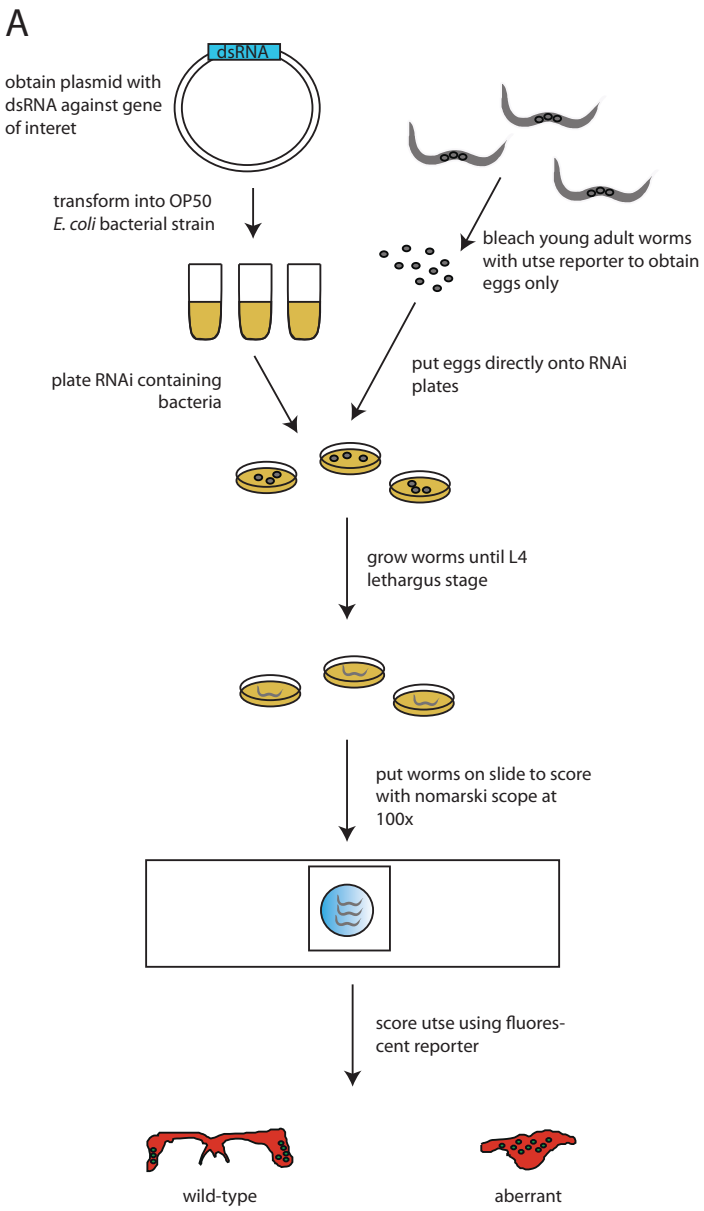

Figure 2: screen schematics

(A) Schematic of how RNAi screen against utse phenotypes was performed.

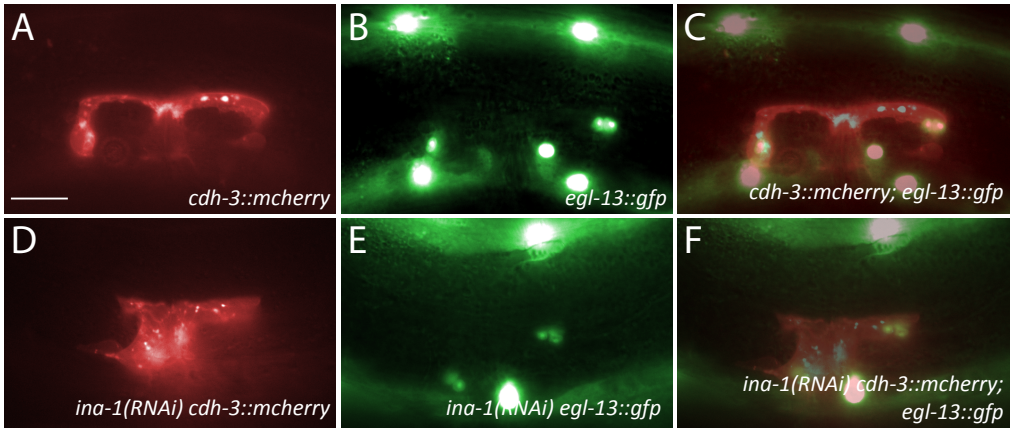

Figure 3: Representative phenotypes

utse cell body maked with *cdh-3::mcherry* and utse nuclei marked with *egl-13::gfp*. **(A-C)** wild-type utse development. **(A)** wild-type utse cell body has properly grown outward along the anterior-posterior axis. **(B)** wild-type utse nuclei have migrated to the anterior and posterior edges of the cell. **(C)** merge of (A) and (B). **(D-F)** utse development in *ina-1(RNAi)* treated animals. **(D)** in *ina-1(RNAi)* treated animals utse cell body has failed to grow the full length along the anterior-posterior axis and cell body is mishappen. **(E)** *ina-1(RNAi)* treated animals exhibit defects in nuclear migration. Nuclei have not properly migration and are mispositioned. **(F)** merge of (D) and (E). Scale bar indicates 100 μm.

CHAPTER 6

Concluding Remarks

6.1 Concluding remarks

This work presents the *C. elegans* uterine seam cell (utse) new model system for studying cell biology. During its development, the utse grows outward along the anterior-posterior axis, changing from an ellipsoidal cell to an elongated H-shaped cell. We have identified spatial and molecular inputs necessary for utse outgrowth, and used the utse as an *in vivo* model to study proteases involved in metastatic cancer.

Chapter 2 describes 11 different *C. elegans* systems that undergo outgrowth and cell shape change. While discussing the different genetic inputs necessary for each system, I observed that certain genes and gene families (netrins, Trio) were controlling outgrowth in multiple systems. It seems that these genes regulate different tissues through differentially interacting with tissue specific factors. A comprehensive study of these master genetic regulators of cell outgrowth in multiple tissues would be an ideal way to identify exactly how these genes are differentially regulated. Furthermore, in many cases I also saw that certain components of a pathway were involved in more than one tissue. For instance, the FGF receptor is involved in utse development, and the FGF ligands and receptor are involved in muscle arm development. These two cell outgrowth systems are spatially distant from one another and have separate functions within the worm. Therefore, it would not be surprising if FGF was affecting other outgrowth systems in *C. elegans*, especially considering that FGF is known to affect cell migration and cell shape change in other organisms. FGF is but one example of a system that begs to be studied in other *C. elegans* tissues that grow outward. By selecting a few candidates that function in multiple systems and whose gene families have known outgrowth function in other organisms, we can identify other master regulators of *C. elegans* cell outgrowth by characterizing their inputs in multiple *C. elegans* growing tissues.

Chapter 3 characterizes spatial and molecular inputs involved in *C. elegans* utse cell outgrowth. Specifically, in Chapter 3 I identified three tissues involved in utse development: the uterine lumen cells uterine toroid 1 and uterine toroid 2, and the sex muscles. I also identified that certain genes expressed in these tissues, *rsef-1* and *unc-73* in the uterine toroids and *unc-53* in the sex muscles, promote utse outgrowth. One experiment that would bolster my findings would involve performing tissue specific rescues within these three tissues. For instance, if a uterine toroid 1 or 2 specific promoter were available, this promoter could specifically drive *unc-73* expression in uterine toroid 1 or 2 of an *unc-73* null mutant. I also identified several genes involved in cell transport that promote utse outgrowth. These include the divergent Rab *rsef-1*, as well as five other RabGTPases.

Interestingly, in most *C. elegans* systems one or two RabGTPases exhibit activity, and therefore the utse is an ideal system to study multiple aspects of intracellular transport. Some interesting future experiment would involve identification of the cargo being transported within the utse as well as imaging experiments to visualize intracellular transport within the utse.

Chapter 4 characterizes three nematode astacin metalloproteases: NAS-21, NAS-22, and TOH-1, which share sequence similarity with meprins (a class of zinc metalloproteases upregulated in metastatic cancers). Meprins function by cleaving/degrading components of the ECM, such as collagen IV, laminin, fibronectin, and nidogen. This cleavage/degradation promotes invasive activities of metasttic cancers. I have shown that NAS-21, NAS-22, and TOH-1 also negatively regulate expression levels of ECM proteins, such as collagen IV, laminin, and syndecan. An interesting future experiment could involve quantifying changes in protein levels of ECM proteins in response to nematode astacin knockdown. This would be done through Western Blot analysis against ECM proteins using utse/uterine lysate. I also performed a specificity assay through characterizing activity of pharyngeal nas genes within the utse and characterizing NAS-21, NAS-22, and TOH-1 activity within the pharynx. Surprisingly, we saw that astacins expressed in the pharynx affected levels of ECM proteins within the uterus and knockdown of these astacins caused low levels of utse outgrowth defects. Knockdown of NAS-21, NAS-22, and TOH-1 also disrupted the integrity of tissues surrounding the pharynx and affected levels of ECM in tissues adjacent to the pharynx. *C. elegans* contains 40 astacins, the majority of which are secreted, and my results show that even if an astacins are expressed in one tissue, knockdown of this astacin can have long range effects on the ECM of many tissues. Future directions would involve characterizing the effects of all 40 astacins on the ECM of tissues that are both proximal and distal to the astacin expression site. Lastly, after generating a *nas-21* overexpression construct, I was able to screen for phenotypes indicative of *nas-21* upregulation and create a network. While building this network, I identified several upstream activators and protease inhibitors whose homologs regulated meprin activity, further bolstering my claim that the utse can be used as a *in vivo* model to studying meprin activity. One experiment I believe would further this claim would be using human meprin contructs to rescue utse defects in a *nas-21* null mutant. Currently a true *nas-21* null does not exist, but could be generated using CRISPR directed mutagenesis.

Chapter 5 details an RNAi screen performed against genes I thought could affect utse development. My screen identified 54 genes whose knockdown significantly perturbs utse development. These

genes are from a wide variety of categories, including genes involved in neruronal regulation, genes that regulate nuclear migration, and genes that regulate cell transport. Detailed study of these genes can create novel roles for genes that have not traditionally been characterized to affect cell outgrowth.

Overall my work shows that the utse is a powerful tool that I have used to learn about a variety of aspects of cell biology. I feel that my work has cemented the utse as a key model system for understanding cell outgrowth, but has only covered the tip of the iceberg of information that can be gleaned from studying this cell. I hope that my work is but one of many studies that will use the utse to learn more about the complicated nature of cell biology.